Strength in Fragility:

Age-dependent Sclerostin Antibody Response in Osteogenesis Imperfecta Craniofacial Structures

Hsiao Hsin Sung Hsieh

RADBOUD UNIVERSITY PRESS

Radboud Dissertation Series

Strength in Fragility:

Age-dependent Sclerostin Antibody Response in Osteogenesis Imperfecta Craniofacial Structures

Hsiao Hsin Sung Hsieh

The research presented in this thesis was conducted at the Orthopaedic Research Laboratory (ORL) within the Department of Orthopaedic Surgery, and in the Department of Oral and Maxillofacial Surgery at the University of Michigan, Ann Arbor, Michigan, USA, in collaboration with the Experimental Rheumatology group, Department of Rheumatology, Radboud University Medical Centre, Nijmegen, the Netherlands.

Strength in Fragility: Age-dependent Sclerostin Antibody Response in Osteogenesis Imperfecta Craniofacial Structures
Hsiao Hsin Sung Hsieh

Radboud Dissertation Series
ISSN: 2950-2772 (Online); 2950-2780 (Print)

Published by RADBOUD UNIVERSITY PRESS
Postbus 9100, 6500 HA Nijmegen, The Netherlands
www.radbouduniversitypress.nl

Design: Proefschrift AIO | Annelies Lips
Cover: Hsiao Hsin Sung Hsieh
Printing: DPN Rikken/Pumbo

ISBN: 9789465153018
DOI: 10.54195/9789465153018
Free download at: https://doi.org/10.54195/9789465153018

RADBOUD
UNIVERSITY
PRESS

Strength in Fragility:

Age-dependent Sclerostin Antibody Response in Osteogenesis Imperfecta Craniofacial Structures

Proefschrift ter verkrijging van de graad van doctor
aan de Radboud Universiteit Nijmegen
op gezag van de rector magnificus prof. dr. J.M. Sanders,
volgens besluit van het college voor promoties
in het openbaar te verdedigen op

maandag 7 september 2026
om 12.30 uur precies

door

Hsiao Hsin Sung Hsieh
geboren op 19 juli 1975
te Taoyuan, Taiwan

Promotoren:
Prof. dr. P.M. van der Kraan
Prof. dr. K.M. Kozloff, University of Michigan, Verenigde Staten

Copromotor:
Dr. E.N. Blaney Davidson

Manuscriptcommissie:
Dr. ing. J.J.J.P. van den Beucken
Prof. dr. A.D. Bakker, ACTA
Prof. dr. A. Forlino, Università di Pavia, Italië

Strength in Fragility:

Age-dependent Sclerostin Antibody Response in Osteogenesis Imperfecta Craniofacial Structures

Dissertation to obtain the degree of doctor
from Radboud University Nijmegen
on the authority of the Rector Magnificus prof. dr. J.M. Sanders,
according to the decision of the Doctorate Board
to be defended in public on

Monday, September 7, 2026
at 12:30 pm

by

Hsiao Hsin Sung Hsieh
born on July 19, 1975
in Taoyuan, Taiwan

PhD supervisors:
Prof. dr. P.M. van der Kraan
Prof. dr. K.M. Kozloff, University of Michigan, United States of America

PhD co-supervisor:
Dr. E.N. Blaney Davidson

Manuscript Committee:
Dr. ing. J.J.J.P. van den Beucken
Prof. dr. A.D. Bakker, ACTA
Prof. dr. A. Forlino, University of Pavia, Italy

Table of Contents

CHAPTER 1

General Introduction

Understanding the mechanisms underlying bone fragility and impaired repair is critical for improving clinical outcomes in patients with genetic disorders affecting connective tissues. Among these conditions, osteogenesis imperfecta (OI) stands out not only for its impact on the long bones, but also for the unique challenges it poses to the craniofacial skeleton and dental tissues. By investigating the genetic and clinical features of OI, and examining how this disorder affects craniofacial development, this thesis aims to identify new opportunities for enhancing bone regeneration. In particular, recent advances in targeting the Wnt signaling pathway, such as sclerostin inhibition, offer promising strategies that may improve craniofacial bone strength and repair in OI.

Osteogenesis Imperfecta

OI, also known as brittle bone disease, is a rare genetic connective tissue disorder. It is most commonly caused by mutations in the COL1A1 and COL1A2 genes, which lead to defective synthesis or processing of type I collagen, the major protein in bone, skin, and tendon matrices[1-4]. The clinical spectrum is broad, ranging from mild forms of OI with increased fracture susceptibility and reduced bone density to severe, life-threatening manifestations of OI in infancy, including crumpled ribs and skull fragility[5-7]. Notable associated features include blue sclerae, short stature, dentinogenesis imperfecta (DI), hearing loss, valvular insufficiency, and aortic root dilation, alongside milder symptoms such as ligamentous laxity and easy bruising[5, 8].

OI is classified based on both clinical features (phenotype) and genetic characteristics (genotype). The traditional classification includes five main types (I–V), which are distinguished by their physical manifestations and underlying genetic mutations. More recently, additional types (VI–XI) have been identified, resulting from new genetic variants that affect collagen biosynthesis or post-translational modifications. Most cases of OI follow an autosomal dominant pattern of inheritance, though autosomal recessive and X-linked forms are also recognized[9-12]. The pathophysiology of osteogenesis imperfecta centers on both quantitative and qualitative abnormalities of type I collagen, with glycine substitutions in the triple helix regions frequently correlating with disease severity[13-16]. As a genetic disorder, OI is highly heritable, with most forms resulting from inherited mutations in collagen genes or from new (de novo) mutations. Epidemiologically, OI occurs in approximately 1 in 15,000–20,000 births, most frequently affecting type I variants[9, 17].

Diagnostic and prognostic systems, such as the Sillence and Shapiro classifications, are used to categorize people with OI based on their symptoms and expected health outcomes. These frameworks help account for the wide variety of physical

differences seen in OI and can provide some guidance regarding survival. However, even within the same subtype, predicting how frequently fractures will occur or how serious they might become remains challenging[6, 9, 18, 19]. Diagnosis of OI involves clinical assessment, radiographic evaluation, and confirmation via molecular genetic testing[10]. Management typically requires multidisciplinary care, ranging from medications to orthopedic surgery, physical rehabilitation, hearing evaluations, cardiac monitoring, and detailed dental management; prognosis and severity remain highly variable[19, 20].

Although much research has focused on how OI affects long bones, leading to well-established approaches for managing fractures and skeletal fragility, comparatively little is known about OI's impact on craniofacial bones and dental tissues. The developmental origins, biological properties, and functional demands of craniofacial bones are distinct from those of long bones. These differences raise important questions, not only about how OI affects the facial skeleton, but also whether therapeutic strategies that work well for long bones will produce similar results in craniofacial sites. Because craniofacial abnormalities can impair essential functions such as eating, speaking, and breathing, and significantly influence appearance and quality of life, this thesis focuses on the unique challenges posed by OI in these structures, aiming to better understand and improve treatment outcomes.

Craniofacial Structures

The craniofacial complications of OI are rooted in the same types of collagen defects described above. Defective COL1 influences skull and jawbone development, leading to conditions such as DI, malocclusion, and mandibular prognathism, which contribute to asymmetrical growth and altered facial proportions. In teeth, type I collagen plays a crucial role in the dentin and periodontal ligament. The dentin is composed of about 20% organic material, mostly collagen type I, crucial for the tooth's mechanical strength[21].The periodontal ligament, a specialized connective tissue surrounding tooth roots, anchors them to the alveolar bone and is rich in type I collagen, connecting the tooth cementum to the alveolar bone socket and offering crucial support against chewing forces. Even when DI is not visibly evident, patients may still experience underlying dental abnormalities due to these collagen defects[22]. This can result in missing teeth, abnormal tooth eruption, and an increased likelihood of dental attrition and enamel fractures[23].

The impact of type I collagen defects in OI is not limited to individual dental or skeletal issues; instead, these abnormalities interact to create complex clinical challenges. Because the same underlying defect compromises both craniofacial

bone and dental tissues, a patient's dental anomalies can further influence the health and function of the jawbones and surrounding structures. For example, abnormal tooth development or loss may place additional stress on weakened bone, increasing the risk of bone resorption or fracture. Conversely, fragile craniofacial bones may impair proper tooth eruption and retention. This bidirectional relationship complicates oral rehabilitation and necessitates treatment strategies that address both the unique biology of craniofacial bones and the interconnected nature of bone and tooth health in OI patients.

Craniofacial bones are distinct from axial and long bones in their embryological origins and modes of ossification. The craniofacial skeleton is composed of eight cranial bones and fourteen facial bones, which predominantly arise from mesenchymal cells derived from the cranial neural crest during embryogenesis[24]. These versatile cells differentiate into osteoblasts and chondrocytes, facilitating the formation of the cranial vault, facial skeleton, and skull base through both endochondral and intramembranous ossification[25, 26]. Unlike long bones, which typically develop through endochondral ossification, most craniofacial bones form via intramembranous ossification, a process that produces bone directly from mesenchymal cells, bypassing a cartilage stage. This results in unique biomechanical properties and presents clinical challenges in addressing congenital defects, trauma, and disease-related bone loss[26]. The specialized anatomy of the craniofacial complex is not only essential for protecting the brain and sensory organs, but also provides crucial attachment sites for muscles involved in chewing, facial expression, and speech[27].

While the craniofacial skeleton undergoes continuous remodeling throughout life in all individuals, these processes are notably disrupted in osteogenesis imperfecta. In the general population, age-related changes in osteoclast and osteoblast activity typically result in decreased bone mineral density and altered microarchitecture, compromising structural integrity and causing gradual changes in facial morphology[28]. In OI patients, however, defects in collagen exacerbate these remodeling imbalances, leading to an even greater risk of bone fragility, deformity, and changes in the craniofacial appearance—often manifesting earlier and more severely than in unaffected individuals. The functional demands placed on craniofacial bones, such as chewing and breathing, further increase the complexity of these remodeling challenges. As a result, regenerative strategies for OI must be tailored to the unique biology and heightened vulnerabilities of craniofacial bones, rather than relying on approaches developed for long bone defects in the general population.

Current reconstructive treatments are based on free flaps for major craniofacial defects as consequence of cancer or trauma. However, harvesting the graft is invasive and limited by available donor bone, increased morbidity, and postoperative pain. For more localized oral rehabilitation, various types of bone grafts and biological treatments, such as bone morphogenetic proteins (BMPs), are employed[29-31]. While these options offer clinical benefits, they can also result in significant swelling and the possibility of excessive or heterotopic bone formation[32]. There is a need for better therapeutic solutions that can autoregulate without causing resorption or overgrowth. Researchers continue to seek improved methods that provide balanced regeneration and stability for craniofacial bone regeneration and reconstruction.

Wnt signaling: Sclerostin inhibition

Recent advances in understanding OI have highlighted the importance of molecular pathways involved in bone formation and repair, particularly in the craniofacial region. One pathway of significant interest is Wnt signaling, which plays a central role in regulating bone growth and osteoblast differentiation. Given that OI is characterized by impaired bone quality and inadequate repair due to defective collagen, targeting molecular mechanisms that enhance bone formation has become an attractive therapeutic strategy. In this context, the Wnt signaling pathway, and interventions such as sclerostin inhibition, have emerged as promising approaches for improving bone strength and regeneration, especially in craniofacial bones.

The Wnt signaling pathway is pivotal in bone biology and plays a particularly important role in craniofacial development. This pathway governs the proliferation and differentiation of osteoprogenitor cells into osteoblasts, which are essential for bone growth and repair[33]. Wnt signaling operates through two main branches: the canonical (β-catenin-dependent) pathway and the non-canonical (β-catenin-independent) pathways. The canonical pathway results in stabilization and nuclear translocation of β-catenin, which then activates genes critical for osteoblast formation and bone regeneration. In contrast, the non-canonical pathways modulate cellular movement, polarity, and other responses independent of β-catenin signaling, and are also implicated in developmental processes and bone cell function[33-35].

Precise regulation of Wnt signaling is crucial for maintaining cranial suture patency and proper bone formation. When this regulation is disrupted, it can lead to craniofacial malformations or diseases such as craniosynostosis[34, 35].

One key regulator within this pathway is sclerostin, a glycoprotein primarily produced by osteocytes. Sclerostin acts by inhibiting the Wnt/β-catenin pathway, thereby suppressing osteoblast activity and promoting bone resorption[37]. In certain genetic disorders, including OI, sclerostin levels are found to be elevated, further impairing bone formation. Conversely, mutations in the SOST gene, which encodes sclerostin, lead to conditions characterized by excessive bone growth, such as sclerosteosis and van Buchem disease[38, 39].

Wnt signaling naturally balances bone formation and remodeling by promoting osteoblast activity and inhibiting osteoclast differentiation, offering a more holistic approach compared to treatments that solely focus on bone formation or resorption[36].

Preclinical studies have shown promise in targeting sclerostin for therapy. Sclerostin antibody (SclAb) treatment has been demonstrated to enhance bone formation and mechanical strength by reactivating Wnt signaling in animal models of OI, notably the Brtl/+ mouse. This mouse model carries a mutation in the col1a1 gene, mimicking moderate OI and presenting with reduced bone mineral density and bone fragility. In these studies, SclAb administration improved cortical bone formation and increased mechanical properties, without increasing brittleness[43-45].

Although SclAb therapy shows benefits for long bones, its effects on craniofacial structures remain less well understood—especially in the OI context. Given that sclerostin mutations can significantly increase bone density in facial bones, understanding the response of craniofacial bone to sclerostin inhibition is essential. Notably, craniofacial bones differ from long bones in their embryological origins and mechanisms of formation, which may lead to unique therapeutic outcomes.

Therefore, this thesis aims to characterize the role of sclersotin and Wnt signaling in craniofacial bone regeneration comprehensively address the multifaceted challenges of craniofacial bone health, fracture risk, and therapeutic strategies in osteogenesis imperfecta (OI), this thesis is structured as follows:

Chapter 2. Preserving alveolar bone: The intersection of aging, remodeling, and Wnt signaling pathways

This chapter characterizes the unique biology of alveolar bone—highlighting its rapid adaptation to chewing forces, oral microbiome exposure, and complex mechanical demands. Central to maintenance and regeneration is the Wnt/β-catenin pathway, a master regulator whose age-related alterations and suppression can drive net bone loss in the oral cavity. The chapter reviews compartment-

specific regulation of this pathway and compares alveolar bone turnover and signaling paradigms to those in long bones. It further considers current evidence for molecular interventions, including sclerostin inhibition, that may support bone health and regeneration in aging and disease.

Given Wnt signaling's central role in craniofacial bone remodeling, it is crucial to determine whether craniofacial bone is a clinically significant site of involvement in OI, motivating a population-based analysis in the next chapter.

Chapter 3. Craniofacial and whole-skeleton fracture patterns in osteogenesis imperfecta: Findings from a nationwide U.S. insurance claims database
In this chapter, a national insurance claims dataset is used to quantify the period prevalence, anatomical distribution, and predictors of fractures in OI, with particular emphasis on craniofacial sites—jaw, skull, and facial bones—that are understudied in prior literature. By stratifying fracture risk by age, sex, proxy-measured disease severity, and insurance type, the research reveals the distinctive burden and demographic patterns of craniofacial fractures in OI. These findings highlight the necessity for ongoing, site-specific monitoring and multidisciplinary management; they also underscore the importance of developing therapies and preventative strategies that address the elevated risk in craniofacial bones.

Recognizing the high real-world burden of craniofacial bone fragility in OI, the thesis next examines whether mouse models replicate patient-specific craniofacial features, essential for testing new therapies.

Chapter 4. Collagen mutation and age contribute to differential craniofacial phenotypes in mouse models of osteogenesis imperfecta
This chapter uses genetically modified mouse strains with distinct type I collagen mutations, including Brtl/+ and G610c/+, to rigorously assess how mutation type, location, and aging affect craniofacial and dentoalveolar bone structure and remodeling. The Brtl/+ model harbors a heterozygous Col1a1 mutation causing a glycine-to-cysteine substitution at position 349 in the α1(I) collagen chain, whereas the G610c/+ model carries a heterozygous Col1a2 mutation producing a glycine-to-cysteine substitution at position 610 in the α2(I) collagen chain. These substitutions occur within the collagen triple-helical domain, where glycine residues are essential for normal helix folding; therefore, both mutations impair type I collagen structure and function through a dominant-negative mechanism.

Detailed morphometric analyses and bone turnover studies are conducted to compare mouse model phenotypes to human OI presentations, facilitating accurate model selection for preclinical studies. The evaluation also supports targeted therapy development by delineating the impact of genotype and age on specific craniofacial bone deficits.

With these validated models reflecting relevant craniofacial abnormalities, the thesis advances to testing molecular therapies targeting pathways implicated in bone defect restoration.

Chapter 5. Sex-Based Differences in Sclerostin Antibody for Craniofacial Bone Disorders with Collagen Defects

This chapter investigates the efficacy of sclerostin antibody (SclAb) therapy in OI mouse models, addressing both craniofacial bone mass restoration and architectural improvement. Comprehensive analysis of SclAb's effects explores sex-specific differences, acknowledging the role of estrogen and testosterone in bone formation, resorption, and density. The results support consideration of individualized approaches for craniofacial bone regeneration in OI, revealing the potential for SclAb therapy beyond traditional bone turnover enhancement.

While increased bone quantity and density are necessary, functional rehabilitation demands successful prosthetic integration. The thesis thus progresses to the challenge of achieving solid osseointegration in compromised bone due to OI.

Chapter 6. Sclerostin Antibody Enhances Implant Osseointegration in Bone with Col1a1 Mutation

Given the challenges of dental and orthopedic implant success in low-density bone, this chapter evaluates whether SclAb-induced improvements in alveolar bone translate to enhanced bone-to-implant contact and fixation in the Brtl/+ mouse model. Using advanced imaging and mechanical testing, the research assesses implant integration, durability, and functional performance. Study outcomes provide the basis for clinical application of SclAb therapy in oral rehabilitation, especially for patients with compromised skeletal health.

Synthesizing these mechanistic, population-level, and therapeutic insights, the final chapter looks forward to future strategies and clinical implementation.

Chapter 7. Conclusion and Future Directions

This chapter integrates the key findings on Wnt signaling, population-based craniofacial fracture risk, model validation, molecular intervention, and implant outcomes in OI. It recommends future research directions such as optimizing localized SclAb delivery and refining patient selection strategies, ultimately aiming to advance craniofacial bone regeneration and rehabilitation for individuals with osteogenesis imperfecta.

References

1. Uttarilli A, Shah H, Bhavani GS, Upadhyai P, Shukla A, Girisha KM. Phenotyping and genotyping of skeletal dysplasias: Evolution of a center and a decade of experience in India. Bone. 2019;120:204-11. Epub 20181106. doi: 10.1016/j.bone.2018.10.026. PubMed PMID: 30408610.
2. Marini JC, Forlino A, Cabral WA, Barnes AM, San Antonio JD, Milgrom S, Hyland JC, Korkko J, Prockop DJ, De Paepe A, Coucke P, Symoens S, Glorieux FH, Roughley PJ, Lund AM, Kuurila-Svahn K, Hartikka H, Cohn DH, Krakow D, Mottes M, Schwarze U, Chen D, Yang K, Kuslich C, Troendle J, Dalgleish R, Byers PH. Consortium for osteogenesis imperfecta mutations in the helical domain of type I collagen: regions rich in lethal mutations align with collagen binding sites for integrins and proteoglycans. Hum Mutat. 2007;28(3):209-21. Epub 2006/11/02. doi: 10.1002/humu.20429. PubMed PMID: 17078022; PMCID: PMC4144349.
3. Nicol L, Morar P, Wang Y, Henriksen K, Sun S, Karsdal M, Smith R, Nagamani SCS, Shapiro J, Lee B, Orwoll E. Alterations in non-type I collagen biomarkers in osteogenesis imperfecta. Bone. 2019;120:70-4. Epub 20181002. doi: 10.1016/j.bone.2018.09.024. PubMed PMID: 30290234.
4. Valadares ER, Carneiro TB, Santos PM, Oliveira AC, Zabel B. What is new in genetics and osteogenesis imperfecta classification? J Pediatr (Rio J). 2014;90(6):536-41. Epub 20140718. doi: 10.1016/j.jped.2014.05.003. PubMed PMID: 25046257.
5. Ablin DS. Osteogenesis imperfecta: a review. Can Assoc Radiol J. 1998;49(2):110-23. PubMed PMID: 9561014.
6. Forlino A, Cabral WA, Barnes AM, Marini JC. New perspectives on osteogenesis imperfecta. Nat Rev Endocrinol. 2011;7(9):540-57. Epub 20110614. doi: 10.1038/nrendo.2011.81. PubMed PMID: 21670757; PMCID: PMC3443407.
7. Marini JC, Forlino A, Bachinger HP, Bishop NJ, Byers PH, Paepe A, Fassier F, Fratzl-Zelman N, Kozloff KM, Krakow D, Montpetit K, Semler O. Osteogenesis imperfecta. Nat Rev Dis Primers. 2017;3:17052. Epub 2017/08/19. doi: 10.1038/nrdp.2017.52. PubMed PMID: 28820180.
8. Pollitt R, McMahon R, Nunn J, Bamford R, Afifi A, Bishop N, Dalton A. Mutation analysis of COL1A1 and COL1A2 in patients diagnosed with osteogenesis imperfecta type I-IV. Hum Mutat. 2006;27(7):716. doi: 10.1002/humu.9430. PubMed PMID: 16786509.
9. Sillence DO, Senn A, Danks DM. Genetic heterogeneity in osteogenesis imperfecta. J Med Genet. 1979;16(2):101-16. doi: 10.1136/jmg.16.2.101. PubMed PMID: 458828; PMCID: PMC1012733.
10. Jain M, Tam A, Shapiro JR, Steiner RD, Smith PA, Bober MB, Hart T, Cuthbertson D, Krischer J, Mullins M, Bellur S, Byers PH, Pepin M, Durigova M, Glorieux FH, Rauch F, Lee B, Sutton VR, Consortium MotBBD, Nagamani SCS. Growth characteristics in individuals with osteogenesis imperfecta in North America: results from a multicenter study. Genet Med. 2019;21(2):275-83. Epub 20180704. doi: 10.1038/s41436-018-0045-1. PubMed PMID: 29970925; PMCID: PMC6320321.
11. Morello R, Bertin TK, Chen Y, Hicks J, Tonachini L, Monticone M, Castagnola P, Rauch F, Glorieux FH, Vranka J, Bachinger HP, Pace JM, Schwarze U, Byers PH, Weis M, Fernandes RJ, Eyre DR, Yao Z, Boyce BF, Lee B. CRTAP is required for prolyl 3- hydroxylation and mutations cause recessive osteogenesis imperfecta. Cell. 2006;127(2):291-304. doi: 10.1016/j.cell.2006.08.039. PubMed PMID: 17055431.
12. van Dijk FS, Nesbitt IM, Zwikstra EH, Nikkels PG, Piersma SR, Fratantoni SA, Jimenez CR, Huizer M, Morsman AC, Cobben JM, van Roij MH, Elting MW, Verbeke JI, Wijnaendts LC, Shaw NJ, Hogler W, McKeown C, Sistermans EA, Dalton A, Meijers-Heijboer H, Pals G. PPIB mutations cause severe osteogenesis imperfecta. Am J Hum Genet. 2009;85(4):521-7. Epub 20090924. doi: 10.1016/j.ajhg.2009.09.001. PubMed PMID: 19781681; PMCID: PMC2756556.

13. Minch CM, Kruse RW. Osteogenesis imperfecta: a review of basic science and diagnosis. Orthopedics. 1998;21(5):558-67; quiz 68-9. PubMed PMID: 9606696.

14. Makareeva E, Mertz EL, Kuznetsova NV, Sutter MB, DeRidder AM, Cabral WA, Barnes AM, McBride DJ, Marini JC, Leikin S. Structural heterogeneity of type I collagen triple helix and its role in osteogenesis imperfecta. J Biol Chem. 2008;283(8):4787-98. Epub 20071211. doi: 10.1074/jbc.M705773200. PubMed PMID: 18073209.

15. Rauch F, Lalic L, Roughley P, Glorieux FH. Relationship between genotype and skeletal phenotype in children and adolescents with osteogenesis imperfecta. J Bone Miner Res. 2010;25(6):1367-74. doi: 10.1359/jbmr.091109. PubMed PMID: 19929435.

16. Selvaraj V, Sekaran S, Dhanasekaran A, Warrier S. Type 1 collagen: Synthesis, structure and key functions in bone mineralization. Differentiation. 2024;136:100757. Epub 20240228. doi: 10.1016/j.diff.2024.100757. PubMed PMID: 38437764.

17. Stoltz MR, Dietrich SL, Marshall GJ. Osteogenesis imperfecta. Perspectives. Clin Orthop Relat Res. 1989(242):120-36. PubMed PMID: 2650946.

18. Shapiro F. Consequences of an osteogenesis imperfecta diagnosis for survival and ambulation. J Pediatr Orthop. 1985;5(4):456-62. doi: 10.1097/01241398-198507000-00014. PubMed PMID: 4019761.

19. Sillence DO, Rimoin DL, Danks DM. Clinical variability in osteogenesis imperfecta-variable expressivity or genetic heterogeneity. Birth Defects Orig Artic Ser. 1979;15(5B):113-29. PubMed PMID: 393318.

20. Grafe I, Yang T, Alexander S, Homan EP, Lietman C, Jiang MM, Bertin T, Munivez E, Chen Y, Dawson B, Ishikawa Y, Weis MA, Sampath TK, Ambrose C, Eyre D, Bachinger HP, Lee B. Excessive transforming growth factor-beta signaling is a common mechanism in osteogenesis imperfecta. Nat Med. 2014;20(6):670-5. Epub 20140504. doi: 10.1038/nm.3544. PubMed PMID: 24793237; PMCID: PMC4048326.

21. Goldberg M, Kulkarni AB, Young M, Boskey A. Dentin: structure, composition and mineralization. Front Biosci (Elite Ed). 2011;3(2):711-35. Epub 20110101. doi: 10.2741/e281. PubMed PMID: 21196346; PMCID: PMC3360947.

22. Ventura L, Verdonk SJE, Zhytnik L, Ridwan-Pramana A, Gilijamse M, Schreuder WH, van Gelderen-Ziesemer KA, Schoenmaker T, Micha D, Eekhoff EMW. Dental Abnormalities in Osteogenesis Imperfecta: A Systematic Review. Calcif Tissue Int. 2024;115(5):461-79. Epub 20240918. doi: 10.1007/s00223-024-01293-2. PubMed PMID: 39294450; PMCID: PMC11531448.

23. Malmgren B, Norgren S. Dental aberrations in children and adolescents with osteogenesis imperfecta. Acta Odontol Scand. 2002;60(2):65-71. doi: 10.1080/000163502753509446. PubMed PMID: 12020117.

24. Chai Y, Jiang X, Ito Y, Bringas P, Jr., Han J, Rowitch DH, Soriano P, McMahon AP, Sucov HM. Fate of the mammalian cranial neural crest during tooth and mandibular morphogenesis. Development. 2000;127(8):1671-9. doi: 10.1242/dev.127.8.1671. PubMed PMID: 10725243.

25. Ortega N, Behonick DJ, Werb Z. Matrix remodeling during endochondral ossification. Trends Cell Biol. 2004;14(2):86-93. doi: 10.1016/j.tcb.2003.12.003. PubMed PMID: 15102440; PMCID: PMC2779708.

26. Percival CJ, Richtsmeier JT. Angiogenesis and intramembranous osteogenesis. Dev Dyn. 2013;242(8):909-22. Epub 20130627. doi: 10.1002/dvdy.23992. PubMed PMID: 23737393; PMCID: PMC3803110.

27. Cray J. Craniofacial biology journals: A review. International Journal of Paleopathology. 2011;1(3-4):130-1.

28. Fang H, Deng Z, Liu J, Chen S, Deng Z, Li W. The Mechanism of Bone Remodeling After Bone Aging. Clin Interv Aging. 2022;17:405-15. Epub 20220405. doi: 10.2147/CIA.S349604. PubMed PMID: 35411139; PMCID: PMC8994557.

29. Jensen AT, Jensen SS, Worsaae N. Complications related to bone augmentation procedures of localized defects in the alveolar ridge. A retrospective clinical study. Oral Maxillofac Surg. 2016;20(2):115-22. Epub 20160302. doi: 10.1007/s10006-016-0551-8. PubMed PMID: 26932593.

30. Nkenke E, Neukam FW. Autogenous bone harvesting and grafting in advanced jaw resorption: morbidity, resorption and implant survival. Eur J Oral Implantol. 2014;7 Suppl 2:S203-17. PubMed PMID: 24977256.

31. Sakkas A, Wilde F, Heufelder M, Winter K, Schramm A. Autogenous bone grafts in oral implantology-is it still a "gold standard"? A consecutive review of 279 patients with 456 clinical procedures. Int J Implant Dent. 2017;3(1):23. Epub 20170601. doi: 10.1186/s40729-017-0084-4. PubMed PMID: 28573552; PMCID: PMC5453915.

32. Smucker JD, Rhee JM, Singh K, Yoon ST, Heller JG. Increased swelling complications associated with off-label usage of rhBMP-2 in the anterior cervical spine. Spine (Phila Pa 1976). 2006;31(24):2813-9. doi: 10.1097/01.brs.0000245863.52371.c2. PubMed PMID: 17108835.

33. Houschyar KS, Tapking C, Borrelli MR, Popp D, Duscher D, Maan ZN, Chelliah MP, Li J, Harati K, Wallner C, Rein S, Pforringer D, Reumuth G, Grieb G, Mouraret S, Dadras M, Wagner JM, Cha JY, Siemers F, Lehnhardt M, Behr B. Wnt Pathway in Bone Repair and Regeneration - What Do We Know So Far. Front Cell Dev Biol. 2018;6:170. Epub 20190107. doi: 10.3389/fcell.2018.00170. PubMed PMID: 30666305; PMCID: PMC6330281.

34. Shimomura T, Kawakami M, Tatsumi K, Tanaka T, Morita-Takemura S, Kirita T, Wanaka A. The Role of the Wnt Signaling Pathway in Upper Jaw Development of Chick Embryo. Acta Histochem Cytochem. 2019;52(1):19-26. Epub 20190223. doi: 10.1267/ahc.18038. PubMed PMID: 30923412; PMCID: PMC6434314.

35. Marchini M, Hu D, Lo Vercio L, Young NM, Forkert ND, Hallgrimsson B, Marcucio R. Wnt Signaling Drives Correlated Changes in Facial Morphology and Brain Shape. Front Cell Dev Biol. 2021;9:644099. Epub 20210329. doi: 10.3389/fcell.2021.644099. PubMed PMID: 33855022; PMCID: PMC8039397.

36. Hoeppner LH, Secreto FJ, Westendorf JJ. Wnt signaling as a therapeutic target for bone diseases. Expert Opin Ther Targets. 2009;13(4):485-96. doi: 10.1517/14728220902841961. PubMed PMID: 19335070; PMCID: PMC3023986.

37. Sutherland MK, Geoghegan JC, Yu C, Turcott E, Skonier JE, Winkler DG, Latham JA. Sclerostin promotes the apoptosis of human osteoblastic cells: a novel regulation of bone formation. Bone. 2004;35(4):828-35. doi: 10.1016/j.bone.2004.05.023. PubMed PMID: 15454089.

38. Balemans W, Van Den Ende J, Freire Paes-Alves A, Dikkers FG, Willems PJ, Vanhoenacker F, de Almeida-Melo N, Alves CF, Stratakis CA, Hill SC, Van Hul W. Localization of the gene for sclerosteosis to the van Buchem disease-gene region on chromosome 17q12-q21. Am J Hum Genet. 1999;64(6):1661-9. doi: 10.1086/302416. PubMed PMID: 10330353; PMCID: PMC1377909.

39. Van Hul W, Balemans W, Van Hul E, Dikkers FG, Obee H, Stokroos RJ, Hildering P, Vanhoenacker F, Van Camp G, Willems PJ. Van Buchem disease (hyperostosis corticalis generalisata) maps to chromosome 17q12-q21. Am J Hum Genet. 1998;62(2):391-9. doi: 10.1086/301721. PubMed PMID: 9463328; PMCID: PMC1376897.

40. Xiaohui T, Wang L, Yang X, Jiang H, Zhang N, Zhang H, Li D, Li X, Zhang Y, Wang S, Zhong C, Yu S, Ren M, Sun M, Li N, Chen T, Ma Y, Li F, Liu J, Yu Y, Yue H, Zhang Z, Zhang G. Sclerostin inhibition in rare bone diseases: Molecular understanding and therapeutic perspectives. J Orthop Translat. 2024;47:39-49. Epub 20240619. doi: 10.1016/j.jot.2024.05.004. PubMed PMID: 39007037; PMCID: PMC11245887.

41. Forlino A, Porter FD, Lee EJ, Westphal H, Marini JC. Use of the Cre/lox recombination system to develop a non-lethal knock-in murine model for osteogenesis imperfecta with an alpha1(I) G349C substitution. Variability in phenotype in BrtlIV mice. J Biol Chem. 1999;274(53):37923-31. doi: 10.1074/jbc.274.53.37923. PubMed PMID: 10608859.

42. Kozloff KM, Carden A, Bergwitz C, Forlino A, Uveges TE, Morris MD, Marini JC, Goldstein SA. Brittle IV mouse model for osteogenesis imperfecta IV demonstrates postpubertal adaptations to improve whole bone strength. J Bone Miner Res. 2004;19(4):614-22. Epub 20040112. doi: 10.1359/JBMR.040111. PubMed PMID: 15005849.

43. Sinder BP, Eddy MM, Ominsky MS, Caird MS, Marini JC, Kozloff KM. Sclerostin antibody improves skeletal parameters in a Brtl/+ mouse model of osteogenesis imperfecta. J Bone Miner Res. 2013;28(1):73-80. Epub 2012/07/28. doi: 10.1002/jbmr.1717. PubMed PMID: 22836659; PMCID: PMC3524379.

44. Sinder BP, Salemi JD, Ominsky MS, Caird MS, Marini JC, Kozloff KM. Rapidly growing Brtl/+ mouse model of osteogenesis imperfecta improves bone mass and strength with sclerostin antibody treatment. Bone. 2015;71:115-23. Epub 2014/12/03. doi: 10.1016/j.bone.2014.10.012. PubMed PMID: 25445450; PMCID: PMC4274252.

45. Sinder BP, White LE, Salemi JD, Ominsky MS, Caird MS, Marini JC, Kozloff KM. Adult Brtl/+ mouse model of osteogenesis imperfecta demonstrates anabolic response to sclerostin antibody treatment with increased bone mass and strength. Osteoporos Int. 2014;25(8):2097-107. Epub 2014/05/08. doi: 10.1007/s00198-014-2737-y. PubMed PMID: 24803333; PMCID: PMC4415164.

CHAPTER 2

The Role of Wnt Signaling in Age-Related Alveolar Bone Loss and Regeneration

Hsiao H Sung [1 2 3], Navya Chalamalasetty [2], Ali Alzainal [1], Hanlong Liu [1], Lexuan Wang [1], Pietra Colacrai Arikita [1], Ivy C X Wei [4], Hom-Lay Wang [5], M H J van den Bosch [3], Michelle S Caird [1], Peter M van der Kraan [3], Kenneth M Kozloff [1], Esmeralda Blaney Davidson [3]

[1.] Orthopaedic Research Laboratories, Department of Orthopaedic Surgery, University of Michigan, Ann Arbor, Michigan, USA.

[2.] Department of Oral and Maxillofacial Surgery, University of Michigan, Ann Arbor, Michigan, USA.

[3.] Experimental Rheumatology, Department of Rheumatology, Radboud University Medical Centre, Nijmegen, the Netherlands.

[4.] Department of Biologic and Materials Sciences & Prosthodontics, University of Michigan, Ann Arbor, Michigan, USA.

[5.] Department of Periodontics and Oral Medicine, University of Michigan, Ann Arbor, Michigan, USA.

J Periodontal Res. 2026 Mar;61(3):237-255. doi: 10.1111/jre.70085. Epub 2026 Feb 4.

Abstract

The periodontium is a uniquely dynamic tissue system requiring precise signaling for lifelong adaptation. The canonical Wnt/β-catenin pathway is a master regulator of bone homeostasis; however, its role in the specialized environment of the alveolar bone-marked by rapid turnover, complex mechanical forces, and exposure to the oral microbiome-remains incompletely understood, particularly in the context of aging. This review critically synthesizes evidence on Wnt signaling in alveolar bone remodeling, with a focus on age-related dysregulation, contrasting established paradigms from long bone biology with emerging oral-tissue-specific data. Wnt/β-catenin signaling is essential for periodontal homeostasis, orchestrating osteoblastogenesis and mechanotransduction. Its activity is compartment-specific within the periodontium and is potently suppressed in pathology. Key mechanisms of age-related decline include the upregulation of Wnt antagonists (e.g., sclerostin, DKK1), cellular senescence, altered FoxO-Wnt crosstalk under oxidative stress, and impaired mechanosensing. These changes converge to disrupt regenerative capacity, tipping the balance toward net alveolar bone loss. Therapeutically, sclerostin inhibition demonstrates robust preclinical efficacy in rescuing bone loss in models of periodontitis and estrogen deficiency. However, the potential cardiovascular risks of systemic Wnt activation suggest that redirecting efforts toward localized delivery strategies could be a promising alternative. Aging induces a multifaceted suppression of regenerative Wnt signaling in the periodontium. Modulating the Wnt pathway shows great potential for oral bone regeneration. However, significant challenges exist, especially in designing local delivery systems that are both safe and effective. Overcoming these hurdles is crucial for successful clinical applications. Future research must bridge the gap between skeletal biology and direct oral-specific investigations to enable targeted therapies that preserve periodontal health in an aging population.

Key Points

The integrity of the periodontium, a uniquely dynamic and mechanically stressed tissue system, is fundamentally governed by Wnt/β-catenin signaling, which orchestrates alveolar bone homeostasis and adaptation. Aging induces a multifaceted decline in this regenerative pathway, driven by the upregulation of antagonists like sclerostin, the accumulation of senescent cells, and the blunting of essential mechanosensory functions. This age-related suppression of Wnt signaling converges with local inflammatory pathology, such as periodontitis, to shift the periodontal balance toward irreversible bone loss. While targeted inhibition of Wnt antagonists demonstrates robust preclinical potential for regenerating alveolar

bone, the translation of this promise into safe clinical reality is challenged by the cardiovascular risks of systemic therapy, underscoring an urgent need for localized delivery strategies and dedicated research to bridge foundational skeletal biology with the unique demands of the oral environment.

Keywords: Wnt signaling; aging; alveolar bone; periodontium.

Graphical Abstract

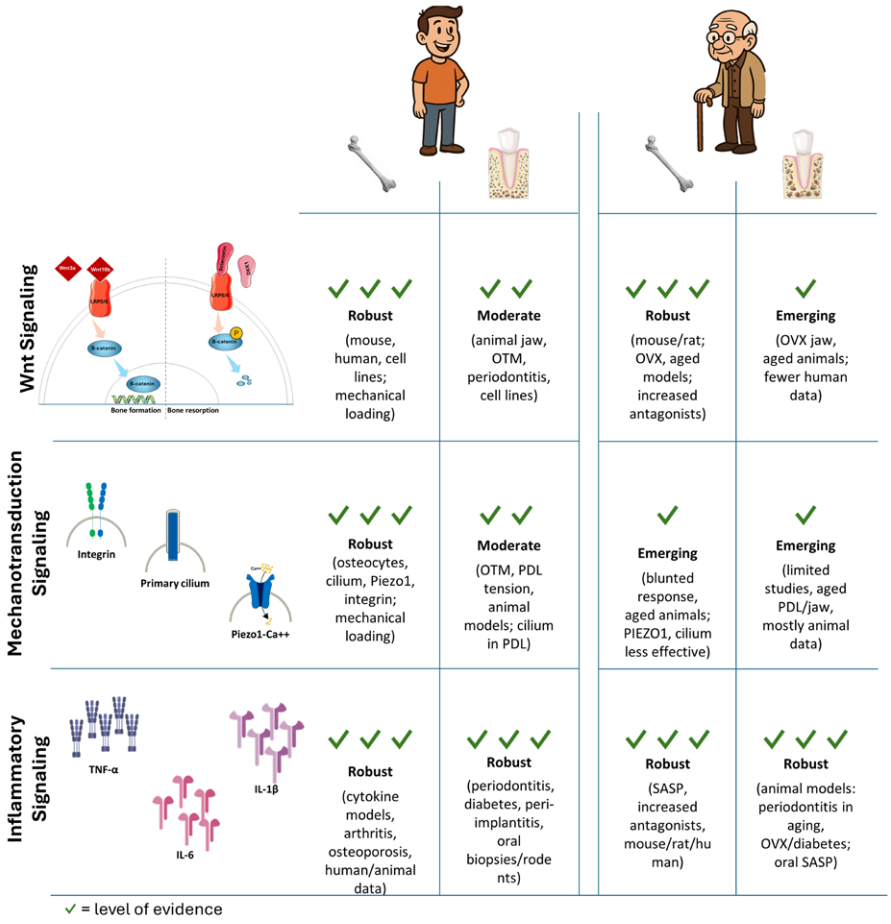

Introduction

The periodontium constitutes a dynamic, integrated tissue complex essential for oral function, comprising alveolar bone, periodontal ligament (PDL), cementum, and gingiva. Through lifelong, coordinated remodeling, this system maintains tooth anchorage and adapts to mechanical forces, environmental exposures, and injury[1-3].

The Wnt signaling pathway is a master regulator of bone formation and resorption in both systemic and oral environments[4, 5]. However, our foundational understanding of Wnt biology, and of bone adaptation more broadly, has been driven predominantly by research in long bones, where it orchestrates osteoblast activity, mechanotransduction, and fracture repair[6-8]. The periodontium presents a fundamentally distinct ecological niche: characterized by rapid turnover rates[9, 10], complex multidirectional mechanical stimuli[11, 12], and tissues that are continuously exposed to the oral microbiome and inflammatory challenges[13, 14]. Consequently, the direct extrapolation of molecular mechanisms and therapeutic strategies from the appendicular skeleton to the oral cavity is fraught with challenge and requires rigorous, tissue-specific validation.

Aging critically disrupts the homeostatic equilibrium of this specialized system. Systemic hallmarks of aging, including declines in stem cell function, Wnt signaling efficacy, and bone quality, combine with local risk factors, such as malocclusion and periodontitis, to disrupt normal regenerative responses and tip the balance toward net bone loss[6, 7, 15, 16]. Clinically, these changes manifest as increased tooth mobility, diminished masticatory function, and heightened vulnerability to oral disease in older adults[14]. The periodontium thus represents a critical, and vulnerable, interface where systemic aging and local pathology intersect.

Emerging research in periodontal biology now highlights the need for targeted investigation into canonical and non-canonical Wnt pathways, local antagonists like sclerostin and Dickkopf-related protein 1 (DKK1), and regenerative strategies tailored to the periodontium itself[17-21]. While therapeutic advances inspired by osteoporosis management offer promising approaches for dental and periodontal conditions, significant translational hurdles remain. These include fragmented direct evidence from oral tissues, safety concerns with systemic therapy, technical barriers to local delivery, and a limited number of clinical trials specific to the oral environment.

This review critically synthesizes current evidence on the role of Wnt signaling within the periodontium, with a focused emphasis on alveolar bone remodeling and its

dysregulation with age. By deliberately contrasting established paradigms from long bone biology with emerging, direct data from oral tissues, we aim to 1) clarify tissue-specific regulatory mechanisms, 2) illuminate critical translational gaps, and 3) propose a refined roadmap for future Wnt-targeted therapeutic innovation. Advancing this field is essential not only for preserving oral health, but also for improving systemic health and quality of life in aging populations (Table 1 and 2).

Table 1. Age-Related Alveolar Bone Loss: Pathophysiological Cascade and Wnt Signaling Dysregulation

Factor	Effect of Aging	Wnt Pathway Role & Mechanism
Bone Quantity & Quality	Bone mineral density, height, and width decrease; trabecular structure weakens.	Aging reduces canonical Wnt signaling → decreased osteoblast-driven bone formation and compromised maintenance.
Osteoblast Function	Number and activity decline; differentiation and regenerative capacity diminish.	Wnt/β-catenin is a key promoter of osteoblast differentiation and activity; this pro-formation signal is dampened with age.
Osteoclast Activity	Resorptive activity often increases, shifting remodeling balance toward net loss.	Reduced Wnt signaling lowers OPG and increases RANKL expression → favors increased osteoclastogenesis and bone resorption.
PDL & Extracellular Matrix (ECM)	PDL space narrows; collagen integrity declines; tissue loses elasticity.	Impaired Wnt signaling and reduced DEL-1 expression compromise PDL fibroblast function and ECM repair/ regeneration.
Local Inflammatory Milieu ("Inflammaging")	Chronic, low-grade inflammation increases pro-resorptive cytokines (e.g., TNF-α, IL-1β, IL-6).	Inflammatory cytokines upregulate secreted Wnt inhibitors (DKK1, sclerostin) → further suppress bone formation.
Key Molecular Shift	↑ Expression of DKK1, sclerostin, SHN3; ↓ Expression of Klotho.	DKK1 & sclerostin directly inhibit Wnt/ β-catenin signaling; SHN3 promotes sclerostin; Klotho decline removes a protective Wnt-enhancing effect.
Tissue Repair & Regeneration Capacity	Healing after extraction, periodontal defect, or implant placement is slower and less predictable.	Exogenous Wnt activation (e.g., L-WNT3A) or neutralization of inhibitors (e.g., sclerostin antibody) can rescue bone healing in aged models.
Therapeutic Implication	Age-related bone loss requires targeted intervention to restore anabolic signaling.	Strategy: Antagonize endogenous inhibitors (anti-sclerostin/DKK1) or provide Wnt agonists to re-establish a pro-formative microenvironment.

Abbreviations: DKK1: Dickkopf-1; IL: interleukin; OPG: osteoprotegerin; PDL: periodontal ligament; RANKL: receptor activator of nuclear factor κB ligand; TNF-α: tumor necrosis factor-alpha.

Table 2. Sources of mechanistic evidence of Wnt signaling in the periodontium.

Mechanism/Pathway	Evidence Source	Direct/ Extrapolated
Canonical Wnt signaling in osteoblasts[1-3]	Long bone (mouse, human)	Extrapolated
Canonical Wnt/β-catenin in alveolar bone	Periodontium (rodent, human)	Direct
Sclerostin antagonism	Long bone; periodontium (rodent)	Both
Mechanotransduction (Piezo1, integrins, cilia)	Periodontium (rodent, cell lines)	Direct / Partial
Non-canonical Wnt signaling	Long bone; periodontium (rodent)	Both
FoxO–Wnt crosstalk	Long bone; emerging in periodontium	Extrapolated / Emerging
Senescence/SASP impact on Wnt	Long bone; periodontium (human, rodent)	Both

Note: This table summarizes the origins and types of mechanistic evidence underpinning current understanding of Wnt signaling pathways in the periodontium. Mechanisms are categorized by their biological context, indicating whether supporting data comes from long bone models, direct studies in periodontal tissues, or extrapolation.

Wnt Signaling and Periodontium

Periodontium: Alveolar Bone structure and remodeling

Alveolar bone is a core component of the periodontium, forming the tooth-supporting sockets within the jaws[22, 23]. Its intimate functional integration with the PDL results in one of the most dynamic osseous environments in the body, characterized by rapid turnover rates[24-26]. This high plasticity is enabled by a specialized, compartmentalized architecture designed for both force transmission and metabolic support.

Closest to the tooth root lies the *bundle bone*, a thin, specialized layer distinguished by the insertion of Sharpey's fibers from the PDL[1, 27, 28]. This interface plays a crucial role in mechanotransduction, allowing the bone to rapidly adapt to varying occlusal forces[1, 11, 12, 27, 29].

Beneath the bundle bone are the *cortical* and *trabecular* compartments, which provide essential structural reinforcement while serving as a metabolic reservoir to support continuous remodeling[22, 23, 30].

Through this integrated structure, the alveolar bone is equipped to translate mechanical signals into anabolic or catabolic responses, a defining feature that sets it apart from the long bones elsewhere in the skeleton[16, 23, 26, 31] (Figure 1).

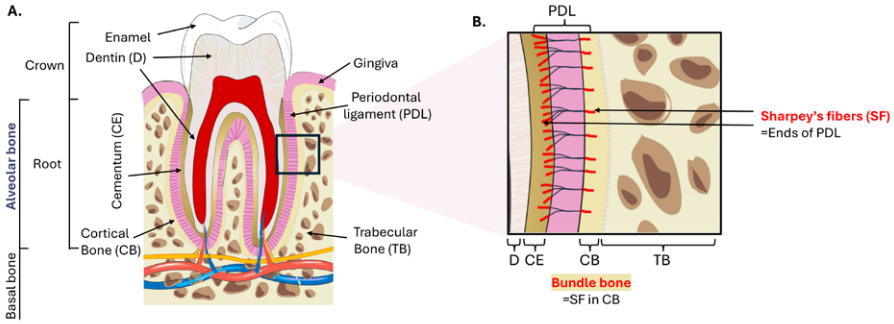

Figure 1. Alveolar bone structure: Alveolar bone is a specialized osseous tissue that forms the tooth sockets (alveoli) within the maxilla and mandible, providing structural support and anchorage for teeth. As part of the periodontium, it interacts dynamically with the gingiva, periodontal ligament (PDL), and cementum to maintain tooth position and masticatory function. Structurally, it comprises two key compartments: (A) the underlying cortical and trabecular bone, which provides structural reinforcement and metabolic support and (B) the bundle bone, which interfaces with the PDL via Sharpey's fibers and facilitates force transmission.

Core Canonical Wnt/β-catenin Signaling in the Periodontium

Bone homeostasis within the periodontium is governed by the canonical Wnt/β-catenin pathway, a mechanism conserved yet distinctly regulated in this environment. Activation begins when Wnt ligands (e.g., Wnt3a, Wnt10b) bind to Frizzled and LRP5/6 co-receptors, triggering phosphorylation of LRP5/6. This event inhibits a cytoplasmic destruction complex, comprising Axin, Adenomatous Polyposis Coli (APC), and Glycogen Synthase Kinase-3β (GSK-3β), that normally targets β-catenin for proteasomal degradation. Consequently, β-catenin accumulates, translocates to the nucleus, and partners with TCF/LEF transcription factors to drive the expression of osteogenic genes (Runx2, COL1A1) and production of Osteoprotegerin (OPG), which inhibits RANKL-mediated osteoclastogenesis[2, 4, 29, 32, 33].

While this core pathway is evolutionarily conserved, its regulation within the periodontium exhibits critical tissue-specific nuances. It is essential to note that foundational knowledge of the Wnt/β-catenin destruction complex, receptor activation, and downstream transcription is derived overwhelmingly from studies in long bones and cancer models. Direct validation of these precise molecular interactions within the unique cellular milieu of the periodontium—particularly in human tissues—remains an important, ongoing effort[16, 31].

Direct periodontal evidence confirms this pathway's central role. Mechanical stimulation from mastication rapidly activates canonical Wnt signaling in alveolar bone[25, 34, 35]. Furthermore, genetic ablation of the Wnt antagonist sclerostin leads to

excessive alveolar bone accumulation[36], while human biopsies from periodontitis patients show elevated levels of sclerostin and DKK1 in alveolar bone and PDL, correlating with bone loss severity[37, 38] (Figure 2).

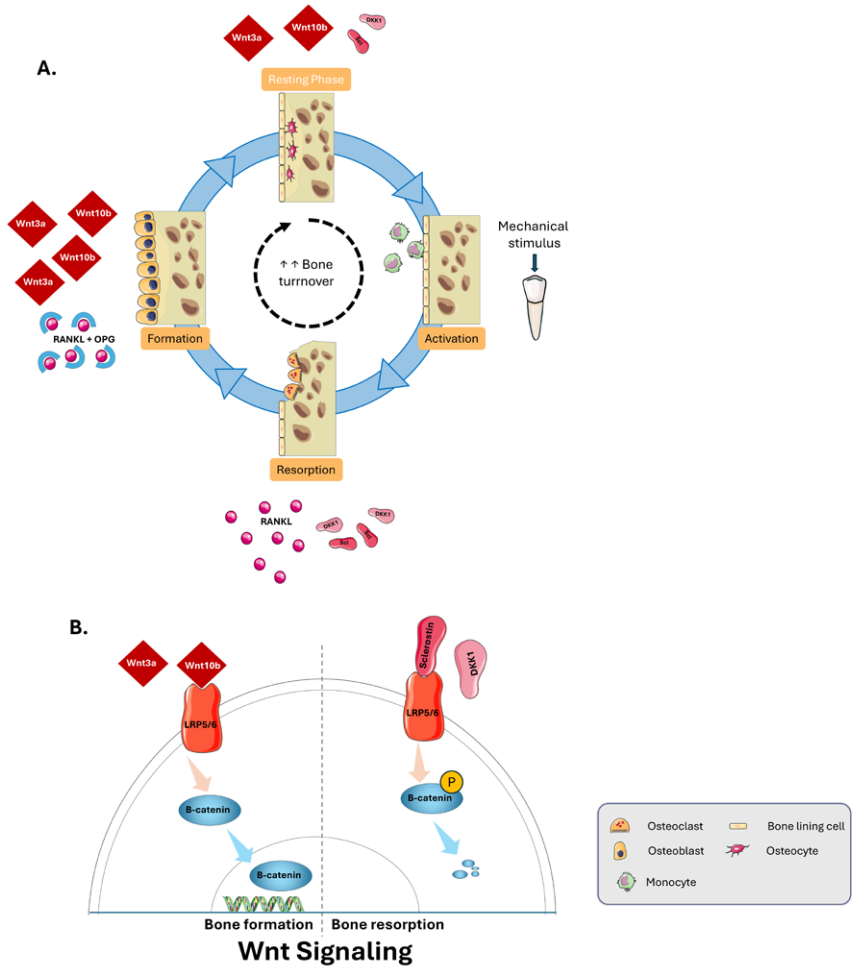

Figure 2. Wnt/β-catenin signaling regulates alveolar bone remodeling in response to mechanical stimuli. (A) Alveolar bone undergoes rapid and dynamic remodeling due to its specialized microstructure and sensitivity to mechanical forces. Mechanical stimulation activates Wnt signaling, with Wnt ligands (such as Wnt3a and Wnt10b) binding to Frizzled receptors and LRP5/6 co-receptors, thereby preventing degradation of β-catenin. (B) Stabilized β-catenin accumulates and translocate into the nucleus, where it promotes transcription of osteogenic genes, enhances osteoblast differentiation, and suppresses osteoclast activity. Conversely, Wnt signaling inhibitors such as sclerostin and Dkk1 bind to Frizzled and LRP5/6, leading to β-catenin phosphorylation and degradation. Overall, the Wnt/β-catenin pathway is central to maintaining alveolar bone homeostasis. It enables adaptive remodeling in response to mechanical (occlusal) forces, balancing bone formation and resorption and helping preserve periodontal integrity.

Wnt Activity Across Periodontal Compartments and Cell Types

The behavior of the Wnt signaling pathway within the periodontium is highly compartmentalized and cell-type specific. In the PDL, mechanical tension such as that exerted by orthodontic forces activates canonical Wnt signaling in fibroblasts and progenitor cells, thereby driving both osteogenic and cementogenic differentiation[39-41]. By contrast, exposure of the PDL to compressive loads or inflammatory stress markedly upregulates several Wnt antagonists, including sclerostin, DKK1, and sFRPs, which serves to suppress new tissue formation and instead promotes resorptive processes[42-45].

A similarly nuanced regulatory role for Wnt signaling exists within cementum. Acute Wnt pathway stimulation in cementoblasts enhances cementogenic gene expression, including genes such as CEMP1 and CAP, and promotes matrix deposition[46-48]. However, persistent Wnt activation, as seen in sclerostin (SOST) knockout mice, does not result in increased cementum thickness and may actually impair cementocyte function[36]. This highlights the necessity for a tightly controlled Wnt signaling environment within the cementum, a process likely governed by additional epigenetic regulators[49-51].

Wnt signaling and Mechanotransduction

Physiological mechanical forces are sensed by osteocytes and PDL fibroblasts via a specialized apparatus including integrins[27], Piezo1 ion channels[42], and primary cilia[52, 53]. In the periodontium, this sensing triggers a conserved anabolic cascade: loading downregulates Wnt antagonists (e.g., sclerostin)[29, 44] and stabilizes β-catenin. This leads to the proliferation and osteogenic differentiation of Wnt-responsive progenitors (e.g., Axin2+ cells), directly coupling force sensing to new bone formation at sites of tension[28, 54]. This process is synergized by the release of other osteogenic factors such as IGF-1 and BMPs[40, 55, 56].

This model provides a compelling, integrated view of periodontal mechanobiology. However, a significant portion of this cascade is inferred from analogous pathways in long bone osteocytes. Direct, real-time visualization of force-induced β-catenin stabilization and progenitor cell fate specification within the living periodontium is lacking. Furthermore, the relative contributions of integrin, Piezo1, and ciliary signaling in initiating this cascade in different periodontal cell types (osteocytes vs. PDL fibroblasts) are not yet resolved, representing a key knowledge gap for targeted therapeutic modulation (Figure 3).

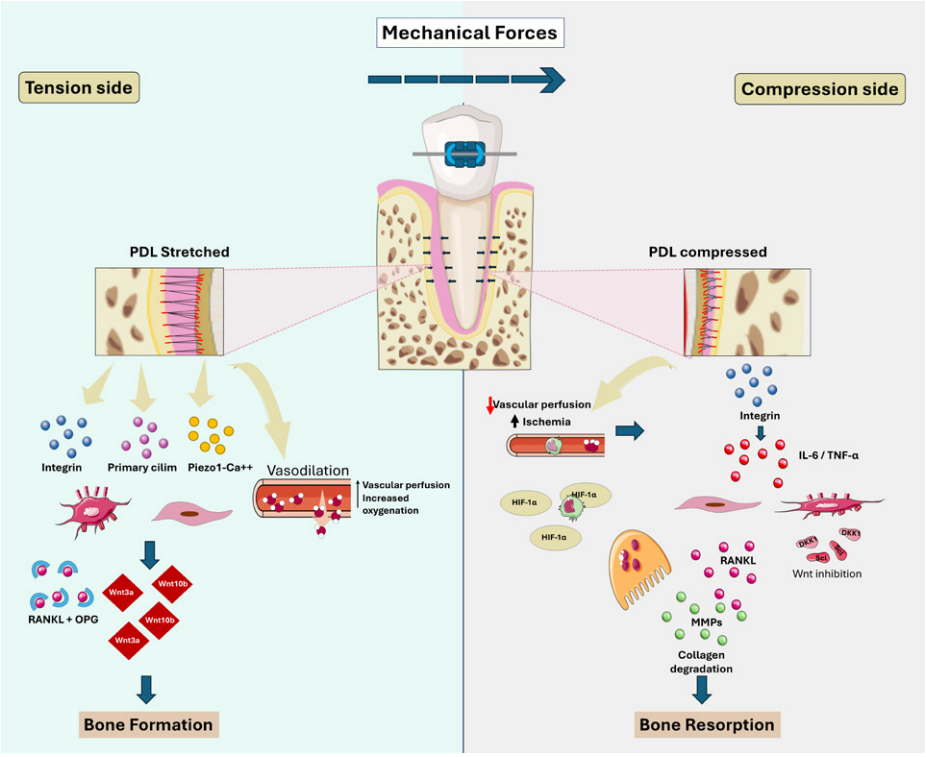

Figure 3. Mechanotransduction pathways in alveolar bone remodeling in an orthodontic tooth movement (OTM) model. Mechanical loading from occlusion or orthodontics creates strain and fluid shear stress that osteocytes detect through integrin signaling and primary cilia deflection, activating calcium and Wnt pathways. (A) In tension zones, PDL stretching triggers Piezo1/2 channel activation, improving blood flow and oxygen levels. This mechanical stimulation boosts Wnt/β-catenin signaling through Wnt3a/10b, stimulating bone formation while inhibiting bone resorption through RANKL suppression. (B) In compression zones, blood vessel squeezing causes hypoxia that stabilizes HIF-1α, increasing TNF-α and IL-6, RANKL and decreasing OPG production. Osteocytes release Wnt blockers (DKK1, sclerostin), allowing osteoclast development. This spatial control of Wnt signaling - activated in tension areas and blocked in compression areas - coordinates tooth movement while protecting the surrounding bone structure.

Pathological Disruption of Regenerative Wnt Signaling

Mechanical Overload

When mechanical stress becomes excessive or chronic (e.g., occlusal trauma, poorly controlled orthodontic forces), the adaptive Wnt response is subverted. Overload induces hypoxia (HIF-1α stabilization)[57, 58] and upregulates Wnt antagonists like sclerostin and DKK1[44, 45, 59], actively suppressing canonical signaling. This shifts the RANKL/OPG balance toward resorption, uncoupling bone turnover and leading to clinical outcomes such as widened PDL spaces and progressive alveolar bone loss[13].

Inflammatory Suppression (e.g., Periodontitis)

Chronic inflammation represents a potent and clinically significant disruptor. Inflammatory cytokines (TNF-α, IL-6) drive a marked upregulation of Wnt antagonists, including sclerostin, DKK1, and sFRP1, within both the PDL and alveolar bone[38]. The severity of this upregulation in human periodontitis correlates directly with clinical attachment loss and radiographic bone loss[38]. Critically, this pathway is therapeutically targetable: genetic deletion or antibody-mediated neutralization of Sost rescues alveolar bone loss in experimental periodontitis, including in challenging conditions like type 2 diabetes[21, 33], establishing a definitive proof-of-principle.

Pathway Crosstalk and Complexity

Pathological breakdown is exacerbated by signaling crosstalk. For instance, NF-κB activation in inflammatory contexts (e.g., apical periodontitis) actively suppresses the Wnt/β-catenin cascade[60]. Regenerative feedback mechanisms exist, such as exosomes from gingival mesenchymal stem cells that can deliver signals inhibiting NF-κB while concurrently activating Wnt signaling[61]. Non-canonical pathways also modulate the disease process, with elevated Wnt-5a in gingival crevicular fluid correlating with inflammatory and osteoclastogenic activity in periodontitis[62].

Implications for Peri-Implantitis

The pathological principles of inflammatory Wnt suppression extend to the bone surrounding dental implants, where the dysregulated host-microbiome interface is a key driver of disease[63]. Peri-implantitis, a biofilm-associated inflammatory disease leading to implant-supporting bone loss, shares etiological features with periodontitis but is characterized by a more aggressive inflammatory response and rapid bone destruction.

Emerging molecular profiling reveals that the peri-implant tissue microenvironment is fundamentally altered. RNA-seq analyses demonstrate significant age-related dysregulation in key pathways, including depressed Wnt signaling alongside heightened immune and inflammatory activity in aged mice compared to young controls[64]. In human disease, this manifests as significant immune dysregulation, including distinct macrophage polarization profiles that contribute to a pro-inflammatory, pro-osteoclastogenic state in peri-implantitis lesions[65].

Within this pathological milieu, it is highly plausible that the potent upregulation of Wnt antagonists (e.g., sclerostin, DKK1) observed in periodontitis also occurs, actively suppressing the osteogenic repair necessary to maintain the bone-implant interface. This represents a critical translational frontier. While direct

evidence linking specific Wnt antagonist levels to peri-implantitis progression is still accruing, proof-of-concept exists: sclerostin antibody treatment can enhance osseointegration in compromised bone[20]. The central, clinically significant question remains whether therapeutic local Wnt pathway activation can subvert the inflammatory suppression of bone formation and stabilize bone around ailing implants—a hypothesis now supported by mechanistic extrapolation and early molecular profiling[63-65], but awaiting targeted interventional validation.

Alveolar Bone Regeneration After Tooth Extraction

The specific role of Wnt signaling in extraction socket healing, a process of intramembranous ossification distinct from long bone fracture repair, remains an active area of investigation with limited direct evidence[66]. Preliminary findings suggest involvement: periodontal ligament stem cells (PDLSCs) contribute to socket healing[66], and local Wnt pathway modulation (e.g., sclerostin inhibition) can enhance bone formation in animal models, particularly in aged or estrogen-deficient states[15, 19]. However, stem cell behavior is complex and context-dependent. While key progenitor populations (Gli1+, Lepr+) are present[67-70], they can adopt pathogenic states; for example, Lepr+ stromal cells in periodontitis can attenuate repair via CCRL2-mediated Wnt inhibition[70]. Dedicated research is needed to clarify the precise regulation of Wnt-responsive stem cells during alveolar socket regeneration (Table 3).

Table 3. Key Wnt antagonists and agonists in oral biology.

Molecule	Cell Source	Role in Periodontium	Effect of Aging	Therapeutic Modulation
Sclerostin	Osteocytes, some PDL cells	Inhibits Wnt/β-catenin; suppresses bone formation	Upregulated	Antibody (Scl-Ab) neutralization rescues bone loss
DKK1	Osteocytes, fibroblasts	Inhibits Wnt signaling	Upregulated	Dual antibody under development
Wnt3a, Wnt10b	Osteoblast-lineage cells	Activates canonical pathway	Diminished expression	Recombinant protein (experimental)
Wnt5a, Wnt11	Multiple (inflammatory cells, fibroblasts)	Modulates non-canonical signaling, inflammation, cementum repair	Increased in disease	Potential small-molecule modulators
sFRP1	Fibroblasts, bone cells	Downregulates canonical pathway	Upregulated	Not clinically targeted

Note: Overview of major Wnt signaling molecules implicated in periodontal bone biology, including their cellular sources, roles within the periodontium, changes associated with aging, and current or potential avenues for therapeutic modulation.

Wnt signaling and Aging

Aging is a dynamic driver of tissue dysfunction, actively altering the responsiveness of cells within the components of the periodontium. The adaptability of these tissues depends on the coordinated activity of Wnt signaling networks, which respond to mechanical forces and inflammatory challenges[4, 35]. However, with advancing age, this regulatory machinery is progressively compromised. This manifests as impaired mechanotransduction[6], increased expression of Wnt antagonists like sclerostin[29, 71], and an exacerbated inflammatory response that further suppresses regenerative signaling[14, 38]. Below, we clarify mechanisms established through direct studies of the periodontium and those extrapolated from research in other bones (primarily long bone models), highlighting the similarities and unique features pertinent to oral health (Figure 4).

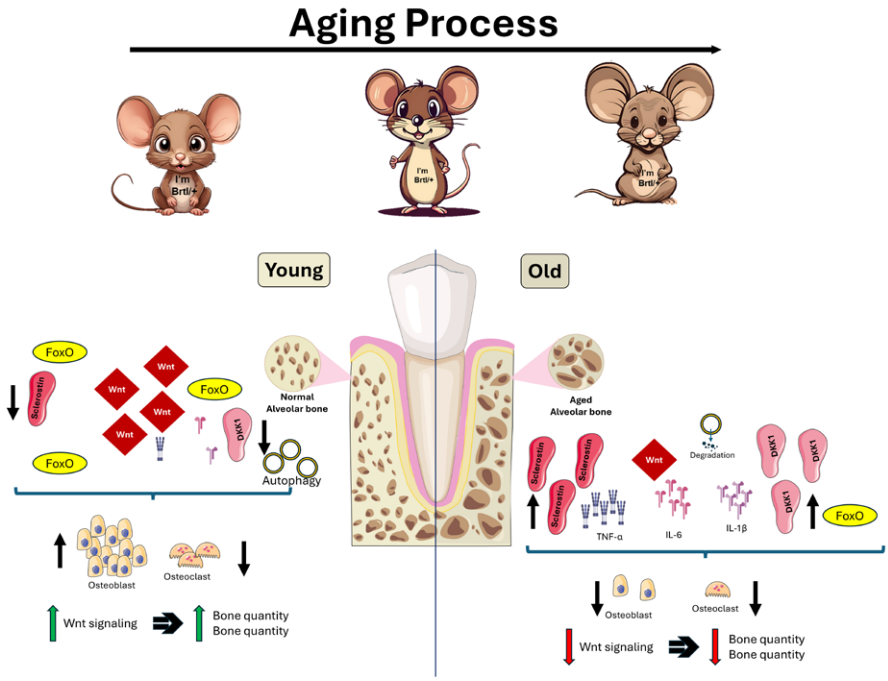

Figure 4. Age-related dysregulation of alveolar bone homeostasis. The left panel depicts a healthy, young alveolar bone unit characterized by robust, homeostatic remodeling. Active osteoblasts, supported by functional osteocytes and efficient autophagy, respond to anabolic signals including potent canonical Wnt/β-catenin activity. The right panel illustrates the aged alveolar bone microenvironment, where regenerative capacity is suppressed by a convergence of mechanisms. These include osteoblast dysfunction, cellular senescence with a pro-inflammatory secretory phenotype (elevating TNF-α, IL-6, IL-1β), and the potent inhibition of Wnt signaling via upregulated antagonists (sclerostin, DKK1), oxidative stress-induced diversion of β-catenin to FoxO transcription factors. Concomitant declines in autophagic clearance further exacerbate cellular stress. Collectively, these changes shift the RANKL/OPG balance, promoting osteoclast activity and leading to net alveolar bone loss.

Canonical Wnt/β-catenin Signaling in Tissue Homeostasis and Aging

The principles of Wnt-mediated regeneration, while promising, must be considered within the context of the systemic biological decline that accompanies aging[4]. In young, healthy tissues, the canonical Wnt/β-catenin pathway orchestrates effective regeneration and repair. However, with advancing age, this same signaling pathway becomes fundamentally dysregulated.

Much of our understanding of age-related impairment in Wnt signaling comes from research on long bones such as the femur and tibia. In these tissues, aging is known to disrupt skeletal homeostasis largely through changes in the canonical Wnt/β-catenin signaling pathway. For instance, mechanical loading robustly activates Wnt signaling and promotes bone formation in younger individuals. As bones age, however, their mechanotransduction capacity diminishes[6, 9]. This reduced responsiveness is attributed primarily to increased secretion of Wnt antagonists, namely sclerostin and DKK1, by osteocytes, which actively suppress the osteogenic Wnt signal[7, 45, 71]. In addition to altered signaling, aged bone marrow stromal cells shift toward adipogenesis rather than osteogenesis, a transition driven by declining β-catenin activity[7, 10]. Collectively, these changes create a systemic environment characterized by reduced anabolic capacity and increased skeletal fragility.

Recent studies demonstrate that many of these mechanisms are mirrored in oral tissues, providing direct evidence that the long bone findings are applicable within a periodontal context. For example, similar to what is observed in long bones, aged alveolar bone within the periodontium exhibits impaired activation of Wnt signaling in response to mechanical loading[6]. This deficit correlates with a failure to properly downregulate sclerostin, resulting in insufficient bone regeneration. Moreover, the expression of sclerostin in aged periodontal tissues is significantly elevated, paralleling the pattern seen in aging long bones[29, 71]. Systemic increases in sclerostin further contribute to bone loss in both skeletal sites, highlighting a shared endocrine-like mechanism of age-related bone degeneration[71].

Adding to this complexity, aging exacerbates inflammatory and resorptive responses in the periodontium[14]., fostering a local environment that further antagonizes regenerative Wnt signaling—an effect similar to that observed in chronic inflammatory conditions affecting bone[38]. Additionally, recent discoveries have identified dysfunctional stem cell populations, such as pathogenic Lepr+ stromal cells, within aged periodontal tissues. These cells disrupt Wnt signaling and impede tissue repair, providing a cellular basis for the impaired regeneration seen in the aging periodontium[70].

Non-Canonical Wnt Signaling (PCP and Ca^{2+} Pathways) in Aging Tissues

Non-canonical Wnt ligands (e.g., Wnt5a, Wnt11) are crucial regulators of cell migration, tissue polarity, and inflammatory responses. Their activity becomes particularly significant in the dysfunctional cellular environment of aged bone, which is characterized by altered osteoblast/osteoclast activity and increased porosity[72, 73]. In this context, inflammatory cytokines like TNF-α can elevate non-canonical signaling. Wnt5a plays a dual role: it is essential for coordinating osteoclast-osteoblast coupling and maintaining bone formation[74], yet its dysregulation is also implicated in age-related stem cell dysfunction[75]. This establishes a core principle from systemic biology: precise regulation of non-canonical Wnt pathways is critical for skeletal homeostasis, and its disruption is a hallmark of aging.

Translating these mechanisms to oral tissues, emerging evidence confirms that non-canonical Wnt signaling is relevant in periodontal aging and pathology. Chronic inflammation from periodontitis elevates WNT-5a levels in gingival crevicular fluid, paralleling increased local inflammation and osteoclast activity[62]. Inflammatory upregulation of Wnt5a can block cementogenic differentiation of periodontal cells, further hindering repair. Interestingly, certain non-canonical Wnt pathways might also offer protection; for example, Wnt4 can inhibit NF-κB–mediated inflammation in bone, raising the possibility of similar benefits in oral tissues.

Yet, many questions remain unanswered. What roles do ligands like Wnt11 and Wnt16 play in the aging of alveolar bone, PDL, and cementum? How do mechanical forces, which are a defining feature of the oral environment, modulate PCP and Ca^{2+} pathways in aged tissues? And is the protective effect of Wnt4 observed in long bones also present in oral tissues? Addressing these gaps will be essential for developing therapies that harness non-canonical Wnt signaling to preserve periodontal health in an aging population.

Crosstalk with Forkhead box O (FoxO) Transcription Factors: Integrating Metabolism and Oxidative Stress Response in aging

FoxO transcription factors play a central role in balancing cellular stress resistance and regenerative ability, an equilibrium that becomes increasingly disrupted with age. In long bones, rising oxidative stress is a major cause of bone loss[76]. Under these conditions, β-catenin shifts from its canonical role with TCF/LEF to partnering with FoxO proteins, prioritizing antioxidant defenses at the expense of bone-forming gene programs[76]. Though this adaptation initially protects cells, chronic FoxO activation ultimately suppresses Wnt signaling and slows bone formation[77]. This effect occurs via mechanisms like β-catenin sequestration[78] and CBP-mediated

acetylation of FOXO4[79]. Over time, FoxO overactivity contributes to age-related bone decline—a process independent of, but worsened by, sex steroid deficiency[80]. Thus, in long bones, the drive for stress survival directly undermines tissue regeneration.

In oral tissues, evidence for FoxO–Wnt crosstalk is just beginning to surface. The periodontium's unique microenvironment, marked by constant inflammatory and metabolic stress from the oral microbiome[14], suggests this signaling axis could be highly relevant locally. Systemic factors may also influence outcomes; for example, parathyroid hormone (PTH) can lower oxidative stress and promote bone formation in aging long bones[81], hinting at ways to restore FoxO–Wnt balance. Early studies show that the FoxO–Wnt interaction shapes the trade-off between resilience and regeneration in oral tissues, with FoxO1 playing varying roles in young and aged models[82].

However, important questions remain. What specific functions do FoxO isoforms (FoxO1, 3a, 4) have in periodontal cells such as osteocytes, ligament stem cells, and cementoblasts? Can anabolic therapies like PTH or Sclerostin antibody also modulate the FoxO–Wnt axis in the periodontium? How do broader aging pathways—such as declines in sirtuin 1 (Sirt1) activity[78] affect FoxO–Wnt signaling in oral tissues?

Clarifying these mechanisms is crucial for future therapies. Strategies such as modulating FoxO acetylation or combining FoxO-targeted approaches with other bone anabolic agents may help rebalance this signaling axis, ultimately enhancing resilience and regeneration of alveolar bone and periodontal tissues as we age.

Wnt Signaling, Cellular Senescence, and Senescence-Associated Inflammation

Research on long bones has established that the accumulation of senescent cells is a hallmark of skeletal aging and a major contributor to osteoporosis[83, 84]. Senescent osteocytes and bone marrow stromal cells develop a robust senescence-associated secretory phenotype (SASP), which fosters a pro-inflammatory and tissue-destructive microenvironment, ultimately weakening bone structure and increasing fragility[85]. Central to this process is the interplay with Wnt signaling: a decline in pro-regenerative Wnt ligands such as Wnt3a is required for mesenchymal stem cells to enter senescence[86], while an increase in certain Wnts, notably Wnt16, can drive osteoblasts toward senescence[87]. Thus, there is a bidirectional relationship, Wnt pathway activity governs cellular senescence, and senescent cells, through their SASP, secrete factors that further suppress Wnt signaling. Interventions targeting this axis, whether by clearing senescent cells (senolytics)[88], or modulating oxidative stress with agents like Astaxanthin or Pyrroloquinoline Quinone[89, 90], have shown

efficacy in mitigating bone loss in aging models, validating this pathway as a therapeutic target in systemic skeletal aging.

Emerging research indicates that this senescence-inflammation–Wnt suppression cycle is also present in oral tissues, but with unique features tied to the periodontal environment. Periodontitis-induced chronic inflammation exposes cells to continuously high levels of cytokines such as TNF-α, IL-1β, and IL-6, which intensify inflammatory responses and promote alveolar bone resorption[14]. This persistent inflammatory milieu favors cellular senescence in the periodontium. Experimental studies parallel findings from long bones: inflamed human periodontal tissues exhibit elevated levels of the Wnt antagonists DKK1 and sclerostin, and these correlate with the severity of clinical bone loss[38]. Importantly, inhibition of sclerostin either genetically or using antibodies, can rescue alveolar bone in animal models of periodontitis[33, 38], confirming the pathogenic role of Wnt suppression. Additionally, non-canonical Wnt signaling contributes to oral tissue inflammation; for example, Wnt4 can dampen bone inflammation by inhibiting NF-κ[91], while its disruption is linked to occlusal trauma[92]. Elevated Wnt5a is also associated specifically with inflammatory periodontitis.

While the "Senescence → SASP → Wnt Suppression → Impaired Regeneration" cycle is well-defined in long bone biology, the oral cavity is exposed to constant microbial and mechanical stresses, likely accelerating both senescence and Wnt pathway inhibition. The unique oral microenvironment, shaped by polymicrobial biofilm and dynamic mechanical loading, may hasten the progression of this pathogenic cycle, making it particularly challenging for periodontal tissues to maintain regenerative capacity. Thus, therapeutically targeting this multiple-hit pathway, whether through senolytics[88], inhibition of Wnt antagonists such as sclerostin[21, 33], or activation of protective Wnt signaling (e.g., Wnt4)[91], holds strong promise for rejuvenating the aged and inflamed periodontium.

Despite these advances, critical questions remain unanswered. How do different subtypes of senolytics interact with Wnt signaling within distinct periodontal niches? What roles do non-canonical Wnt ligands play in modulating or mitigating senescence-induced inflammation in the periodontium? Can senolytic or Wnt-based therapies developed for long bone disease be adapted to the unique microenvironmental challenges of the oral cavity, and if so, how do we optimize their efficacy?

Autophagy, Mitochondrial Dysfunction, and Wnt Signaling in Aging

Long bone studies offer crucial insights into the cellular mechanisms underlying bone maintenance and aging. Robust autophagy and mitochondrial function

within osteoblast lineage cells are essential for preserving bone mass and strength. Elevating autophagy, such as through genetic upregulation of TFEB—results in increased bone mass[93, 94], whereas suppressing autophagy in osteocytes causes a skeletal phenotype that mimics aging[95, 96]. Mitochondrial health is equally important; oxidative stress or reduced autophagy in osteoblasts impairs the bone's ability to respond to mechanical forces, recapitulating age-related decline[97]. Furthermore, in disease contexts, autophagy can negatively regulate Wnt signaling and its suppression can drive inflammatory bone resorption[98]. Mitochondrial dysfunction is also a key mediator in systemic diseases such as Leigh syndrome, contributing to osteoporosis and fragile bone[99, 100]. These findings establish autophagy and mitochondrial health as key, cell-intrinsic requirements for bone formation, adaptation, and resistance to inflammatory and metabolic stress.

Recent research indicates that similar cellular pathways are relevant in oral tissues but manifest in distinct, site-specific ways. In the periodontium, diabetes is known to worsen periodontitis by promoting mitochondrial dysfunction[101], and infection with P. gingivalis directly triggers mitochondrial fragmentation and dysfunction in host cells[102]. Unlike long bones, the oral environment's unique exposure to microbial biofilms and frequent inflammation means impaired autophagy and mitochondrial failure are likely common and may converge to suppress regenerative Wnt signaling, compromising alveolar bone and PDL maintenance. Studies also show that mitochondrial quality governs the differentiation of dental stem cells, and its failure potentially impairs oral tissue repair[99]. Non-canonical crosstalk has been observed where autophagy and mitochondrial dysfunction interact with inflammatory and Wnt pathways, further aggravating periodontal breakdown[98, 101].

Given the parallels seen in cellular stress responses, the foundational knowledge from long bone biology strongly informs hypotheses for oral tissues. However, direct studies in the periodontium remain limited, and major questions persist: How does autophagic flux specifically affect Wnt signaling in human periodontal ligament stem cells or cementoblasts? Can interventions that activate TFEB or protect mitochondria rescue periodontal cell function under inflammatory conditions? Would regimens that combine a Wnt activator (like sclerostin antibody) with an autophagy inducer offer synergistic benefits for periodontal regeneration?

Mechanosensing Dysfunction: Impaired Wnt Response in the Aged Periodontal Complex

Mechanotransduction, the conversion of mechanical forces into cellular signals, is essential for maintaining bone integrity throughout life. Pivotal research in long

bones has demonstrated that aging impairs mechanotransduction by diminishing the activation of Wnt signaling in response to mechanical loading[6] and reducing the transcriptional responsiveness of bone cells to force[9]. As a result, these deficits are recognized as key contributors to age-related systemic bone loss[71], setting a precedent for the study of mechanotransduction in other tissues, such as the periodontium.

Building lessons from skeletal biology, direct research in oral tissues has identified PIEZO1 as a principal mechanosensor in periodontal health and disease. PIEZO1 is necessary for force-driven alveolar bone remodeling via Wnt signaling in PDL cells[42], supports tension-induced osteogenic differentiation in PDL stem cells[103], and controls the balance between proliferation and mineralization in human cementoblasts[104]. Experimental findings also show that activating PIEZO1 can safeguard against periodontitis exacerbated by traumatic occlusion[105]. Remarkably, PIEZO1's impact varies by cell type and context: in osteoclasts, it protects against inflammatory bone loss through a mechanism independent of Ca^{2+} signaling[106]. Collectively, these observations establish PIEZO1 as a pivotal regulator of adaptation, remodeling, and inflammation in periodontal tissues.

While the principle that mechanosensing capacity declines with age is established in long bones, it remains unclear how aging affects PIEZO1-mediated mechano-transduction in the periodontium. Does PIEZO1's expression, sensitivity, or cell-type specific protective functions decrease with age, potentially contributing to periodontal fragility? Is the anti-inflammatory, bone-protective role of osteoclastic PIEZO1 compromised in older individuals, accelerating bone loss in periodontitis? Does anabolic signaling through PIEZO1 in PDL stem cells become uncoupled as tissues age? The constant mechanical and inflammatory stresses unique to the oral cavity may place exceptional demands on this network, making its age-related degradation a probable factor in periodontal breakdown.

Systemic Influences: Sex Hormones and Their Interaction with Wnt in Aging

Sex hormones, such as estrogen is essential for maintaining bone health, largely by regulating the Wnt signaling pathway. In long bones, these hormones promote bone formation and strength through several coordinated mechanisms. Estrogen increases Wnt activity in osteoblasts and suppresses Wnt inhibitors like sclerostin, supporting bone-building processes[107]. Crucially, estrogen receptors and Wnt/β-catenin signaling work together to encourage osteogenic differentiation of mesenchymal progenitor cells[107]. Androgens also boost Wnt activity, further enhancing the environment for bone growth. This synergy between sex hormones and Wnt signaling is a cornerstone of skeletal endocrinology.

As individuals age, hormone levels, especially estrogen, decline, most notably after menopause. This hormonal shift disrupts the balance with Wnt signaling, leading to weaker bone formation and increased bone resorption[71, 108]. As a result, bone metabolism tips toward loss, making osteoporosis more likely. Long bone research has defined the molecular details: reduced estrogen not only diminishes Wnt signaling but also increases expression of Wnt antagonists such as sclerostin and DKK1, which suppress the activity of osteoblasts and contribute to bone mass erosion[71]. Notably, some Wnt-mediated protective effects, particularly those involving Wnt16, remain active even without estrogen[109], highlighting the complexity of the regulatory system. Furthermore, reduced estrogen impairs the bone's ability to activate Wnt signaling in response to mechanical loading[108]. Therapeutically, targeting these molecular interactions has shown promise. For example, using antibodies to block sclerostin can restore Wnt pathway activity and reverse hormone-related bone loss in animal models and clinical trials, confirming that Wnt activation can effectively compensate for declining sex hormones[110-112].

Recent research provides direct evidence for these hormonal and molecular mechanisms in the oral cavity. In rodent models simulating menopause through ovariectomy, estrogen deficiency sharply accelerates alveolar bone loss by suppressing Wnt pathway activity and promoting bone resorption[113, 114]. This effect is compounded by increased production of local Wnt antagonists and pro-resorptive cytokines[14], mirroring the mechanisms seen in long bones. Importantly, targeted therapies that modulate Wnt signaling have been shown to be effective in the oral context: for example, antibody-mediated inhibition of sclerostin corrects alveolar bone loss in models of ovariectomized rats or type 2 diabetic periodontitis[21, 115] and enhances socket repair after estrogen withdrawal in rats[19]. These findings directly affirm that reversing Wnt suppression can support oral bone regeneration in hormonally compromised situations. Additionally, systemic rises in sclerostin remain associated with age-related and estrogen withdrawal-related bone loss in the periodontium[71].

Despite strong mechanistic parallels, emerging evidence confirms that the molecular landscape in the craniofacial bone is distinct from that of long bones. Site-specific differences in osteoblast phenotype, mechanical loading response, and estrogen receptor-related gene expression have been documented[116]. These insights show the need for continued oral-specific research, rather than simple extrapolation from skeletal models, to define the precise regulation of Wnt and related pathways in the aging craniofacial bone.

Wnt-Targeted Therapeutic Strategies for Alveolar Bone Regeneration

The Wnt/β-catenin signaling pathway is essential for skeletal homeostasis and tissue regeneration. Its dysregulation drives age-related bone loss, making it a prime target for intervention in both systemic osteoporosis and oral bone health. Therapeutic strategies now range from FDA-approved systemic approaches to innovative experimental treatments focused on localized oral regeneration.

FDA-Approved Systemic Therapy

Sclerostin antibody (SclAb), clinically known as Romosozumab, is a monoclonal antibody developed to neutralize sclerostin, a potent and secreted inhibitor of canonical Wnt signaling, a central regulator of bone formation[4]. Sclerostin, produced by osteocytes, binds LRP5/6 co-receptors on osteoblasts and blocks Wnt ligands from activating the signaling cascade required for β-catenin stabilization and osteogenic gene expression[4, 29]. This action provides a physiological brake on bone mass formation. However, in aging and chronic inflammation, sclerostin levels rise, systemically[71] and locally in inflamed periodontal tissues[28], contributing to suppressed bone regeneration. SclAb restores Wnt activation, re-engaging osteoblast function, stimulating bone formation, and suppress resorption.

Clinically, Romosozumab is administered monthly via subcutaneous injection and is FDA-approved for up to 12 months in postmenopausal women at high fracture risk. It rapidly increases bone formation, reduces resorption, and achieves significant gains in bone mineral density, with up to 73% reduction in vertebral fracture risk compared to placebo[112].

The therapeutic potential of sclerostin inhibition extends to diverse models of bone disease and oral pathology. In rodent models of estrogen deficiency, SclAb restores alveolar bone mass and improves healing post-extraction[19]. In periodontitis models, both genetic deletion and antibody blockade of sclerostin rescue alveolar bone loss[17, 33]. In type 2 diabetic periodontitis, SclAb reverses severe bone loss[21]. SclAb also enhances alveolar bone quality and dental implant osseointegration in conditions such as osteoporosis, osteogenesis imperfecta, and X-linked hypophosphatemia[18, 20, 115, 117, 118], demonstrating its capacity to overcome multiple barriers to oral bone regeneration.

Studies using systemic administration of SclAb have reported increased bone mass even in wild-type mice, indicating that SclAb therapy has potential for bone augmentation in healthy individuals[20, 21, 115]. Preclinical models show that local administration of SclAb in alveolar bone defects leads to significant enhancement

of bone formation when delivered at sufficiently high concentrations, resulting in marked increases in bone volume and trabecular thickness. This targeted delivery method enables focused bone regeneration at specific defect sites and may help limit systemic side effects. However, the benefits are dose-dependent, as lower-dose local formulations have not provided meaningful improvements compared to controls[117, 119].

Despite its anabolic benefits, systemic romosozumab carries a black-box warning for increased major adverse cardiovascular events (MACE), as shown in the ARCH trial[120]. Sclerostin serves a protective role in vascular health, and its inhibition may promote arterial calcification and proliferation, raising cardiovascular risk[121, 122]. Consequently, systemic therapy is restricted to one year and only prescribed for patients without cardiovascular risk factors.

The evidence for local efficacy, coupled with systemic safety limitations, strongly supports the need for advanced localized SclAb delivery systems in oral medicine. However, it is important to note that local delivery has been assessed exclusively in preclinical animal studies; no clinical trials in humans have yet tested this approach. A significant challenge remains: the pharmacokinetics of locally administered SclAb, including its absorption, retention, and release profile within the oral environment, have not been fully characterized even in these animal studies. Technical obstacles such as rapid salivary clearance, masticatory forces, and microbial degradation further complicate sustained and controlled drug availability. Future progress will rely on engineered biomaterials that preserve biological integrity and ensure precise, site-specific activation. Combination protocols with anti-inflammatories or senolytics may further improve outcomes, especially in complex or aged tissues. Ultimately, the goal is to deliver potent local bone regeneration, as established in preclinical models, while thoroughly understanding and optimizing local pharmacokinetics to maximize efficacy and minimize risk—before considering human clinical application (Table 4).

Table 4. Comparative summary of modalities for alveolar bone regeneration.

Modality	Delivery Route	Clinical Evidence	Efficacy in Aging Models	Advantages	Limitations/Risks
Sclerostin Ab (Romosozumab)	Systemic/subcutaneous	FDA-approved (osteoporosis), preclinical oral	Proven in rodents (aged, estrogen-def.)	Potent anabolic, robust rescue	Cardiovascular risk, need for local delivery
Local Sclerostin Ab	Local/injectable/graft	Preclinical only	Effective in aged rodents	Enhanced targeting, reduced systemic risk	Uncharacterized PK/ delivery in oral tissues
DKK1 Ab	Systemic/experimental	Early stage	Potent in some models	Synergistic with Scl-Ab	No safety profile yet
BMP-2	Local/scaffold	FDA-approved (craniofacial)	Safe, effective	Well-established, osteoinductive	Limited efficacy in severe Wnt suppression, cost
EMD	Local/graft	FDA-cleared	Effective, long-term studies	Soft tissue & bone healing	Less effective in severe bone loss
MSC/exosome therapy	Local/scaffold	Preclinical	Promising	Immunomodulatory, less invasive	Experimental, unclear long-term outcomes

Note: Comparison of current and emerging therapeutic modalities for alveolar bone regeneration, detailing delivery routes, level of supporting clinical or preclinical evidence (including efficacy in aged models), main advantages, limitations and risks. This table facilitates an at-a-glance evaluation of the translational and clinical readiness of each approach.

Experimental Wnt Therapies: Dual Inhibitor Antibodies and Wnt Agonists

Building on the therapeutic principle of Wnt pathway activation, research is moving beyond single-target inhibition such as sclerostin or DKK1 alone, to multi-target strategies for greater efficacy. Notably, concurrent inhibition of both sclerostin and DKK1 in a rat model of alveolar bone loss more effectively preserves and augments bone volume compared to single-target approaches[123]. This establishes direct proof that dual antagonism of Wnt inhibitors may be superior for oral bone regeneration. Along these lines, newly developed bispecific antibodies that neutralize both sclerostin and DKK1 have shown synergistic osteogenic effects in systemic skeletal models, improving bone mass and fracture repair[124]. Mechanistically, this approach releases the full osteoanabolic potential of DKK1 inhibition that would otherwise be reduced by compensatory upregulation of sclerostin[125]. DKK1 blockade also shows efficacy in genetic bone fragility, such as osteogenesis imperfecta[126], broadening its therapeutic promise. Together, these findings support continued development of bispecific agents for complex oral bone defects.

Direct Wnt pathway agonism through recombinant Wnt proteins is a complementary frontier. Here, lipid-mediated stabilization technologies enable the delivery and efficacy of proteins such as Wnt3A for therapeutic use[127]. Liposomal Wnt3A (L-Wnt3A) formulations enhance in vivo stability and allow for precise local application. Studies show that these protein therapies can rejuvenate bone-forming capacity, even in autografts from aged animals[15], and accelerate healing in rodent injury models by activating Wnt-responsive osteoprogenitors. Regenerative potential is further increased when combined with biomaterial scaffolds. However, these protein-based strategies remain experimental; open questions remain regarding their durability in the oral environment, optimal biomaterial integration, and long-term safety before clinical use.

Mesenchymal Stem Cell (MSC) Therapies, including exosome-, scaffold-, or cell-based approaches, remain experimental for oral bone regeneration. Preclinical studies are promising, showing enhanced healing. Relevant to this review, exosomes derived from gingival MSCs have been shown to cross-regulate Wnt and NF-κB signaling in the periodontal inflammatory microenvironment[61], and direct application of a WNT protein therapeutic can improve bone formation in grafts from aged animals[15], providing proof-of-principle for Wnt-mediated regeneration.

Comparisons to Current Clinical Modalities

Wnt-targeted therapies must be considered alongside well-established clinical modalities, particularly bone morphogenetic protein-2 (BMP-2) and enamel matrix derivative (EMD).

BMP-2 is FDA-approved for certain craniofacial indications including sinus augmentation and ridge preservation. Its osteoinductive activity is intimately linked to the Wnt pathway, as BMP-2 facilitates osteoblast differentiation and mineralization through an autocrine Wnt loop[128]. Preclinically, BMP-2 incorporated into biomimetic grafts promotes periodontal and alveolar regeneration in large animal models[129, 130], and randomized clinical trials confirm rhBMP-2's efficacy in augmenting alveolar ridge volume in humans[131].

EMD is an FDA-cleared biologic derived from porcine tooth buds and widely used for periodontal regeneration. EMD supports soft tissue healing and modulates inflammation[132], in part by inducing growth factor and Wnt target gene expression. Clinically, combining EMD with bone grafts treats severe intrabony defects effectively[133], and EMD combined with guided tissue regeneration yields predictable outcomes[134]. Long-term studies indicate stable periodontal regeneration with EMD use over a decade[135].

Both BMP-2 and EMD are valued for their safety, accessibility, and ability to engage the patient's endogenous Wnt pathway. However, their efficacy can be diminished in patients with severely suppressed Wnt signaling—a hallmark of advanced age, diabetes, or metabolic disease, where Wnt antagonists like sclerostin are elevated. In these contexts, direct Wnt pathway activation via sclerostin-neutralizing antibodies has demonstrated robust preclinical efficacy in models of diabetic and osteoporotic periodontitis[19, 21]. Therefore, while BMP-2 and EMD remain clinical mainstays, next-generation Wnt-targeted strategies are poised to overcome age-related regenerative deficits, potentially enabling future combination or sequential therapeutic paradigms.

Future Perspectives and Research Directions in Wnt signaling /aging

Despite dramatic advances in our understanding of Wnt signaling and its role in skeletal aging, there remain substantial limitations and knowledge gaps when it comes to the craniofacial complex and oral tissues. Much of today's mechanistic insight into Wnt comes from long bone studies, but the periodontium—composed of the alveolar bone, PDL, and cementum—offers a more dynamic microenvironment, exposed to unique mechanical, inflammatory, and microbial stresses. Direct research focusing on Wnt signaling in these oral tissues is still in its infancy, making extrapolation from systemic skeletal models an interim solution with inherent shortcomings.

One key limitation is the incomplete mapping of Wnt-responsive cell populations within the periodontium. While recent work has identified populations such as

Gli1-positive and Lepr-positive cells, the full diversity of stem/progenitor groups, their fate decisions, and their responses to aging remain unresolved. Additionally, mechanosensing pathways—like those involving PIEZO1 channels and integrins—are increasingly recognized as pivotal in translating chewing forces into cellular regenerative signals via Wnt, yet how aging alters these sensors and their downstream effects is poorly understood in oral tissues compared to the femur or tibia. Does the aged periodontium lose its ability to "sense" and respond to force, and if so, by what cellular and molecular mechanisms?

Crosstalk with inflammatory pathways further complicates the landscape. Chronic oral inflammation, often driven by lifelong exposure to microbial biofilms, intensifies Wnt suppression via antagonists like sclerostin and DKK1. The precise molecular mechanisms by which inflammatory and senescent processes inhibit Wnt-mediated regeneration in aged oral tissues are not fully delineated. Non-canonical Wnt ligands (such as Wnt5a, Wnt11, and Wnt16) also play underexplored roles in modulating immune responses and cell polarity in the periodontium, presenting intriguing but poorly defined therapeutic targets.

Therapeutic translation encounters its own set of challenges. While systemic sclerostin antibody (romosozumab) is effective for osteoporosis, its cardiovascular risks limit long-term use. Local delivery of Wnt-targeted drugs in the oral cavity is promising but unproven: How do these agents behave in a saliva-rich, mechanically active environment, and can they maintain stability and efficacy within aged tissue? Preclinical models suggest potent results, but clinical studies, especially in older human populations, are almost nonexistent.

Senescence—the progressive decline in cell renewal capacity—is another frontier where oral research lags behind skeletal biology. The "vicious cycle" of senescence-associated inflammation promoting Wnt suppression (and vice versa) is established in long bones but remains largely hypothetical in the periodontium. Moreover, whether emerging interventions like senolytics or autophagy enhancers can rejuvenate aged periodontal tissue through Wnt pathway modulation is a tantalizing but unanswered question.

Finally, hormonal factors, particularly the decline of estrogen with age, are known to interact with Wnt signaling and accelerate bone loss. Rodent studies have shown parallels in oral bone, yet the nuances of hormone–Wnt interactions—and optimal therapies to counteract their decline—require much deeper exploration in clinical settings.

Looking ahead, the field faces an exciting challenge. There is a clear need for direct oral-specific research, employing advanced lineage tracing, single-cell profiling, and in vivo mechanotransduction studies in aged models. Novel drug delivery systems—perhaps using bioengineered scaffolds or hydrogels customized for periodontal tissues—must be developed and rigorously tested for efficacy and safety. Exploring combination therapies that integrate Wnt agonism, senolytic agents, autophagy enhancers, and hormone replacement could offer synergistic regenerative effects. Importantly, understanding how mechanical forces, chronic inflammation, and the oral microbiome interact with aging and Wnt signaling would allow for multi-pronged interventions targeting the root causes of periodontal decline.

Moreover, unraveling the roles of non-canonical Wnt ligands and mapping their specific effects across different cell types of the periodontium may reveal overlooked protective mechanisms or novel targets for therapy. Lastly, translating preclinical successes to human trials, especially those focused on older, medically complex patients, will be critical to achieve tangible improvements in oral regenerative medicine (table 5).

Table 5. Knowledge gaps and future research directions in periodontal Wnt signaling.

Knowledge Gap	Clinical Relevance	Suggested Research Direction	Potential Impact
Aging effect on PIEZO1 and mechanosensors	Explains failed adaptation in elders	In vivo imaging, single-cell analysis in aging models	More effective mechano-based therapies
Fate & function of Wnt-responsive stem cells (Gli1+, Lepr+)	Targeting regeneration after injury/extraction	Lineage tracing, molecular profiling in aged/human tissues	Development of targeted regeneration strategies
Local vs. systemic pharmacokinetics of Wnt modulators	Safety, efficacy, side-effects	PK/PD studies, biomaterial release optimization	Safer, targeted local therapies
Non-canonical Wnt roles in inflammation, cementum repair	Precision therapies for periodontitis/peri-implantitis	Direct tissue-level mechanistic studies, new modulators	Better outcomes in oral inflammatory diseases
Effect of metabolic disease (diabetes) on Wnt therapy response	Higher risk population, poor outcomes	Integrated metabolic/Wnt modulation research	Broader therapy applicability
Combination therapy (Wnt agonism + senolytics/autophagy)	Addressing multi-pathway aging	Preclinical studies in aged, complex models	Synergistic, robust regeneration

Note: Critical areas where knowledge remains limited regarding Wnt biology and therapeutic modulation in the periodontium, paired with the direct clinical relevance of each gap. Suggested future research directions propose methodologies to address these uncertainties and outline the potential impact on clinical practice and patient outcomes.

Conclusion

Aging in the periodontium leads to profound shifts in tissue dynamics, with Wnt signaling at the heart of maintaining bone and ligament integrity. As age-related disruption of Wnt pathways drives periodontal degeneration, the consequences extend far beyond oral health, compromised periodontium exacerbates systemic diseases and worsens quality of life through pain, impaired function, and increased risk of tooth loss. Together, these insights reveal a strong clinical rationale for creating interventions that reactivate Wnt pathways and support periodontal regeneration in aging individuals. Innovative approaches targeting Wnt signaling offer promising solutions, providing not only the potential to preserve or restore dental support but also to improve overall health outcomes. Continued research focused on translating these findings into safe, effective clinical strategies is essential for enhancing well-being and longevity in the aging population.

References

1. H S. The periodontium. L OAV, editor. Berlin, Germany: Springer-Verlag; 1986.
2. Hlaing E, Ishihara Y, Odagaki N, Wang Z, Ikegame M, Kamioka H. The expression and regulation of Wnt1 in tooth movement-initiated mechanotransduction. Am J Orthod Dentofacial Orthop. 2020;158(6):e151-e60. Epub 20201101. doi: 10.1016/j.ajodo.2020.08.006. PubMed PMID: 33139146.
3. Li A, Thomas RZ, van der Sluis L, Tjakkes GH, Slot DE. Definitions used for a healthy periodontium-A systematic review. Int J Dent Hyg. 2020;18(4):327-43. Epub 20200524. doi: 10.1111/idh.12438. PubMed PMID: 32330350; PMCID: PMC7687205.
4. Duan P, Bonewald LF. The role of the wnt/beta-catenin signaling pathway in formation and maintenance of bone and teeth. Int J Biochem Cell Biol. 2016;77(Pt A):23-9. Epub 20160519. doi: 10.1016/j.biocel.2016.05.015. PubMed PMID: 27210503; PMCID: PMC4958569.
5. Tokavanich N, Wein MN, English JD, Ono N, Ono W. The Role of Wnt Signaling in Postnatal Tooth Root Development. Front Dent Med. 2021;2. Epub 20211112. doi: 10.3389/fdmed.2021.769134. PubMed PMID: 35782525; PMCID: PMC9248717.
6. Holguin N, Brodt MD, Silva MJ. Activation of Wnt Signaling by Mechanical Loading Is Impaired in the Bone of Old Mice. J Bone Miner Res. 2016;31(12):2215-26. Epub 20160907. doi: 10.1002/jbmr.2900. PubMed PMID: 27357062; PMCID: PMC5397287.
7. Rauner M, Sipos W, Pietschmann P. Age-dependent Wnt gene expression in bone and during the course of osteoblast differentiation. Age (Dordr). 2008;30(4):273-82. Epub 20080902. doi: 10.1007/s11357-008-9069-9. PubMed PMID: 19424851; PMCID: PMC2585653.
8. Zhong Z, Ethen NJ, Williams BO. WNT signaling in bone development and homeostasis. Wiley Interdiscip Rev Dev Biol. 2014;3(6):489-500. Epub 20140930. doi: 10.1002/wdev.159. PubMed PMID: 25270716; PMCID: PMC4199871.
9. Chermside-Scabbo CJ, Harris TL, Brodt MD, Braenne I, Zhang B, Farber CR, Silva MJ. Old Mice Have Less Transcriptional Activation But Similar Periosteal Cell Proliferation Compared to Young-Adult Mice in Response to in vivo Mechanical Loading. J Bone Miner Res. 2020;35(9):1751-64. Epub 20200601. doi: 10.1002/jbmr.4031. PubMed PMID: 32311160; PMCID: PMC7486279.
10. Galea GL, Meakin LB, Harris MA, Delisser PJ, Lanyon LE, Harris SE, Price JS. Old age and the associated impairment of bones' adaptation to loading are associated with transcriptomic changes in cellular metabolism, cell-matrix interactions and the cell cycle. Gene. 2017;599:36-52. Epub 20161110. doi: 10.1016/j.gene.2016.11.006. PubMed PMID: 27840164; PMCID: PMC5139832.
11. McCormack SW, Witzel U, Watson PJ, Fagan MJ, Groning F. Inclusion of periodontal ligament fibres in mandibular finite element models leads to an increase in alveolar bone strains. PLoS One. 2017;12(11):e0188707. Epub 20171130. doi: 10.1371/journal.pone.0188707. PubMed PMID: 29190785; PMCID: PMC5708643.
12. Zhong J, Shibata Y, Wu C, Watanabe C, Chen J, Zheng K, Hu J, Swain MV, Li Q. Functional non-uniformity of periodontal ligaments tunes mechanobiological stimuli across soft- and hard-tissue interfaces. Acta Biomater. 2023;170:240-9. Epub 20230825. doi: 10.1016/j.actbio.2023.08.047. PubMed PMID: 37634832.
13. Nakatsu S, Yoshinaga Y, Kuramoto A, Nagano F, Ichimura I, Oshino K, Yoshimura A, Yano Y, Hara Y. Occlusal trauma accelerates attachment loss at the onset of experimental periodontitis in rats. J Periodontal Res. 2014;49(3):314-22. Epub 20130701. doi: 10.1111/jre.12109. PubMed PMID: 23808820.
14. Song Y, Chung J. Aging Aggravates Periodontal Inflammatory Responses and Alveolar Bone Resorption by Porphyromonas gingivalis Infection. Curr Issues Mol Biol. 2023;45(8):6593-604. Epub 20230808. doi: 10.3390/cimb45080416. PubMed PMID: 37623235; PMCID: PMC10453897.

15. Chen T, Li J, Cordova LA, Liu B, Mouraret S, Sun Q, Salmon B, Helms J. A WNT protein therapeutic improves the bone-forming capacity of autografts from aged animals. Sci Rep. 2018;8(1):119. Epub 20180108. doi: 10.1038/s41598-017-18375-x. PubMed PMID: 29311710; PMCID: PMC5758817.

16. Mavropoulos A, Rizzoli R, Ammann P. Different responsiveness of alveolar and tibial bone to bone loss stimuli. J Bone Miner Res. 2007;22(3):403-10. Epub 2006/12/22. doi: 10.1359/jbmr.061208. PubMed PMID: 17181394.

17. Ahn H, Park W, Choi SH, Hong N, Huh J, Jung S. Effect of anti-sclerostin antibody on orthodontic tooth movement in ovariectomized rats. Prog Orthod. 2024;25(1):45. Epub 20241125. doi: 10.1186/s40510-024-00544-0. PubMed PMID: 39581932; PMCID: PMC11586325.

18. Carpenter KA, Alkhatib DO, Dulion BA, Guirado E, Patel S, Chen Y, George A, Ross RD. Sclerostin antibody improves alveolar bone quality in the Hyp mouse model of X-linked hypophosphatemia (XLH). Int J Oral Sci. 2023;15(1):47. Epub 20231010. doi: 10.1038/s41368-023-00252-1. PubMed PMID: 37813865; PMCID: PMC10562382.

19. Marcantonio CC, Perles GH, Lopes MES, Soares LFF, da Costa PI, Cerri PS, Cirelli JA. Influence of anti-sclerostin monoclonal antibody in the repair of post-extraction sockets of ovariectomized rats. Arch Oral Biol. 2024;162:105962. Epub 20240322. doi: 10.1016/j.archoralbio.2024.105962. PubMed PMID: 38569446.

20. Sung HH, Kwon HH, Stephan C, Reynolds SM, Dai Z, Van der Kraan PM, Caird MS, Blaney Davidson EN, Kozloff KM. Sclerostin antibody enhances implant osseointegration in bone with Col1a1 mutation. Bone. 2024;186:117167. Epub 20240613. doi: 10.1016/j.bone.2024.117167. PubMed PMID: 38876270; PMCID: PMC11243590.

21. Turkkahraman H, Flanagan S, Zhu T, Akel N, Marino S, Ortega-Gonzalez D, Yuan X, Bellido T. Sclerostin antibody corrects periodontal disease in type 2 diabetic mice. JCI Insight. 2024;9(16). Epub 20240718. doi: 10.1172/jci.insight.181940. PubMed PMID: 39171525; PMCID: PMC11343605.

22. Huja SS, Beck FM. Bone remodeling in maxilla, mandible, and femur of young dogs. Anat Rec (Hoboken). 2008;291(1):1-5. Epub 2007/12/19. doi: 10.1002/ar.20619. PubMed PMID: 18085627.

23. Randall LE, Beck FM, Huja SS. Bone remodeling surrounding primary teeth in skeletally immature dogs. Angle Orthod. 2011;81(6):931-7. Epub 20110601. doi: 10.2319/021611-114.1. PubMed PMID: 21631293; PMCID: PMC8903844.

24. Akintoye SO, Lam T, Shi S, Brahim J, Collins MT, Robey PG. Skeletal site-specific characterization of orofacial and iliac crest human bone marrow stromal cells in same individuals. Bone. 2006;38(6):758-68. Epub 20060103. doi: 10.1016/j.bone.2005.10.027. PubMed PMID: 16403496.

25. Tsuchida S, Nakayama T. Recent Clinical Treatment and Basic Research on the Alveolar Bone. Biomedicines. 2023;11(3). Epub 20230310. doi: 10.3390/biomedicines11030843. PubMed PMID: 36979821; PMCID: PMC10044990.

26. Wang JY, Huo L, Yu RQ, Rao NJ, Lu WW, Zheng LW. Skeletal Site-Specific Response of Jawbones and Long Bones to Surgical Interventions in Rats Treated with Zoledronic Acid. Biomed Res Int. 2019;2019:5138175. Epub 20191218. doi: 10.1155/2019/5138175. PubMed PMID: 31930124; PMCID: PMC6942746.

27. Barczyk M, Bolstad AI, Gullberg D. Role of integrins in the periodontal ligament: organizers and facilitators. Periodontol 2000. 2013;63(1):29-47. doi: 10.1111/prd.12027. PubMed PMID: 23931052; PMCID: PMC3791550.

28. Liang Y, Hu Z, Chang B, Liu X. Quantitative characterizations of the Sharpey's fibers of rat molars. J Periodontal Res. 2020;55(2):307-14. Epub 20191201. doi: 10.1111/jre.12716. PubMed PMID: 31788804; PMCID: PMC7082191.

29. Odagaki N, Ishihara Y, Wang Z, Ei Hsu Hlaing E, Nakamura M, Hoshijima M, Hayano S, Kawanabe N, Kamioka H. Role of Osteocyte-PDL Crosstalk in Tooth Movement via SOST/Sclerostin. J Dent Res. 2018;97(12):1374-82. Epub 20180604. doi: 10.1177/0022034518771331. PubMed PMID: 29863952.

30. Lee JH, Kim HJ, Yun JH. Three-dimensional microstructure of human alveolar trabecular bone: a micro-computed tomography study. J Periodontal Implant Sci. 2017;47(1):20-9. Epub 20170228. doi: 10.5051/jpis.2017.47.1.20. PubMed PMID: 28261521; PMCID: PMC5332332.

31. Son C, Choi MS, Park JC. Different Responsiveness of Alveolar Bone and Long Bone to Epithelial-Mesenchymal Interaction-Related Factor. JBMR Plus. 2020;4(8):e10382. Epub 2020/08/18. doi: 10.1002/jbm4.10382. PubMed PMID: 32803111; PMCID: PMC7422712.

32. Enomoto H, Shiojiri S, Hoshi K, Furuichi T, Fukuyama R, Yoshida CA, Kanatani N, Nakamura R, Mizuno A, Zanma A, Yano K, Yasuda H, Higashio K, Takada K, Komori T. Induction of osteoclast differentiation by Runx2 through receptor activator of nuclear factor-kappa B ligand (RANKL) and osteoprotegerin regulation and partial rescue of osteoclastogenesis in Runx2-/- mice by RANKL transgene. J Biol Chem. 2003;278(26):23971-7. Epub 20030415. doi: 10.1074/jbc.M302457200. PubMed PMID: 12697767.

33. Ren Y, Han X, Ho SP, Harris SE, Cao Z, Economides AN, Qin C, Ke H, Liu M, Feng JQ. Removal of SOST or blocking its product sclerostin rescues defects in the periodontitis mouse model. FASEB J. 2015;29(7):2702-11. Epub 20150310. doi: 10.1096/fj.14-265496. PubMed PMID: 25757567; PMCID: PMC4478802.

34. Kuroda S, Wazen R, Moffatt P, Tanaka E, Nanci A. Mechanical stress induces bone formation in the maxillary sinus in a short-term mouse model. Clin Oral Investig. 2013;17(1):131-7. Epub 20120229. doi: 10.1007/s00784-012-0686-4. PubMed PMID: 22373776.

35. Seddiqi H, Klein-Nulend J, Jin J. Osteocyte Mechanotransduction in Orthodontic Tooth Movement. Curr Osteoporos Rep. 2023;21(6):731-42. Epub 20231004. doi: 10.1007/s11914-023-00826-2. PubMed PMID: 37792246; PMCID: PMC10724326.

36. Phanrungsuwan A, Chavez MB, Eltilib LA, Kolli TN, Mohamed FF, Tan MH, Salmon CR, Nociti FH, Jr., Foster BL. Disparate effects of sclerostin deletion on alveolar bone and cellular cementum in mice. J Periodontol. 2025;96(1):82-96. Epub 20240716. doi: 10.1002/JPER.24-0025. PubMed PMID: 39012429; PMCID: PMC11735692.

37. Chatzopoulos GS, Jiang Z, Marka N, Wolff LF. Periodontal Disease, Tooth Loss, and Systemic Conditions: An Exploratory Study. Int Dent J. 2024;74(2):207-15. Epub 20231012. doi: 10.1016/j.identj.2023.08.002. PubMed PMID: 37833208; PMCID: PMC10988265.

38. Miranda TS, Napimoga MH, Feres M, Marins LM, da Cruz DF, da Silva HDP, Duarte PM. Antagonists of Wnt/beta-catenin signalling in the periodontitis associated with type 2 diabetes and smoking. J Clin Periodontol. 2018;45(3):293-302. Epub 20180112. doi: 10.1111/jcpe.12854. PubMed PMID: 29243300.

39. Li Y, Jacox LA, Little SH, Ko CC. Orthodontic tooth movement: The biology and clinical implications. Kaohsiung J Med Sci. 2018;34(4):207-14. Epub 20180203. doi: 10.1016/j.kjms.2018.01.007. PubMed PMID: 29655409.

40. Yu Y, Mu J, Fan Z, Lei G, Yan M, Wang S, Tang C, Wang Z, Yu J, Zhang G. Insulin-like growth factor 1 enhances the proliferation and osteogenic differentiation of human periodontal ligament stem cells via ERK and JNK MAPK pathways. Histochem Cell Biol. 2012;137(4):513-25. Epub 20120107. doi: 10.1007/s00418-011-0908-x. PubMed PMID: 22227802.

41. Ziegler N, Alonso A, Steinberg T, Woodnutt D, Kohl A, Mussig E, Schulz S, Tomakidi P. Mechano-transduction in periodontal ligament cells identifies activated states of MAP-kinases p42/44 and p38-stress kinase as a mechanism for MMP-13 expression. BMC Cell Biol. 2010;11:10. Epub 20100128. doi: 10.1186/1471-2121-11-10. PubMed PMID: 20109185; PMCID: PMC2824740.

42. Jiang Y, Guan Y, Lan Y, Chen S, Li T, Zou S, Hu Z, Ye Q. Mechanosensitive Piezo1 in Periodontal Ligament Cells Promotes Alveolar Bone Remodeling During Orthodontic Tooth Movement. Front Physiol. 2021;12:767136. Epub 20211122. doi: 10.3389/fphys.2021.767136. PubMed PMID: 34880779; PMCID: PMC8645976.

43. Rizk M, Niederau C, Florea A, Kiessling F, Morgenroth A, Mottaghy FM, Schneider RK, Wolf M, Craveiro RB. Periodontal ligament and alveolar bone remodeling during long orthodontic tooth movement analyzed by a novel user-independent 3D-methodology. Sci Rep. 2023;13(1):19919. Epub 20231114. doi: 10.1038/s41598-023-47386-0. PubMed PMID: 37964111; PMCID: PMC10646115.

44. Shu R, Bai D, Sheu T, He Y, Yang X, Xue C, He Y, Zhao M, Han X. Sclerostin Promotes Bone Remodeling in the Process of Tooth Movement. PLoS One. 2017;12(1):e0167312. Epub 20170112. doi: 10.1371/journal.pone.0167312. PubMed PMID: 28081119; PMCID: PMC5230762.

45. Tu X, Rhee Y, Condon KW, Bivi N, Allen MR, Dwyer D, Stolina M, Turner CH, Robling AG, Plotkin LI, Bellido T. Sost downregulation and local Wnt signaling are required for the osteogenic response to mechanical loading. Bone. 2012;50(1):209-17. Epub 20111030. doi: 10.1016/j.bone.2011.10.025. PubMed PMID: 22075208; PMCID: PMC3246572.

46. Cheng D, Yuan X, Ma Z, Lin X, Zhu Z, Wang J, Zhang C, Wang Y, Zhou J, Wang S, Hu L. Canonical Wnt Pathway Enhanced Dental Pulp Mesenchymal Stem Cells-Mediated Cementum Regeneration. J Oral Rehabil. 2025;52(10):1571-82. Epub 20250514. doi: 10.1111/joor.14001. PubMed PMID: 40369784.

47. Nottmeier C, Liao N, Simon A, Decker MG, Luther J, Schweizer M, Yorgan T, Kaucka M, Bockamp E, Kahl-Nieke B, Amling M, Schinke T, Petersen J, Koehne T. Wnt1 Promotes Cementum and Alveolar Bone Growth in a Time-Dependent Manner. J Dent Res. 2021;100(13):1501-9. Epub 20210519. doi: 10.1177/00220345211012386. PubMed PMID: 34009051; PMCID: PMC8649456.

48. Ono Y, Kaku M, Thant L, Iwama H, Arai M, Mizukoshi M, Dobashi A, Kitami M, Taketo MM, Ohazama A, Saito I, Uoshima K. Wnt/beta-catenin Promotes Cementum Apposition in Periodontal Regeneration. J Dent Res. 2025;104(2):183-92. Epub 20241125. doi: 10.1177/00220345241286490. PubMed PMID: 39586793; PMCID: PMC11752650.

49. Ding Y, Luan J, Malmstrom HS, Luan X, Diekwisch TGH. Mir-27 Promotes Periodontal Regeneration via Osteogenesis/Angiogenesis. J Dent Res. 2025:220345251366279. Epub 20251016. doi: 10.1177/00220345251366279. PubMed PMID: 41102998.

50. Ma L, Li M, Xuan G, Dai Y. METTL14-mediated m6A RNA methylation promotes the osteogenic differentiation of pPDLSCs by regulating WNT3A. Odontology. 2025;113(4):1701-11. Epub 20250418. doi: 10.1007/s10266-025-01097-2. PubMed PMID: 40249476.

51. Tan D, Li Q, Chen Z, Zhang H, Rao P, Li J, Tao Q, Xiao J, Song J. YTHDC1 Modulates the Osteogenic Capacity of hPDLSCs via Wnt/beta-Catenin Signalling Pathway for the Treatment of Bone Defects in Osteoporosis Rats. Cell Prolif. 2025;58(8):e70020. Epub 20250317. doi: 10.1111/cpr.70020. PubMed PMID: 40097906; PMCID: PMC12336452.

52. Chang PE, Li S, Kim HY, Lee DJ, Choi YJ, Jung HS. BBS7-SHH Signaling Activity Regulates Primary Cilia for Periodontal Homeostasis. Front Cell Dev Biol. 2021;9:796274. Epub 20211207. doi: 10.3389/fcell.2021.796274. PubMed PMID: 34957122; PMCID: PMC8703258.

53. Hampl M, Cela P, Szabo-Rogers HL, Kunova Bosakova M, Dosedelova H, Krejci P, Buchtova M. Role of Primary Cilia in Odontogenesis. J Dent Res. 2017;96(9):965-74. Epub 20170612. doi: 10.1177/0022034517713688. PubMed PMID: 28605602; PMCID: PMC5524235.

54. Wang K, Xu C, Xie X, Jing Y, Chen PJ, Yadav S, Wang Z, Taylor RW, Wang J, Feng JQ. Axin2+ PDL Cells Directly Contribute to New Alveolar Bone Formation in Response to Orthodontic Tension Force. J Dent Res. 2022;101(6):695-703. Epub 20220109. doi: 10.1177/00220345211062585. PubMed PMID: 35001706; PMCID: PMC9124907.

55. Grgurevic L, Novak R, Salai G, Trkulja V, Hamzic LF, Popovic VZ, Bozic D. Identification of bone morphogenetic protein 4 in the saliva after the placement of fixed orthodontic appliance. Prog Orthod. 2021;22(1):19. Epub 20210712. doi: 10.1186/s40510-021-00364-6. PubMed PMID: 34250561; PMCID: PMC8273045.

56. Wang M, Fan J, Wang A, Jin X, Zhang Z, Hu X, Liu L, Zhao Y, Li Y. Effect of local application of bone morphogenetic protein -2 on experimental tooth movement and biological remodeling in rats. Front Physiol. 2023;14:1111857. Epub 20230418. doi: 10.3389/fphys.2023.1111857. PubMed PMID: 37143931; PMCID: PMC10151543.

57. Narasimhan S, Al Kawas S, Shetty SR, Al-Daghestani HS, Samsudin R. Impact of hypoxia on alveolar bone dynamics and remodeling. Heliyon. 2024;10(23):e40868. Epub 20241202. doi: 10.1016/j.heliyon.2024.e40868. PubMed PMID: 39717576; PMCID: PMC11664270.

58. Ploysongsang K, Kobayashi Y, Lu Y, Niki Y, Chavanavesh J, Moriyama K. The effects of systemic and sustained hypoxia on orthodontic tooth movement in rats. Sci Rep. 2025;15(1):21468. Epub 20250701. doi: 10.1038/s41598-025-07949-9. PubMed PMID: 40594863; PMCID: PMC12219902.

59. Morse A, Ko FC, McDonald MM, Lee LR, Schindeler A, van der Meulen MCH, Little DG. Increased anabolic bone response in Dkk1 KO mice following tibial compressive loading. Bone. 2020;131:115054. Epub 20190912. doi: 10.1016/j.bone.2019.115054. PubMed PMID: 31521827.

60. Guan X, He Y, Wei Z, Shi C, Li Y, Zhao R, Pan L, Han Y, Hou T, Yang J. Crosstalk between Wnt/beta-catenin signaling and NF-kappaB signaling contributes to apical periodontitis. Int Immunopharmacol. 2021;98:107843. Epub 20210619. doi: 10.1016/j.intimp.2021.107843. PubMed PMID: 34153668.

61. Hu Y, Wang Z, Fan C, Gao P, Wang W, Xie Y, Xu Q. Human gingival mesenchymal stem cell-derived exosomes cross-regulate the Wnt/beta-catenin and NF-kappaB signalling pathways in the periodontal inflammation microenvironment. J Clin Periodontol. 2023;50(6):796-806. Epub 20230305. doi: 10.1111/jcpe.13798. PubMed PMID: 36843393.

62. Kornsuthisopon C, Chansaenroj A, Manokawinchoke J, Tompkins KA, Pirarat N, Osathanon T. Non-canonical Wnt signaling participates in Jagged1-induced osteo/odontogenic differentiation in human dental pulp stem cells. Sci Rep. 2022;12(1):7583. Epub 20220509. doi: 10.1038/s41598-022-11596-9. PubMed PMID: 35534526; PMCID: PMC9085777.

63. Alves CH, Russi KL, Rocha NC, Bastos F, Darrieux M, Parisotto TM, Girardello R. Host-microbiome interactions regarding peri-implantitis and dental implant loss. J Transl Med. 2022;20(1):425. Epub 20220923. doi: 10.1186/s12967-022-03636-9. PubMed PMID: 36138430; PMCID: PMC9502891.

64. Turajane K, Ji G, Chinenov Y, Chao M, Ayturk U, Suhardi VJ, Greenblatt MB, Ivashkiv LB, Bostrom MP, Yang X. RNA-seq Analysis of Peri-Implant Tissue Shows Differences in Immune, Notch, Wnt, and Angiogenesis Pathways in Aged Versus Young Mice. JBMR Plus. 2021;5(11):e10535. Epub 20210909. doi: 10.1002/jbm4.10535. PubMed PMID: 34761143; PMCID: PMC8567488.

65. Li Y, Li X, Guo D, Meng L, Feng X, Zhang Y, Pan S. Immune dysregulation and macrophage polarization in peri-implantitis. Front Bioeng Biotechnol. 2024;12:1291880. Epub 20240129. doi: 10.3389/fbioe.2024.1291880. PubMed PMID: 38347915; PMCID: PMC10859439.

66. Ulm C, Strbac GD, Stavropoulos A, Esfandeyari A, Dobsak T, Bertl K. Improved access to the bone marrow space by multiple perforations of the alveolar bundle bone after tooth extraction-A case report. Clin Exp Dent Res. 2022;8(1):3-8. Epub 20210723. doi: 10.1002/cre2.474. PubMed PMID: 34296542; PMCID: PMC8874110.

67. Fan Y, Lyu P, Bi R, Cui C, Xu R, Rosen CJ, Yuan Q, Zhou C. Creating an atlas of the bone microenvironment during oral inflammatory-related bone disease using single-cell profiling. Elife. 2023;12. Epub 20230201. doi: 10.7554/eLife.82537. PubMed PMID: 36722472; PMCID: PMC9925051.

68. Hosoya A, Shalehin N, Takebe H, Fujii S, Seki Y, Mizoguchi T, Shimo T, Iijima M, Irie K. Stem cell properties of Gli1-positive cells in the periodontal ligament. J Oral Biosci. 2020;62(4):299-305. Epub 20200831. doi: 10.1016/j.job.2020.08.002. PubMed PMID: 32882366.

69. Zhang D, Lin W, Jiang S, Deng P, Liu L, Wang Q, Sheng R, Shu HS, Wang L, Zou W, Zhou BO, Jing J, Ye L, Yu B, Zhang S, Yuan Q. Lepr-Expressing PDLSCs Contribute to Periodontal Homeostasis and Respond to Mechanical Force by Piezo1. Adv Sci (Weinh). 2023;10(29):e2303291. Epub 20230808. doi: 10.1002/advs.202303291. PubMed PMID: 37553778; PMCID: PMC10582421.

70. Chen Y, Weng Y, Huang J, Li Q, Sun B, Wang H, Wang Z. Leptin receptor (+) stromal cells respond to periodontitis and attenuate alveolar bone repair via CCRL2-mediated Wnt inhibition. J Bone Miner Res. 2024;39(5):611-26. doi: 10.1093/jbmr/zjae036. PubMed PMID: 38477792.

71. Todd H, Galea GL, Meakin LB, Delisser PJ, Lanyon LE, Windahl SH, Price JS. Wnt16 Is Associated with Age-Related Bone Loss and Estrogen Withdrawal in Murine Bone. PLoS One. 2015;10(10):e0140260. Epub 20151009. doi: 10.1371/journal.pone.0140260. PubMed PMID: 26451596; PMCID: PMC4599960.

72. Piemontese M, Almeida M, Robling AG, Kim HN, Xiong J, Thostenson JD, Weinstein RS, Manolagas SC, O'Brien CA, Jilka RL. Old age causes de novo intracortical bone remodeling and porosity in mice. JCI Insight. 2017;2(17). Epub 20170907. doi: 10.1172/jci.insight.93771. PubMed PMID: 28878136; PMCID: PMC5621920.

73. Becerikli M, Jaurich H, Schira J, Schulte M, Dobele C, Wallner C, Abraham S, Wagner JM, Dadras M, Kneser U, Lehnhardt M, Behr B. Age-dependent alterations in osteoblast and osteoclast activity in human cancellous bone. J Cell Mol Med. 2017;21(11):2773-81. Epub 20170426. doi: 10.1111/jcmm.13192. PubMed PMID: 28444839; PMCID: PMC5661248.

74. Roberts JL, Liu G, Paglia DN, Kinter CW, Fernandes LM, Lorenzo J, Hansen MF, Arif A, Drissi H. Deletion of Wnt5a in osteoclasts results in bone loss through decreased bone formation. Ann N Y Acad Sci. 2020;1463(1):45-59. Epub 20200109. doi: 10.1111/nyas.14293. PubMed PMID: 31919867.

75. Tiwari RL, Mishra P, Martin N, George NO, Sakk V, Soller K, Nalapareddy K, Nattamai K, Scharffetter-Kochanek K, Florian MC, Geiger H. A Wnt5a-Cdc42 axis controls aging and rejuvenation of hair-follicle stem cells. Aging (Albany NY). 2021;13(4):4778-93. Epub 20210225. doi: 10.18632/aging.202694. PubMed PMID: 33629967; PMCID: PMC7950224.

76. Almeida M, Han L, Martin-Millan M, Plotkin LI, Stewart SA, Roberson PK, Kousteni S, O'Brien CA, Bellido T, Parfitt AM, Weinstein RS, Jilka RL, Manolagas SC. Skeletal involution by age-associated oxidative stress and its acceleration by loss of sex steroids. J Biol Chem. 2007;282(37):27285-97. Epub 20070710. doi: 10.1074/jbc.M702810200. PubMed PMID: 17623659; PMCID: PMC3119455.

77. Iyer S, Ambrogini E, Bartell SM, Han L, Roberson PK, de Cabo R, Jilka RL, Weinstein RS, O'Brien CA, Manolagas SC, Almeida M. FOXOs attenuate bone formation by suppressing Wnt signaling. J Clin Invest. 2013;123(8):3409-19. Epub 20130715. doi: 10.1172/JCI68049. PubMed PMID: 23867625; PMCID: PMC3726166.

78. Iyer S, Han L, Bartell SM, Kim HN, Gubrij I, de Cabo R, O'Brien CA, Manolagas SC, Almeida M. Sirtuin1 (Sirt1) promotes cortical bone formation by preventing beta-catenin sequestration by FoxO transcription factors in osteoblast progenitors. J Biol Chem. 2014;289(35):24069-78. Epub 20140707. doi: 10.1074/jbc.M114.561803. PubMed PMID: 25002589; PMCID: PMC4148840.

79. Huang Q, Wang J. CBP-mediated FOXO4 acetylation facilitates postmenopausal osteoporosis (PMO) progression through the inhibition of the Wnt/beta-catenin signaling pathway. Histol Histopathol. 2024;39(8):1017-24. Epub 20231127. doi: 10.14670/HH-18-680. PubMed PMID: 38037460.

80. Ucer S, Iyer S, Kim HN, Han L, Rutlen C, Allison K, Thostenson JD, de Cabo R, Jilka RL, O'Brien C, Almeida M, Manolagas SC. The Effects of Aging and Sex Steroid Deficiency on the Murine Skeleton Are Independent and Mechanistically Distinct. J Bone Miner Res. 2017;32(3):560-74. Epub 20161103. doi: 10.1002/jbmr.3014. PubMed PMID: 27714847; PMCID: PMC5340621.

81. Jilka RL, Almeida M, Ambrogini E, Han L, Roberson PK, Weinstein RS, Manolagas SC. Decreased oxidative stress and greater bone anabolism in the aged, when compared to the young, murine skeleton with parathyroid hormone administration. Aging Cell. 2010;9(5):851-67. doi: 10.1111/j.1474-9726.2010.00616.x. PubMed PMID: 20698835; PMCID: PMC2958819.

82. Xiong Y, Zhang Y, Zhou F, Liu Y, Yi Z, Gong P, Wu Y. FOXO1 differentially regulates bone formation in young and aged mice. Cell Signal. 2022;99:110438. Epub 20220816. doi: 10.1016/j.cellsig.2022.110438. PubMed PMID: 35981656.

83. Pignolo RJ, Law SF, Chandra A. Bone Aging, Cellular Senescence, and Osteoporosis. JBMR Plus. 2021;5(4):e10488. Epub 20210402. doi: 10.1002/jbm4.10488. PubMed PMID: 33869998; PMCID: PMC8046105.

84. Pignolo RJ, Chandra A. Insights into age-related osteoporosis from senescence-based preclinical models and human accelerated aging paradigms. Mech Ageing Dev. 2025;224:112025. Epub 20250111. doi: 10.1016/j.mad.2025.112025. PubMed PMID: 39805505; PMCID: PMC11938943.

85. Teissier T, Temkin V, Pollak RD, Cox LS. Crosstalk Between Senescent Bone Cells and the Bone Tissue Microenvironment Influences Bone Fragility During Chronological Age and in Diabetes. Front Physiol. 2022;13:812157. Epub 20220321. doi: 10.3389/fphys.2022.812157. PubMed PMID: 35388291; PMCID: PMC8978545.

86. Lehmann J, Narcisi R, Franceschini N, Chatzivasileiou D, Boer CG, Koevoet W, Putavet D, Drabek D, van Haperen R, de Keizer PLJ, van Osch G, Ten Berge D. WNT/beta-catenin signalling interrupts a senescence-induction cascade in human mesenchymal stem cells that restricts their expansion. Cell Mol Life Sci. 2022;79(2):82. Epub 20220120. doi: 10.1007/s00018-021-04035-x. PubMed PMID: 35048158; PMCID: PMC8770385.

87. Jo S, Weon S, Nam B, Jang MA, Kang H, Kim TJ, Park YS, Kim TH. WNT16 elevation induced cell senescence of osteoblasts in ankylosing spondylitis. Arthritis Res Ther. 2021;23(1):301. Epub 20211208. doi: 10.1186/s13075-021-02670-0. PubMed PMID: 34879876; PMCID: PMC8653593.

88. Weng K, He Y, Weng X, Yuan Y. Exercise alleviates osteoporosis by regulating the secretion of the Senescent Associated Secretory Phenotype. Bone. 2025;196:117485. Epub 20250409. doi: 10.1016/j.bone.2025.117485. PubMed PMID: 40216288.

89. Geng Q, Wang S, Heng K, Zhai J, Song X, Xia L, Wang L, Lin Q, Li H, Guo Y. Astaxanthin attenuates irradiation-induced osteoporosis in mice by inhibiting oxidative stress, osteocyte senescence, and SASP. Food Funct. 2022;13(22):11770-9. Epub 20221114. doi: 10.1039/d2fo01673g. PubMed PMID: 36285709.

90. Geng Q, Gao H, Yang R, Guo K, Miao D. Pyrroloquinoline Quinone Prevents Estrogen Deficiency-Induced Osteoporosis by Inhibiting Oxidative Stress and Osteocyte Senescence. Int J Biol Sci. 2019;15(1):58-68. Epub 20190101. doi: 10.7150/ijbs.25783. PubMed PMID: 30662347; PMCID: PMC6329928.

91. Yu B, Chang J, Liu Y, Li J, Kevork K, Al-Hezaimi K, Graves DT, Park NH, Wang CY. Wnt4 signaling prevents skeletal aging and inflammation by inhibiting nuclear factor-kappaB. Nat Med. 2014;20(9):1009-17. Epub 20140810. doi: 10.1038/nm.3586. PubMed PMID: 25108526; PMCID: PMC4159424.

92. Xu W, Lu Q, Qu M, Fan R, Leng S, Wang L, Liu L, Yang F, Zhou X, Huang D, Zhang L. Wnt4 regulates bone metabolism through IKK-NF-kappaB and ROCK signaling under occlusal traumatic periodontitis. J Periodontal Res. 2022;57(3):461-9. Epub 20220208. doi: 10.1111/jre.12975. PubMed PMID: 35137408.

93. James A, Hendrixson JA, Kadhim I, Marques-Carvalho A, Laster J, Crawford J, Thostenson J, Wanchai V, Sato AY, Nookaew I, Xiong J, Almeida M, Onal M. Elevation of master autophagy regulator Tfeb in osteoblast lineage cells increases bone mass and strength. JCI Insight. 2025;10(17). Epub 20250729. doi: 10.1172/jci.insight.191688. PubMed PMID: 40728889; PMCID: PMC12487674.

94. Onal M. TFEB-mediated autophagy stimulation as an anabolic strategy for bone: insights from TFEB activation in the osteoblast lineage. Autophagy Rep. 2025;4(1):2596422. Epub 20251208. doi: 10.1080/27694127.2025.2596422. PubMed PMID: 41377164; PMCID: PMC12688215.

95. Onal M, Piemontese M, Xiong J, Wang Y, Han L, Ye S, Komatsu M, Selig M, Weinstein RS, Zhao H, Jilka RL, Almeida M, Manolagas SC, O'Brien CA. Suppression of autophagy in osteocytes mimics skeletal aging. J Biol Chem. 2013;288(24):17432-40. Epub 20130503. doi: 10.1074/jbc.M112.444190. PubMed PMID: 23645674; PMCID: PMC3682543.

96. Piemontese M, Onal M, Xiong J, Han L, Thostenson JD, Almeida M, O'Brien CA. Low bone mass and changes in the osteocyte network in mice lacking autophagy in the osteoblast lineage. Sci Rep. 2016;6:24262. Epub 20160411. doi: 10.1038/srep24262. PubMed PMID: 27064143; PMCID: PMC4827128.

97. Resende-Coelho A, Ali MM, James A, Warren A, Gatrell L, Kadhim I, Fu Q, Xiong J, Onal M, Almeida M. Mitochondrial oxidative stress or decreased autophagy in osteoblast lineage cells is not sufficient to mimic the deleterious effects of aging on bone mechanoresponsiveness. Aging (Albany NY). 2025;17(3):610-29. Epub 20250318. doi: 10.18632/aging.206213. PubMed PMID: 40105873; PMCID: PMC11984430.

98. Chen L, Yang Y, Bao J, Wang Z, Xia M, Dai A, Tan J, Zhou L, Wu Y, Sun W. Autophagy negative-regulating Wnt signaling enhanced inflammatory osteoclastogenesis from Pre-OCs in vitro. Biomed Pharmacother. 2020;126:110093. Epub 20200318. doi: 10.1016/j.biopha.2020.110093. PubMed PMID: 32199225.

99. Kato H, Han X, Yamaza H, Masuda K, Hirofuji Y, Sato H, Pham TTM, Taguchi T, Nonaka K. Direct effects of mitochondrial dysfunction on poor bone health in Leigh syndrome. Biochem Biophys Res Commun. 2017;493(1):207-12. Epub 20170909. doi: 10.1016/j.bbrc.2017.09.045. PubMed PMID: 28899781.

100. Zhang H, Zhao R, Wang X, Qi Y, Sandai D, Wang W, Song Z, Liang Q. Interruption of mitochondrial symbiosis is associated with the development of osteoporosis. Front Endocrinol (Lausanne). 2025;16:1488489. Epub 20250203. doi: 10.3389/fendo.2025.1488489. PubMed PMID: 39963284; PMCID: PMC11830588.

101. Sun X, Mao Y, Dai P, Li X, Gu W, Wang H, Wu G, Ma J, Huang S. Mitochondrial dysfunction is involved in the aggravation of periodontitis by diabetes. J Clin Periodontol. 2017;44(5):463-71. Epub 20170412. doi: 10.1111/jcpe.12711. PubMed PMID: 28207937.

102. Xu T, Dong Q, Luo Y, Liu Y, Gao L, Pan Y, Zhang D. Correction to: Porphyromonas gingivalis infection promotes mitochondrial dysfunction through Drp1-dependent mitochondrial fission in endothelial cells. Int J Oral Sci. 2022;14(1):3. Epub 20220112. doi: 10.1038/s41368-021-00153-1. PubMed PMID: 35022392; PMCID: PMC8755809.

103. Du Y, Zheng J, Xu B, Peng C, Yang K. Piezo1 participates in the tension-driven osteogenic differentiation of periodontal ligament stem cells. BMC Oral Health. 2025;25(1):1155. Epub 20250713. doi: 10.1186/s12903-025-06427-y. PubMed PMID: 40653466; PMCID: PMC12257747.

104. Hasegawa T, Ouchi T, Kurashima R, Kimura M, Asoda S, Nakagawa T, Shibukawa Y. Piezo1 negatively regulates proliferation, but enhances mineralization in human cementoblasts. J Oral Biosci. 2025;67(4):100705. Epub 20251101. doi: 10.1016/j.job.2025.100705. PubMed PMID: 41274689.

105. Wang X, Xie B, Guo Y, Wan H, He X, Chen J, He Y. Agonism of PIEZO1 prevents aggravated periodontitis with traumatic occlusion via MAPK signaling pathway. iScience. 2025;28(11):113688. Epub 20251008. doi: 10.1016/j.isci.2025.113688. PubMed PMID: 41234768; PMCID: PMC12605257.

106. Shindo S, Nakamura S, Hawthorne A, Heidari A, Pastore MR, Okamoto M, Suzuki M, Salinas M, Memida T, Minond D, Bontempo A, Cayabyab M, Yang Y, Crane JL, Hernandez M, Vardar S, Hardigan P, Han X, Kaltman S, Kawai T. Piezo1 protects against inflammatory bone loss via a unique Ca(2+)-independent mechanism in osteoclasts. Front Immunol. 2025;16:1661538. Epub 20250925. doi: 10.3389/fimmu.2025.1661538. PubMed PMID: 41080556; PMCID: PMC12507952.

107. Gao Y, Huang E, Zhang H, Wang J, Wu N, Chen X, Wang N, Wen S, Nan G, Deng F, Liao Z, Wu D, Zhang B, Zhang J, Haydon RC, Luu HH, Shi LL, He TC. Crosstalk between Wnt/beta-catenin and estrogen receptor signaling synergistically promotes osteogenic differentiation of mesenchymal progenitor cells. PLoS One. 2013;8(12):e82436. Epub 20131205. doi: 10.1371/journal.pone.0082436. PubMed PMID: 24340027; PMCID: PMC3855436.

108. Liedert A, Nemitz C, Haffner-Luntzer M, Schick F, Jakob F, Ignatius A. Effects of Estrogen Receptor and Wnt Signaling Activation on Mechanically Induced Bone Formation in a Mouse Model of Postmenopausal Bone Loss. Int J Mol Sci. 2020;21(21). Epub 20201105. doi: 10.3390/ijms21218301. PubMed PMID: 33167497; PMCID: PMC7663944.

109. Moverare-Skrtic S, Wu J, Henning P, Gustafsson KL, Sjogren K, Windahl SH, Koskela A, Tuukkanen J, Borjesson AE, Lagerquist MK, Lerner UH, Zhang FP, Gustafsson JA, Poutanen M, Ohlsson C. The bone-sparing effects of estrogen and WNT16 are independent of each other. Proc Natl Acad Sci U S A. 2015;112(48):14972-7. Epub 20151116. doi: 10.1073/pnas.1520408112. PubMed PMID: 26627248; PMCID: PMC4672787.

110. Zhang D, Hu M, Chu T, Lin L, Wang J, Li X, Ke HZ, Qin YX. Sclerostin antibody prevented progressive bone loss in combined ovariectomized and concurrent functional disuse. Bone. 2016;87:161-8. Epub 20160208. doi: 10.1016/j.bone.2016.02.005. PubMed PMID: 26868528; PMCID: PMC4862887.

111. MacNabb C, Patton D, Hayes JS. Sclerostin Antibody Therapy for the Treatment of Osteoporosis: Clinical Prospects and Challenges. J Osteoporos. 2016;2016:6217286. Epub 20160526. doi: 10.1155/2016/6217286. PubMed PMID: 27313945; PMCID: PMC4899597.

112. Cosman F, Crittenden DB, Adachi JD, Binkley N, Czerwinski E, Ferrari S, Hofbauer LC, Lau E, Lewiecki EM, Miyauchi A, Zerbini CA, Milmont CE, Chen L, Maddox J, Meisner PD, Libanati C, Grauer A. Romosozumab Treatment in Postmenopausal Women with Osteoporosis. N Engl J Med. 2016;375(16):1532-43. Epub 20160918. doi: 10.1056/NEJMoa1607948. PubMed PMID: 27641143.

113. Momesso NR, Bacelar-Marcolino ACZ, Biguetti CC, Ortiz RC, Ervolino E, Matsumoto MA. Comparative effects of ovariectomy and chemically induced menopause on alveolar bone healing in zoledronate-treated female mice. Bone. 2025;201:117655. Epub 20250924. doi: 10.1016/j.bone.2025.117655. PubMed PMID: 41005449.

114. Furlan CC, Freire AR, Ferreira-Pileggi BC, Watanabe LNO, Botacin PR, Prado FB, Rossi AC. Does Ovariectomy Affect the Mechanics of the Mandibular Alveolar Bone Structure of Wistar Rats Subjected to Tooth Loss and Modified Diet?-A FEA Study. Biology (Basel). 2024;13(11). Epub 20241106. doi: 10.3390/biology13110906. PubMed PMID: 39596861; PMCID: PMC11592268.

115. Chen H, Xu X, Liu M, Zhang W, Ke HZ, Qin A, Tang T, Lu E. Sclerostin antibody treatment causes greater alveolar crest height and bone mass in an ovariectomized rat model of localized periodontitis. Bone. 2015;76:141-8. Epub 20150411. doi: 10.1016/j.bone.2015.04.002. PubMed PMID: 25868799.

116. Gharibi B, Ghuman MS, Cama G, Rawlinson SCF, Grigoriadis AE, Hughes FJ. Site-specific differences in osteoblast phenotype, mechanical loading response and estrogen receptor-related gene expression. Mol Cell Endocrinol. 2018;477:140-7. Epub 20180619. doi: 10.1016/j.mce.2018.06.011. PubMed PMID: 29928929.

117. Yao Y, Kauffmann F, Maekawa S, Sarment LV, Sugai JV, Schmiedeler CA, Doherty EJ, Holdsworth G, Kostenuik PJ, Giannobile WV. Sclerostin antibody stimulates periodontal regeneration in large alveolar bone defects. Sci Rep. 2020;10(1):16217. Epub 20201001. doi: 10.1038/s41598-020-73026-y. PubMed PMID: 33004873; PMCID: PMC7530715.

118. Yu SH, Hao J, Fretwurst T, Liu M, Kostenuik P, Giannobile WV, Jin Q. Sclerostin-Neutralizing Antibody Enhances Bone Regeneration Around Oral Implants. Tissue Eng Part A. 2018;24(21-22): 1672-9. Epub 2018/06/21. doi: 10.1089/ten.TEA.2018.0013. PubMed PMID: 29921173; PMCID: PMC6916116.

119. Ergunol E, Semsi R, Dayanir D, Akgun RO, Ekim O, Uludamar A, Ozkul A, Sepici Dincel A. Sclerostin antibody promotes alveolar bone regeneration after tooth extraction. Biomol Biomed. 2025. Epub 20251022. doi: 10.17305/bb.2025.12999. PubMed PMID: 41123196.

120. Saag KG, Petersen J, Brandi ML, Karaplis AC, Lorentzon M, Thomas T, Maddox J, Fan M, Meisner PD, Grauer A. Romosozumab or Alendronate for Fracture Prevention in Women with Osteoporosis. N Engl J Med. 2017;377(15):1417-27. Epub 20170911. doi: 10.1056/NEJMoa1708322. PubMed PMID: 28892457.

121. Gonzalez-Salvatierra S, Garcia-Fontana C, Lacal J, Andujar-Vera F, Martinez-Heredia L, Sanabria-de la Torre R, Ferrer-Millan M, Moratalla-Aranda E, Munoz-Torres M, Garcia-Fontana B. Cardioprotective function of sclerostin by reducing calcium deposition, proliferation, and apoptosis in human vascular smooth muscle cells. Cardiovasc Diabetol. 2023;22(1):301. Epub 20231102. doi: 10.1186/s12933-023-02043-8. PubMed PMID: 37919715; PMCID: PMC10623848.

122. Golledge J, Thanigaimani S. Role of Sclerostin in Cardiovascular Disease. Arterioscler Thromb Vasc Biol. 2022;42(7):e187-e202. Epub 20220512. doi: 10.1161/ATVBAHA.122.317635. PubMed PMID: 35546488.

123. Liu M, Kurimoto P, Zhang J, Niu QT, Stolina M, Dechow PC, Feng JQ, Hesterman J, Silva MD, Ominsky MS, Richards WG, Ke H, Kostenuik PJ. Sclerostin and DKK1 Inhibition Preserves and Augments Alveolar Bone Volume and Architecture in Rats with Alveolar Bone Loss. J Dent Res. 2018;97(9):1031-8. Epub 20180404. doi: 10.1177/0022034518766874. PubMed PMID: 29617179.

124. Florio M, Gunasekaran K, Stolina M, Li X, Liu L, Tipton B, Salimi-Moosavi H, Asuncion FJ, Li C, Sun B, Tan HL, Zhang L, Han CY, Case R, Duguay AN, Grisanti M, Stevens J, Pretorius JK, Pacheco E, Jones H, Chen Q, Soriano BD, Wen J, Heron B, Jacobsen FW, Brisan E, Richards WG, Ke HZ, Ominsky MS. A bispecific antibody targeting sclerostin and DKK-1 promotes bone mass accrual and fracture repair. Nat Commun. 2016;7:11505. Epub 20160527. doi: 10.1038/ncomms11505. PubMed PMID: 27230681; PMCID: PMC4894982.

125. Witcher PC, Miner SE, Horan DJ, Bullock WA, Lim KE, Kang KS, Adaniya AL, Ross RD, Loots GG, Robling AG. Sclerostin neutralization unleashes the osteoanabolic effects of Dkk1 inhibition. JCI Insight. 2018;3(11). Epub 20180607. doi: 10.1172/jci.insight.98673. PubMed PMID: 29875318; PMCID: PMC6124404.

126. Ko JY, Wang FS, Lian WS, Yang FS, Chen JW, Huang PH, Liao CY, Kuo SJ. Dickkopf-1 (DKK1) blockade mitigates osteogenesis imperfecta (OI) related bone disease. Mol Med. 2024;30(1):66. Epub 20240521. doi: 10.1186/s10020-024-00838-3. PubMed PMID: 38773377; PMCID: PMC11106911.

127. Tuysuz N, van Bloois L, van den Brink S, Begthel H, Verstegen MM, Cruz LJ, Hui L, van der Laan LJ, de Jonge J, Vries R, Braakman E, Mastrobattista E, Cornelissen JJ, Clevers H, Ten Berge D. Lipid-mediated Wnt protein stabilization enables serum-free culture of human organ stem cells. Nat Commun. 2017;8:14578. Epub 20170306. doi: 10.1038/ncomms14578. PubMed PMID: 28262686; PMCID: PMC5343445.

128. Rawadi G, Vayssiere B, Dunn F, Baron R, Roman-Roman S. BMP-2 controls alkaline phosphatase expression and osteoblast mineralization by a Wnt autocrine loop. J Bone Miner Res. 2003;18(10):1842-53. doi: 10.1359/jbmr.2003.18.10.1842. PubMed PMID: 14584895.

129. Wei L, Teng F, Deng L, Liu G, Luan M, Jiang J, Liu Z, Liu Y. Periodontal regeneration using bone morphogenetic protein 2 incorporated biomimetic calcium phosphate in conjunction with barrier membrane: A pre-clinical study in dogs. J Clin Periodontol. 2019;46(12):1254-63. Epub 20191007. doi: 10.1111/jcpe.13195. PubMed PMID: 31518453; PMCID: PMC6899729.

130. Jiang S, Liu T, Wu G, Li W, Feng X, Pathak JL, Shi J. BMP2-Functionalized Biomimetic Calcium Phosphate Graft Promotes Alveolar Defect Healing During Orthodontic Tooth Movement in Beagle Dogs. Front Bioeng Biotechnol. 2020;8:517. Epub 20200529. doi: 10.3389/fbioe.2020.00517. PubMed PMID: 32548104; PMCID: PMC7272671.

131. Nam JW, Khureltogtokh S, Choi HM, Lee AR, Park YB, Kim HJ. Randomised controlled clinical trial of augmentation of the alveolar ridge using recombinant human bone morphogenetic protein 2 with hydroxyapatite and bovine-derived xenografts: comparison of changes in volume. Br J Oral Maxillofac Surg. 2017;55(8):822-9. Epub 20170830. doi: 10.1016/j.bjoms.2017.07.017. PubMed PMID: 28864147.

132. Miron RJ, Dard M, Weinreb M. Enamel matrix derivative, inflammation and soft tissue wound healing. J Periodontal Res. 2015;50(5):555-69. Epub 20141123. doi: 10.1111/jre.12245. PubMed PMID: 25418917.

133. Kitamura M, Yamashita M, Miki K, Ikegami K, Takedachi M, Kashiwagi Y, Nozaki T, Yamanaka K, Masuda H, Ishihara Y, Murakami S. An exploratory clinical trial to evaluate the safety and efficacy of combination therapy of REGROTH(R) and Cytrans(R) granules for severe periodontitis with intrabony defects. Regen Ther. 2022;21:104-13. Epub 20220621. doi: 10.1016/j.reth.2022.06.001. PubMed PMID: 35785043; PMCID: PMC9234541.

134. Sculean A, Windisch P, Chiantella GC, Donos N, Brecx M, Reich E. Treatment of intrabony defects with enamel matrix proteins and guided tissue regeneration. A prospective controlled clinical study. J Clin Periodontol. 2001;28(5):397-403. doi: 10.1034/j.1600-051x.2001.028005397.x. PubMed PMID: 11350501.

135. De Ry SP, Roccuzzo A, Lang NP, Sculean A, Salvi GE. Long-term clinical outcomes of periodontal regeneration with enamel matrix derivative: A retrospective cohort study with a mean follow-up of 10 years. J Periodontol. 2022;93(4):548-59. Epub 20210908. doi: 10.1002/JPER.21-0347. PubMed PMID: 34258767; PMCID: PMC9373923.

CHAPTER 3

Craniofacial and whole-skeleton fracture patterns in osteogenesis imperfecta: Findings from a nationwide U.S. insurance claims database

Hsiao H Sung [1 2 3], Daniel G. Whitney[1 4], Kenneth M Kozloff [1], Michelle S Caird [1]

[1.] Orthopaedic Research Laboratories, Department of Orthopaedic Surgery, University of Michigan, Ann Arbor, USA

[2.] Department of Oral and Maxillofacial Surgery, University of Michigan, Ann Arbor, USA

[3.] Experimental Rheumatology, Department of Rheumatology, Radboud Medical Centre, Nijmegen, The Netherlands.

[4.] Institute for Healthcare Policy and Innovation, University of Michigan, Ann Arbor, USA.

Bone. 2026 Mar:204:117762. doi: 10.1016/j.bone.2025.117762. Epub 2025 Dec 15.

Abstract

Background: Osteogenesis imperfecta (OI) is an inherited connective tissue disease characterized by lifelong skeletal fragility and recurrent fractures. While most prior research has focused on long bone fractures in selected clinical cohorts, population-based estimates of craniofacial and site-specific fracture risk in OI remain largely limited. This study used insurance claims data to quantify the period prevalence, anatomical distribution, and predictors of fractures in individuals with versus without OI.

Methods: A retrospective cohort study was conducted using the IBM® MarketScan® Multi-State Medicaid (2016-2022, all ages) and Commercial Databases (2016-2022, < 65 years old). Diagnosis of OI and all fractures were identified using ICD and CPT codes recorded during healthcare encounters. The first full year of enrollment was used to determine 1-year period prevalence and counts of fractures overall and by site, stratified by age (<5, 6-9, 10-13, 14-18, 19-25, ten-year intervals to >55). Differences between cohorts were estimated using relative risk (RR). Associations with demographic and clinical factors were assessed via logistic regression. Proxy measures of OI severity and medical device use were applied, as clinical classification and exposure to treatments could not be directly adjudicated.

Results: Among 4294 individuals with OI and approximately 54.8 million controls, the overall fracture prevalence was 33.9 % in the OI cohort versus 2.5 % in controls (RR 13.6), with elevated rates observed at all anatomical sites. Jaw (craniofacial) fractures were nearly seven times more frequent in OI (0.40 % vs. 0.06 %; RR 6.7), while femur fractures showed the greatest disparity (RR 119.4). Age-specific analysis revealed the highest fracture risk for individuals with OI in early childhood, particularly at craniofacial and axial sites, with risk increasing further in those with greater proxy-measured disease severity. Female was associated with lower odds of fracture compared to males, and Medicaid coverage correlated with increased risk at select skeletal sites. Limitations include inability to distinguish fracture etiology (spontaneous, traumatic, or iatrogenic), unmeasured exposure to treatments, inability to apply clinical OI classifications, and exclusion of uninsured individuals.

Conclusions: Individuals with OI face a markedly greater and distinctive burden of fractures, including craniofacial involvement, than the general population. This work provides the first large-scale, population-based estimates of craniofacial fracture burden in OI, highlighting distinct age- and site-specific risk patterns. These findings reinforce the importance of ongoing, site-specific monitoring and

integrated multidisciplinary care for individuals with OI, supporting clinicians in anticipatory guidance and tailored prevention strategies.

Keywords: Craniofacial; Fractures; Insurance claims; Osteogenesis imperfecta.

Introduction

Osteogenesis imperfecta (OI) is now recognized as a genetically and clinically heterogeneous group of conditions, rather than a single disorder. The term OI encompasses a spectrum of inheritable diseases characterized mainly by bone fragility, and arises from mutations in multiple genes—primarily those involved in the synthesis or processing of type I collagen[1, 2]. Individuals affected by this spectrum experience lifelong skeletal fragility, with fractures serving as a hallmark manifestation and contributing substantially to clinical, functional, and psychosocial impact[3-5]. While the pattern and frequency of fractures are central to understanding OI, most published research is limited to small or selected patient cohorts or fracture sites[6-9], hindering comprehensive epidemiologic insight.

Beyond long bone and axial fractures, individuals with OI commonly exhibit a distinct craniofacial phenotype. This craniofacial phenotype encompasses both skeletal and dental abnormalities, which often become more pronounced in severe forms of the disorder. A primary dental concern is Dentinogenesis Imperfecta (DI), which affects between 30–70% of OI patient. DI causes fragile, discolored teeth prone to accelerated wear and periapical pathology[10-12] . These dental issues are frequently accompanied by significant malocclusion, particularly Class III (anterior crossbite), open bite, and vertical maxillary deficiency, is frequently reported[13-15], and contributes to difficulties in mastication, speech, and aesthetics. Craniofacial skeletal deformities, such as mandibular prognathism and reduced facial height, are also prevalent, especially in severe phenotypes[16]. Not only do these features predispose individuals to functional impairment, but they may also increase susceptibility to jaw fractures, either spontaneous or iatrogenic during dental procedures[17, 18].

Insurance claims databases offer opportunities to characterize fracture epidemiology on a broader scale. Although OI is identified in these datasets using International Classification of Diseases (ICD) and Current Procedural Terminology (CPT) codes that do not disaggregate the various genetic subtypes, and thus introduce limitations in clinical specificity, claims-based studies remain valuable for assessing overall trends in fracture risk, anatomical distribution, and healthcare burden. Prior research utilizing these databases has largely been restricted to commercially insured populations, thereby excluding individuals covered by Medicaid or Medicare and limiting the generalizability of findings[19, 20], which excludes a substantial portion of the OI community covered by Medicaid or Medicare. Such limitations restrict both socioeconomic representation and the generalizability of findings, and may underestimate the full spectrum of fracture severity, distribution, and healthcare burden among individuals with OI.

To date, most epidemiologic studies on OI fractures have focused on the long and axial bones, as fractures at these sites are the most common and often the most disabling[6-9, 20-22]. In contrast, craniofacial fractures in OI remain understudied, despite their significant impact on appearance, communication, mastication, and quality of life. Existing knowledge about craniofacial fractures is primarily drawn from case reports and small series[23-25], often related to oral surgeries[26-29], leaving the true prevalence and distribution of these injuries in the broader OI population unclear. Importantly, craniofacial fractures in children may be misattributed to non-accidental trauma[30-33], potentially resulting in serious social and legal consequences. Robust, population-level epidemiologic data on craniofacial and other skeletal fractures in OI are therefore essential to inform clinical care, guide anticipatory counseling, and support evidence-based prevention strategies.

To address these gaps, we conducted a large-scale, retrospective cohort study using nationwide public and commercial claims databases. Our objectives were to: (1) compare the 1-year period prevalence and fracture count in individuals with and without OI. overall and stratified by age group; (2) assess the effects of sex, OI severity, and insurance type on age-stratified fracture outcomes; and (3) determine the distribution of fractures sites, with a particular focus on craniofacial fractures, to identify sites of increased vulnerability. By providing a comprehensive epidemiologic analysis, we aim to inform clinical care, anticipatory counseling, and prevention strategies for individuals across the OI spectrum.

Methods

Data source

This was a retrospective cohort study using the IBM® Watson Health MarketScan® Research Databases to analyze patient-level claims data from January 1, 2016 to December 31, 2022.

The IBM® MarketScan® Commercial Database captures health insurance claims for insured employees and their non-Medicare-eligible dependents under employer-sponsored plans, covering individuals from birth through age 65. The Commercial Database draws from approximately 350 different U.S. insurance payers, providing robust representation across the private health insurance landscape.

The IBM® MarketScan® Multi-State Medicaid Database includes people of all ages covered by state Medicaid programs from multiple, geographically diverse states, encompassing both fee-for-service and managed care plans.

Health conditions (such as OI and fractures) and equipment use (such as wheelchairs) were identified using International Classification of Diseases, Tenth Revision, Clinical Modification (ICD-10-CM) codes and Healthcare Common Procedure Coding System (HCPCS) codes. Details are provided in **Supplementary Table 1**. All data were de-identified, and the study was deemed exempt by the University of Michigan Institutional Review Board.

Cohort selection

Individuals of any age and with ≥1 year of continuous enrollment in a health plan between 2016 and 2022 were included in this study.

OI cohort: Individuals were classified as having OI if they had at least one inpatient claim with an OI ICD code, or two outpatient claims with an OI ICD code on different days within 12 months.

Non-OI comparator cohort: Individuals with no OI claims.

Of 4,925 individuals identified with OI (Commercial, n=2,416; Medicaid, n=2,509), 4,294 (87.2%) had ≥1 year of continuous health plan enrollment and were included. Among 72,706,051 without OI claims (Commercial, n=53,742,214; Medicaid, n=18,963,837), 54,750,885 (75.3%) met the same enrollment requirement.

Fracture outcomes

Fractures were identified using a single ICD code from both inpatient and outpatient claims and classified as: All cause fracture: including fragility, pathological, non-fragility fractures

By location: jaw; other skull and facial bones (excluding the jaw); vertebral column (cervical through lumbar region); shoulder (e.g., shoulder girdle); humerus; forearm (i.e., radius, ulna); wrist and hand; hip (including femoral neck); other femur; leg (including tibia, fibula) and ankle; foot and toes; and other/unspecified sites.

Fracture outcomes were measured in two ways:

1. One year period prevalence: Number of people with at least one fracture in a cohort per year, divided by the total cohort size. Although the MarketScan databases provide up to six years of coverage, we elected to calculate 1-year period prevalence and fracture counts. This approach maximizes sample size and the representativeness of the study population by minimizing the selection bias that occurs when longer continuous enrollment periods are

required. Longer observation intervals would substantially reduce the number of eligible participants, disproportionately including individuals with more stable insurance coverage and potentially skewing estimates. This approach offers robust, interpretable estimates of fracture burden across all age groups and insurance types.

2. Fracture count (rate): Total number of distinct fracture events per site, divided by the cohort sample size multiplied by 100.

Distinct fracture events were defined as claims for the same fracture site separated by at least 4 months. This approach helps to ensure that follow-up claims or procedures (such as cast removal) related to the same initial fracture event are not counted as new events. Prior studies have used gaps of 3- or 6-month intervals to distinguish new fractures.[34-36] The 4-month gap in this study was used to balance the potentially longer fracture recovery and higher fracture-related healthcare visits among people with OI compared to those without OI. Given the 1-year study period, the 4-month gap also ensured we could reasonably capture multiple distinct events per year for both groups. As a result, a maximum of four distinct fractures per site could be recorded during the study period.

Covariates

Date of birth (as the year of birth) and sex were retrieved from the databases. Age was calculated as the difference between the study entry year and the year of birth. To examine fracture pattern across the life span, age was grouped into intervals reflecting key stages of bone development, regardless of sex: ≤5 years old, 6-9 years old, 10-13 years old, 14-18 years old, 19-25 years old, and then 10-year intervals until ≥56 years old. The number of OI cohort older than 65 years old (n=78) was too small for reliable fracture estimates, partly because the Commercial database includes individuals only up to age 65.

Because the ICD coding system does not specify OI severity, we used proxy indicators based on comorbid diagnoses and assistive device use. Medical claims were searched for diagnoses of dentinogenesis imperfecta, hearing loss, and scoliosis, while durable medical equipment claims were searched for wheelchairs (including parts and accessories) and orthotics (see **Supplementary Table 1** for a list of codes). Each of these five indicators contributed one point, resulting in a severity score ranging from 0 to 5. Since these proxies are not exclusive to OI, we collected them for both the OI and non-OI cohorts.

The Commercial database lacked complete race data, while the Medicaid database intentionally excluded geographic variables as part of the contractual agreements made between IBM® MarketScan® and their business partners. Therefore, common descriptive characteristics including race, ethnicity, and geography (e.g., state, U.S. region, rural/urban) were not included in this study.

Statistical analysis

Baseline descriptive characteristics were summarized as percentages and counts for the OI cohort, and as percentages only for the non-OI cohort to enhance readability given the large sample size. For both OI and non-OI groups, the 1-year period prevalence and count of fractures at any site, as well as by specific fracture site, were summarized both overall and stratified by age group. The relative risk (RR) with 95% confidence intervals (CI) was estimated by comparing the OI cohort to the non-OI cohort.

To assess whether sex, OI severity, or insurance type modified the association between OI cohort and fracture prevalence across age group, logistic regression models were applied. These models included the main effects of cohort (OI vs. non-OI) and each factor, as well as their two-way interaction terms. For statistical power and to account for similar age-related patterns, fracture sites were grouped as follows: (1) all skull/facial sites including the jaw, (2) vertebral column and pelvis, (3) all upper extremity sites, and (4) all lower extremity sites. Models were stratified by age group.

If the interaction term for a given factor (e.g. sex) was statistically significant ($p \leq 0.05$) in at least 3 consecutive age groups, estimates were reported to illustrate how the effect differed by OI status. In the absence of strong evidence for effect modification, subsequent analyses focused on the OI cohort alone, consistent with the primary objective of characterizing fracture epidemiology in OI. In these cases, models were simplified by removing interaction terms, and odds ratios (OR) for each factor were estimated within the OI group, adjusting for age as a continuous variable.

For each cohort, the proportion of fractures by site (excluding unspecified sites) was calculated. As individuals could experience multiple fractures at different sites, proportions were determined as the number of fractures at each site divided by the total number of fractures. As part of the Data Use Agreement, estimates with $n<11$ cases were suppressed for patient de-identification purposes. SAS version 9.4 was used and $P \leq 0.05$ (two-tailed) was considered statistically significant.

Results

Cohort characteristics

A total of 4,294 individuals with OI and 54.8 million individuals without OI were included (**Table 1**). The median age in the OI cohort was 8 years younger than in the non-OI cohort. Medicaid insurance coverage was present in 54.0% of the OI group, compared with 29.0% in the non-OI group. Among individuals with OI, 4.9% used 2 or more types of medical or durable medical equipment, compared with only 0.1%, in the non-OI cohort used multiple devices.

Table 1. Descriptive characteristics for the cohorts with osteogenesis imperfecta (OI) and without OI (non-OI).

	OI (n=4,294)	Non-OI (n=54,750,885)
	% (n)	%
Age in years, median (IQR)	21 (9, 39)	29 (13, 47)
≤5 years old	18.0 (772)	12.5
6-9 years old	8.9 (383)	6.6
10-13 years old	9.6 (414)	6.7
14-18 years old	10.7 (461)	8.1
19-25 years old	10.4 (445)	10.2
26-35 years old	13.1 (564)	14.8
36-45 years old	10.1 (433)	13.6
46-55 years old	10.1 (434)	13.8
≥56 years old	9.0 (388)	13.7
Sex		
Male	42.7 (1,834)	46.3
Female	57.3 (2,460)	53.7
Insurance type		
Commercial	46.0 (1,975)	71.0
Medicaid	54.0 (2,319)	29.0
Year study entry		
2016	57.2 (2,456)	51.8
2017	9.3 (397)	9.9
2018	9.0 (387)	10.9
2019	11.3 (484)	10.2
2020	7.2 (307)	9.6
2021	6.1 (263)	7.7

Table 1. Continued

	OI (n=4,294)	Non-OI (n=54,750,885)
	% (n)	%
Proxy items for OI severity		
Dentinogenesis imperfecta	1.6 (70)	<0.1
Hearing loss	1.9 (82)	0.5
Scoliosis	9.5 (406)	0.7
Wheelchair use	6.2 (266)	0.1
Orthotics	9.2 (396)	1.2
Proxy OI severity count		
0 items	77.3 (3,319)	97.6
1 item	17.8 (764)	2.3
≥2 items	4.9 (211)	0.1

IQR, interquartile range.

Fracture prevalence and count (rate)

Despite the younger age, the prevalence of fractures at any site was much higher in the OI cohort (33.9%) compared to the non-OI cohort (2.5%), corresponding to an RR of 13.6 (95% CI=13.0, 14.2) (**Table 2**). The total fracture rate, defined as the count of fractures per 100 individuals, yielded an RR of 20.2 (95% CI=19.7, 20.7) for OI versus non-OI. Jaw fracture prevalence was 0.40% for OI and 0.06% for non-OI, with an RR of 6.7 (95% CI=4.2, 10.7). For leg/ankle fractures, the prevalence was 10.95% in OI; the most common sites of fracture in the non-OI group was foot/toes fractures, with a prevalence of 0.59%. The RR for femur fractures was especially high at 119.4 (95% CI=108.8, 131.0).

Table 2. 1-year period prevalence and count of fractures by site, and relative risk (RR) of fracture for the cohorts with osteogenesis imperfecta (OI) and without OI (non-OI).

	OI (n=4,294)	Non-OI (n=54,750,885)	OI vs. Non-OI (reference: non-OI)
	% (n)	% (n)	RR (95% CI)
Prevalence (% of cohort with at least 1 fracture)			
Any site	33.86 (1,454)	2.49 (1,364,447)	13.6 (13.0, 14.2)
Jaw	0.40 (17)	0.06 (31,101)	6.7 (4.2, 10.7)
Skull/face, excluding jaw	1.37 (59)	0.15 (83,515)	9.1 (7.1, 11.8)
Vertebral column and pelvis	0.93 (40)	0.06 (32,057)	15.5 (11.4, 21.1)
Shoulder	2.49 (107)	0.14 (74,630)	17.8 (14.8, 21.5)
Humerus	5.40 (232)	0.18 (100,335)	30.0 (26.5, 34.0)
Forearm	7.64 (328)	0.46 (254,444)	16.6 (15.0, 18.4)

Table 2. Continued

	OI (n=4,294)	Non-OI (n=54,750,885)	OI vs. Non-OI (reference: non-OI)
	% (n)	% (n)	RR (95% CI)
Wrist/hand	4.68 (201)	0.58 (319,392)	8.1 (7.1, 9.2)
Hip	4.54 (195)	0.08 (41,242)	56.8 (49.5, 65.1)
Femur	9.55 (410)	0.08 (44,311)	119.4 (108.8, 131.0)
Leg/ankle	10.95 (470)	0.46 (250,180)	23.8 (21.9, 25.9)
Foot/toes	5.12 (220)	0.59 (321,751)	8.7 (7.6, 9.9)
Count (Number of fractures per cohort x 100)			
Any site	59.59 (2,559)	2.95 (1,613,545)	20.2 (19.7, 20.7)
Jaw	0.44 (19)	0.07 (38,864)	6.3 (4.0, 9.8)
Skull/face, excluding jaw	1.42 (61)	0.16 (85,132)	8.9 (6.9, 11.4)
Vertebral column and pelvis	0.93 (40)	0.06 (33,191)	15.5 (11.4, 21.1)
Shoulder	2.56 (110)	0.14 (76,093)	18.3 (15.2, 22.0)
Humerus	5.96 (256)	0.19 (102,900)	31.4 (27.9, 35.3)
Forearm	8.06 (346)	0.47 (259,188)	17.1 (15.5, 19.0)
Wrist/hand	4.84 (208)	0.59 (323,516)	8.2 (7.2, 9.4)
Hip	4.77 (205)	0.08 (43,291)	59.6 (52.2, 68.2)
Femur	10.74 (461)	0.09 (46,556)	119.3 (109.4, 130.1)
Leg/ankle	12.06 (518)	0.47 (258,275)	25.7 (23.7, 27.8)
Foot/toes	5.52 (237)	0.60 (327,693)	9.2 (8.1, 10.4)

Age-specific fracture patterns

When stratified by age group, both fracture prevalence (**Figure 1A**) and count (**Figure 1B**) at any site were higher in the OI cohort compared to the non-OI across group across the age range, with the difference particularly pronounced earlier in life. Age-stratified prevalence and count of fractures by site are shown in **Figure 2** (skull/facial sites and vertebral column, including pelvis), **Figure 3** (upper extremity), and **Figure 4** (lower extremity). For certain sites with limited events, age groups were consolidated based on the number of fracture events and clinical relevance. Fracture estimates for the jaw could not be reported due to insufficient sample sizes, though jaw fractures were observed across the adult lifespan at higher rates in the OI cohort.

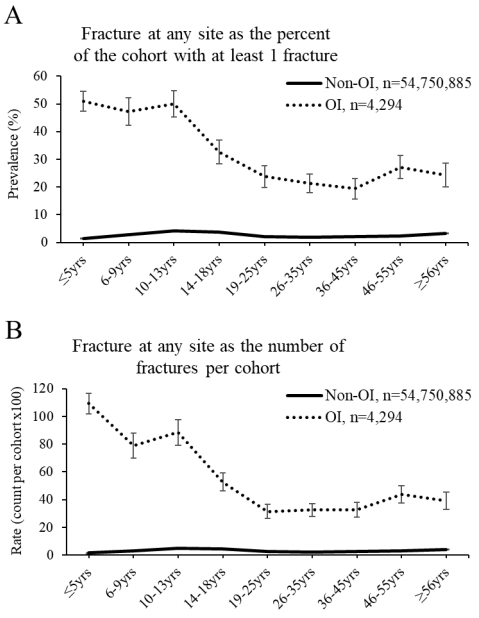

Figure 1. Risk of fracture at any site as (A) the percent of each cohort with at least 1 fracture and (B) the total number of fractures per cohort by age group, for the cohort with osteogenesis imperfecta (OI) (n = 4294) and without OI (n = 54,750,885).

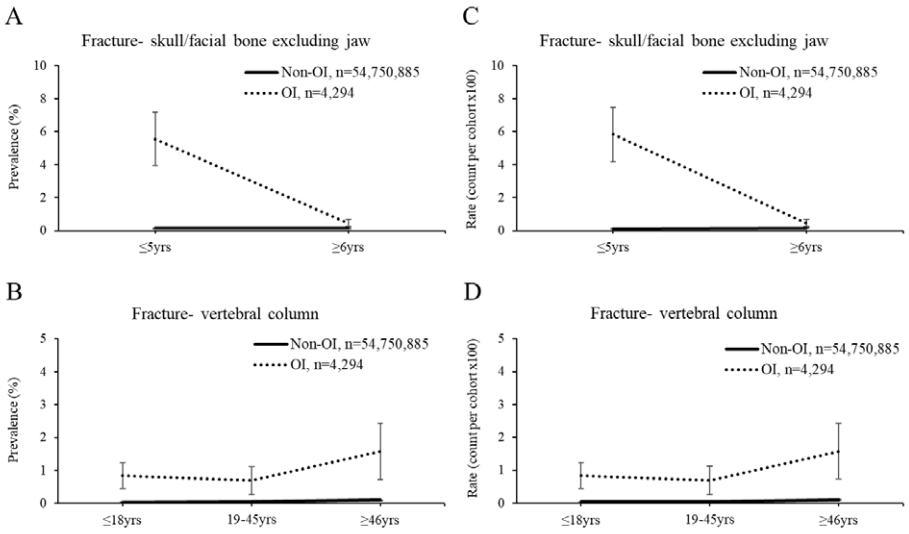

Figure 2. Risk of fracture by site as (A,B) the percent of each cohort with at least 1 fracture at that site and (C,D) the total number of fractures at that site per cohort by age groups for the (A,C) skull and facial bones (excluding the jaw) and (B,D) vertebral column (including pelvis) for the cohort with osteogenesis imperfecta (OI) (n = 4294) and without OI (n = 54,750,885).

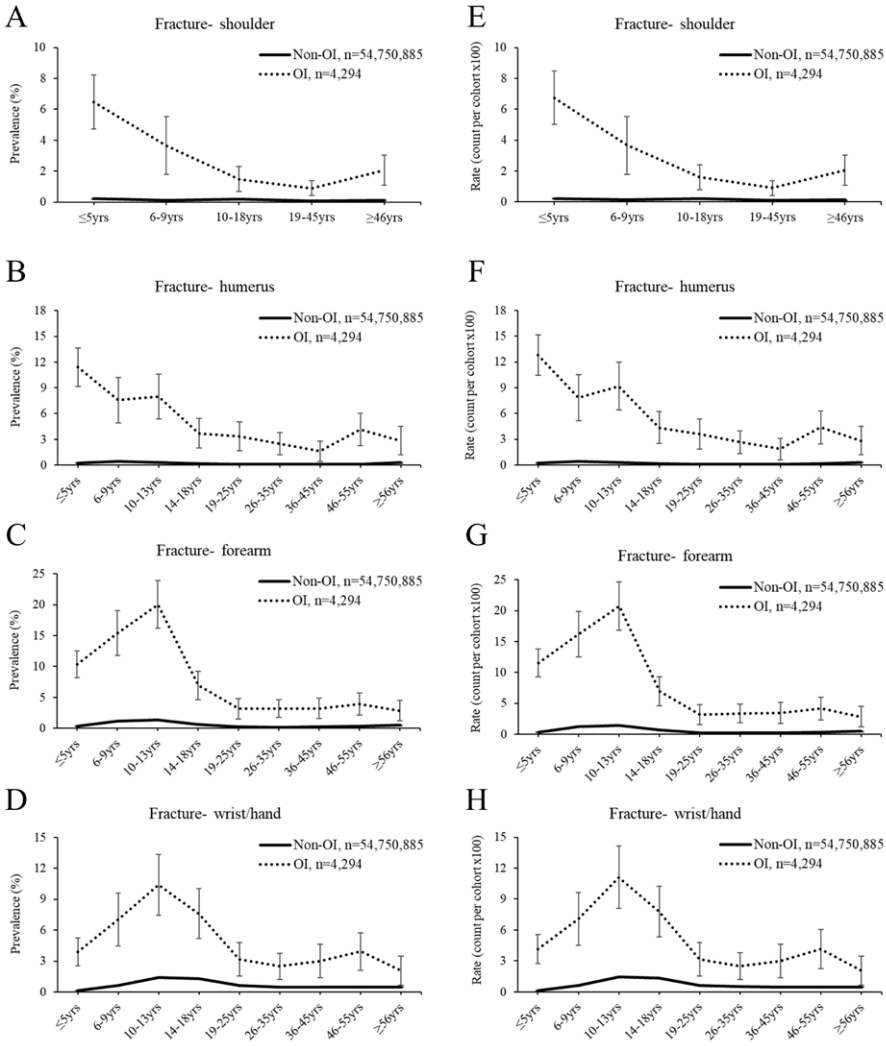

Figure 3. Risk of fracture by site as (A,B,C,D) the percent of each cohort with at least 1 fracture at that site and (E,F,G,H) the total number of fractures at that site per cohort by age groups for the upper extremity sites for the cohort with osteogenesis imperfecta (OI) (n = 4294) and without OI (n = 54,750,885).

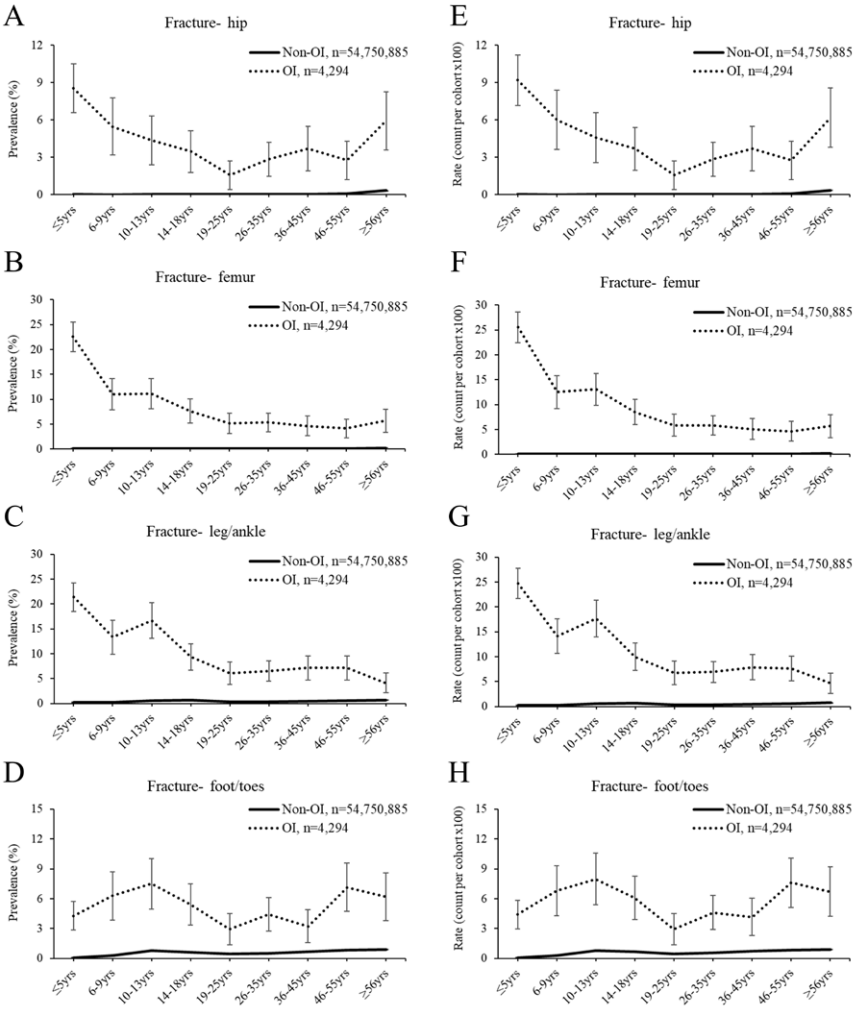

Figure 4. Risk of fracture by site as (A,B,C,D) the percent of each cohort with at least 1 fracture at that site and (E,F,G,H) the total number of fractures at that site per cohort by age groups for the lower extremity sites for the cohort with osteogenesis imperfecta (OI) (n = 4294) and without OI (n = 54,750,885).

Effect Modification by Sex, OI Severity, and Insurance

Effect modification was observed between the OI severity proxy and risk of lower extremity fractures in at least 3 consecutive age groups (*p* for interaction ranged from <0.001 to 0.007, except for the oldest group [≥56 years old], *p*=0.059). In the non-OI cohort, subgroups with 1 or 2+ equipment items showed increasing or stable fracture trends with age. Among OI patients with 1 or 2+ items, trends were more variable but generally decreased with age (**Figure 5)**.

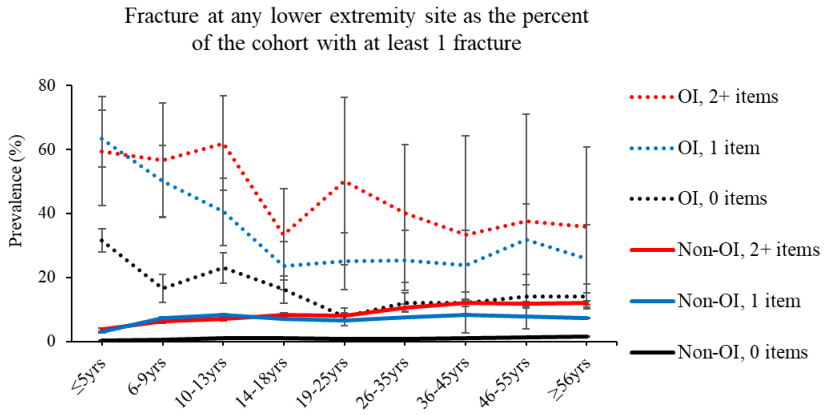

Figure 5. Risk of fracture at any of the lower extremity sites based on evidence of an interaction between cohort (OI vs. non-OI) and the proxy variable for OI severity based on 0, 1, or 2 or more items used to assess the severity of OI.

For outcomes without strong evidence of effect modification, the OR for sex and insurance coverage within the OI cohort are presented in **Table 3.** Females with OI had a lower OR of fractures at any site and in grouped sites compared to males with OI; however, only total and upper extremities reached statistical significance. Individuals with OI covered by Medicaid had a similar overall fracture prevalence as those with Commercial insurance, but higher OR of skull/face and vertebral (including pelvis) fractures, with only vertebral fractures reaching statistical significance.

Table 3. Age-adjusted odds ratio (OR) of the fracture prevalence outcomes by sex and insurance coverage for the cohort with osteogenesis imperfecta (OI) (n = 4294).

	Females (ref: males)	**Medicaid insurance coverage (ref: Commercial)**
	OR (95% CI)	**OR (95% CI)**
Fracture site		
Any site	0.85 (0.75, 0.97)	0.96 (0.84, 1.09)
Skull/face	0.72 (0.45, 1.17)	1.42 (0.85, 2.36)
Vertebral column and pelvis	0.62 (0.33, 1.17)	2.11 (1.07, 4.16)
Upper extremities	0.74 (0.63, 0.88)	0.98 (0.83, 1.16)
Lower extremities	0.91 (0.79, 1.06)	0.99 (0.86, 1.15)

The associations between the OI severity proxy and fracture prevalence are presented in **Table 4**. A severity score of 1 was associated with a significantly higher OR of fracture at any site and all grouped sites compared to a score of 0. A score of 2+ was associated with a further increased OR for most fractured outcomes.

Table 4. Age-adjusted odds ratio (OR) of the fracture prevalence outcomes by the proxy variable for osteogenesis imperfecta (OI) severity for the cohort with OI (n = 4294).

	Proxy of OI severity (ref: 0 items)
	OR (95% CI)
Fracture site	
Any site	
1 item	1.95 (1.66, 2.30)
2+ items	2.86 (2.14, 3.81)
Skull/face	
1 item	2.11 (1.24, 3.58)
2+ items	1.55 (0.60, 3.96)
Vertebral column and pelvis	
1 item	2.62 (1.28, 5.36)
2+ items	6.30 (2.61, 15.19)
Upper extremities	
1 item	1.15 (0.93, 1.43)
2+ items	1.40 (1.00, 1.98)
Lower extremities*	
1 item	2.56 (2.15, 3.06)
2+ items	4.07 (3.05, 5.43)

CI, confidence intervals. All models are adjusted for age (as continuous).
[a]Strong evidence of effect modification between cohort (OI vs. non-OI) and age group; see Fig. 5.

Table 5. Proportion of all fractures by fracture site for the cohorts with osteogenesis imperfecta (OI) and without OI (non-OI).

	OI (n=4,294)	Non-OI (n=54,750,885)
Fracture site		
Jaw	0.8	2.4
Skull/face excluding jaw	2.5	5.3
Vertebral column and pelvis	1.6	2.1
Shoulder	4.5	4.8
Humerus	10.4	6.5
Forearm	14.1	16.3
Wrist/hand	8.5	20.3
Hip	8.3	2.7
Femur	18.7	2.9
Leg/ankle	21.0	16.2
Foot/toes	9.6	20.5

CI, confidence intervals. All models are adjusted for age (as continuous).

Fracture Distribution by Skeletal Site

The distribution of fractures by anatomical site for both cohorts is presented in **Table 5**. The pattern of fracture sites differed markedly between cohorts. Jaw, skull/face, wrist/hand, and foot/toes fractures accounted for ~2 to 3x greater proportion of the total fractures in the non-OI cohort than in the OI. Conversely, hip and femur fractures constituted ~3 to 7x greater proportion of all fractures in the OI cohort. The proportion of all fractures by site, stratified by age group, is presented in **Figure 6**.

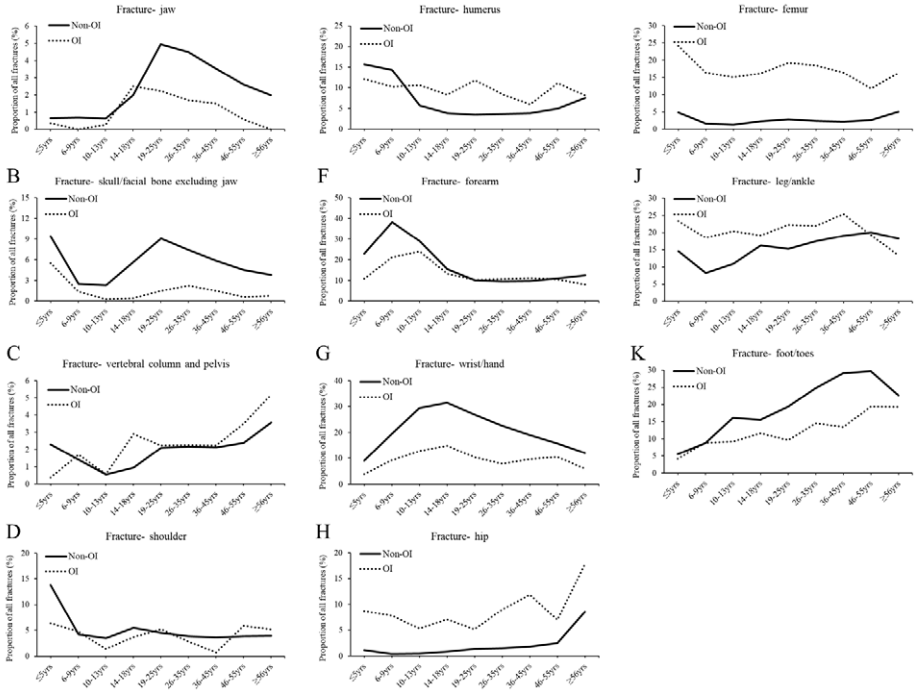

Figure 6. The proportion of all fractures (as the total count) by fracture site for the cohort with osteogenesis imperfecta (OI) (n = 4294) and without OI (n = 54,750,885) by age group.

Discussion

This large, nationwide study advances understanding of fracture epidemiology across the OI spectrum in the United States, providing population-level estimates for craniofacial and whole-skeleton fractures throughout the lifespan. Leveraging extensive and heterogeneous national claims data, our analysis documents fracture risk, age-specific patterns, and site-specific distribution in this rare disease population.

A principal insight of this study is the high and dynamic burden of skeletal fragility in OI. Fracture risk among individuals with OI was found to be highest in early childhood, declining through adolescence and young adulthood, and increasing again later in life[19, 20, 22]. The observed overall fracture prevalence (33.9% in OI) and relative risk (13.6-fold higher than non-OI) closely aligns with previous U.S. insurance claims-based estimates (e.g., a 40% one-year occurrence) and international registry data indicating that fracture risk is a near-universal clinical hallmark of OI[20, 22]. Our findings reinforce the persistent and elevated risk throughout life and echo similar age-related fracture trajectories reported in other rare disease registries[22].

Importantly, our results further elucidate the role of insurance and socioeconomic factors in shaping fracture risk and ascertainment. Notably, OI individuals with Medicaid coverage had higher odds of craniofacial and vertebral fractures than those with commercial insurance, though the overall fracture prevalence was similar. This may reflect the complex interplay of medical eligibility (children with more severe OI more likely to qualify for Medicaid), differences in healthcare access and utilization, and demographic or socioeconomic disparities. Additionally, occupation and physical activity levels—often linked to insurance status—may also contribute, although such specifics are not captured in claims data. These findings highlight the potential for ascertainment bias in claims-based studies, as insurance coverage influences both access to care and the likelihood of fractures being clinically reported.

The current study extends the literature by providing robust population-level estimates of craniofacial fracture risk in OI. Previous research has primarily described craniofacial fractures in OI through case reports or small series[23, 24, 26], often focusing on iatrogenic jaw injuries from dental procedures[37, 38]. While our study confirms that craniofacial fractures, especially of the jaw, are more frequent in individuals with OI compared to the general population, their absolute prevalence remains low relative to fractures of long bones and the spine. Due to limitations in claims data, we were unable to distinguish between traumatic, spontaneous, and procedure-related (iatrogenic) jaw fractures. This limitation may lead to an overestimation of spontaneous jaw fracture rates in the OI population, and future studies using more granular clinical data are warranted to differentiate these causes.

Our detailed analysis of fracture site distribution further builds on previous registry and hospital-based studies[8, 19-22]. The notably high proportion of femur and hip fractures seen here aligns with earlier hospital and registry reports, where femoral involvement was reported in up to 50–65% of OI fracture cases[8, 22]. Similarly, the

observed pattern of vertebral fractures increasing with age mirrors the osteoporotic tendency and vertebral vulnerability described in OI and osteoporosis literature[39-41]. In contrast, the relative scarcity of craniofacial fractures compared to long bone involvement underlines important biomechanical and anatomical distinctions.

Several clinical and sociodemographic factors were associated with fracture risk. More severe diseases, measured by the use of multiple assistive devices or related condition, were linked to higher fracture risk at axial sites, consistent with prior findings showing the impact of disease severity on OI morbidity. Medicaid coverage was associated with higher odds of fractures specifically at craniofacial and vertebral sites. This pattern may reflect, in part, that children with more severe or complex OI, who are at higher risk for such fractures, are more likely to be enrolled in Medicaid due to medical eligibility criteria, rather than solely economic need. Additionally, variations in access to specialty care, healthcare utilization, or surveillance practices among Medicaid recipients may contribute to these findings. Thus, differences in fracture risk by insurance type likely reflect a combination of medical complexity, access, and policy differences rather than straightforward socioeconomic status alone.

Our methodological approach has strengths and limitations inherent to claim-based research. Large databases such as MarketScan® permit broad, real-world epidemiologic analyses of diverse cohorts beyond what single-center studies can offer. Recent studies in other rare diseases such as Duchenne muscular dystrophy and Ehlers-Danlos syndromes have demonstrated similar strengths and limitations in MarketScan-based research, highlighting its utility for investigating treatment patterns and healthcare costs, while recognizing issues of coverage gaps and coding accuracy[42, 43]. To further improve precision and population coverage, future research should integrate complementary data sources, such as Medicare claims, patient registries, and clinical records to improve precision and extend representation.

Several limitations must be considered when interpreting our findings. First, the MarketScan® Commercial Database excludes individuals aged 65 and older, those who are uninsured, and people with other public insurance, which restricts generalizability—particularly for older adults living with osteogenesis imperfecta (OI). While the Multi-State Medicaid database covers all ages, regional variation in Medicaid programs may affect case capture and introduce further heterogeneity.

A key limitation of administrative claims data is the reliance on ICD and CPT codes for identifying fractures. These codes capture diagnoses and treatments but do not

provide information about fracture etiology—such as whether injuries are sports-related, spontaneous, or iatrogenic—or about lifestyle risk factors and exposure to fracture-altering treatments. Consequently, the specific context of injury events, which can be especially relevant in healthy children and adolescents, cannot be discerned. However, this limitation is less consequential in OI, where intrinsic bone fragility results in fractures from minimal or unidentifiable trauma, making etiological distinctions both clinically challenging and less critical[44]. Since physical activity is recommended for individuals with OI[44-46], the overall fracture propensity described here serves as a pragmatic and meaningful measure of skeletal health, reflecting real-world risk for those encouraged to remain active.

Additionally, our proxies for OI severity were informed by prior studies but remain unvalidated, and the inability to apply recognized classification systems like Sillence precludes differentiation between milder and more severe disease forms[14]. While radiographic evidence, such as documentation of vertebral fractures or bone deformities, might provide further insight into clinical severity, such measures are not consistently available and remain unvalidated for use in claims data. Future research should aim to refine and validate these proxies to improve risk assessment.

Furthermore, administrative claims analysis are limited to periods of health plan enrollment, potentially missing fractures that occurred prior to study entry and preventing lifelong cumulative incidence estimates. The prevalence of undiagnosed OI in the general population is poorly characterized, meaning that claims-based approaches may underestimate the true burden. Although database constraints precluded age- and sex-standardized fracture rate calculations, we performed site-, age-, and sex-stratified analyses that yield actionable insights into subgroup-specific risks—an important consideration in heterogeneous rare diseases like OI.

It should be noted that, although our databases span up to six years of enrollment, we opted for a 1-year period prevalence design to maximize sample size and minimize selection bias associated with requiring longer continuous coverage. We recognize, however, that longitudinal analyses could offer more comprehensive insights into fracture incidence, recurrence, and the effects of treatments over time in individuals with OI. Future research utilizing longer periods of observation is warranted to explore these temporal dynamics in greater detail.

Despite these limitations, this study is highly valuable in addressing critical gaps in our understanding of fracture risk among individuals with OI. Not all patients are captured by national registries or advocacy organizations such as the OI

Foundation, and clinical cohorts at any single center are typically small due to the rarity of the disease. By leveraging large, national claims databases, our study provides a broader, population-based perspective, capturing real-world experiences of individuals with OI who might otherwise be overlooked. This national scope enhances the relevance and generalizability of our findings, offering pragmatic and clinically meaningful insights into fracture risk and disease burden among a diverse OI population that has historically been difficult to study. These results are therefore an important contribution to the evidence base and can inform improved care and resource allocation for individuals with OI nationwide.

In summary, this study offers a comprehensive, population-based assessment of fracture risk and distribution in OI, including new insights into craniofacial and jaw involvement. Our findings provide a foundation for improved anticipatory guidance, interdisciplinary care, and targeted prevention strategies for individuals with OI. As claims-based epidemiology continues to evolve, future research should triangulate claims data with clinical, genetic, and dental sources to optimize outcomes for the OI community.

References

1. Marini JC, Forlino A, Bachinger HP, Bishop NJ, Byers PH, Paepe A, Fassier F, Fratzl-Zelman N, Kozloff KM, Krakow D, Montpetit K, Semler O. Osteogenesis imperfecta. Nat Rev Dis Primers. 2017;3:17052. Epub 2017/08/19. doi: 10.1038/nrdp.2017.52. PubMed PMID: 28820180.
2. Marini JC, Forlino A, Cabral WA, Barnes AM, San Antonio JD, Milgrom S, Hyland JC, Korkko J, Prockop DJ, De Paepe A, Coucke P, Symoens S, Glorieux FH, Roughley PJ, Lund AM, Kuurila-Svahn K, Hartikka H, Cohn DH, Krakow D, Mottes M, Schwarze U, Chen D, Yang K, Kuslich C, Troendle J, Dalgleish R, Byers PH. Consortium for osteogenesis imperfecta mutations in the helical domain of type I collagen: regions rich in lethal mutations align with collagen binding sites for integrins and proteoglycans. Hum Mutat. 2007;28(3):209-21. Epub 2006/11/02. doi: 10.1002/humu.20429. PubMed PMID: 17078022; PMCID: PMC4144349.
3. Rork WC, Hertz AG, Wiese AD, Kostick KM, Nguyen D, Schneider SC, Shepherd WS, Cho H, Members of the B, Murali CN, Lee B, Sutton VR, Storch EA. A qualitative exploration of patient perspectives on psychosocial burdens and positive factors in adults with osteogenesis imperfecta. Am J Med Genet A. 2023;191(9):2267-75. Epub 20230615. doi: 10.1002/ajmg.a.63323. PubMed PMID: 37317786; PMCID: PMC10525007.
4. Hill M, Hammond J, Sharmin M, Lewis C, Heathfield M, Crowe B, Gotherstrom C, Chitty LS, DeVile C. Living with osteogenesis imperfecta: A qualitative study exploring experiences and psychosocial impact from the perspective of patients, parents and professionals. Disabil Health J. 2022;15(1):101168. Epub 20210708. doi: 10.1016/j.dhjo.2021.101168. PubMed PMID: 34266787.
5. Marom R, Rabenhorst BM, Morello R. Osteogenesis imperfecta: an update on clinical features and therapies. Eur J Endocrinol. 2020;183(4):R95-R106. doi: 10.1530/EJE-20-0299. PubMed PMID: 32621590; PMCID: PMC7694877.
6. Chhabra BN, Phillips T, Mitchell TW, Gattu N, Ezeokoli EU, Bell B. Pediatric Hand and Wrist Fractures in Osteogenesis Imperfecta: An Analysis of Incidence, Patient-specific Risk Factors, and Fracture-specific Characteristics. J Pediatr Orthop. 2023;43(8):e680-e5. Epub 20230605. doi: 10.1097/BPO.0000000000002449. PubMed PMID: 37278060.
7. Joshi KK, Siafarikas A, Prince R. The Natural History of Symptomatic Fractures in Children and Adolescents with Osteogenesis Imperfecta Type 1: A Cohort Study from Western Australia. JBMR Plus. 2023;7(9):e10782. Epub 20230621. doi: 10.1002/jbm4.10782. PubMed PMID: 37701152; PMCID: PMC10494498.
8. Philippoteaux C, Lefevre C, Saint-Dizier C, Paccou J, Chazard E. Mortality and fracture risk in children with osteogenesis imperfecta: Results from the French nationwide hospital discharge database. Bone. 2025;200:117607. Epub 20250811. doi: 10.1016/j.bone.2025.117607. PubMed PMID: 40803492.
9. Riley E, Elgarwany S, Arundel P, Bishop NJ, Offiah AC. An observational study of the prevalence of classic metaphyseal fractures in children with osteogenesis imperfecta in the first two years of life. Clin Radiol. 2025;87:106964. Epub 20250517. doi: 10.1016/j.crad.2025.106964. PubMed PMID: 40505223.
10. Waltimo-Siren J, Tuurala H, Saamaki E, Holst P, Evalahti M, Arponen H. Dental and dentoalveolar dimensions in individuals with osteogenesis imperfecta. Acta Odontol Scand. 2021;79(5):390-5. Epub 20210215. doi: 10.1080/00016357.2021.1881160. PubMed PMID: 33587862.
11. Stephen LX, Beighton P. Dental management of severe dentinogenesis imperfecta in a mild form of osteogenesis imperfecta. J Clin Pediatr Dent. 2002;26(2):131-6. doi: 10.17796/jcpd.26.2.r852g46052604266. PubMed PMID: 11878277.
12. Barron MJ, McDonnell ST, Mackie I, Dixon MJ. Hereditary dentine disorders: dentinogenesis imperfecta and dentine dysplasia. Orphanet J Rare Dis. 2008;3:31. Epub 20081120. doi: 10.1186/1750-1172-3-31. PubMed PMID: 19021896; PMCID: PMC2600777.

13. Malmgren B, Norgren S. Dental aberrations in children and adolescents with osteogenesis imperfecta. Acta Odontol Scand. 2002;60(2):65-71. doi: 10.1080/000163502753509446. PubMed PMID: 12020117.

14. Van Dijk FS, Sillence DO. Osteogenesis imperfecta: clinical diagnosis, nomenclature and severity assessment. Am J Med Genet A. 2014;164A(6):1470-81. Epub 20140408. doi: 10.1002/ajmg.a.36545. PubMed PMID: 24715559; PMCID: PMC4314691.

15. Lund AM, Hansen M, Kollerup G, Juul A, Teisner B, Skovby F. Collagen-derived markers of bone metabolism in osteogenesis imperfecta. Acta Paediatr. 1998;87(11):1131-7. doi: 10.1080/080352598750031112. PubMed PMID: 9846914.

16. Van Dijk FS, Pals G, Van Rijn RR, Nikkels PG, Cobben JM. Classification of Osteogenesis Imperfecta revisited. Eur J Med Genet. 2010;53(1):1-5. Epub 20091028. doi: 10.1016/j.ejmg.2009.10.007. PubMed PMID: 19878741.

17. Andersson K, Dahllof G, Lindahl K, Kindmark A, Grigelioniene G, Astrom E, Malmgren B. Mutations in COL1A1 and COL1A2 and dental aberrations in children and adolescents with osteogenesis imperfecta - A retrospective cohort study. PLoS One. 2017;12(5):e0176466. Epub 20170512. doi: 10.1371/journal.pone.0176466. PubMed PMID: 28498836; PMCID: PMC5428910.

18. O'Connell AC, Marini JC. Evaluation of oral problems in an osteogenesis imperfecta population. Oral Surg Oral Med Oral Pathol Oral Radiol Endod. 1999;87(2):189-96. doi: 10.1016/s1079-2104(99)70272-6. PubMed PMID: 10052375.

19. Abraham P, Miles G, Petruski-Ivleva N, Hawaldar K, Robinson C, Berger KI. A real-world analysis of the clinical and healthcare burden associated with osteogenesis imperfecta. Bone. 2025;200:117572. Epub 20250628. doi: 10.1016/j.bone.2025.117572. PubMed PMID: 40588112.

20. Yang Ec, O; Gupta, R; Shen, Y; Sader, s; Beyers, H; Jain, M; Franzone, J. Real World Data of Fracture Rates and Musculoskeletal Disorders for Patients Living with Osteogenesis Imperfecta (OI). JBMR *plus*. 2025.

21. Park SH, Yoon H, Yoon S, Chung J, Kim JH, Lee S. Analyses of Osteogenesis Imperfecta in South Korea Using the Nationwide Health Insurance Service Claim Data: A Propensity Score-Matched Study. Calcif Tissue Int. 2024;115(6):915-22. Epub 20240816. doi: 10.1007/s00223-024-01274-5. PubMed PMID: 39150494.

22. Folkestad L, Hald JD, Ersboll AK, Gram J, Hermann AP, Langdahl B, Abrahamsen B, Brixen K. Fracture Rates and Fracture Sites in Patients With Osteogenesis Imperfecta: A Nationwide Register-Based Cohort Study. J Bone Miner Res. 2017;32(1):125-34. Epub 20160829. doi: 10.1002/jbmr.2920. PubMed PMID: 27448250.

23. Ehrenfeld M, Schwenzer N. [Fracture of the mandible in osteogenesis imperfecta]. Aktuelle Traumatol. 1989;19(3):107-9. PubMed PMID: 2568078.

24. Ehrenfeld M, Schwenzer N. [Fracture of the mandible in osteogenesis imperfecta. Case report and literature review]. Dtsch Z Mund Kiefer Gesichtschir. 1989;13(1):49-53. PubMed PMID: 2689022.

25. Urquiza-Fornovi I, Redondo-Alamillos M, Garcia R, II, Romance-Garcia AI. Mandible fracture in a child with osteogenesis imperfecta on bisphosphonates. Open versus closed treatment? A case report. Dent Traumatol. 2020;36(6):692-6. Epub 20200909. doi: 10.1111/edt.12596. PubMed PMID: 32790945.

26. Kobayashi Y, Satoh K, Mizutani H. Osteogenesis Imperfecta Diagnosed from Mandibular and Lower Limb Fractures: A Case Report. Craniomaxillofac Trauma Reconstr. 2016;9(2):141-4. Epub 20150428. doi: 10.1055/s-0035-1550063. PubMed PMID: 27162570; PMCID: PMC4858426.

27. Reece MKJ, Quillin K, Homewood TJ, Bunevich J. Surgical Treatment of a Bilateral Mandibular Fracture in a Patient with Osteogenesis Imperfecta Type III. Plast Reconstr Surg Glob Open. 2021;9(7):e3702. Epub 20210719. doi: 10.1097/GOX.0000000000003702. PubMed PMID: 34290943; PMCID: PMC8288904.

28. Masroor T, Chappell AG, Shahzad F. Anesthetic and Surgical Considerations in Osteogenesis Imperfecta: A Case Report of Mandible Fracture Management. Eplasty. 2022;22:e12. Epub 20220505. PubMed PMID: 35611149; PMCID: PMC9108419.

29. Gallego L, Junquera L, Pelaz A, Costilla S. Pathological mandibular fracture after simple molar extraction in a patient with osteogenesis imperfecta treated with alendronate. Med Oral Patol Oral Cir Bucal. 2010;15(6):e895-7. Epub 20101101. doi: 10.4317/medoral.15.e895. PubMed PMID: 20526255.

30. Altalib A, Althomali A, Alshahrani A, Alfrayyan A, Aljughaiman MS. Osteogenesis Imperfecta and Child Abuse From a Forensic Point of View. Cureus. 2021;13(1):e12790. Epub 20210119. doi: 10.7759/cureus.12790. PubMed PMID: 33628660; PMCID: PMC7891677.

31. Pepin MG, Byers PH. What every clinical geneticist should know about testing for osteogenesis imperfecta in suspected child abuse cases. Am J Med Genet C Semin Med Genet. 2015;169(4): 307-13. Epub 20151114. doi: 10.1002/ajmg.c.31459. PubMed PMID: 26566591.

32. D'Eufemia P, Palombaro M, Lodato V, Zambrano A, Celli M, Persiani P, De Bari MP, Sangiorgi L. Child abuse and osteogenesis imperfecta: how can they be still misdiagnosed? A case report. Clin Cases Miner Bone Metab. 2012;9(3):195-7. Epub 20121220. PubMed PMID: 23289038; PMCID: PMC3535999.

33. Ojima K, Matsumoto H, Hayase T, Fukui Y. An autopsy case of osteogenesis imperfecta initially suspected as child abuse. Forensic Sci Int. 1994;65(2):97-104. doi: 10.1016/0379-0738(94)90264-x. PubMed PMID: 8206461.

34. Keshishian A, Boytsov N, Burge R, Krohn K, Lombard L, Zhang X, Xie L, Baser O. Examining the Effect of Medication Adherence on Risk of Subsequent Fracture Among Women with a Fragility Fracture in the U.S. Medicare Population. J Manag Care Spec Pharm. 2017;23(11):1178-90. doi: 10.18553/jmcp.2017.17054. PubMed PMID: 29083977.

35. Liu J, Guo H, Rai P, Pinto L, Barron R. Medication persistence and risk of fracture among female Medicare beneficiaries diagnosed with osteoporosis. Osteoporos Int. 2018;29(11):2409-17. Epub 2018/07/20. doi: 10.1007/s00198-018-4630-6. PubMed PMID: 30022254.

36. Whitney DG, Clines GA, Leis AM, Caird MS, Hurvitz EA. Five-year risk of fracture and subsequent fractures among adults with cerebral palsy. Bone Rep. 2022;17:101613. Epub 2022/09/03. doi: 10.1016/j.bonr.2022.101613. PubMed PMID: 36052289; PMCID: PMC9424353.

37. Kim MY, Kim CH. Iatrogenic mandibular fracture after open reduction and internal fixation in a patient with osteogenesis imperfecta. Br J Oral Maxillofac Surg. 2017;55(9):971-3. Epub 20171014. doi: 10.1016/j.bjoms.2017.09.003. PubMed PMID: 29037585.

38. Tieghi R, Consorti G, Clauser LC. Pathololgic fracture of the mandible after removal of follicular cyst. J Craniofac Surg. 2011;22(5):1779-80. doi: 10.1097/SCS.0b013e31822e77c6. PubMed PMID: 21959430.

39. Kanis JA, McCloskey EV. Epidemiology of vertebral osteoporosis. Bone. 1992;13 Suppl 2:S1-10. doi: 10.1016/8756-3282(92)90189-4. PubMed PMID: 1385718.

40. Loffler MT, Kallweit M, Niederreiter E, Baum T, Makowski MR, Zimmer C, Kirschke JS. Epidemiology and reporting of osteoporotic vertebral fractures in patients with long-term hospital records based on routine clinical CT imaging. Osteoporos Int. 2022;33(3):685-94. Epub 20211014. doi: 10.1007/s00198-021-06169-x. PubMed PMID: 34648040; PMCID: PMC8844161.

41. Nguyen HT, Nguyen BT, Thai THN, Tran AV, Nguyen TT, Vo T, Mai LD, Tran TS, Nguyen TV, Ho-Pham LT. Prevalence, incidence of and risk factors for vertebral fracture in the community: the Vietnam Osteoporosis Study. Sci Rep. 2024;14(1):32. Epub 20240102. doi: 10.1038/s41598-023-50145-w. PubMed PMID: 38168502; PMCID: PMC10761939.

42. Klimchak AC, Signorovitch J, Innis B, Laverty CG, Gooch K. Assessment of Phosphorodiamidate Morpholino Oligomer Treatment Patterns for Patients with Duchenne Muscular Dystrophy: A MarketScan Claims Analysis. Adv Ther. 2025;42(1):523-36. Epub 20241111. doi: 10.1007/s12325-024-03044-z. PubMed PMID: 39527337; PMCID: PMC11782370.

43. Schubart JR, Schaefer EW, Knight DRT, Mills SE, Francomano CA. Estimates of the excess cost burden of Ehlers-Danlos syndromes: a United States MarketScan(R) claims database analysis. Front Public Health. 2024;12:1365712. Epub 20240703. doi: 10.3389/fpubh.2024.1365712. PubMed PMID: 39022417; PMCID: PMC11252068.

44. Nijhuis W, Franken A, Ayers K, Damas C, Folkestad L, Forlino A, Fraschini P, Hill C, Janus G, Kruse R, Lande Wekre L, Michiels L, Montpetit K, Panzeri L, Porquet-Bordes V, Rauch F, Sakkers R, Salles JP, Semler O, Sun J, To M, Tosi L, Yao Y, Yeung EHK, Zhytnik L, Zillikens MC, Verhoef M. A standard set of outcome measures for the comprehensive assessment of osteogenesis imperfecta. Orphanet J Rare Dis. 2021;16(1):140. Epub 20210320. doi: 10.1186/s13023-021-01682-y. PubMed PMID: 33743784; PMCID: PMC7980586.

45. Nijhuis W, Verhoef M, van Bergen C, Weinans H, Sakkers R. Fractures in Osteogenesis Imperfecta: Pathogenesis, Treatment, Rehabilitation and Prevention. Children (Basel). 2022;9(2). Epub 20220216. doi: 10.3390/children9020268. PubMed PMID: 35204988; PMCID: PMC8869965.

46. Gilani M, Todd S, Wong SC, McDevitt H, Kyriakou A, Mason A. Acceptability and Barriers of Exercise in Children With Osteogenesis Imperfecta. Arch Rehabil Res Clin Transl. 2025;7(3):100458. Epub 20250428. doi: 10.1016/j.arrct.2025.100458. PubMed PMID: 40980517; PMCID: PMC12447189.

Supplementary

Supplementary Table 1. International Classification of Diseases, Tenth Revision, Clinical Modification (ICD) codes and Healthcare Common Procedure Coding System (HCPCS) codes used to identify study variables.

Variable	ICD codes	HCPCS codes
Osteogenesis imperfecta	Q78.0	
Dentinogenesis imperfecta	K00.5	
Hearing loss	H90.x	
Scoliosis	M41.x	
Wheelchair parts and accessories		E0950-E1299
Orthotics		L0112-L2136
Fracture	M80.x, M84.3x, M8.4x, M84.6x, M84.7x, S02.x, S12.x, S22.x, S32.x, S42.x, S52.x, S62.x, S72.x, S82.x, S92.x	

CHAPTER 4

Collagen mutation and age contribute to differential craniofacial phenotypes in mouse models of osteogenesis imperfecta

Hsiao H Sung [1 2 3], Wyatt J Spresser [2], Joseph P Hoffmann [2], Zongrui Dai [4], Peter M Van der Kraan [3], Michelle S Caird [1], Esmeralda Blaney Davidson [3], Kenneth M Kozloff [1]

[1.] Orthopaedic Research Laboratories, Department of Orthopaedic Surgery, University of Michigan, Ann Arbor, MI 48109, United States.

[2.] Department of Oral and Maxillofacial Surgery, University of Michigan, Ann Arbor, MI 48109, United States.

[3.] Experimental Rheumatology, Department of Rheumatology, Radboud Medical Centre, Nijmegen, The Netherlands, 6525 GA.

[4.] Department of Biostatistics, University of Michigan, Ann Arbor, MI 48109, United States.

JBMR Plus. 2024 Jan 4;8(1):ziad004. doi: 10.1093/jbmrpl/ziad004. eCollection 2024 Jan.

Abstract

Craniofacial and dentoalveolar abnormalities are present in all types of osteogenesis imperfecta (OI). Mouse models of the disorder are critical to understand these abnormalities and underlying OI pathogenesis. Previous studies on severely affected OI mice report a broad spectrum of craniofacial phenotypes, exhibiting some similarities to the human disorder. The Brtl/+ and G610c/+ are moderately severe and mild-type IV OI, respectively. Little is known about the aging effects on the craniofacial bones of these models and their homology to human OI. This study aimed to analyze the Brtl/+ and G610c/+ craniofacial morphometries during aging to establish suitability for further OI craniofacial bone intervention studies. We performed morphological measurements on the micro-CT-scanned heads of 3-wk-old, 3-mo-old, and 6-mo-old female Brtl/+ and G610c/+ mice. We observed that Brtl/+ skulls are shorter in length than WT ($P < .05$), whereas G610c/+ skulls are similar in length to their WT counterparts. The Brtl/+ mice exhibit alveolar bone with a porotic-like appearance that is not observed in G610c/+. As they age, Brtl/+ mice show severe bone resorption in both the maxilla and mandible ($P < .05$). By contrast, G610c/+ mice experience mandibular resorption consistently across all ages, but maxillary resorption is only evident at 6 mo ($P < .05$). Western blot shows high osteoclastic activities in the Brtl/+ maxilla. Both models exhibit delayed pre-functional eruptions of the third molars ($P < .05$), which are similar to those observed in some bisphosphonate-treated OI subjects. Our study shows that the Brtl/+ and G610c/+ mice display clear features found in type IV OI patients; both show age-related changes in the craniofacial growth phenotype. Therefore, understanding the craniofacial features of these models and how they age will allow us to select the most accurate mouse model, mouse age, and bone structure for the specific craniofacial bone treatment of differing OI groups.

Keywords: alveolar bone; mandible; maxilla; micro-CT imaging; osteogenesis imperfecta; teeth.

Lay Summary

Brtl/+ and G610c/+ are distinct Osteogenesis Imperfecta (OI) mouse models with unique collagen1 mutations. Brtl/+ mice exhibit shorter skulls, porotic-like alveolar bone, and age-related bone resorption in both the maxilla and mandible. In contrast, G610c/+ mice resemble wild-type in alveolar bone appearance but also display age-related mandibular resorption. Both models show delayed third molar eruptions, resembling some OI patients. These model differences provide valuable insights for studying OI-related craniofacial bone treatments and the effects of aging on craniofacial features.

Graphical Abstract

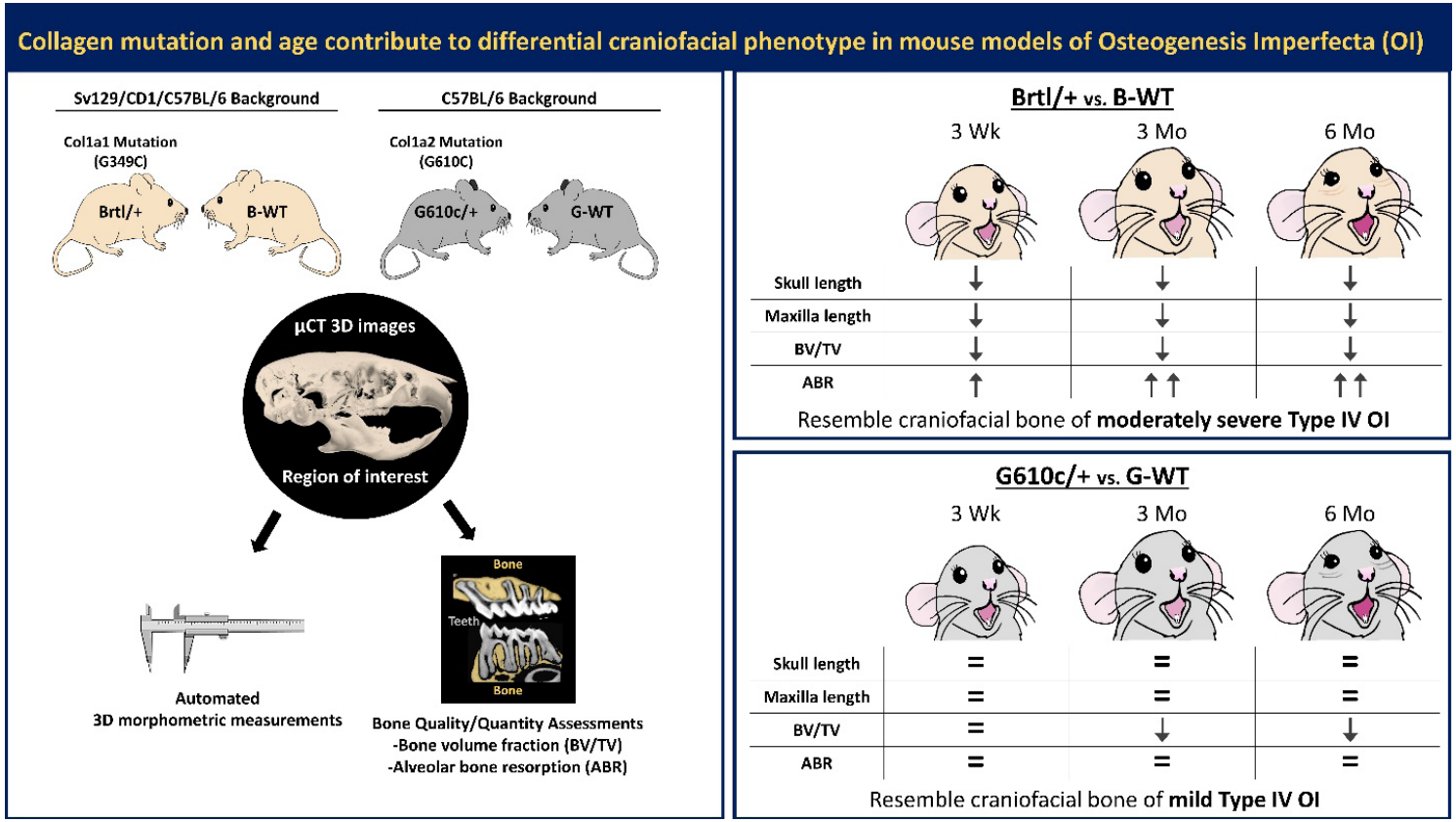

Introduction

Osteogenesis imperfecta (OI) is a congenital disease characterized by bone dysplasia due to an abnormality in the synthesis and/or processing of the main protein of the bone extracellular matrix (ECM), type I collagen[1]. OI is mainly caused by *COL1A1* or *COL1A2* gene mutations[2] and less commonly by mutations in genes encoding collagen-associated proteins (recessive forms)[3]. These mutations contribute to more than 22 OI types, with types I to IV being the most common[4]. Type I collagen (Col1) is the most abundant protein found in bone[5]. Defects in Col1 can result in bone quality, quantity, and/or morphologic alterations, as seen in OI[5]. These Col1 alterations induce a unique facial appearance in OI, differing significantly from the non-OI population.

Type IV OI is highly variable, with symptoms ranging from mild to moderately severe bone deformity, reduced bone mineral density (BMD), and abnormal bone microarchitecture[6,7]. Fracture rates in type IV OI children tend to decrease with age, typically after puberty[8]. Type IV OI subjects also exhibit abnormal craniofacial morphologies, such as relative macrocephaly, brachycephaly, variable Dentinogenesis Imperfecta expression, tooth agenesis, increased hypodontia, and poor dentoalveolar bone development[7, 9-14].

These high clinical heterogeneities are governed by the mutated gene, the mutation type, the mutation position along the gene, and the patient's genetic background[15]. Mouse models of the disorder are critical in understanding both the normal physiology, underlying OI pathogenesis, and response to medication therapies. Brtl/+ and G610c/+ mice are type IV OI mouse models extensively studied in long bones for bone growth deficiencies, impaired fracture healing, defective mineralization of developing bone, and disrupted osteoblast differentiation[16-20]. Both models have a glycine substitution in *Col1a1/2* genes, one of the most common mutation types in OI patients[21,22]. The Brtl/+ mouse has *COL1A1* missense mutations that change an obligatory glycine to a cysteine at the 349th amino-acid residue of the triple-helical domain[23]. Similarly, the G610c/+ mouse has *COL1A2* missense mutations that change an obligatory glycine to a cysteine at the 610th amino-acid residue of the triple-helical domain[24]. Despite the similar mutation type, different causative genes, mutation positions, and mouse genetic backgrounds cause these two mice to exhibit different OI severities and aging characteristics. In our previous work examining Brtl/+ calvarial bones treated with the anabolic sclerostin antibody, we found that the genotype has a modest influence on skull shape[25]. Brtl/+ displayed a slightly larger, straighter lambda angle and a smaller, sharper bregma angle, resulting in a mildly domed skull appearance compared to the WT[25].

However, there is a notable gap in the literature concerning craniofacial growth and development, especially of the maxilla and mandible, in both Brtl/+ and G610c/+ genotypes, with a particular emphasis on the effects of aging on these bones.

As humans, these mice have two distinct ossification modes, intramembranous and endochondral, that differentially develop the craniofacial and long bone microarchitectures, respectively[26]. Therefore, study results assessing long-bone morphology and aging characteristics in Brtl/+ and G610c/+ are not necessarily applicable to the craniofacial bone. Thus, this study aimed to analyze the Brtl/+ and G610c/+ craniofacial morphometrics and characteristics with aging to establish whether they are suitable models for studying efficient and safe OI craniofacial bone therapeutic interventions.

Material and method

Experimental animals

The University of Michigan's Committee on the Use and Care of Animals approved all protocols and procedures. All animals were bred and housed in an AAALAC-accredited vivarium. Female Brtl/+ mice have a mixed background of SV129/CD1/C57BL/6 and were derived from heterozygous Brtl/+ and WT parental strains. Female G610c/+ have a background of C57BL/6 and were derived from heterozygous G610c/+ and WT parental strains. Mice were euthanized at 3 weeks (3w), 3 months (3m), or 6 months (6m) of age (Table 1).

Table 1. Sample size

Strain	Female Brtl		Female G610c	
Age / geno	WT	Brtl/+ (Het)	WT	G610c/+ (Het)
3w	11	10	11	10
3m	12	11	12	10
6m	10	10	10	10
Total	**33**	**31**	**33**	**30**

Micro-computed tomography (µCT) & analysis

A total of 127 mouse skulls were scanned with high-resolution µCT (Bruker Skyscan 1176; Bruker, Kontich, Belgium) (Table 1). Image acquisition was performed using our previously reported protocol[25]. Individual 2D cross-sectional images were reconstructed into 3D volumes with 9-µm isotropic voxel size using NRecon

software (version 1.6.5.8; Bruker). Dragonfly 2.0 (ORS, Denver, USA) was used to delineate the region of interest and to perform crania, maxilla, and mandible measurements, segmentations, and bone volume fraction analysis.

1. Craniofacial linear measurements*:* Measurements were performed on 3D reconstructed volumes. Landmarks (Figure S1) were placed manually on the 3D reconstructed images, and the measurements were processed with an automated plug-in provided by ORS Dragonfly Team. Most of these parameters have been defined previously[27,28]. All measurements were conducted by three users to ensure precision in landmark placement. The resulting standard errors across evaluators were below 5%.

2. Maxilla alveolar bone volume fraction*:* Alveolar bone was evaluated at a region of interest that includes anteroposteriorly the mesial side of the first molar to the distal side of the 3rd molar, supero-inferiorly from the alveolar crest to the molar apex, and transversally from the buccal to palatal plates.

3. Alveolar bone resorption*:* 3D reconstructions of the maxillary and mandibular teeth were standardized to the same scale value prior to resorption measurements using Image J (NIH, Bethesda, Maryland, USA). The bone recession was measured from the alveolar crest to the cementoenamel junction. Three measurements were conducted on each tooth (mesial, middle, and distal side of the tooth), totaling 9 measurements per sample.

4. 3rd molar eruption stage. The eruption stage of the third molar was determined by comparing the percentage emergence of its crown to the full eruption height. The full eruption height was measured from the alveolar crest (between the 2nd and 3rd molar to the occlusal plane of the second molar's distal cusp. The 3rd molar crown's emergence was measured from the alveolar crest to its own occlusal plane. Crown emergence measurements for bilateral third molars were performed and then averaged. All measurements were performed using Image J software (NIH, Bethesda, Maryland, USA).

5. Interfrontal bone (IFB)*:* We used 3D reconstructed µCT images to determine whether an ossicle was present within the interfrontal (metopic) suture for each sample. An ossicle was defined as an IFB if completely separated from the frontal bone by the metopic suture. For samples with an IFB, we segmented both the frontal and interfrontal bones, quantified their volumes, and calculated the ratio of the IFB volume relative to the frontal bone volume.

Western blot

Harvested maxillae underwent snap freeze in liquid nitrogen and stored at -80ºC until protein extraction. Maxillary alveolar bone protein extracts from 3 week-, 3 month-, and 6 month-old Brtl+/– (n=3 per age group) and WT littermates (n=3 per age group) were obtained by grinding with RIPA lysis buffer. The protein concentration was measured using a BCA kit (Thermo Fisher Scientific). The sample solutions were heated at 95°C for 5 min with 4X Nupage buffers. For each sample, proteins (20 µg) were separated on 4-12% polyacrylamide gel and then transferred onto a PVDF membrane (MilliporeSigma). Before immunodetection, gel sample loading was preliminary proved to be equivalent by Ponceau Red staining (0.2% w/v Ponceau S in 3% w/v trichloroacetic acid). 5% non-fat dry milk and 0.05% Tween 20 was used to block the membrane, followed by overnight incubation with primary antibody: osteocalcin sc-376835 (Santa Cruz Biotechnology San Jose, CA, USA) as osteoblastic activity marker; Osteopontin sc-21742 (Santa Cruz Biotechnology San Jose, CA, USA) as late osteogenic differentiation marker; Nfatc1 sc-7294 Santa Cruz Biotechnology (San Jose, CA, USA) as osteoclastic differentiation marker; Mmp9 af-909 (R&D Systems Minneapolis, MN, USA) as osteoclastic activity marker. Western blots were washed with 0.05% TBS-tween before 30 min room temperature incubation with anti-mouse secondary antibody sc-516102 (Santa Cruz Biotechnology San Jose, CA, USA). Immunostained bands were visualized using SuperSignal™ West Pico PLUS Chemiluminescent Substrate detection reagents (Thermo Scientific, Waltham, MA, USA). Chemiluminescent signals were captured by ImageQuant LAS 4000 (GE Healthcare) digital imaging system. Band intensities were determined using an XRS+ Chemidoc system and Image Lab software (Biorad, Hercules, CA, USA). β-actin immunoblotting ensured equal loading of samples.

Statistical analysis

All height, width, and length data, comprising a total of 204 comparisons, including genotype, age, and mutant, were analyzed using nonparametric tests to avoid assumptions about variance or distribution. The Krustal-Wallis test was applied to determine whether there were any significant differences within multi-groups, and the post-hoc Dunn test with Benjamin Hochberg correction was applied to determine the p-values for each comparison. These analyses were performed using R Statistical Software (v4.1.0, R Core Team 2020). All the other data were analyzed using two-way ANOVA for the main effects of age and genotype. Differences between heterozygous and their corresponding WT were assessed using the student's two-tailed unpaired *t-test*, modified with Welch's two-sample *t-test* when interaction was present or to evaluate for type-1 error. These analyses and all graphs were performed using GraphPad Prism (v.9 for Windows, GraphPad Software, San Diego, USA). In all experiments, a p-value ≤0.05 was considered significant.

Results

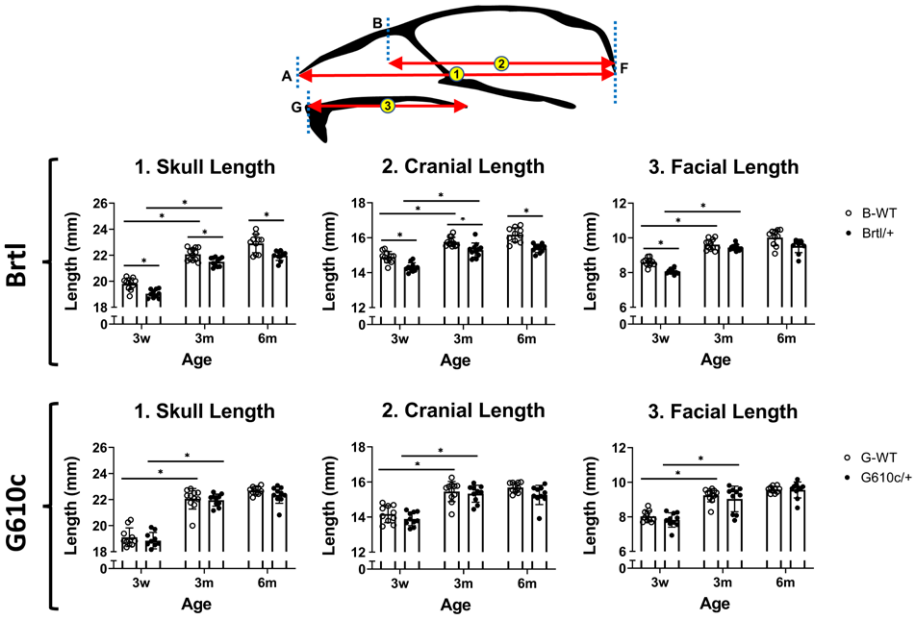

Figure 1. Craniofacial length measurements. Craniofacial length graphs, asterisk representing P-value ≤ .05. Points A = nasale, B = nasion, F = opisthion, G = Prosthion, and J = most caudal point of palatal bone. B-WT, Brtl WT, G-WT, G610c WT. Arrows illustrate the measurements.

Brtl/+ mouse has a shorter skull and facial length

Both Brtl/+ and WT show skull anteroposterior growth with age. The average Brtl/+ skull lengths were 19.04±0.31mm, (3w), 21.48±0.33mm (3m), and 21.96±0.36mm (6m), which were significantly smaller than age-matched WT (19.80±0.44mm, 22.06±0.46mm, 22.90±0.71mm respectively, $p<0.05$) (Figure 1, S2, S3). The average Brtl/+ cranial lengths were 14.31±0.26mm (3w), 15.30±0.4mm (3m), and 15.39±0.24mm (6m). These values were significantly smaller than age-matched WT (14.90±0.32mm, 15.76±0.26mm, 16.17±0.40mm, respectively, $p<0.05$) (Figure 1, S2, S3). Both, Brtl+ and WT exhibited significant progressive anteroposterior growth from 3w to 3m (skull length $p=0.006$, cranial length $p=0.003$). The skull and cranial length show a significant growth pattern between 3w and 3m. However, the growth rate decreases between 3m and 6m (Figure 1). No significant differences were found in anterior and middle cranial height between Brtl/+ and WT and across different age groups. However, Brtl/+ posterior cranial height is significantly smaller (6.10±0.18mm) than WT (6.38±0.21mm, $p=0.013$) at 3m. This increase can be attributed to the significant growth in posterior cranial height observed in both groups at 3 months (Figures 2, 4, and S2). Brtl/+ has

shorter facial length (8.06±0.15) and height (4.07±0.08) compared with WT (8.60±0.22 and 4.25±0.16, respectively, $p<0.05$) at 3w. At 6m, the Brtl/+ facial measurements almost reach the WT measurements, except the facial width (6.24±0.02.4), which is smaller than those of WT (6.53±0.19, $p=0.04$) (Figure 1, 2, 3, S3).

G610c/+ mice display mild craniofacial disturbances

The average G610c/+ skull length (3w-18.84±0.62. 3m-21.95±0.46, 6m-22.35±0.64) is similar to WT (3w-19.10±0.71, 3m-22.05±0.47, 6m-22.68±0.29), and while slightly smaller, was not statistically significant (Figure 1, S2-3). Similar differences were observed in the G610c/+ cranial lengths (3w-13.90±0.39. 3m-15.33±0.49, 6m-15.39±0.24), similar to those found in WT (3w-14.17±0.48, 3m-15.45±0.58, 6m-15.69±0.28). No significant differences were found in the cranial heights between G610c/+ and WT. However, G610c/+ exhibited a significant increase in anterior cranial height from 3m (6.14±0.22) to 6m (6.34±0.12, $p=0.042$). On the other hand, the WT exhibited increases in posterior cranial height from 3w (5.86±0.16) to 3m (5.90±0.12, $p=0.013$) (Figure 2, S3).

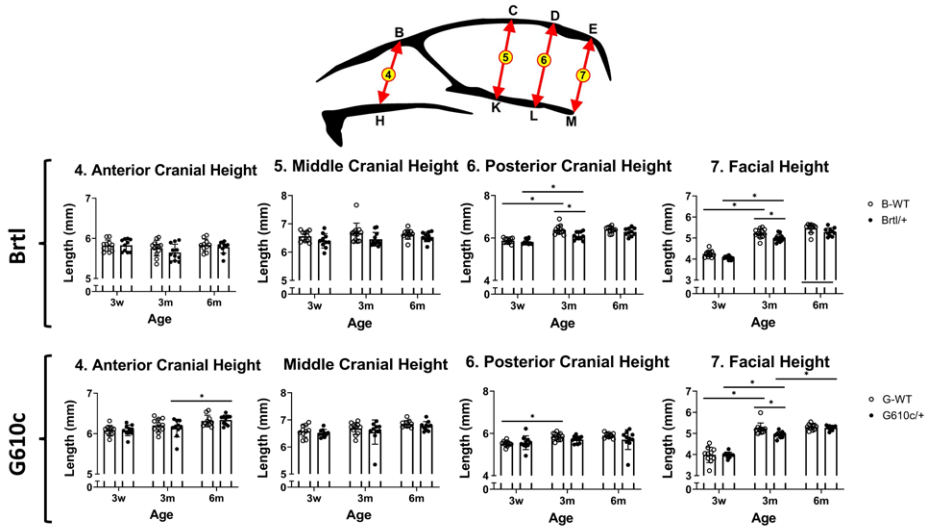

Figure 2. Craniofacial height measurements. Craniofacial height graphs, asterisk representing P-value ≤ .05. Points B = nasion, C=Bregma, D = intersection parietal bone with interparietal bone, E = intersection interparietal bone with squamous portion of the occipital bone, H = intersection maxilla and premaxilla, K = most ventral point of ISS, L = most ventral point of SOS, and M = most caudal point of basioccipital bone. B-WT, Brtl WT, G-WT, G610c WT. Arrows illustrate the measurements.

Brtl/+ and G610c/+ exhibit a few craniofacial morphometric differences

Both the Brtl/+ and G610c/+ show similar skull and cranial lengths. However, there is a significant difference in cranial heights. G610c/+ exhibits an increase in cranial height (dome-shaped skull) across the age compared to Brtl/+. G610c/+ tends to be more brachycephalic, primarily due to a wider frontal bone (3w-4.91±0.17, 3m-5.23±0.14, 6m-5.25±0.13) compared to Brtl/+ (3w-4.83±0.10, 3m-5.22±0.16, 6m-5.23±0.12, $p<0.05$). Brtl/+ tends to have narrower craniofacial widths, especially nasal width at 6m (2.04±009) compared to G610c/+ (2.19±0.18, $p=0.04$). Additionally, Brtl/+ tends to have taller anterior mandibular heights than G610c/+, especially at 6m (1.85±0.12, 1.66±0.12, $p=0.016$). (Figure S4, S5).

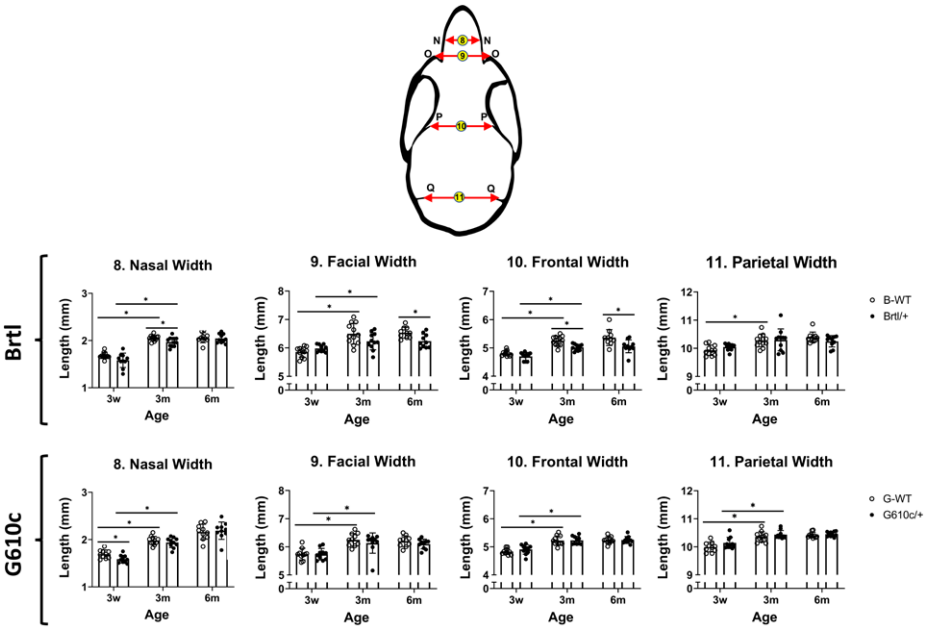

Figure 3. Craniofacial width measurements. Craniofacial width graphs, asterisk representing P-value ≤ .05. Points N = external margin of the nasal bone, O = anterior notch of the zygomatic process, P = frontal squamosal intersection, and Q = intersection of parietal-interparietal and occipital bones. B-WT, Brtl WT, G-WT, G610c WT. Arrows illustrate the measurements.

Brtl-WT (B-WT) tends to be larger than G610c-WT (G-WT) across all three age groups

There are no significant differences in skull length between B-WT and G-WT. However, the cranial length of B-WT (3w-14.90±0.32mm, 3m-15.76±0.26mm, and 6m-16.17±0.40mm) are longer than G-WT (3w-14.17±0.48, 3m-15.45±0.58, and 6m-15.69±0.28), with significant differences observed at 3w (p=0.007) and 6m (p=0.03). In general, the craniofacial morphometrics, except for cranial height, tend to be larger in B-WT compared to G-WT (Figure S4, S6).

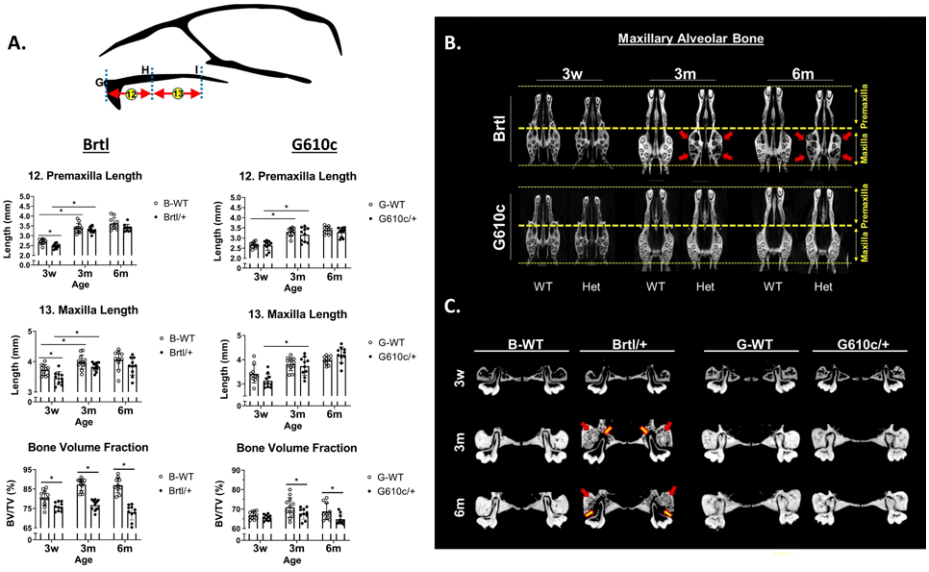

Figure 4. Maxilla measurements. (A) Premaxilla and maxilla lengths and alveolar bone vol fraction graphs, asterisk representing P-value ≤ .05. Points G = Prosthion, H = intersection maxilla and premaxilla, I = intersection maxilla and palatal bone. B-WT, Brtl WT, and G-WT, G610c WT. (B) Axial view showing the maxilla's length and the alveolar bone's appearance. The red arrow highlights the bone with a porotic-like appearance. (C) Coronal view showing the alveolar bone at the level of the first molar. The yellow arrow highlights the enlargement of the tooth sockets resulting from alveolar bone resorption, while the red arrow indicates the bone with a porotic-like appearance.

Brtl/+ mice have shorter, narrower, and pneumatized maxillary alveolar bone

The premaxilla of Brtl/+ (3w-2.48±0.12, 3m-3.30±0.15, and 6m-3.39±0.18) tends to be shorter than WT (3w-2.70±0.13, 3m-3.39±0.24, and 6m-3.62±0.30) across all ages, with a significant difference observed at 3w (p=0.013) (Figure 4A-B, S3). The Brtl/+ maxilla (3w-3.46±0.21, 3m-3.83±0.14, and 6m-3.85±0.29) also tend to be shorter than that of WT (3w-3.72±0.17, 3m-3.99±0.23, and 6m-4.05±0.32), with a significant difference observed at 3 weeks (p=0.042) (Figure 4A-B, S3). G610c/+ premaxilla (3w-2.63±0.24, 3m-3.16±0.35, and 6m-3.29±0.23) and maxilla lengths (3w-3.13±0.29, 3m-3.73±0.38, and 6m-3.97±0.17) are similar to those of WT (3w-2.66±0.14, 3m-3.30±0.20, and 6m-3.39±0.18, and 3w-3.41±0.37, 3m-3.82±0.27, and 6m-4.02±0.32, respectively) (Figure 4A-B, S3). The maxilla bone volume fraction (BV/TV) of the bones in the immediate vicinity of the maxillary teeth is reduced in the Brtl/+ (3w-75.99%, 3m-76.72%, 6m-73.08%) compared with WT (3w-80.45%, 3m-87.29%, 6m-86.32%, p<0.05) (Figure 4A). The BV/TV of G610c/+ (65.63%) is similar to WT (66.80%) at 3w. With age, G610c/+ BVTV (3m-67.74%, 6m-64.80%) become smaller than WT (3m-70.87%, 6m-68.79%, p<0.05) (Figure 4A). With age, Brtl/+ alveolar bone becomes more pneumatized (porotic-like appearance) (Figure 4B-C). G610c/+ mice do not exhibit alveolar bone with a porotic-like appearance (Figure 4B-C).

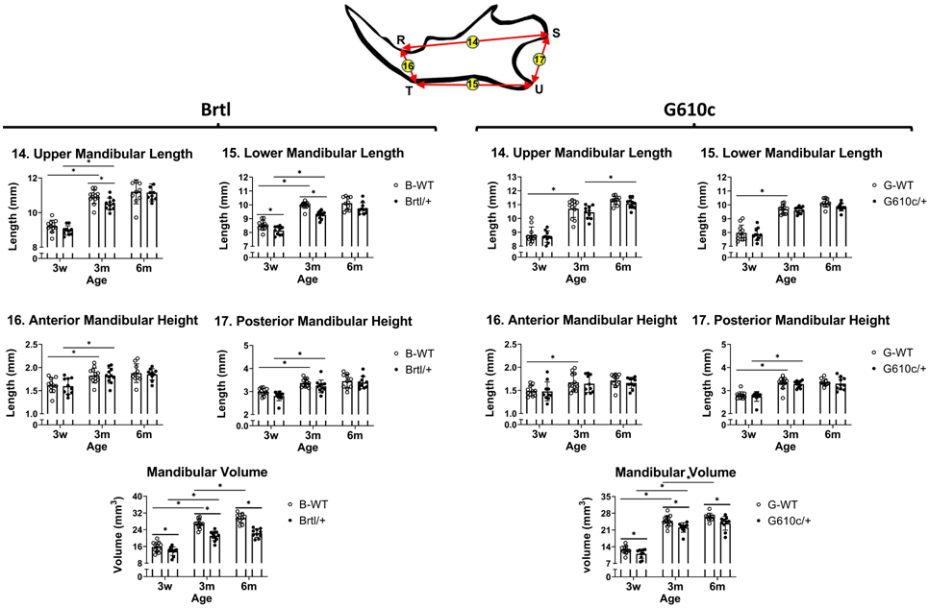

Figure 5. Mandibular measurements. Mandibular lengths, heights, and vol graphs. Asterisk representing P-value ≤ .05. R = superior rim of lower incisor alveolus (bone-tooth junction), S = most posterior point of the condyle, T = inferior rim of lower incisor alveolus (bone-tooth junction), U = tip of the mandibular angle. B-WT, Brtl WT, and G-WT, G610c WT.

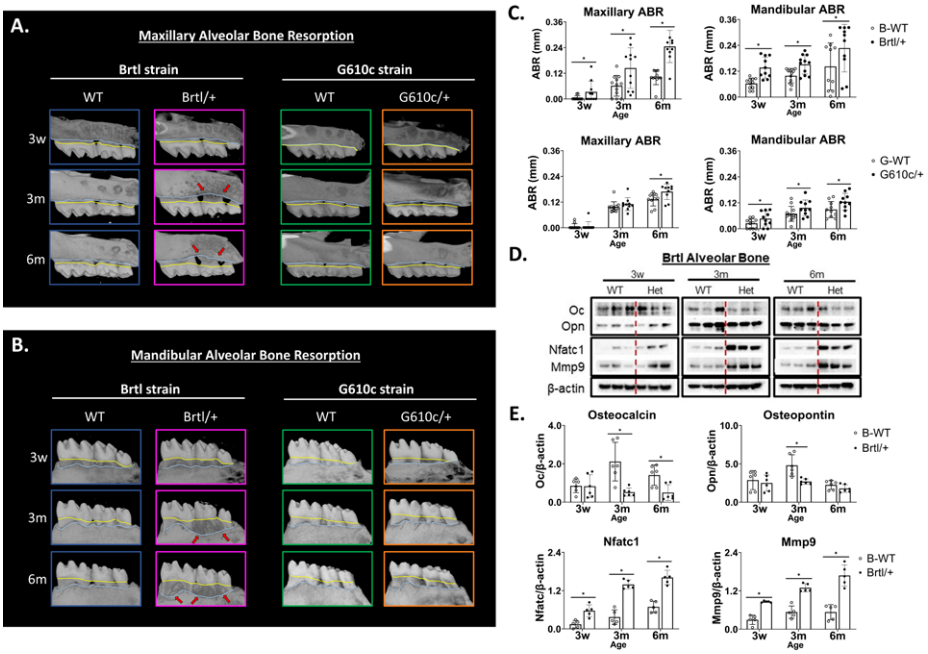

Figure 6. Alveolar bone resorption. (A) Sagittal μCT images of maxillary alveolar bone showing bone resorption by genotype and age, with cyan line depicting the alveolar bone level and yellow line depicting the cementoenamel junction; red arrows indicate severe resorption sites. (B) Sagittal μCT images of mandibular alveolar bone showing bone resorption by genotype and age, with cyan line depicting the alveolar bone level and yellow line depicting the cementoenamel junction; red arrows indicate severe resorption sites. (C) Brtl and G610c maxillary and mandibular alveolar bone resorption graphs, with asterisk representing P-value ≤ .05. (D) Western blot of Brtl alveolar bone. (E) Western blot graphs asterisk representing P-value ≤ .05.

Brtl/+ and G610c/+ mandibles are slightly smaller compared to their corresponding WT

Brtl/+ tends to be slightly smaller compared to WT. This is mainly due to the significant anterior mandibular height reduction (3w-1.48±0.21 vs 1.60±0.18, 3m-1.64±0.19 vs 1.83±0.16, and 6m-1.66±0.12 vs 1.85±0.12 p=0.017) at 6m (Figure 5, S3). G610c/+ mandible also is overall slightly shorter compared to their WT, although it was not statistically significant (Figure 5, S3). Brtl/+ mandibular volume (3w-13.72mm^3, 3m-21.04mm^3, 6m-22.31mm^3) is smaller compared with WT (3w-15.72mm^3, 3m-26.88mm^3, 6m-29.54mm^3, p<0.05). G610c/+ mandibular volume (3w-11.02mm^3, 3m-22.06mm^3, 6m-22.91mm^3) is also smaller than their age-matched WT (3w-12.74mm^3, 3m-24.82mm^3, 6m-26.45mm^3, p<0.05) (Figure 5). Brtl/+ shows a smaller growth rate (3w-3m: 34.80%) than WT (3w-3m: 41.52%;). G610c/+ exhibits a similar growth rate (3w-3m: 50.06%; 3m-6m: 3.71%) to WT (3w-3m: 48.69%; 3m-6m: 6.15%) (Figure 5). The G610c mutants are smaller than Brtl mutants at 3w (13.72mm^3

vs 11.02mm^3), but with aging, G610c/+ exhibit higher growth, surpassing the average size of the Brtl/+ (Figure S5). WT-Brtl are larger than WT-G610c (3w-15.72mm^3 vs 12.74mm^3, 3m-26.88mm^3 vs 24.82mm^3, 6m-29.54mm^3 vs 26.45mm^3) (Figure S4, S6). Overall, the biggest mandibular growth happens between 3w to 3m, which slows down between 3m to 6m. Like the maxilla, the mandibular alveolar bone exhibits a porotic-like appearance that is not observed in WT or G610c (Figure S7).

Aged Brtl/+ and G610c/+ have severe alveolar bone resorption

Brtl/+ maxilla (3w-0.01mm, p=0.01; 3m-0.07mm, p≤0.01; 6m-0.11mm, p≤0.01) and mandibular (3w-0.07mm, p≤0.01; 3m-0.10mm, p≤0.01; 6m-0.15mm, p=0.03) alveolar bone exhibit signs of resorption that worsen with age. This progressive resorption compromises more teeth with aging (Figure 6A-C). This resorption is corroborated with western blots that show decreased osteoblastic and increased osteoclastic activities in Brtl/+ alveolar bone that become exacerbated with age (Figure 6D-E). G610c/+ mice show mild alveolar bone resorption with aging compared to Brtl/+. While this resorption becomes significantly more accentuated at 6 months compared to earlier ages, resorption remains less severe than Brtl/+ (Figure 6A-C).

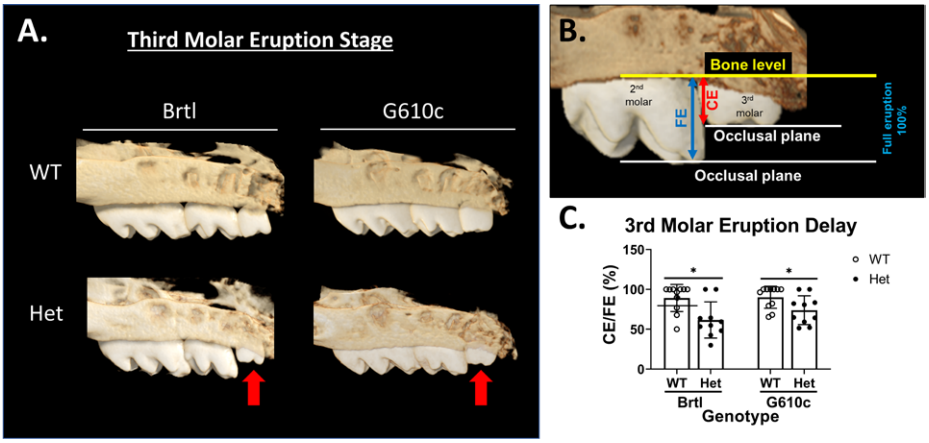

Figure 7. Third molar eruption delay. (A) 3D µCT reconstruction of 3w Brtl and G610c maxilla third molars (representative mean sample); the red arrow indicates the third molar crown emergence height. The blue arrow indicates the full eruption height measured from the alveolar crest to the occlusal plane of the second molar distal cusp. (B) Schematic that illustrates the method used to calculate the crown emergence (CE). (C) Graph illustrates the percentage of third molar CE of Brtl and G610c, with asterisk representing P-value ≤ .05.

Brtl/+ display delayed third molar eruption

Both Brtl/+ and G610c/+ mice show a significant pre-functional eruption delay of their third molars. From the analyzed samples, the average crown emergence for

Brtl/+ was 68.8%, compared to 90.4% of their littermate WT (p=0.01). The average crown emergence of G610c/+ was 68.8%, contrasting with 95.2% of their WT (p=0.03). Among the Brtl/+ third molars that have not reached the occlusal plane, the crown emergence was 68.8%. For G610c/+, it was 79.1% (Figure 7A-C).

Brtl/+ and G610c/+ mice exhibit interfrontal bones

During morphometric measurements, we observed the presence of a midline ossicle (Figure 8A). IFB was observed in 84% of the Brtl/+ and 77% of the G610c/+ calvarial bones (Figure 8B). In contrast, only 39% of B-WT and 61% of G-WT mice exhibit the presence of these IFBs (Figure 8B). When present, Brtl/+ IFB demonstrated a larger volume compared with those present in WT. In contrast, both G610c/+ mutant and WT exhibited a smaller IFB, with IFB on average 2% of corresponding frontal bone volume. Brtl/+ IFB is 4.9% of their frontal bone volume, while WT is substantially smaller (0.8%).

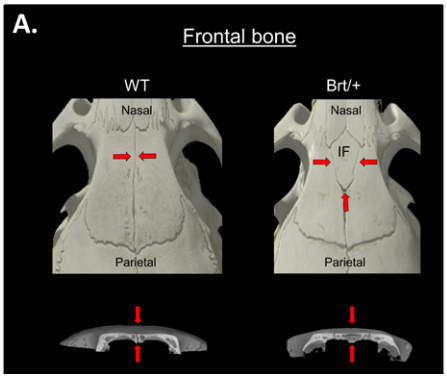

B. Interfrontal Bones

Strain	Brtl		G610c	
Age / geno	WT	Brtl/+	WT	G610c/+
3w	4/11 (36%)	9/10 (90%)	8/11 (73%)	8/10 (80%)
3m	6/12 (50%)	9/11 (82%)	7/12 (58%)	7/10 (70%)
6m	3/10 (30%)	8/10 (80%)	5/10 (50%)	6/10 (60%)
Total	**13/33 (39%)**	**26/31 (84%)**	**20/33 (61%)**	**23/30 (77%)**

Figure 8. Interfrontal bone (IFB). (A) µCT images of 3D reconstructed WT and Brtl/+ skull showing the presence of IFB in between the frontal bone. (B) Summary table of the IFB in Brtl and G610c at each age. Geno, genotype.

G610c/+ mice and anterior cranial compartment misalignment

A subset of 3w G610c/+ mice (n=3) presented with anterior compartment deformation with misalignment of the midline (Figure S8). This unexpected finding was observed during µCT analysis.

Discussion

Mutations in Col1 commonly induce a unique facial appearance, differing significantly from the non-OI population. A detailed cephalometric radiographic analysis of OI patients reveals deficiencies in the anterior cranial base and shorter maxillary, palatine, and mandibular lengths compared to age-matched controls[11, 14]. Brtl/+ reflects a moderate-to-severe type IV OI exhibiting overall reduced cranial, maxilla, and mandibular morphometric indices compared with WT. Some Brtl/+ craniofacial morphometric reductions are more pronounced at 3w and tend to reach WT values at 6mo age. This "catch-up" pattern is similar to what we previously observed in the long bone phenotype[16-19]. This pattern could be explained by possible matrix-level adaptations that improve whole bone strength without corresponding increases in structural geometry, especially after mice reach puberty, generally after 42 days of age[29, 30]. Notably, these observations resemble findings observed in OI patients, where fracture rates tend to decrease after puberty[8]. Brtl/+ mice show a reduced skull and cranial anteroposterior (A-P) length similar to those previously reported in Col1a1^{jrt}/+ and OIM/- mice[31, 32]. Both the Col1a1^{jrt}/+ and OIM-/-mice have been described with a craniofacial resemblance to severe type OI patients[31, 32]. Similar results were observed here in Brtl/+, but not G610c/+ mice, which exhibited a milder craniofacial phenotype, and their overall cranial morphometric indices are very similar to WT. Despite Brtl/+ and G610c/+ having the same type of missense mutation in the Col1, they exhibit phenotype heterogeneity, likely due, in part, to different mutation positions (Brtl/+ at Col1a1 G349C and G610c/+ at Col1a2 G610C) and differing genetic backgrounds (Brt/+ from a mixed of SV129/CD1/C57BL/6 and G610c/+ from C57BL/6). This could also explain the lack of similarity between Brtl/+ and G610c to the *Crtap*$^{-/-}$ mice, which have a mutation in collagen-associated genes and displays brachycephalic skull shape characterized by nasofrontal suture and facial bone fusions[33]. This fusion leads to mid-face retrusion[33] not observed in the mice of this study.

The most substantial and significant morphometric changes were observed within each genotype and strain between 3w to 3m. Surprisingly, no significant differences were observed between 3m to 6m. This occurrence could be attributed to the fact that mice reach their maturation stage between 3m to 6m. It is plausible to suggest that after the craniofacial growth peak, which typically occurs around postnatal 60 days[34], a gradual growth rate deceleration occurs, resulting in fewer discernible differences during this later period.

Overall, we found that the B-WT craniofacial bones are larger than G-WT, particularly at 3w and 3m. It may be explained that these mice have different growth peaks.

Eventually, around 6m G-WT is able to reach close to the B-WT size. It seems G-WT exhibit a delayed growth peak compared to B-WT, eventually reaching a size that closely resembles the B-WT as they age. On the other hand, while the heterozygous mice initially exhibit similar craniofacial sizes at a younger age, these differences become more pronounced with aging. These observed differences between the strains highlight that, despite both Col1 mutations, the WT mice are not strain interchangeable. To ensure an accurate comparison, it is crucial to compare each mutant to its corresponding WT littermates[35].

We observed a significant impact of aging on both the Brtl/+ maxilla and mandible, resulting in severe alveolar bone loss. This severe alveolar resorption has been described as decreased alveolar bone in a previous Brtl/+ mandibular study[36]. We also observed a similar pattern of bone loss in 6m G610c/+ mice, while younger mice did not exhibit such changes. Similar reduced alveolar bone has also been reported in *crtap-/-* mice, which harbor mutations in collagen-associated genes [33]. Furthermore, this alveolar bone loss is associated with an upregulation of osteoclastic activity, specifically Mmp9, and Nfatc1. These severe alveolar resorptions observed with aging may be secondary to the poor bone quantity and quality inherent to OI[1, 3, 6, 37]. Previous study shows that the Brtl/+ mice are more prone to microdamage accumulation compared to age-matched WT. This was evident when the B rtl/+ ulnae exposed to typical cage activities showed a significantly greater amount of cortical microdamage than those of the WT[38]. If this observation extends to the maxilla and mandible bones, it can be assumed that high biomechanical loading from chewing cycles (occlusion) may exacerbate pre-existing microdamage in Brtl/+. Given this, it seems plausible to suggest that the increased alveolar resorption in Brtl/+ might result from this cumulative loading effect on the compromised Brtl/+ bone quality, which aligns with observations described in Col1a1^{jrt}/+ mice[31].

Interestingly, the maxillary and mandibular alveolar BV/TV exhibit a noteworthy reduction as both Brtl and G610c mice age, especially when comparing across the ages. This finding aligns with the reported observations in humans, where a decline in trabecular BV/TV has been consistently associated with the natural aging process[39].

We found a delay in the upper third molar eruptions in both Brtl/+ and G610c/+ mice. Tooth eruption has two stages--intraosseous and supraosseous. The intraosseous stage requires osteoclastic activity to create the eruption path by removing the bone. Once the tooth cusps reach the alveolar crest, the eruption pathway is complete. Then, the tooth transitions to the supra osseous stage, which requires bone apposition apical to the developing tooth in order to push the tooth

to the occlusal plane[40, 41]. Delayed tooth eruption has been found following the administration of bisphosphonates to newborn rats. Evidence for similar effects in humans is sparse, since only a few studies show tooth maturity and eruption delay in bisphosphonate-treated OI patients compared to non-OI children[42, 43]. As these studies compare the tooth eruption of OI patients with non-OI children instead of non-bisphosphonate-treated OI patients, bisphosphonates may not be the only factor affecting eruption in this population. Rather, the poor OI bone quantity and quality could also be participating in the tooth eruption delay. Poor OI bone may not produce proper and sufficient apical bone to induce the propulsion movement for tooth eruption at the same pace as non-OI subjects.

Our OI mice differed from *Crtap−/−* mice regarding cranial bone fusions. While cranial fusions disturbances were not observed in our mice, they did exhibit interfrontal bone ossicles (IFB), which was not observed in the *Crtap*$^{-/-}$ mice[33]. As a radiographic finding, we observed a higher IFB in Brtl/+ and G610c/+ than in their corresponding WT. The IFB are small irregular bones that are present within sutures or fontanelles. Our IFB seems to be a Wormian bone. Wormian bones have been described as an idiopathic minor skeletal variant that could be present in numerous recognized syndromes[44]. In fact, many OI subjects have an abnormally large number of Wormian bones visible on a skull radiograph[45]. It has been proposed that abnormal mechanical stresses across cranial sutures are the common denominator for various conditions associated with the presence of Wormian bones[45]. A previous study found the presence of Wormian bones in most OI types III and IV, but less in OI type I individuals[45]. Wormian bones appear more frequently in more severely affected OI patients and seem to develop mostly in utero[45]. Our Brtl/+ and G610c emulate type IV OI, and their interfrontal or Wormian bones are completely surrounded by the metopic suture, separating them from the frontal bones. However, previous studies on various inbred mouse strains observed the presence of an ossicle residing between the frontal bones[46]. IFB was described as a quasi-continuous trait that exhibits, when present, morphological variability. C57BL6 and CBA mice also consistently exhibit IFB[46]. The Brtl/+ has a mixed background, unlike the G610c/+, which is genetically more homogeneous. However, the presence of a C57BL6 background in both Brtl/+ and G610c/+ may explain the presence of the IFB due to genetic components in C57BL6 mice. Heterozygous mutants, however, show a higher incidence of IFB than WT counterparts, which are larger in size when measured related to their corresponding frontal bone sizes. Therefore, the presence of IFB could also be influenced by the Col1 mutation. A better understanding of the genetic and environmental factors that influence IFB development may be relevant to understanding the presence of OI Wormian bone formation.

In summary, our study shows that the Brtl/+ and G610c/+ mice display clear features found in type IV OI patients; more importantly, they show similar age-related changes in craniofacial growth phenotype. Based on our findings, these mild and moderately severe models can be used to study mechanisms underlying craniofacial abnormalities of OI patients. Therefore, understanding the craniofacial features of these models and how they age will allow us to select the most accurate mouse model, mouse age and bone structure for treatment of a specific craniofacial site of differing OI groups.

References

1. Marini JC, Forlino A, Bachinger HP, Bishop NJ, Byers PH, Paepe A, Fassier F, Fratzl-Zelman N, Kozloff KM, Krakow D, Montpetit K, Semler O. Osteogenesis imperfecta. Nat Rev Dis Primers. 2017;3:17052. Epub 20170818. doi: 10.1038/nrdp.2017.52. PubMed PMID: 28820180.
2. Marini JC, Forlino A, Cabral WA, Barnes AM, San Antonio JD, Milgrom S, Hyland JC, Korkko J, Prockop DJ, De Paepe A, Coucke P, Symoens S, Glorieux FH, Roughley PJ, Lund AM, Kuurila-Svahn K, Hartikka H, Cohn DH, Krakow D, Mottes M, Schwarze U, Chen D, Yang K, Kuslich C, Troendle J, Dalgleish R, Byers PH. Consortium for osteogenesis imperfecta mutations in the helical domain of type I collagen: regions rich in lethal mutations align with collagen binding sites for integrins and proteoglycans. Hum Mutat. 2007;28(3):209-21. doi: 10.1002/humu.20429. PubMed PMID: 17078022; PMCID: PMC4144349.
3. Kang H, Aryal ACS, Marini JC. Osteogenesis imperfecta: new genes reveal novel mechanisms in bone dysplasia. Transl Res. 2017;181:27-48. Epub 20161119. doi: 10.1016/j.trsl.2016.11.005. PubMed PMID: 27914223.
4. Garibaldi N, Besio R, Dalgleish R, Villani S, Barnes AM, Marini JC, Forlino A. Dissecting the phenotypic variability of osteogenesis imperfecta. Dis Model Mech. 2022;15(5). Epub 20220516. doi: 10.1242/dmm.049398. PubMed PMID: 35575034; PMCID: PMC9150118.
5. Chen Y, Yang S, Lovisa S, Ambrose CG, McAndrews KM, Sugimoto H, Kalluri R. Type-I collagen produced by distinct fibroblast lineages reveals specific function during embryogenesis and Osteogenesis Imperfecta. Nat Commun. 2021;12(1):7199. Epub 20211210. doi: 10.1038/s41467-021-27563-3. PubMed PMID: 34893625; PMCID: PMC8664945.
6. Marini JC DDA. Osteogenesis Imperfecta 2020.
7. Basel D, Steiner RD. Osteogenesis imperfecta: recent findings shed new light on this once well-understood condition. Genet Med. 2009;11(6):375-85. doi: 10.1097/GIM.0b013e3181a1ff7b. PubMed PMID: 19533842.
8. Marini JC. Osteogenesis imperfecta: comprehensive management. Adv Pediatr. 1988;35:391-426. PubMed PMID: 3055864.
9. Gjorup H, Jacobsen PE, Hald JD, Haubek D. Craniofacial morphology in adults with osteogenesis imperfecta-A cross-sectional study. Orthod Craniofac Res. 2022. Epub 20220822. doi: 10.1111/ocr.12607. PubMed PMID: 36054241.
10. Jain E, Valiathan A, Kumar S, Natrajan M. Osteogenesis imperfecta and pneumatization of bone-- a hidden reality. Orthodontics (Chic). 2013;14(1):e150-5. doi: 10.11607/ortho.947. PubMed PMID: 23646325.
11. Jensen BL, Lund AM. Osteogenesis imperfecta: clinical, cephalometric, and biochemical investigations of OI types I, III, and IV. J Craniofac Genet Dev Biol. 1997;17(3):121-32. PubMed PMID: 9338855.
12. Rousseau M, Retrouvey JM, Members of the Brittle Bone Disease C. Osteogenesis imperfecta: potential therapeutic approaches. PeerJ. 2018;6:e5464. Epub 20180817. doi: 10.7717/peerj.5464. PubMed PMID: 30128210; PMCID: PMC6100848.
13. Tsipouras P, Barabas G, Matthews WS. Neurologic correlates of osteogenesis imperfecta. Arch Neurol. 1986;43(2):150-2. doi: 10.1001/archneur.1986.00520020044016. PubMed PMID: 3947255.
14. Waltimo-Siren J, Kolkka M, Pynnonen S, Kuurila K, Kaitila I, Kovero O. Craniofacial features in osteogenesis imperfecta: a cephalometric study. Am J Med Genet A. 2005;133A(2):142-50. doi: 10.1002/ajmg.a.30523. PubMed PMID: 15666304.

15. Marom R, Rabenhorst BM, Morello R. Osteogenesis imperfecta: an update on clinical features and therapies. Eur J Endocrinol. 2020;183(4):R95-R106. doi: 10.1530/EJE-20-0299. PubMed PMID: 32621590; PMCID: PMC7694877.

16. Sinder BP, Eddy MM, Ominsky MS, Caird MS, Marini JC, Kozloff KM. Sclerostin antibody improves skeletal parameters in a Brtl/+ mouse model of osteogenesis imperfecta. J Bone Miner Res. 2013;28(1):73-80. doi: 10.1002/jbmr.1717. PubMed PMID: 22836659; PMCID: PMC3524379.

17. Sinder BP, Lloyd WR, Salemi JD, Marini JC, Caird MS, Morris MD, Kozloff KM. Effect of anti-sclerostin therapy and osteogenesis imperfecta on tissue-level properties in growing and adult mice while controlling for tissue age. Bone. 2016;84:222-9. Epub 20160106. doi: 10.1016/j.bone.2016.01.001. PubMed PMID: 26769006; PMCID: PMC4757447.

18. Sinder BP, Salemi JD, Ominsky MS, Caird MS, Marini JC, Kozloff KM. Rapidly growing Brtl/+ mouse model of osteogenesis imperfecta improves bone mass and strength with sclerostin antibody treatment. Bone. 2015;71:115-23. Epub 20141023. doi: 10.1016/j.bone.2014.10.012. PubMed PMID: 25445450; PMCID: PMC4274252.

19. Sinder BP, White LE, Salemi JD, Ominsky MS, Caird MS, Marini JC, Kozloff KM. Adult Brtl/+ mouse model of osteogenesis imperfecta demonstrates anabolic response to sclerostin antibody treatment with increased bone mass and strength. Osteoporos Int. 2014;25(8):2097-107. Epub 20140507. doi: 10.1007/s00198-014-2737-y. PubMed PMID: 24803333; PMCID: PMC4415164.

20. Masci M, Wang M, Imbert L, Barnes AM, Spevak L, Lukashova L, Huang Y, Ma Y, Marini JC, Jacobsen CM, Warman ML, Boskey AL. Bone mineral properties in growing Col1a2(+/G610C) mice, an animal model of osteogenesis imperfecta. Bone. 2016;87:120-9. Epub 20160413. doi: 10.1016/j.bone.2016.04.011. PubMed PMID: 27083399; PMCID: PMC4862917.

21. Andersson K, Dahllof G, Lindahl K, Kindmark A, Grigelioniene G, Astrom E, Malmgren B. Mutations in COL1A1 and COL1A2 and dental aberrations in children and adolescents with osteogenesis imperfecta - A retrospective cohort study. PLoS One. 2017;12(5):e0176466. Epub 20170512. doi: 10.1371/journal.pone.0176466. PubMed PMID: 28498836; PMCID: PMC5428910.

22. Ho Duy B, Zhytnik L, Maasalu K, Kandla I, Prans E, Reimann E, Martson A, Koks S. Mutation analysis of the COL1A1 and COL1A2 genes in Vietnamese patients with osteogenesis imperfecta. Hum Genomics. 2016;10(1):27. Epub 20160812. doi: 10.1186/s40246-016-0083-1. PubMed PMID: 27519266; PMCID: PMC4983065.

23. Forlino A, Porter FD, Lee EJ, Westphal H, Marini JC. Use of the Cre/lox recombination system to develop a non-lethal knock-in murine model for osteogenesis imperfecta with an alpha1(I) G349C substitution. Variability in phenotype in BrtlIV mice. J Biol Chem. 1999;274(53):37923-31. doi: 10.1074/jbc.274.53.37923. PubMed PMID: 10608859.

24. Daley E, Streeten EA, Sorkin JD, Kuznetsova N, Shapses SA, Carleton SM, Shuldiner AR, Marini JC, Phillips CL, Goldstein SA, Leikin S, McBride DJ, Jr. Variable bone fragility associated with an Amish COL1A2 variant and a knock-in mouse model. J Bone Miner Res. 2010;25(2):247-61. doi: 10.1359/jbmr.090720. PubMed PMID: 19594296; PMCID: PMC3153383.

25. Scheiber AL, Barton DK, Khoury BM, Marini JC, Swiderski DL, Caird MS, Kozloff KM. Sclerostin Antibody-Induced Changes in Bone Mass Are Site Specific in Developing Crania. J Bone Miner Res. 2019;34(12):2301-10. Epub 20191107. doi: 10.1002/jbmr.3858. PubMed PMID: 31441963; PMCID: PMC7458133.

26. Galea GL, Zein MR, Allen S, Francis-West P. Making and shaping endochondral and intramembranous bones. Dev Dyn. 2021;250(3):414-49. Epub 20201228. doi: 10.1002/dvdy.278. PubMed PMID: 33314394; PMCID: PMC7986209.
27. Vora SR, Camci ED, Cox TC. Postnatal Ontogeny of the Cranial Base and Craniofacial Skeleton in Male C57BL/6J Mice: A Reference Standard for Quantitative Analysis. Front Physiol. 2015;6:417. Epub 20160112. doi: 10.3389/fphys.2015.00417. PubMed PMID: 26793119; PMCID: PMC4709510.
28. Wei X, Thomas N, Hatch NE, Hu M, Liu F. Postnatal Craniofacial Skeletal Development of Female C57BL/6NCrl Mice. Front Physiol. 2017;8:697. Epub 2017/09/30. doi: 10.3389/fphys.2017.00697. PubMed PMID: 28959213; PMCID: PMC5603710.
29. Kozloff KM, Carden A, Bergwitz C, Forlino A, Uveges TE, Morris MD, Marini JC, Goldstein SA. Brittle IV mouse model for osteogenesis imperfecta IV demonstrates postpubertal adaptations to improve whole bone strength. J Bone Miner Res. 2004;19(4):614-22. Epub 20040112. doi: 10.1359/JBMR.040111. PubMed PMID: 15005849.
30. Dutta S, Sengupta P. Men and mice: Relating their ages. Life Sci. 2016;152:244-8. Epub 2015/11/26. doi: 10.1016/j.lfs.2015.10.025. PubMed PMID: 26596563.
31. Eimar H, Tamimi F, Retrouvey JM, Rauch F, Aubin JE, McKee MD. Craniofacial and Dental Defects in the Col1a1Jrt/+ Mouse Model of Osteogenesis Imperfecta. J Dent Res. 2016;95(7):761-8. Epub 20160307. doi: 10.1177/0022034516637045. PubMed PMID: 26951553.
32. Menegaz RA, Ladd SH, Organ JM. Craniofacial allometry in the OIM(-/-) mouse model of osteogenesis imperfecta. FASEB J. 2020;34(8):10850-9. Epub 20200627. doi: 10.1096/fj.202000715R. PubMed PMID: 32592291.
33. Xu H, Lenhart SA, Chu EY, Chavez MB, Wimer HF, Dimori M, Somerman MJ, Morello R, Foster BL, Hatch NE. Dental and craniofacial defects in the Crtap(-/-) mouse model of osteogenesis imperfecta type VII. Dev Dyn. 2020;249(7):884-97. Epub 20200312. doi: 10.1002/dvdy.166. PubMed PMID: 32133710; PMCID: PMC7727892.
34. Maga AM. Postnatal Development of the Craniofacial Skeleton in Male C57BL/6J Mice. J Am Assoc Lab Anim Sci. 2016;55(2):131-6. Epub 2016/03/31. PubMed PMID: 27025802; PMCID: PMC4783629.
35. Adams A, McBratney-Owen B, Newby B, Bowen ME, Olsen BR, Warman ML. Presphenoidal synchondrosis fusion in DBA/2J mice. Mamm Genome. 2013;24(1-2):54-62. Epub 20121121. doi: 10.1007/s00335-012-9437-8. PubMed PMID: 23179633; PMCID: PMC3560942.
36. Boskey AL, Verdelis K, Spevak L, Lukashova L, Beniash E, Yang X, Cabral WA, Marini JC. Mineral and matrix changes in Brtl/+ teeth provide insights into mineralization mechanisms. Biomed Res Int. 2013;2013:295812. Epub 20130529. doi: 10.1155/2013/295812. PubMed PMID: 23802117; PMCID: PMC3681234.
37. Marini JC, Dang Do AN. Osteogenesis Imperfecta. In: Feingold KR, Adler RA, Ahmed SF, Anawalt B, Blackman MR, Chrousos G, Corpas E, de Herder WW, Dhatariya K, Dungan K, Hamilton E, Hofland J, Jan de Beur S, Kalra S, Kaltsas G, Kapoor N, Kim M, Koch C, Kopp P, Korbonits M, Kovacs CS, Kuohung W, Laferrere B, Levy M, McGee EA, McLachlan R, Muzumdar R, Purnell J, Rey R, Sahay R, Shah AS, Sperling MA, Stratakis CA, Trence DL, Wilson DP, editors. Endotext. South Dartmouth (MA)2000.
38. Davis MS, Kovacic BL, Marini JC, Shih AJ, Kozloff KM. Increased susceptibility to microdamage in Brtl/+ mouse model for osteogenesis imperfecta. Bone. 2012;50(3):784-91. Epub 20111220. doi: 10.1016/j.bone.2011.12.007. PubMed PMID: 22207275; PMCID: PMC3443405.
39. Chen H, Zhou X, Fujita H, Onozuka M, Kubo KY. Age-related changes in trabecular and cortical bone microstructure. Int J Endocrinol. 2013;2013:213234. Epub 2013/04/11. doi: 10.1155/2013/213234. PubMed PMID: 23573086; PMCID: PMC3614119.
40. Marks SC, Jr., Schroeder HE. Tooth eruption: theories and facts. Anat Rec. 1996;245(2):374-93. doi: 10.1002/(SICI)1097-0185(199606)245:2<374::AID-AR18>3.0.CO;2-M. PubMed PMID: 8769674.

41. Proffit WR, Frazier-Bowers SA. Mechanism and control of tooth eruption: overview and clinical implications. Orthod Craniofac Res. 2009;12(2):59-66. doi: 10.1111/j.1601-6343.2009.01438.x. PubMed PMID: 19419448.

42. Kamoun-Goldrat A, Ginisty D, Le Merrer M. Effects of bisphosphonates on tooth eruption in children with osteogenesis imperfecta. Eur J Oral Sci. 2008;116(3):195-8. doi: 10.1111/j.1600-0722.2008.00529.x. PubMed PMID: 18471236.

43. Malmgren B, Tsilingaridis G, Monsef-Johansson N, Qahtani ZHA, Dahllof G, Astrom E. Bisphosphonate Therapy and Tooth Development in Children and Adolescents with Osteogenesis Imperfecta. Calcif Tissue Int. 2020;107(2):143-50. Epub 20200525. doi: 10.1007/s00223-020-00707-1. PubMed PMID: 32451573; PMCID: PMC7343730.

44. Bellary SS, Steinberg A, Mirzayan N, Shirak M, Tubbs RS, Cohen-Gadol AA, Loukas M. Wormian bones: a review. Clin Anat. 2013;26(8):922-7. Epub 20130820. doi: 10.1002/ca.22262. PubMed PMID: 23959948.

45. Semler O, Cheung MS, Glorieux FH, Rauch F. Wormian bones in osteogenesis imperfecta: Correlation to clinical findings and genotype. Am J Med Genet A. 2010;152A(7):1681-7. doi: 10.1002/ajmg.a.33448. PubMed PMID: 20583157.

46. Zimmerman H, Yin Z, Zou F, Everett ET. Interfrontal Bone Among Inbred Strains of Mice and QTL Mapping. Front Genet. 2019;10:291. Epub 20190402. doi: 10.3389/fgene.2019.00291. PubMed PMID: 31001328; PMCID: PMC6454051.

Supplemental Figures

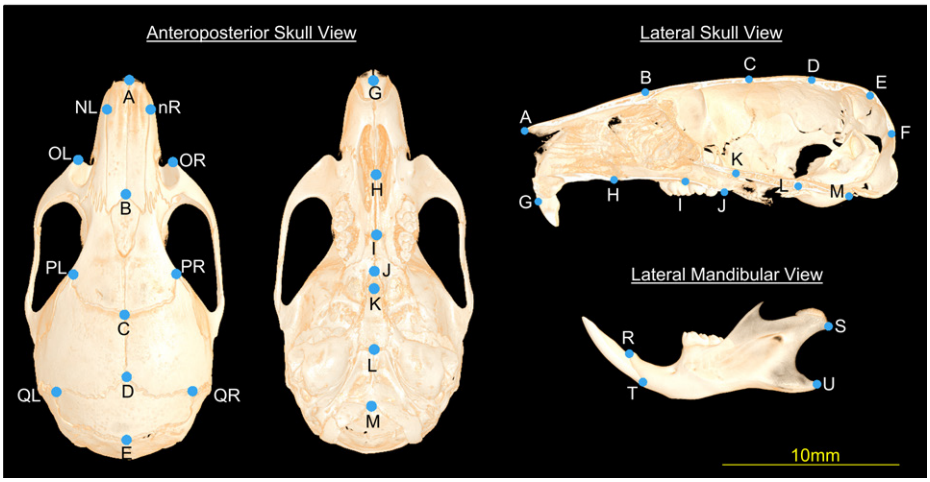

Supplemental Figure 1. Micro-CT Craniofacial landmarks. The representative 3D craniofacial reconstruction images illustrate the landmark points utilized for automated craniofacial lengths, heights, and widths measurements.

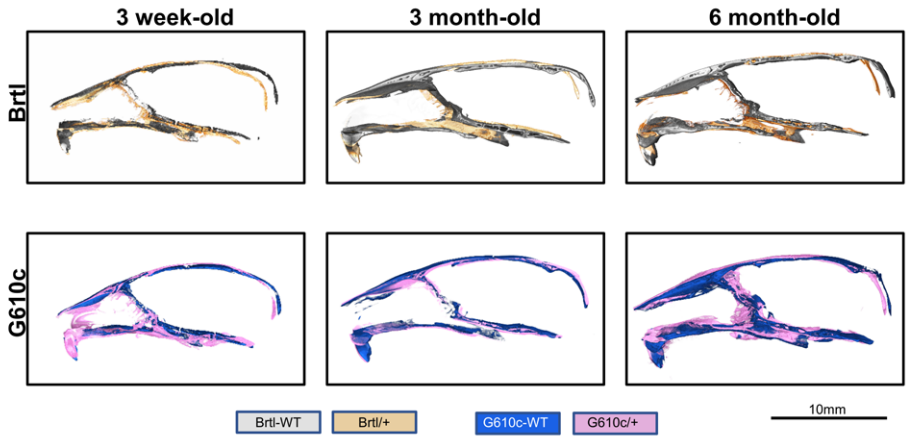

Supplemental Figure 2. 3D Skull µCT reconstruction images overlapped by genotype. The lateral view of the 3D µCT reconstruction images were obtained from the midsagittal slab, demonstrating the overlapping of the WT and Heterozygous (Het) samples from each age and mutation strain. The skulls overlapping were aligned based on the nasospinale and prosthion reference points. It shows the overlap of the WT and Het of each age and mutation strain. Representative 3D slabs were selected from samples that had the average length within each group. The silver line illustrates Brtl-WT, the orange line represents Brtl/+, the blue line illustrates G610c-WT, and the pink line illustrates G610c/+.

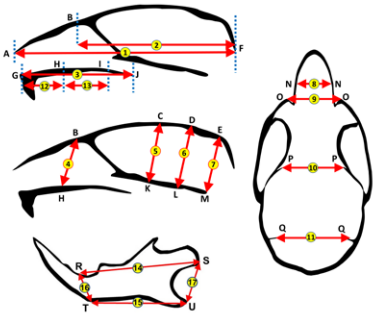

Supplemental Table 1. Craniofacial measurements

Landmark		Age	Brtl			G610c		
			WT	Brtl/+	p-value	WT	G610c/+	p-value
Length	1. Skull	3w	19.80±0.44	19.04±0.31	**0.007**	19.10±0.71	18.84±0.62	0.533
		3m	22.06±0.46	21.48±0.33	**0.036**	22.05±0.47	21.95±0.46	0.445
		6m	22.90±0.71	21.96±0.36	**0.040**	22.68±0.29	22.35±0.64	0.271
	2. Cranial	3w	14.90 ± 0.32	14.31 ± 0.26	**0.005**	14.17 ± 0.48	13.90 ± 0.39	0.271
		3m	15.76 ± 0.26	15.30 ± 0.40	**0.007**	15.45 ± 0.58	15.33 ± 0.49	0.529
		6m	16.17 ± 0.40	15.39 ± 0.24	**0.002**	15.69 ± 0.28	15.39 ± 0.24	0.055
	3. Facial	3w	8.60 ± 0.22	8.06 ± 0.15	**0.001**	8.03 ± 0.32	7.82 ± 0.42	0.365
		3m	9.61 ± 0.30	9.44 ± 0.17	0.273	9.24 ± 0.38	9.03 ± 0.74	0.929
		6m	10.02 ± 0.46	9.54 ± 0.38	0.075	9.58 ± 0.18	9.56 ± 0.46	0.577
	12. Premaxilla	3w	2.70 ± 0.13	2.48 ± 0.12	**0.013**	2.66 ± 0.14	2.63 ± 0.24	0.821
		3m	3.39 ± 0.24	3.30 ± 0.15	0.550	3.30 ± 0.20	3.16 ± 0.35	0.566
		6m	3.62 ± 0.30	3.39 ± 0.18	0.064	3.39 ± 0.18	3.29 ± 0.23	0.534
	13. Maxilla	3w	3.72 ± 0.17	3.46 ± 0.21	**0.042**	3.41 ± 0.37	3.13 ± 0.29	0.150
		3m	3.99 ± 0.23	3.83 ± 0.14	0.124	3.82 ± 0.27	3.73 ± 0.38	0.760
		6m	4.05 ± 0.32	3.85 ± 0.29	0.169	4.02 ± 0.32	3.97 ± 0.17	0.075
	14. Upper Mandibular	3w	9.22 ± 0.35	8.97 ± 0.27	0.112	8.80 ± 0.58	8.69 ± 0.41	1.000
		3m	10.91 ± 0.39	10.50 ± 0.34	**0.042**	10.68 ± 4.51	10.44 ± 0.47	0.086
		6m	11.21 ± 0.69	11.16 ± 0.50	0.619	11.30 ± 0.31	11.08 ± 0.36	0.245
	15. Lower Mandibular	3w	8.51 ± 0.34	8.13 ± 0.30	**0.042**	7.97 ± 0.56	7.88 ± 0.44	0.960
		3m	9.98 ± 0.24	9.27 ± 0.27	**0.001**	9.68 ± 4.07	9.61 ± 0.25	0.446
		6m	10.12 ± 0.46	9.75 ± 0.41	0.191	10.13 ± 0.30	9.83 ± 0.28	0.064
Height	4. Anterior cranial	3w	5.79 ± 0.13	5.83 ± 0.15	0.882	6.08 ± 0.13	6.08 ± 0.13	1.000
		3m	5.76 ± 0.20	5.65 ± 0.21	0.355	6.20 ± 0.16	6.14 ± 0.22	0.682
		6m	5.83 ± 0.15	5.78 ± 0.15	0.698	6.31 ± 0.14	6.34 ± 0.12	0.662
	5. Middle cranial	3w	6.56 ± 0.18	6.40 ± 0.25	0.154	6.58 ± 0.22	6.51 ± 0.13	0.786
		3m	6.60 ± 0.16	6.45 ± 0.24	0.078	6.68 ± 0.22	6.55 ± 0.45	0.614
		6m	6.63 ± 0.17	6.53 ± 0.17	0.271	6.85 ± 0.13	6.77 ± 0.17	0.365
	6. Posterior cranial	3w	5.87 ± 0.12	5.81 ± 0.12	0.327	5.52 ± 0.13	5.56 ± 0.32	0.960
		3m	6.38 ± 0.21	6.10 ± 0.18	**0.013**	5.86 ± 0.16	5.70 ± 0.17	0.098
		6m	6.40 ± 0.15	6.28 ± 0.18	0.271	5.90 ± 0.12	5.70 ± 0.47	0.335
	7. Facial	3w	4.25 ± 0.16	4.07 ± 0.08	**0.023**	3.98 ± 0.37	3.98 ± 0.13	0.662
		3m	5.22 ± 0.21	4.99 ± 0.18	**0.037**	5.23 ± 0.26	4.93 ± 0.15	**0.008**
		6m	5.47 ± 0.22	5.29 ± 0.19	0.075	5.30 ± 0.14	5.27 ± 0.11	0.619
	16. Anterior Mandibular	3w	1.61 ± 0.16	1.60 ± 0.18	0.760	1.49 ± 0.11	1.48 ± 0.21	0.682
		3m	1.83 ± 0.16	1.83 ± 0.16	0.963	1.66 ± 0.51	1.64 ± 0.19	0.486
		6m	1.88 ± 0.20	1.85 ± 0.12	0.960	1.72 ± 0.15	1.66 ± 0.12	0.271
	17. Posterior Mandibular	3w	2.99 ± 0.16	2.81 ± 0.20	0.065	2.8 ± 0.15	2.74 ± 0.21	0.717
		3m	3.37 ± 0.18	3.23 ± 0.27	0.139	3.33 ± 1.35	3.28 ± 0.15	0.182
		6m	3.45 ± 0.31	3.39 ± 0.27	0.698	3.35 ± 0.15	3.3 ± 0.27	0.446
Width	8. Nasal	3w	1.68 ± 0.07	1.58 ± 0.15	0.127	1.69 ± 0.09	1.59 ± 0.08	**0.047**
		3m	2.05 ± 0.06	1.97 ± 0.10	**0.042**	1.98 ± 0.08	1.94 ± 0.11	0.624
		6m	2.06 ± 0.11	2.04 ± 0.09	0.619	2.16 ± 0.16	2.19 ± 0.18	0.786
	9. Facial	3w	5.85 ± 0.18	5.98 ± 0.13	0.277	5.74 ± 0.21	5.74 ± 0.20	0.872
		3m	6.50 ± 0.37	6.23 ± 0.30	0.206	6.25 ± 0.22	6.13 ± 0.36	0.795
		6m	6.53 ± 0.19	6.24 ± 0.24	**0.041**	6.20 ± 0.19	6.10 ± 0.17	0.365
	10. Frontal	3w	4.81 ± 0.09	4.70 ± 0.14	0.182	4.83 ± 0.11	4.91 ± 0.17	0.271
		3m	5.25 ± 0.17	5.02 ± 0.11	**0.011**	5.22 ± 0.17	5.23 ± 0.14	0.786
		6m	5.37 ± 0.28	5.05 ± 0.23	0.047	5.24 ± 0.12	5.25 ± 0.13	0.922
	11. Interparietal	3w	9.93 ± 0.18	10.05 ± 0.12	0.204	9.99 ± 0.17	10.14 ± 0.20	0.245
		3m	10.27 ± 0.22	10.30 ± 0.39	0.821	10.36 ± 0.20	10.44 ± 0.18	0.466
		6m	10.40 ± 0.19	10.25 ± 0.20	0.365	10.41 ± 0.10	10.45 ± 0.09	0.365

Supplemental Figure 3. Genotype and age measurement results. A. Figure showing the measurements analyzed in this study. **B.** Summary table showing genotype data (WT vs Het) categorized by age and mutation.

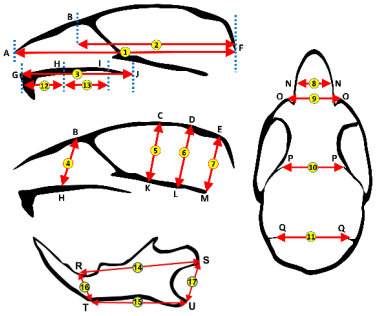

Supplemental Table 2. Craniofacial measurements

Landmark		Age	Het			WT		
			Brtl/+	G610c/+	p-value	B-WT	G-WT	p-value
Length	1. Skull	3w	19.04±0.31	18.84±0.62	0.335	19.80±0.44	19.10±0.71	0.057
		3m	21.48±0.33	21.95±0.46	0.075	22.06±0.46	22.05±0.47	0.82
		6m	21.96±0.36	22.35±0.64	0.075	22.90±0.71	22.68±0.29	0.301
	2. Cranial	3w	14.31 ± 0.26	13.90 ± 0.39	0.075	14.90 ± 0.32	14.17 ± 0.48	**0.007**
		3m	15.30 ± 0.40	15.33 ± 0.49	0.882	15.76 ± 0.26	15.45 ± 0.58	0.446
		6m	15.39 ± 0.24	15.39 ± 0.24	0.741	16.17 ± 0.40	15.69 ± 0.28	**0.035**
	3. Facial	3w	8.06 ± 0.15	7.82 ± 0.42	0.169	8.60 ± 0.22	8.03 ± 0.32	**0.005**
		3m	9.44 ± 0.17	9.03 ± 0.74	0.568	9.61 ± 0.30	9.24 ± 0.38	0.062
		6m	9.54 ± 0.38	9.56 ± 0.46	0.960	10.02 ± 0.46	9.58 ± 0.18	0.055
	12. Premaxilla	3w	2.48 ± 0.12	2.63 ± 0.24	0.114	2.70 ± 0.13	2.66 ± 0.14	0.682
		3m	3.30 ± 0.156	3.16 ± 0.35	0.882	3.39 ± 0.24	3.30 ± 0.20	0.791
		6m	3.39 ± 0.18	3.29 ± 0.23	0.741	3.6229 ± 0.30	3.39 ± 0.18	0.150
	13. Maxilla	3w	3.46 ± 0.21	3.13 ± 0.29	0.035	3.72 ± 0.17	3.41 ± 0.37	**0.037**
		3m	3.83 ± 0.14	3.73 ± 0.38	0.760	3.99 ± 0.23	3.82 ± 0.27	0.273
		6m	3.85 ± 0.29	4.20 ± 0.32	0.064	4.05 ± 0.32	3.97 ± 0.17	0.365
	14. Upper Mandibular	3w	8.97 ± 0.27	8.69 ± 0.41	0.114	9.22 ± 0.35	8.80 ± 0.58	0.082
		3m	10.50 ± 0.34	10.44 ± 0.47	0.960	10.91 ± 0.39	10.68 ± 4.51	1.000
		6m	11.16 ± 0.50	11.08 ± 0.36	1.000	11.21 ± 0.69	11.30 ± 0.31	0.960
	15. Lower Mandibular	3w	8.13 ± 0.30	7.88 ± 0.44	0.217	8.51 ± 0.34	7.97 ± 0.56	**0.032**
		3m	9.27 ± 0.27	9.61 ± 0.25	0.256	9.98 ± 0.24	9.68 ± 4.07	**0.047**
		6m	9.75 ± 0.41	9.83 ± 0.28	0.301	10.12 ± 0.46	10.13 ± 0.30	0.821
Height	4. Anterior cranial	3w	5.83 ± 0.15	6.08 ± 0.13	**0.004**	5.79 ± 0.13	6.08 ± 0.13	**0.008**
		3m	5.65 ± 0.21	6.14 ± 0.22	**0.003**	5.76 ± 0.20	6.20 ± 0.16	**0.001**
		6m	5.78 ± 0.15	6.34 ± 0.12	**0.001**	5.83 ± 0.15	6.31 ± 0.14	**0.001**
	5. Middle cranial	3w	6.40 ± 0.25	6.51 ± 0.13	0.365	6.56 ± 0.18	6.58 ± 0.22	0.717
		3m	6.45 ± 0.24	6.55 ± 0.45	0.182	6.60 ± 0.16	6.68 ± 0.22	0.482
		6m	6.53 ± 0.17	6.77 ± 0.17	**0.020**	6.63 ± 0.17	6.85 ± 0.13	**0.011**
	6. Posterior cranial	3w	5.81 ± 0.12	5.56 ± 0.32	**0.025**	5.87 ± 0.12	5.52 ± 0.13	**0.008**
		3m	6.10 ± 0.18	5.70 ± 0.17	**0.002**	6.38 ± 0.21	5.86 ± 0.16	**0.001**
		6m	6.28 ± 0.18	5.70 ± 0.47	**0.004**	6.40 ± 0.15	5.90 ± 0.12	**0.001**
	7. Facial	3w	4.07 ± 0.08	3.98 ± 0.13	0.131	4.25 ± 0.16	3.98 ± 0.37	0.098
		3m	4.99 ± 0.18	4.93 ± 0.15	0.649	5.22 ± 0.21	5.23 ± 0.26	0.550
		6m	5.29 ± 0.19	5.27 ± 0.11	0.821	5.47 ± 0.22	5.30 ± 0.14	0.064
	16. Anterior Mandibular	3w	1.60 ± 0.18	1.48 ± 0.21	0.169	1.61 ± 0.16	1.49 ± 0.11	0.082
		3m	1.83 ± 0.16	1.64 ± 0.19	0.127	1.83 ± 0.16	1.66 ± 0.51	0.124
		6m	1.85 ± 0.12	1.66 ± 0.12	**0.017**	1.88 ± 0.20	1.72 ± 0.15	0.191
	17. Posterior Mandibular	3w	2.81 ± 0.20	2.74 ± 0.21	0.271	2.99 ± 0.16	2.8 ± 0.15	**0.037**
		3m	3.23 ± 0.27	3.28 ± 0.15	0.446	3.37 ± 0.18	3.33 ± 1.35	0.717
		6m	3.39 ± 0.27	3.3 ± 0.27	0.534	3.45 ± 0.31	3.35 ± 0.15	0.619
Width	8. Nasal	3w	1.58 ± 0.15	1.59 ± 0.08	0.821	1.68 ± 0.07	1.69 ± 0.09	0.795
		3m	1.97 ± 0.10	1.94 ± 0.11	0.795	2.05 ± 0.06	1.98 ± 0.08	**0.047**
		6m	2.04 ± 0.09	2.19 ± 0.18	**0.047**	2.06 ± 0.11	2.16 ± 0.16	0.169
	9. Facial	3w	5.98 ± 0.13	5.74 ± 0.20	**0.020**	5.85 ± 0.18	5.74 ± 0.21	0.277
		3m	8.23 ± 0.30	6.13 ± 0.36	0.795	6.50 ± 0.37	6.25 ± 0.22	0.154
		6m	6.24 ± 0.24	6.10 ± 0.17	0.365	6.53 ± 0.19	6.20 ± 0.19	**0.006**
	10. Frontal	3w	4.70 ± 0.14	4.91 ± 0.17	**0.030**	4.81 ± 0.09	4.83 ± 0.11	0.717
		3m	5.02 ± 0.11	5.23 ± 0.14	**0.020**	5.25 ± 0.17	5.22 ± 0.17	0.899
		6m	5.05 ± 0.23	5.25 ± 0.13	**0.047**	5.37 ± 0.28	5.24 ± 0.12	0.335
	11. Interparietal	3w	10.05 ± 0.12	10.14 ± 0.20	0.786	9.93 ± 0.18	9.99 ± 0.17	0.529
		3m	10.30 ± 0.39	10.44 ± 0.18	0.368	10.27 ± 0.22	10.36 ± 0.20	0.446
		6m	10.25 ± 0.20	10.45 ± 0.09	**0.025**	10.40 ± 0.19	10.41 ± 0.10	0.619

Supplemental Figure 4. Mutation and strain measurement results. A. Figure showing the measurements analyzed in this study. **B.** Summary table showing mutation data (Brt/+ vs G610c/+) and strain data (Brtl-WT vs G610c-WT) categorized by age.

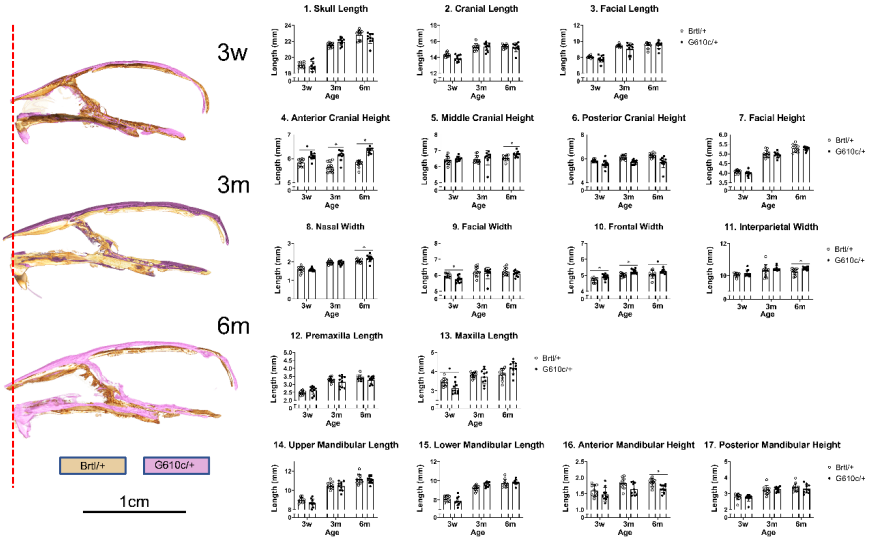

Supplemental Figure 5. Brtl/+ vs G610c/+ Craniofacial measurements. A. Representative 3D µCT images of Brtl/+ and G610c/+. Images are overlapped by age. **B.** Craniofacial measurement graphs, asterisk representing *p-value*≤0.05.

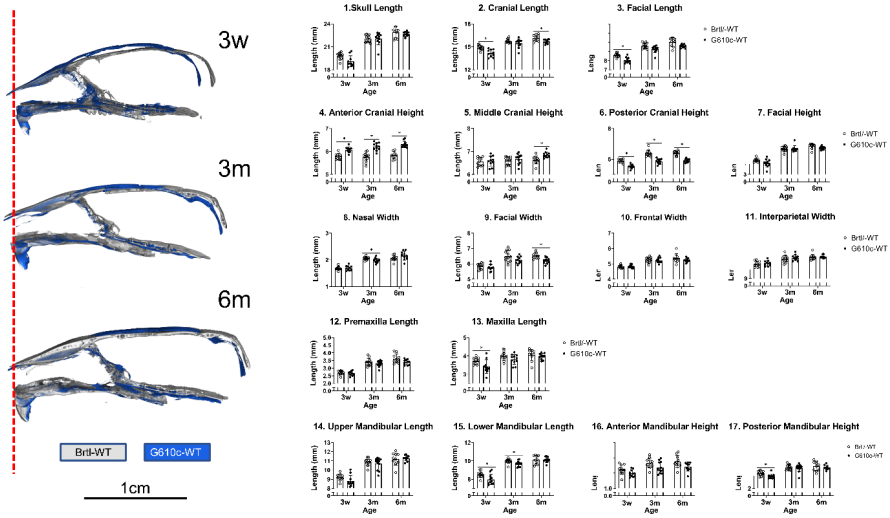

Supplemental Figure 6. Brtl-WT vs G610c-WT Craniofacial measurements. A. Representative 3D µCT images of Brtl-WT and G610c-WT. Images are overlapped by age. **B.** Craniofacial measurement graphs, asterisk representing *p-value*≤0.05.

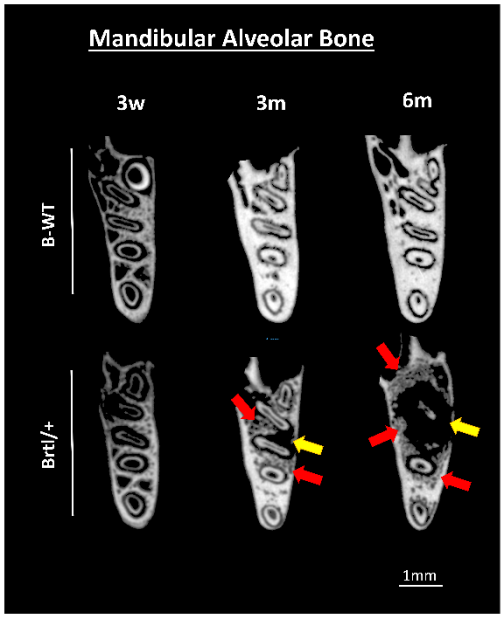

Supplemental Figure 7. Mandibular alveolar bone resorption. Axial view of the mandibular alveolar bone. The red arrow highlights the bone with a porotic-like appearance, and the yellow arrow highlights the enlargement of the tooth sockets resulting from alveolar bone resorption.

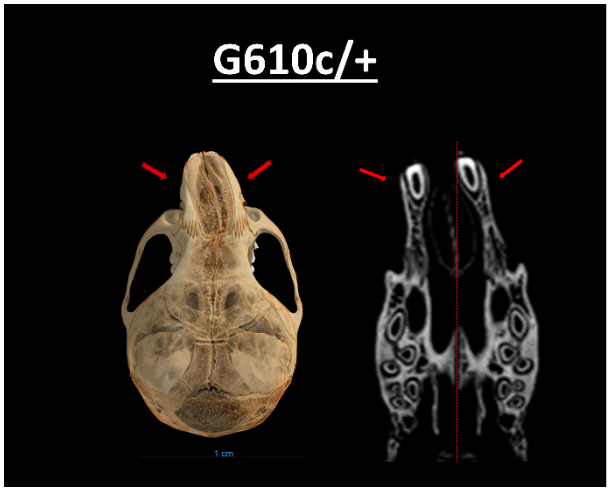

Supplemental Figure 8. G610c/+ skull malformations. Red arrows indicate the midline deviation in 3D µCT reconstruction and axial view of anterior cranial compartment malformations.

CHAPTER 5

Sex-Based Differences in Sclerostin Antibody for Craniofacial Bone Disorders with Collagen Defects

Hsiao H Sung [1 2 3], Ali Alzainal [1], Zongrui Dai [4], Rob Goulet [1], Peter M van der Kraan [3], Michelle S Caird [1], Esmeralda Blaney Davidson [3], Kenneth M Kozloff [1].

[1.] Orthopaedic Research Laboratories, Department of Orthopaedic Surgery, University of Michigan, Ann Arbor, USA.
[2.] Department of Oral and Maxillofacial Surgery, University of Michigan, Ann Arbor, USA.
[3.] Experimental Rheumatology, Department of Rheumatology, Radboud Medical Centre, Nijmegen, The Netherlands,
[4.] Department of Biostatistics, University of Michigan, Ann Arbor, USA.

Abstract

Osteogenesis imperfecta (OI) is a genetic connective tissue disorder marked by bone fragility and craniofacial abnormalities. While most OI research has focused on long bones, the impact on craniofacial bones, formed by both endochondral (cranial base, condyle) and intramembranous (jaw, alveolar bone) ossification, is less understood. Importantly, these ossification types may exhibit unique pathological changes and respond differently to anabolic treatments, with recent evidence suggesting that sex-specific factors may further influence disease severity and therapeutic outcomes. This study aimed to characterize sex-specific craniofacial bone pathology and evaluate the efficacy of sclerostin antibody (SclAb) therapy in Brtl/+ mice, a moderate-to-severe OI model.

Micro-computed tomography was used to evaluate bone volume fraction (BV/TV), trabecular thickness (Tb.Th), bone mineral density (BMD), cortical bone integrity, alveolar bone resorption, and morphometric parameters in wild-type and Brtl/+ mice, both untreated and following SclAb treatment. Data were stratified by sex. Statistical comparisons among the genotype, control, and treated groups performed using ANOVA, with $p \leq 0.05$ considered significant.

Brtl/+ mice exhibited significant reductions in craniofacial BV/TV, Tb.Th, BMD, and jaw thickness, as well as increased alveolar bone resorption compared to wild-type controls, with notable effects across both endochondral and intramembranous skeletal compartments. SclAb treatment markedly improved bone volume, thickness, mineralization, and reduced bone resorption, partially or fully restoring Brtl/+ bone phenotypes to wild-type values. Sex-specific analyses revealed that females responded more robustly in terms of decreased mandibular alveolar bone resorption (intramembranous ossification), while males demonstrated greater improvements in condylar and cranial base thickness (endochondral ossification). Craniofacial morphometric measurements are not affected by SclAb therapy.

Distinct craniofacial bone compartments and sex significantly influence pathology and therapeutic response in OI. These findings highlight the need for personalized, compartment- and sex-specific treatment strategies to optimize craniofacial bone repair. Further research should target mechanisms driving these differences to enhance outcomes for individuals with OI.

Keywords: Sclerostin antibody, osteogenesis imperfecta, craniofacial bone, sex differences

Introduction

Osteogenesis imperfecta (OI) is a heritable connective tissue disorder[1]. Most cases (85%) are attributed to COL1A1 or COL1A2 mutations that disrupt type I collagen production, resulting in abnormal bone mineralization, skeletal fragility, and increased fracture risk[1, 2]. Crucially, OI also leads to craniofacial and dentoalveolar abnormalities across all types, complicating oral rehabilitation and interventions because of poor bone quality and excessive bone resorption[3-5].

The craniofacial skeleton protects the brain and supports vital functions including sensory perception, mastication, speech, and respiration[6]. Its diverse anatomy arises from two developmental pathways: intramembranous ossification (IO) forms the calvarial bones, maxilla, and mandibular body, while endochondral ossification (EO) generates the cranial base and mandibular condyle[7-9]. These processes confer distinct structural and biomechanical properties and can influence how bones respond to disease and treatment[8].

Sex differences in bone disease are well-documented in long bones of the oim/oim mouse model for type III OI: females often display more severe cortical deficits and altered mineralization, even when overall bone mineral content is higher[10]. However, little is known about the presence or extent of sex-dependent differences in craniofacial bones, particularly those with different ossification origins.

Recent advances in bone therapeutics have shown the role of sclerostin as a key inhibitor of bone formation encoded by the SOST gene[11]. Mutations causing sclerosteosis and Van Buchem disease lead to excessive craniofacial bone growth, demonstrating sclerostin's critical regulatory function[12-14]. In OI mouse models, treatment with sclerostin antibody (SclAb) effectively increases bone mass and improves structural properties, including in craniofacial regions such as the calvarial bones, maxilla, and mandibular body[15-17]. Although sex-dependent effects of sclerostin inhibition are documented in long bones, where females exhibit rapid trabecular gains and males show more sustained cortical improvements[18], it is unclear whether similar variations occur in craniofacial sites.

Further insight into sex-dependent bone response comes from fracture healing studies. In these models, male rodents tend to form a larger, cartilage-rich callus (reflecting endochondral ossification dominance), while females progress more quickly to direct bone formation via intramembranous ossification[19]. Moreover, treatment with anabolic agents such as parathyroid hormone (PTH) leads to

early increases in callus volume and strength in males, versus more refined bone deposition in females[20, 21]. These observations suggest that both biological sex and ossification mechanism may influence how craniofacial bones respond to anabolic therapies. Consequently, it is plausible that craniofacial sites with different developmental origins will demonstrate varying responses to sclerostin inhibition according to sex, further underscoring the need to investigate these factors in the context of OI therapy.

This study aims to determine whether anatomical sites, ossification types, and biological sex influence the craniofacial bone response to SclAb in Brtl/+ mice. By clarifying these variables, we seek to advance the development of targeted OI therapies optimized for individual patient factors and craniofacial regions.

Material and Methods

Animals

All protocols and procedures involving animals were approved by the University of Michigan's Committee on Use and Care of Animals. Wildtype (WT) and Brtl/+ mice with a mixed background of SV129/CD-1/C57BL/6S were derived from heterozygous Brtl/+ and WT parental strains. The Brtl/+ mouse is a heterozygous knock-in model for OI, featuring a Gly349Cys substitution in a COL1A1 allele, which has also been found in subjects affected by a moderately severe form of OI (type IV)[22]. 3-month-old mice were randomly assigned to SclAb (25mg/kg SclAb VI, Amgen, Thousand Oaks, CA) or vehicle injection (PBS) subcutaneously, two times per week for 5 weeks following our previously described protocol[23] (Table 1).

Table 1. Sample size

Genotype	Treatment	Female n	Male n	Total n
WT	PBS (control) (WP)	11	6	17
Brtl/+	PBS (control) (BP)	10	6	16
WT	SclAb (WS)	11	8	19
Brtl/+	SclAb (BS)	12	11	23

Micro-computed tomography (µCT) & analysis

A total of 75 mouse skulls were scanned with high-resolution µCT (Bruker Skyscan 1176; Bruker, Kontich, Belgium). Image acquisition was performed using our previously reported protocol[16]. Individual 2D cross-sectional images were reconstructed into 3D volumes with 9-µm isotropic voxel size using NRecon software (version 1.6.5.8; Bruker). Dragonfly 2.0 (ORS, Denver, USA) was used to delineate the region of interest and to perform crania, maxilla, and mandible measurements, segmentations, and cTAn (version 1.6.5.8; Bruker) were used to assess the bone volume fraction analysis.

1. Craniofacial linear measurements*:* Measurements were performed on 3D reconstructed volumes. Landmarks were placed manually on the 3D reconstructed images, and the measurements were processed with an automated plug-in provided by ORS Dragonfly Team. Most of these parameters have been defined previously[24, 25].

2. Craniofacial thickness measurements*:* Measurements were performed on 3D reconstructed volumes. The thickness measurements were processed with an automated plug-in. Most of these parameters have been defined previously[16].

3. Maxilla and mandibular alveolar bone volume fraction*:* Alveolar bone was evaluated at a region of interest that includes the inter-radicular bone of the 1st molar, superoinferiorly from the alveolar crest to the molar apex, and transversally from the buccal to palatal plates.

3. Alveolar bone resorption*:* Measurements were performed on 3D reconstructed volumes. The thickness measurements were processed with an automated plug-in. The bone recession was measured from the alveolar crest to the cementoenamel junction. Three measurements were conducted on each tooth (mesial, middle, and distal side of the tooth), totaling 9 measurements per sample.

Quantitative PCR (qPCR) for Cytokine Expression

Alveolar bone tissue was isolated from mice and preserved in RNA later. Total RNA was extracted using miRNasy kit and quantified by nanodrop. Complementary DNA (cDNA) was synthesized from 1 µg of total RNA using SuperScript III Reverse Transcriptase according to the manufacturer's instructions. Quantitative PCR was performed using SYBR Green Master Mix (Applied Biosystems) and specific primers for Il1, Il6, TNF, and GAPDH (for normalization). Reactions were run on a Applied Biosystems 7500 Real-Time PCR System and analyzed with the ΔΔCt method. Cytokine expression was normalized to the housekeeping gene and expressed as relative fold change compared to wild-type controls. All samples were run in technical triplicates.

TRAP Staining for Osteoclastic Activity

Osteoclastic activity in the alveolar bone was assessed by tartrate-resistant acid phosphatase (TRAP) staining. Tissue samples were fixed in 10% neutral-buffered formalin, decalcified inimunocal (3 days), and embedded in paraffin. Sections (5 µm) were mounted on slides and deparaffinized. TRAP staining was performed using the Sigma-Aldrich Acid Phosphatase, Leukocyte (TRAP) Kit following the manufacturer's protocol. Briefly, sections were incubated with naphthol AS-BI phosphate and Fast Red Violet LB salt in the presence of tartrate, visualizing TRAP-positive multinucleated cells as indicators of osteoclastic activity. Sections were counterstained with light green, imaged under light microscopy.

Statistical analysis

All height, width, length, and thickness data were analyzed using nonparametric tests to avoid assumptions about variance or distribution. The Krustal-Wallis test was applied to determine whether there were any significant differences within multi-groups, and the post-hoc Dunn test with Benjamin Hochberg correction was applied to determine the p-values for each comparison. These analyses were performed using R Statistical Software (v4.1.0, R Core Team 2020). All the other data were analyzed using two-way ANOVA for the main effects of sex and genotype. Differences between heterozygous and their corresponding WT were assessed using the student's two-tailed unpaired *t-test*, modified with Welch's two-sample *t-test* when interaction was present or to evaluate for type-1 error. These analyses and all graphs were performed using GraphPad Prism (v.9 for Windows, GraphPad Software, San Diego, USA). In all experiments, a p-value ≤ 0.05 was considered significant.

Results

Sclerostin Antibody Improves Trabecular Bone Volume Fraction (BV/TV) in Both Genotypes

Bone volume fraction (BV/TV) of trabecular bone was measured in interradicular regions of the first molar in both the maxilla and mandible. In the maxilla, WT controls exhibited a mean BV/TV of 62.29, increasing to 65.76 in wild-type mice treated with SclAb (WS; WP vs WS: $p = 0.021$). Brtl/+ non-treated mice (BP) showed a marked reduction to 48.24 (WP vs BP: $p = 3.73 \times 10^{-7}$). In contrast, Brtl/+ treated with AclAb (BS) demonstrated substantial restoration (60.67), comparable to WT controls (WP vs BS: $p = 0.166$; BP vs BS: $p = 5.84 \times 10^{-8}$). In the mandible, a similar trend was observed: WP was 57.10, WS increased to 62.26 (WP vs WS: $p = 0.0014$),

BP was lowest at 49.01 (WP vs BP: $p = 3.20 \times 10^{-5}$), and BS recovered to 56.06 (WP vs BS: $p = 0.254$; BP vs BS: $p = 7.49 \times 10^{-5}$).

In the maxilla of female mice, WT controls demonstrated a BV/TV of 62.17, while SclAb-treated WT reached 65.49. In contrast, untreated Brtl/+ mice displayed a significantly reduced BV/TV (49.08, $p = 0.000$ versus WT), but SclAb therapy in Brtl/+ restored this value to 61.70, fully rescuing the deficit ($p = 0.000$ compared to untreated Brtl/+). The female mandibular region followed a similar trend: BV/TV decreased from 57.99 in WT to 51.77 in untreated Brtl/+ mice ($p = 0.003$) but was significantly improved to 58.57 after SclAb treatment ($p = 0.001$ versus untreated Brtl/+).

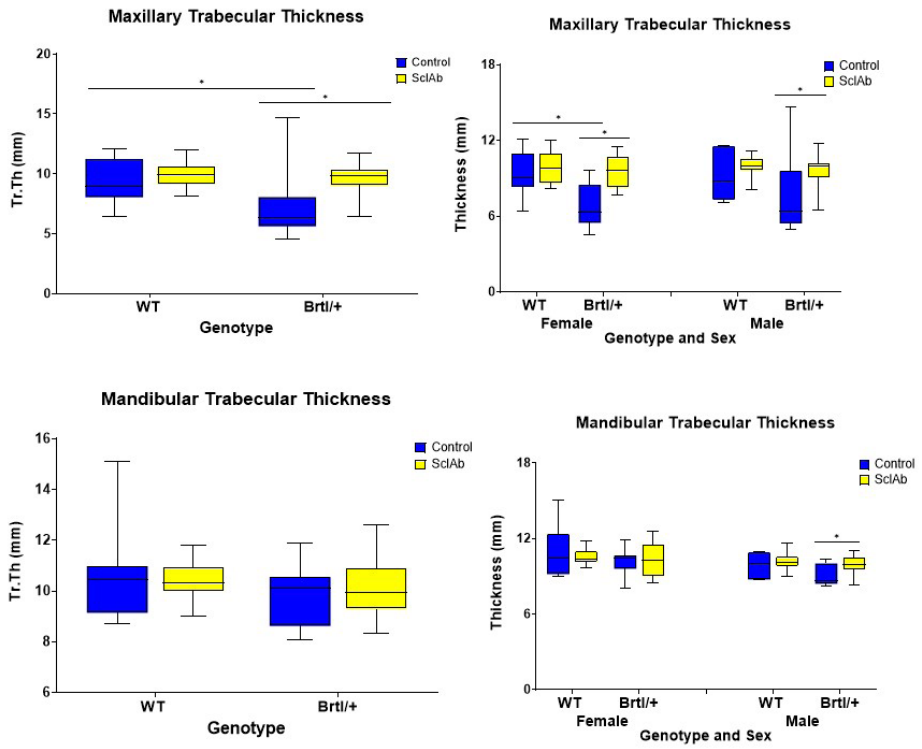

Figure 1: Bone volume fraction (BV/TV) in the maxilla and mandible. The graph displays total BV/TV values for maxillary and mandibular regions, comparing male and female groups across experimental conditions (wild-type control, wild-type SclAb-treated, Brtl/+ untreated, and Brtl/+ SclAb-treated). SclAb administration significantly improved BV/TV in Brtl/+ mice, restoring bone volume toward wild-type levels in both sexes and bone types.

Male mice exhibited comparable effects. In the maxilla, BV/TV fell from 62.51 in WT to 46.84 in Brtl/+ mice ($p = 0.0016$), with SclAb therapy raising BV/TV to 59.54 ($p = 0.0003$

versus untreated Brtl/+). Similarly, mandibular BV/TV dropped from 55.47 in WT to 44.41 in Brtl/+ ($p = 0.0004$) and rebounded to 53.32 after SclAb administration ($p = 0.0001$).

These findings collectively indicate that SclAb robustly improved BV/TV across both sexes and jawbones in Brtl/+ mice, restoring bone volume to levels comparable to WT controls (Figure 1).

Sclerostin Antibody Restores Trabecular Thickness in Maxilla and Maintains Stability in Mandible

In the mandible, trabecular thickness (Tb.Th) remained relatively stable across all groups: WP 10.56 µm, WS 10.43 µm, BP 9.77 µm, and BS 10.13 µm, with no significant differences overall. For females, WP was 10.93 µm, WS 10.58 µm, BP 10.21 µm, and BS 10.34 µm, and males had WP 9.88 µm, WS 10.22 µm, BP 9.05 µm, and BS 9.90 µm, with only BP vs BS reaching marginal significance in males ($p = 0.025$).

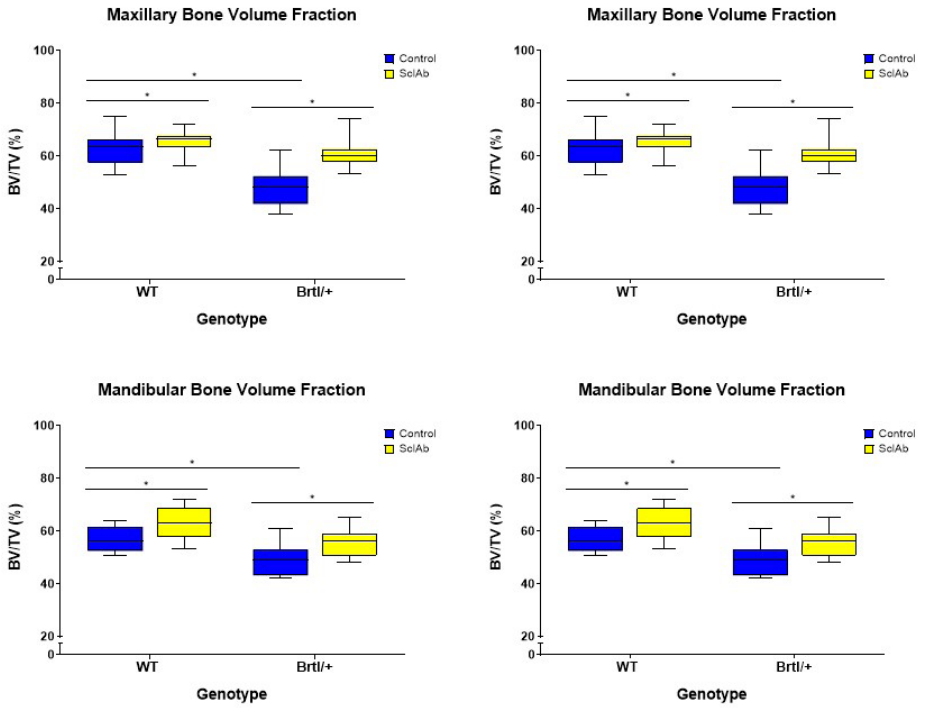

Figure 2. Trabecular thickness (Tb.Th) in the mandible and maxilla. The graph illustrates mean Tb.Th values for each experimental group, shown separately for maxillary and mandibular regions and for male and female mice. In the mandible, Tb.Th remained relatively stable across groups, with only a marginal improvement observed in SclAb-treated Brtl/+ males. In contrast, significant reductions in maxillary Tb.Th were seen in Brtl/+ mice compared to WT, which were restored to WT levels following SclAb treatment in both sexes.

In the maxilla, the genotype effect was more pronounced. WP mice had a mean Tb.Th of 9.32 µm, whereas BP dramatically reduced to 7.14 µm (WP vs BP: $p = 0.004$). Sclerostin antibody restored thickness to 9.88 µm in WS and 9.68 µm in BS, with BS significantly higher than BP (BP vs BS: $p = 0.0001$). In females, WP was 9.40 µm, WS 9.85 µm, BP 6.84 µm, and BS 9.63 µm (WP vs BP: $p = 0.002$; BP vs BS: $p = 0.000$), while males had WP 9.18 µm, WS 9.94 µm, BP 7.64 µm, and BS 9.75 µm (BP vs BS: $p = 0.050$). Sclerostin antibody thus reversed maxillary thinning due to Brtl/+ mutation, with mandibular thickness less affected (Figure 2).

Sclerostin Antibody Normalizes Aberrant Trabecular Number in Maxillary Brtl/+ Mice

In the mandible, the number of trabeculae (Tb.N) was generally low and showed minimal differences between wild-type and Brtl/+ genotypes. Both wild-type phosphate-buffered (WP) and Brtl/+ phosphate-buffered (BP) mice averaged 0.05, while wild-type SclAb-treated (WS) and Brtl/+ SclAb-treated (BS) groups had slightly higher values of 0.06. The modest increase observed with SclAb in wild-type mice was statistically significant (WP vs WS: $p = 0.0004$), but overall, differences between genotypes and treatment in the mandible were limited. Similar trends were seen in males and females, with minor variations and only slight, statistically significant increases following SclAb in some cases.

In contrast, the maxilla showed pronounced genotype effects. Brtl/+ mice (BP) exhibited a marked increase in Tb.N (0.08) compared to wild-type controls (0.06; WP vs BP: $p = 0.0004$). SclAb treatment normalized this value, bringing Tb.N in Brtl/+ SclAb-treated (BS) mice back down to 0.06 (BP vs BS: $p < 0.0001$), similar to wild-type levels. This corrective effect was present in both sexes. For example, Brtl/+ females showed increased Tb.N (0.08 vs wild-type 0.06; $p = 0.000$), but SclAb reduced it to 0.07 (BP vs BS: $p = 0.002$). In males, BP mice had 0.070, and BS dropped to 0.060 (BP vs BS: $p = 0.006$).

Overall, SclAb treatment effectively corrected the increased number of trabeculae in the maxilla caused by the Brtl/+ mutation, restoring normal bone architecture. In the mandible, SclAb had only minor effects on trabecular number (Figure 3).

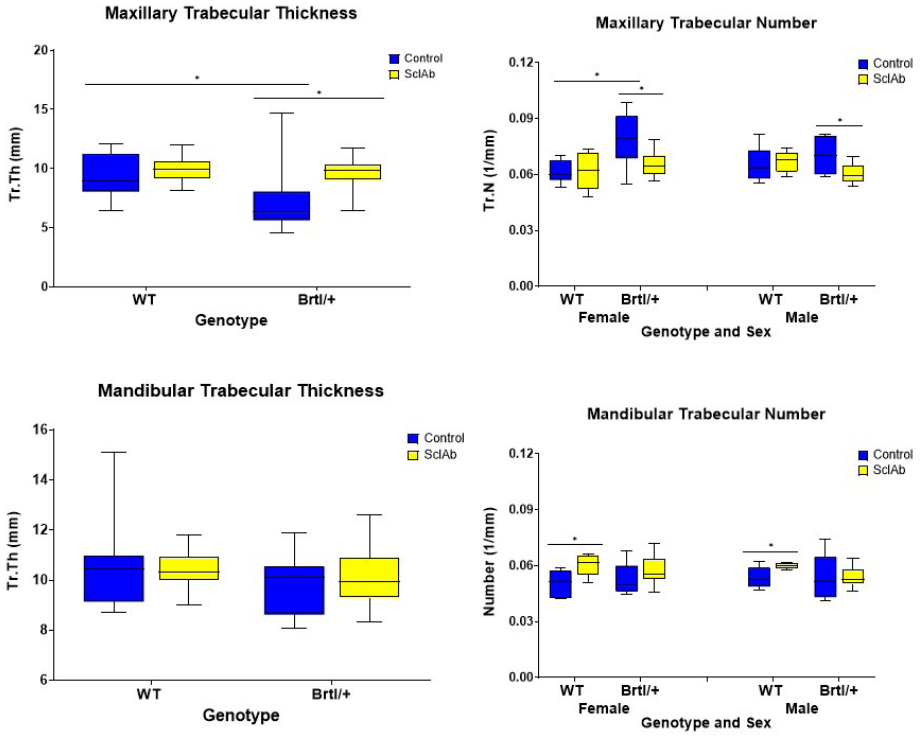

Figure 3. Trabecular number (Tb.N) in the maxilla and mandible. The graph illustrates the Tb.N was markedly increased in the maxilla of Brtl/+ mice compared to WT, with SclAb therapy restoring values toward normal levels in both sexes. In the mandible, Tb.N differences were minimal between genotypes and treatment groups.

Sclerostin Antibody Elevates Bone Mineral Density (BMD)

In the maxilla, bone mineral density (BMD) was substantially reduced in Brtl/+ mice, with an average of 0.85 g/cm^3 compared to 1.22 g/cm^3 in WT, a highly significant difference. SclAb restored BMD in Brtl/+ mice to 1.21 g/cm^3, nearly matching wild-type levels, while WT mice receiving SclAb showed an increase to 1.34 g/cm^3. These improvements were statistically significant, with SclAb treatment leading to a complete rescue in the Brtl/+ group.

Analysis by sex showed a consistent pattern. Female WT mice exhibited a BMD of 1.23 g/cm^3, which increased to 1.32 g/cm^3 following SclAb administration. Brtl/+ females had a markedly lower BMD of 0.87 g/cm^3, but SclAb treatment elevated this to 1.24 g/cm^3, restoring bone density to near control values. In males, WT BMD was 1.21 g/cm^3 and increased to 1.36 g/cm^3 with SclAb. Untreated Brtl/+ males had a BMD of 0.81 g/cm^3, whereas SclAb treatment improved this to 1.17 g/cm^3.

Overall, sclerostin antibody therapy produced clear and substantial improvements in bone density within the maxilla, effectively normalizing BMD in Brtl/+ mice of both sexes (Figure 4).

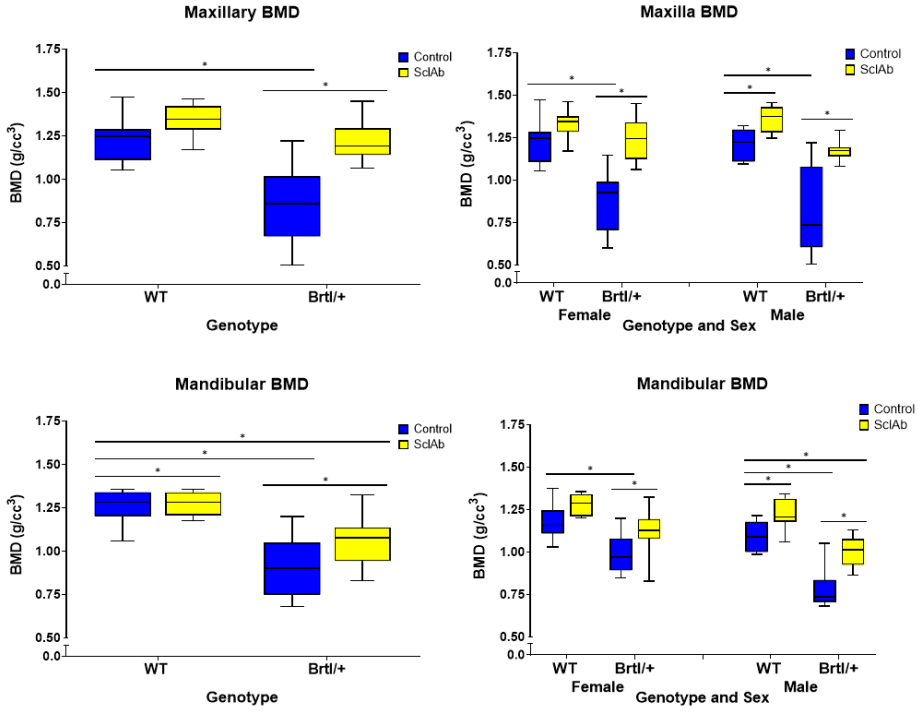

Figure 4. Bone mineral density (BMD) in the maxilla and mandible. Sclerostin antibody treatment significantly increased BMD in Brtl/+ mice and restored bone density to WT levels in both maxilla and mandible, with similar improvements observed in both sexes.

Cortical Bone Structure is Recovered by Sclerostin Antibody Therapy

Cortical bone measurements were performed only in the mandible, as the maxilla does not possess a defined cortical region suitable for consistent analysis due to its thin and fenestrated anatomical structure. Cortical BV/TV in the mandible was sharply reduced in Brtl/+ mice compared to wild-type controls, dropping from 95.3% to 88.2%. This deficit was effectively reversed by sclerostin antibody treatment, which restored BV/TV in Brtl/+ mice to 94.5%, nearly matching wild-type levels. SclAb also boosted BV/TV in wild-type mice, reaching 96.5%. Results were consistent in both female and male subgroups, with significant improvements after treatment in Brtl/+ mice of both sexes.

Other measures of cortical bone quality, including bone area (B.Ar) and bone perimeter (B.Pm), showed similar patterns. Brtl/+ mice had reduced bone area and perimeter compared to wild-type controls, but antibody treatment brought both measures back to or near control values. For example, total bone area was 15,727 μm^2 in wild-type, dropped to 13,867 μm^2 in Brtl/+ mice, and rebounded to 15,789 μm^2 following SclAb therapy. Bone perimeter in Brtl/+ mice was 1442 µm, significantly lower than the wild-type value of 1520 µm, but SclAb restored it to 1513 µm. These improvements were observed in both males and females, with treatment consistently reversing the deficits caused by the Brtl/+ mutation.

Overall, sclerostin antibody treatment robustly restored mandibular cortical bone volume, area, and perimeter in Brtl/+ mice to levels comparable to healthy controls, with similar benefits seen in both sexes (Figure 5).

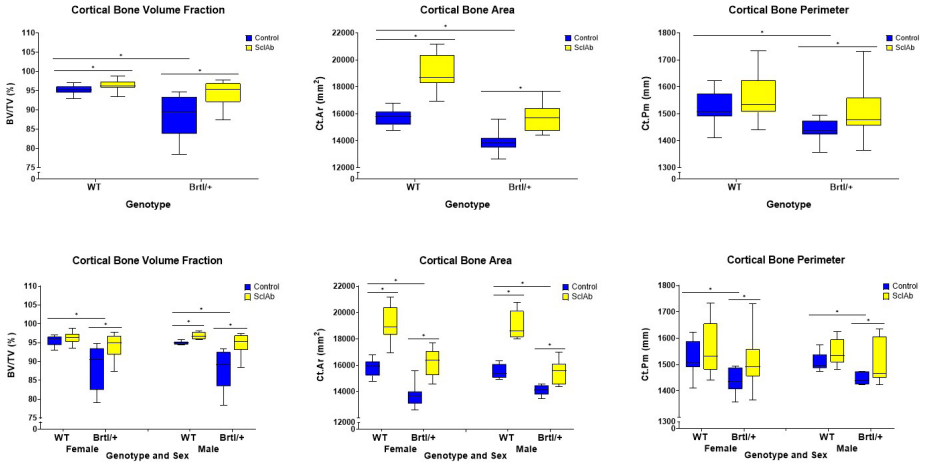

Figure 5. Mandibular cortical bone parameters in Brtl/+ and wild-type mice. The graphs present cortical bone volume fraction (BV/TV), bone area (B.Ar), and bone perimeter (B.Pm). Sclerostin antibody treatment effectively restored cortical bone volume, area, and perimeter in Brtl/+ mice to levels comparable to WT controls, with similar improvements observed in both male and female mice.

Sclerostin Antibody Enhances Condylar Thickness in Both Genotypes

The mandibular condyle, unlike the maxillary bone and the mandibular body which develop via intramembranous ossification, forms through endochondral ossification and represents a critical site for craniofacial growth and remodeling.

In the combined cohort, WT mice had a mean condylar thickness of 0.065 mm, while Brtl/+ animals showed a significant reduction to 0.041 mm (WP vs BP: $p = 0.0005$). SclAb treatment significantly increased condylar thickness in WT mice to 0.091 mm

(WP vs WS: p = 0.017), and partially rescued condylar thickness in Brtl/+ mice to 0.063 mm (BP vs BS: p = 0.0065). No significant difference remained between WT controls and Brtl/+ mice after SclAb treatment (WP vs BS: p = 0.45).

Sex-specific analysis revealed the effect was most prominent in male mice. Females displayed a smaller, statistically non-significant difference in condylar thickness between WT and Brtl/+ groups (WP: 0.064 mm; BP: 0.046 mm; p = 0.12), with SclAb having positive but nonsignificant effects. Males showed a significant reduction in Brtl/+ mice (WP: 0.066 mm; BP: 0.031 mm; p = 0.002), and SclAb treatment increased thickness in both genotypes, with Brtl/+ treated males recovering to 0.062 mm (BP vs BS: p = 0.057).

The Brtl/+ mutation significantly reduces mandibular condylar thickness—an endochondral compartment effect—which is partially rescued by SclAb treatment. The effect is statistically robust when sexes are combined and most evident in males (figure 6).

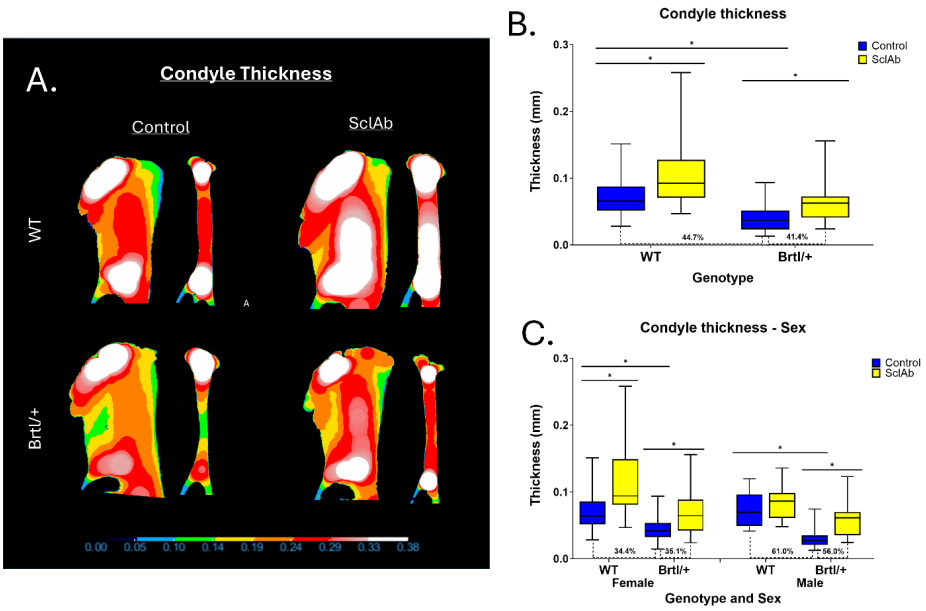

Figure 6. Analysis of Mandibular Condyle Thickness. A. displays the representative mean thickness of the samples for each group. **B**. shows the overall comparison of condyle thickness across all samples, highlighting the general distribution and mean values. **C**. illustrates the comparison of thickness in male and female samples, respectively. All graphs include error bars representing standard deviation and statistical significance p<0.05.

Sclerostin Antibody Enhances Jaw thickness in Both Genotypes

Jaw thickness was assessed in the border of the jaw at the incisor level across all experimental groups. WT mice exhibited an average jaw thickness of 0.258 mm, while Brtl/+ mice demonstrated a significant reduction to 0.194 mm (WP vs BP: $p = 6.5 \times 10^{-7}$), indicating the deleterious effect of the mutation. SclAb treatment substantially increased jaw thickness in both genotypes: SclAb-treated WT mice reached 0.299 mm (WP vs WS: p = 0.0039), and Brtl/+ SclAb-treated mice improved to 0.225 mm (BP vs BS: p = 0.0026; WP vs BS: p = 0.0003). Nevertheless, jaw thickness in treated Brtl/+ mice remained below the values observed in treated WT controls.

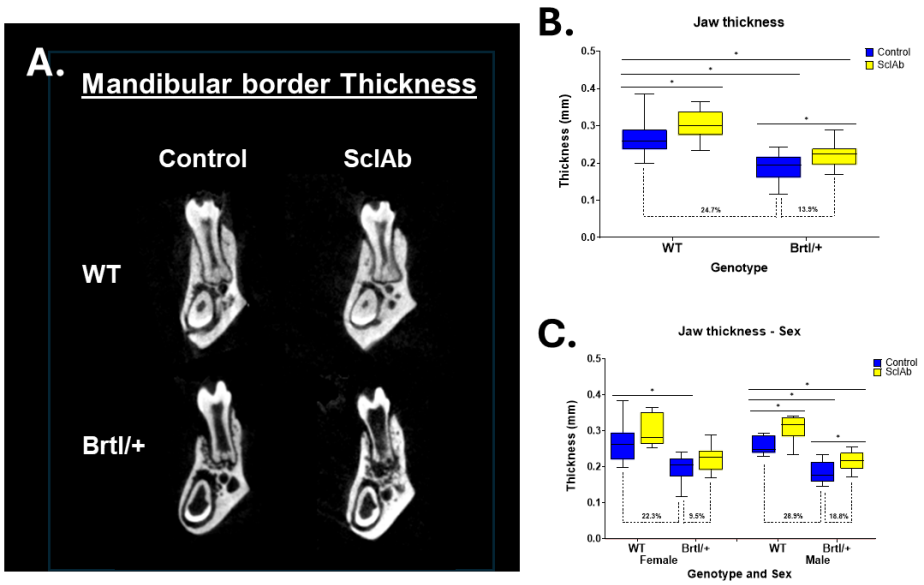

Figure 7. Scl-Ab Partially Rescues Mandibular Border Thickness in Brtl/+ Mice with Sex. A. Representative micro-CT images of the mandibular thickness (intramembranous origin). **B.** Brtl/+ jaw thickness is thinner than WT, and both are increased by SclAb, but Brtl/+ is not fully rescued to WT levels. **C.** Males show stronger responses than females. * $p<0.05$.

Sex-stratified analysis revealed consistent findings. In females, WT jaw thickness measured 0.263 mm, and Brtl/+ had 0.205 mm (WP vs BP: p = 0.0007). Treatment with SclAb raised thickness in Brtl/+ females to 0.226 mm (BP vs BS: p = 0.032), while treated WT females reached 0.281 mm. In males, jaw thickness in WT was 0.248 mm and fell to 0.176 mm in Brtl/+ mice (WP vs BP: $p = 6.5 \times 10^{-5}$); SclAb therapy increased jaw thickness to 0.217 mm in treated Brtl/+ males (BP vs BS: p = 0.015; WP vs BS: p = 0.0013), and to 0.317 mm in treated wild-type males (WP vs WS: p = 0.0038).

The Brtl/+ mutation significantly reduces jaw thickness, and SclAb therapy provides a statistically robust partial rescue in both WT and Brtl/+ mice. Although this treatment improves jaw dimensions in both sexes, it does not fully restore jaw thickness in Brtl/+ animals to healthy WT levels. These results highlight the beneficial effect of sclerostin inhibition on jaw morphology in OI. (Figure 7).

Sclerostin Antibody Improves Cranial Base thickness in Both Genotypes

The cranial base is a key craniofacial structure formed by endochondral ossification, similar to the mandibular condyle. WT mice displayed an average thickness of 0.492 mm, while Brtl/+ mice had a significantly thinner thickness at 0.358 mm (WP vs BP: p = 0.0001), demonstrating the impact of the OI mutation. SclAb treatment increased thickness in both genotypes: WT SclAb-treated mice reached 0.517 mm (WP vs WS: p = 0.047), and treated Brtl/+ mice improved to 0.463 mm (BP vs BS: p = 0.0002). Although the treated Brtl/+ group approached the WT values, the difference did not reach statistical significance (WP vs BS: p = 0.111).

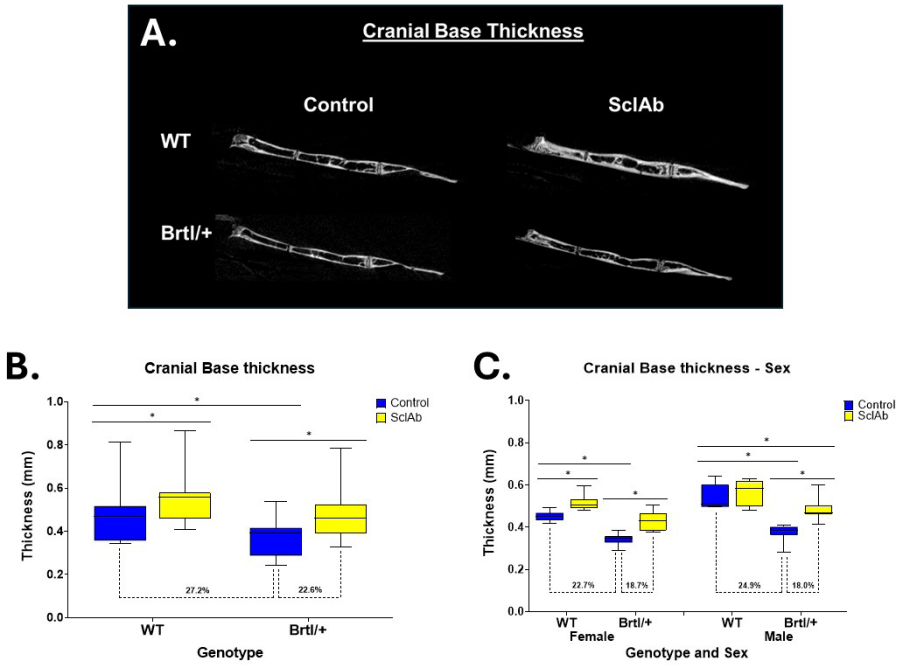

Figure 8. SclAb Rescues Cranial Base Thickness in Brtl/+ Mice with Sex-Dependent Effects. **A)** Representative micro-CT images of cranial base thickness in WT and Brtl/+ with and without SclAb treatment. **B)** Brtl/+ exhibit significantly thinner cranial base bones compared to WT. SclAb restores thickness to WT levels in Brtl/+ but also increases WT bone thickness. **C)** Sex-stratified analysis reveals that females maintain SclAb-induced thickening in both WT and Brtl/+, while males show minimal response in WT and incomplete rescue in Brtl/+. * $p < 0.05$.

When stratified by sex, similar improvements were observed. In females, WT mice had a scranial base thickness of 0.451 mm, while Brtl/+ mice were significantly thinner at 0.349 mm (WP vs BP: $p = 0.00062$). SclAb treatment increased thickness to 0.503 mm in treated WT and to 0.429 mm in treated Brtl/+ females, with a significant improvement seen in the Brtl/+ group (BP vs BS: $p = 0.001$).

In males, WT thickness was 0.510 mm and Brtl/+ mice showed a reduction to 0.383 mm (WP vs BP: $p = 0.003$). Treated WT males reached 0.583 mm, and treated Brtl/+ males measured 0.467 mm, which was significantly higher than untreated Brtl/+ (BP vs BS: $p = 0.002$) and similar to WT controls (WP vs BS: $p = 0.003$).

Brtl/+ mice have a marked decrease in cranial base thickness, but SclAb treatment significantly increases thickness in both WT and mutant animals. Although the therapy brings treated Brtl/+ mice closer to WT values, full recovery is not always achieved (Figure 8).

Sclerostin Antibody Increases Calvarial Bone Thickness in Both Wild-Type and Brtl/+ Mice

Calvarial bone thickness was measured at the frontal, parietal, and occipital bones along the sagittal midline. These regions comprise flat bones formed by intramembranous ossification.

WT mice displayed an average calvarial thickness of 0.487 mm. Brtl/+ mice showed a substantial reduction to 0.336 mm (WP vs BP: $p = 9.6 \times 10^{-13}$), highlighting the impact of the mutation. SclAb treatment increased thickness in WT animals to 0.514 mm (WP vs WS: $p = 0.059$) and significantly improved thickness in treated Brtl/+ mice to 0.452 mm (BP vs BS: $p = 4.8 \times 10^{-9}$; WP vs BS: $p = 0.017$), approaching WT levels.

Sex-specific analysis showed the same trend. In females, WT thickness was 0.470 mm and Brtl/+ thickness dropped to 0.345 mm (WP vs BP: $p = 7.8 \times 10^{-7}$). SclAb increased thickness to 0.514 mm in treated WT (WP vs WS: $p = 0.0085$) and to 0.445 mm in treated Brtl/+ females (BP vs BS: $p = 1.8 \times 10^{-5}$; WP vs BS: $p = 0.054$). In males, WT controls measured 0.508 mm, Brtl/+ mice had 0.324 mm (WP vs BP: $p = 2.1 \times 10^{-7}$), and SclAb raised thickness to 0.515 mm in treated WT and 0.459 mm in treated Brtl/+ males (BP vs BS: $p = 6.2 \times 10^{-5}$; WP vs BS: $p = 0.054$).

Calvarial bone thickness is markedly reduced in Brtl/+ mice, reflecting the effects of OI on intramembranously ossified flat bones. SclAb therapy robustly increases thickness in both WT and Brtl/+ mice, nearly restoring Brtl/+ values to those of WTs (Figure 9).

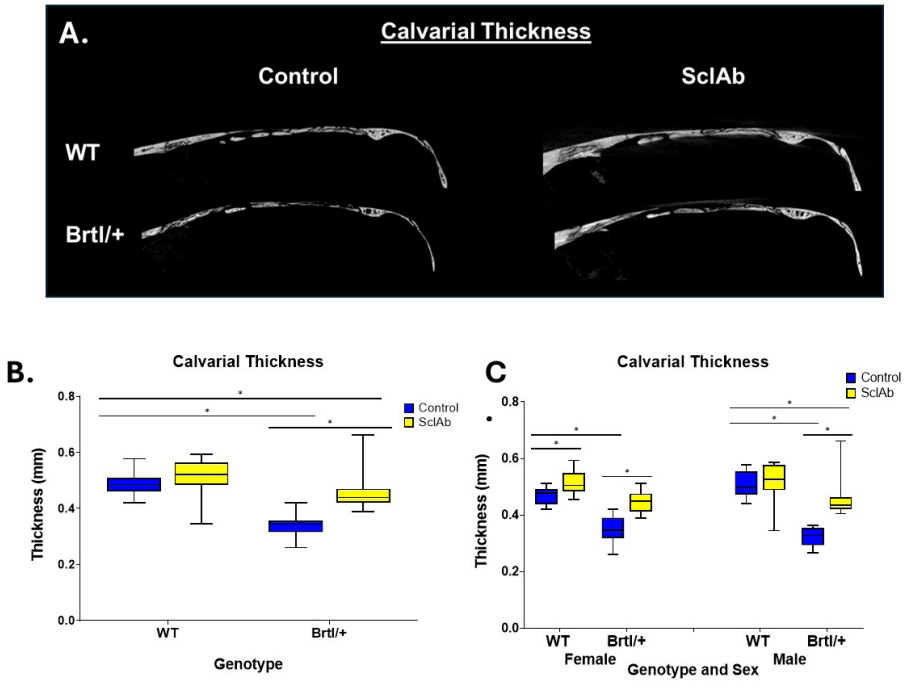

Figure 9. SclAb Partially Restores Calvarial Bone Thickness in Brtl/+ Mice. Micro-CT analysis of calvarial bone. **A.** Representative 3D reconstructions of the calvarial bones (frontal, parietal, and occipital bones). **B.** Quantification of bone thickness across regions. Brtl/+ exhibit significantly thinner calvarial bones compared to WT. SclAb increases thickness in Brtl/+. C. SclAb increased calvarial thickness in Brtl/+ mice of both sexes, partially restoring values toward WT levels.

Sclerostin Antibody Selectively Modifies Craniofacial morphometric measurements

Total skull length was significantly reduced in Brtl/+ non-treated mice (22.07 mm) compared to WT controls (22.73 mm; WP vs BP: $p = 0.015$). Treatment with sclerostin antibody showed a trend toward increased length in WT (WS: 23.01 mm; WP vs WS: $p = 0.31$) and Brtl/+ (BS: 22.51 mm) mice, but these changes did not reach statistical significance.

Cranial length was also significantly shorter in Brtl/+ non-treated mice (15.86 mm) relative to WT controls (16.34 mm; WP vs BP: $p = 0.019$), with no significant differences observed after antibody treatment.

Several additional landmarks demonstrated significant genotype effects. Frontal crest height was elevated in Brtl/+ mice (4.16 mm) compared to WT (3.90 mm; WP vs BP: $p = 0.041$), and facial height was reduced in Brtl/+ non-treated mice (10.17 mm) versus WT controls (10.58 mm; WP vs BP: $p = 0.015$).

Mandibular inferior length was significantly shorter in Brtl/+ non-treated mice (9.69 mm) compared to WT (10.15 mm; WP vs BP: p = 0.085), with SclAb treatment in Brtl/+ animals resulting in a minor, yet statistically significant, increase (BS: 10.21 mm; BP vs BS: p = 0.041).

No statistically significant differences were detected for nasal length, parietal, interparietal, occipital, facial length, premaxilla, maxilla, palate, presphenoid, basisphenoid, or basioccipital measures, nor in anterior, middle, or posterior cranial vault dimensions and heights.

Table 2. Morphometric measurements

Anatomical sites	Measurements (mm)				pvalues			
	WP	BP	WS	BS	WP/BP	WP/WS	WP/BS	BP/BS
total length	22.73	22.07	23.01	22.51	0.01	0.31	0.41	0.13
cranial length	16.34	15.86	16.45	16.14	0.02	0.76	0.22	0.31
nasal length	6.90	6.77	6.90	6.85	0.54	0.95	0.92	0.68
frontal	7.26	6.97	7.24	7.04	0.13	0.83	0.34	0.76
parietal	4.05	4.19	4.08	4.25	0.68	0.92	0.41	0.87
interparietal	3.63	3.43	3.77	3.47	0.30	0.31	0.31	0.92
occipital	6.07	5.81	6.15	5.80	0.17	0.70	0.21	0.92
facial length	11.85	11.52	12.02	11.77	0.06	0.60	0.73	0.26
premaxilla	5.57	5.45	5.64	5.48	0.48	0.83	0.56	0.73
maxilla	3.94	3.72	3.97	3.93	0.17	1.00	0.92	0.18
palate	2.42	2.48	2.49	2.44	0.57	0.63	1.00	0.57
Presphenoid length	2.49	2.35	2.40	2.37	0.13	0.31	0.31	0.92
Basisphenoid length	3.92	3.90	3.96	3.93	0.92	0.63	0.92	0.83
basioccipital length	3.60	3.48	3.69	3.54	0.26	0.34	0.67	0.65
cranial base	9.97	9.71	10.02	9.82	0.13	0.65	0.33	0.68
mandibular inf length	10.15	9.69	10.29	10.21	0.09	0.68	0.85	0.04
mandibular sup length	11.30	10.83	11.35	11.35	0.09	0.90	0.90	0.06
Mid-face length	14.72	14.45	14.80	14.60	0.31	0.73	0.60	0.64
anterior cranial vault	6.36	6.30	6.34	6.28	0.44	0.92	0.49	1.00
Mid-cranial vault	6.17	6.22	6.12	6.17	0.74	0.76	0.95	0.48
posterior cranial vault	5.52	5.65	5.40	5.48	0.31	0.39	0.70	0.12
frontal crest height	3.90	4.16	3.81	4.05	0.04	0.41	0.26	0.33
facial height	10.58	10.17	10.56	10.39	0.01	1.00	0.22	0.22
anterior nasal height	3.16	3.11	3.03	3.09	0.57	0.06	0.31	0.92
posterior nasal height	1.80	1.71	1.78	1.70	0.13	0.68	0.06	0.92
anterior pharyngeal height	1.50	1.33	1.50	1.43	0.02	0.87	0.30	0.31
Upper central incisor	3.38	3.38	3.35	3.39	0.85	0.63	0.92	0.85
Lower central incisor	3.08	3.32	3.18	3.30	0.16	0.46	0.21	0.92
mandibular anterior height	3.52	3.25	3.38	3.26	0.06	0.31	0.28	0.70
Mandibular posterior height	2.79	2.78	2.82	2.94	0.90	0.87	0.21	0.14
magnum height	4.25	4.19	4.26	4.17	0.57	0.92	0.33	0.83

Craniofacial linear dimensions including total skull length, cranial length, frontal crest height, facial height, and mandibular inferior length are significantly reduced in Brtl/+ mice, confirming the impact of this mutation on craniofacial growth.

SclAb treatment leads to partial correction in mandibular length but does not fully normalize other cranial or facial metrics (Table 2).

Genotype Effect and Sclerostin Antibody Response in Maxilla and Mandible

In the maxilla, WT controls exhibited a mean resorption value of 0.208, while Brtl/+ non-treated mice showed a significantly higher value of 0.265 (WP vs BP: $p = 4.00 \times 10^{-5}$), indicating greater bone loss in the mutant genotype. SclAb treatment led to pronounced reductions in resorption: WT-treated mice showed a value of 0.192 (WP vs WS: $p = 0.004$), and Brtl/+ treated animals had 0.240 (WP vs BS: $p = 0.004$; BP vs BS: $p = 0.017$).

Sex-specific analysis confirmed these patterns. In females, WP, BP, WS, and BS values were 0.217, 0.253, 0.192, and 0.241, respectively; significant differences were found between WP and BP ($p = 0.0012$), WP and WS ($p = 0.0011$), and WP and BS ($p = 0.03$). In males, WP, BP, WS, and BS were 0.193, 0.280, 0.192, and 0.237; treatment resulted in significant reductions (WP vs BP: $p = 0.00044$; WP vs BS: $p = 0.01$; BP vs BS: $p = 0.01$).

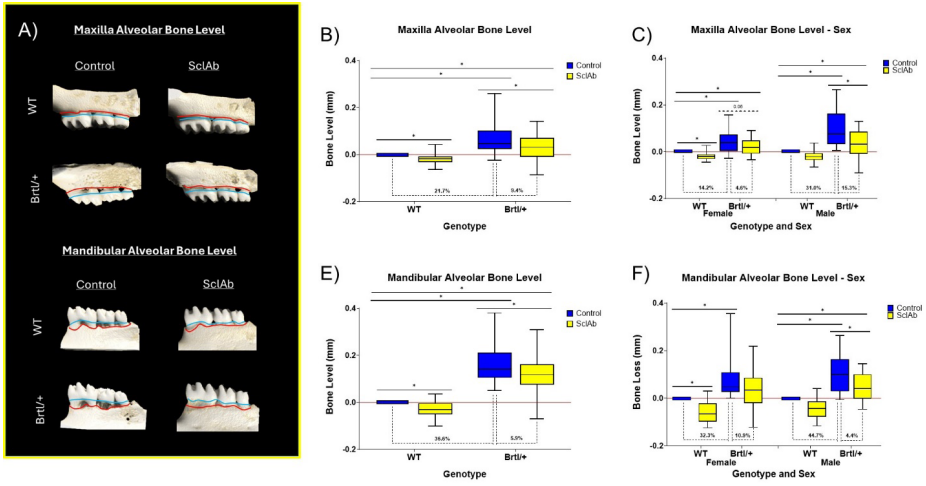

Figure 10. SclAb Partially Rescues Alveolar Bone Loss. A. Representative micro-CT images of the maxillary/mandibular alveolar bone levels (intramembranous origin). **B-C.** Maxillary and **E-F.** mandibular alveolar bone levels. Brtl/+ shows significant bone loss vs. WT. SclAb improves alveolar bone in both genotypes, but Brtl/+ doesn't reach WT levels. Graph bone level is taking the WT level as the reference (point 0) represented with a red dotted line. SclAb treatment reduced bone resorption in both WT and Brtl/+ mice, restoring values toward wild-type levels, with effects most pronounced in males for the maxilla and females for the mandible.

In the mandible, WT displayed a mean resorption of 0.27, while Brtl/+ was markedly increased to 0.42 (WP vs BP: p = 0.0001). SclAb reduced resorption to 0.25 in WS (WP vs WS: p = 0.037) and 0.40 in BS (WP vs BS: p = 0.0006; BP vs BS: p = 0.037). For females, WP, BP, WS, and BS were 0.28, 0.42, 0.25, and 0.37, with all comparisons showing statistical significance (WP vs BP: p = 0.0001; WP vs WS: p = 0.0078; WP vs BS: p = 0.001; BP vs BS: p = 0.009). In males, WP, BP, WS, and BS resorption values were 0.25, 0.45, 0.25, and 0.43; WP vs BP (p = 0.0001), WP vs BS (p = 0.0007), but the difference between BP and BS (p = 0.52) did not reach statistical significance.

Brtl/+ was associated with significantly increased alveolar bone resorption in both maxilla and mandible across sexes. SclAb treatment reduced bone resorption in both WT and Brtl/+ mice, restoring values toward wild-type levels, with effects most pronounced in males for the maxilla and females for the mandible. These results emphasize the genotype-driven increase in alveolar bone loss and highlight the therapeutic benefit of sclerostin inhibition in both craniofacial sites (Figure 10).

SclAb decreased inflammatory reaction in Brtl/+ mice

After observing a decrease in alveolar bone resorption following SclAb treatment in both sexes, we performed quantitative PCR and TRAP staining to evaluate local inflammatory activity and osteoclastogenesis in the alveolar bone.

Quantitative PCR analysis was performed to assess the expression of inflammatory cytokines Il1, Il6, and TNF in the alveolar bone.

For all three cytokines, Brtl/+ untreated mice displayed significantly elevated expression compared to WTs. Specifically, Il1 expression increased from 0.0006 in WP to 0.0033 in BP (WP vs BP: p = 0.0007), Il6 rose from 0.0002 to 0.0009 (WP vs BP: p = 0.0025), and TNF was upregulated from 0.0004 to 0.0018 (WP vs BP: p = 0.0328), indicating a heightened pro-inflammatory state in the Brtl/+ genotype.

SclAb treatment effectively reduced cytokine expression in Brtl/+ mice. For Il1, levels fell from 0.0033 (BP) to 0.0005 (BS; BP vs BS: p = 0.0006). Il6 expression decreased from 0.0009 (BP) to 0.0002 (BS; BP vs BS: p = 0.0019), and TNF values dropped from 0.0018 (BP) to 0.0006 (BS; BP vs BS: p = 0.0466). Expression levels in SclAb-treated Brtl/+ mice were not significantly different from WT controls.

No statistically significant differences were found between WT controls and SclAb-treated wild-types for any cytokine (WP vs WS: all p > 0.05), suggesting that SclAb does not alter baseline cytokine expression in healthy animals.

Brtl/+ mice exhibit elevated inflammatory cytokine expression, which is normalized by SclAb treatment. These results suggest that SclAb effectively reduces the pro-inflammatory gene expression signature associated with OI (Figure 11).

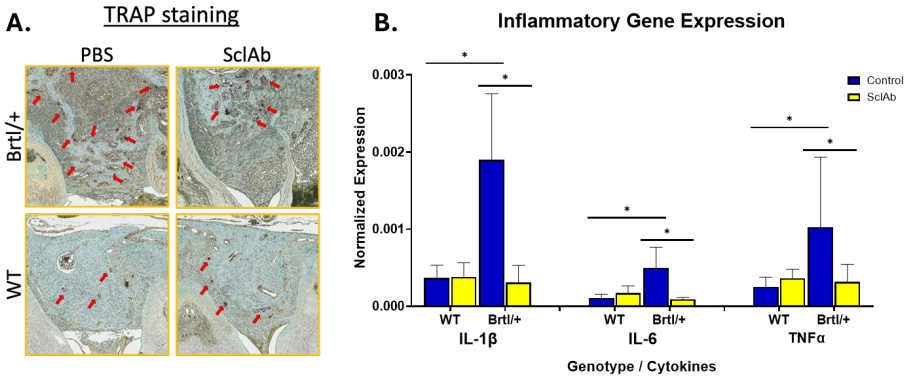

Figure 11. Inflammatory expression in Brtl/+ alveolar bone. A. Representative TRAP staining images demonstrating increased osteoclastic activity in Brtl/+ untreated mice compared to WT and SclAb-treated groups. B. Relative mRNA expression levels of Il1, Il6, and TNF determined by qPCR. Brtl/+ untreated mice show significantly elevated cytokine expression, which is reduced to near WT levels following SclAb treatment.

Discussion

Osteogenesis imperfecta (OI) is a heritable connective tissue disorder characterized predominantly by abnormal collagen synthesis, leading to bone fragility, dental abnormalities, and craniofacial deformity throughout the lifespan[3, 4]. Although much of the existing literature has focused on the appendicular skeleton and axial bones, our study broadens the scope by demonstrating that both intramembranous and endochondral bones of the craniofacial complex are substantially compromised in OI. Through analysis of the Brtl/+ mouse model representing moderate–severe OI, we uncovered pronounced baseline deficits in bone volume, mineral density, and architectural parameters across the maxilla, mandible, calvaria, cranial base, jaw, and condyle. These findings mirror the clinical phenotype of poor oral health, alveolar bone loss, and craniofacial dysmorphology observed in individuals living with OI[4, 26, 27].

Detailed analysis of genotype effects showed that intramembranous bones (maxilla, mandible, calvaria, jaw border) and endochondral structures (mandibular condyle, cranial base) are both impacted, but endochondral sites exhibited especially marked thinning and reduced bone quality in Brtl/+ mice, a pattern analogous to

the vulnerability seen in long bones[23, 28, 29]. Importantly, SclAb therapy produced robust improvements in both bone compartments. In intramembranous bones, SclAb almost fully restored bone volume fraction, mineral density, and thickness—consistent with previous calvarial bone study[16]. Males, in contrast, responded more strongly in condylar and cranial base thickness, pointing to possible influences of sex hormones or developmental timing on endochondral bone repair[23, 28, 29]. These findings reinforce the importance of considering "sex as a biological variable" in skeletal disease management, and highlight a need for further research into the hormonal and molecular mechanisms driving these differences in order to optimize care for all patients.

Consistent with previous reports[18], our findings revealed sex-dependent variations in both OI bone pathology and response to SclAb therapy. Compared to males, females showed greater benefit from SclAb in measures of mandibular bone resorption and density, likely reflecting inherent differences in estrogen-mediated bone turnover and osteoclast activity[30]. Conversely, males exhibited a more pronounced response in condylar and cranial base thickness after SclAb, suggesting sex hormones or developmental timing modulate the reparative capacity of endochondral bone[31]. These observations reinforce the growing appreciation of "sex as a biological variable" in skeletal disease management and should guide clinicians toward individualized dosing and therapy selection according to patient sex and developmental stage.

The mechanism underpinning the efficacy of SclAb relates to its antagonism of sclerostin, a Wnt pathway inhibitor expressed by osteocytes that restrain bone formation[32]. By blocking sclerostin, SclAb unleashes Wnt signaling, thereby stimulating osteoblast differentiation, activity, and matrix production[33, 34]. Notably, benefits were seen in both Brtl/+ mutants and wild-type controls, with no evidence of the pathological hyperostosis seen in sclerosteosis or Van Buchem disease[12-14], suggesting a favorable safety profile for craniofacial applications with appropriate dosing.

Recent studies indicate that OI is accompanied by chronic inflammation, evidenced by elevated cytokines such as IFN and TNFα in patients and mouse models[35]. Such a pro-inflammatory state exacerbates bone loss and metabolism dysfunction, as observed in rheumatoid arthritis and osteoporosis[36, 37], and may further contribute to OI pathology through changes in the bone marrow niche[38]. Building on this, our results show that SclAb therapy not only improves craniofacial bone mass but also reduces alveolar bone resorption and normalizes inflammatory cytokines

(Il1, Il6, TNF) in Brtl/+ mice. This dual anabolic and anti-inflammatory activity may synergistically enhance bone healing, osseointegration, and orthodontic success. Translationally, this suggests improved dental implant stability, informed craniofacial surgical planning, and better rehabilitation strategies for OI and allied skeletal fragility disorders.

Despite notable increases in bone mass and reduced resorption with SclAb, certain morphometric features—such as skull length, cranial height, and overall facial dimensions—were only partially restored. This likely reflects the limited plasticity of craniofacial shape and size after skeletal maturity. Our findings imply that interventions targeting craniofacial morphometry may need to be applied during critical periods of growth, while anabolic agents like SclAb are highly effective for improving bone quality and volume in post-developmental patients, with particular value for surgical and dental applications. Integrating pharmacologic therapy with early orthodontic or surgical approaches may yield optimal outcomes for individuals with OI.

While mouse models replicate many aspects of human OI and craniofacial biology, not all findings will directly translate; thus, validation in patient cohorts, clinical trials, and advanced human tissue models is essential. Additionally, although no adverse hyperostosis was observed, future research should include dose-escalation studies and long-term monitoring to ensure a safe therapeutic window in craniofacial bone growth contexts.

In summary, our study provides strong evidence for the use of SclAb as both a disease-modifying and adjunctive therapy for craniofacial bone augmentation. The sex-, compartment-, and genotype-specific responses observed here should inform future clinical trial designs and guide the development of personalized, evidence-based management algorithms for OI and craniofacial rehabilitation.

Conclusion

This study demonstrates that sclerostin antibody therapy is an effective intervention for craniofacial bone deficits in moderate-to-severe OI, as modeled by the Brtl/+ mouse. Scl-Ab substantially improves bone volume, thickness, mineralization, and reduces bone resorption in both endochondral and intramembranous bones. These restorative effects are consistent across sexes, with nuanced differences in response between male and female mice. Despite these improvements, some morphometric

deficits related to craniofacial size remain incompletely corrected, suggesting the potential necessity for earlier intervention or combination therapies. Overall, the data support SclAb as a promising approach for enhancing craniofacial bone health and implant success in OI, emphasizing the need for sex-aware personalized treatment strategies in translational and clinical practice

References

1. Marini JC, Forlino A, Bachinger HP, Bishop NJ, Byers PH, Paepe A, Fassier F, Fratzl-Zelman N, Kozloff KM, Krakow D, Montpetit K, Semler O. Osteogenesis imperfecta. Nat Rev Dis Primers. 2017;3:17052. Epub 2017/08/19. doi: 10.1038/nrdp.2017.52. PubMed PMID: 28820180.
2. Rodriguez Celin M, Steiner RD, Basel D. COL1A1- and COL1A2-Related Osteogenesis Imperfecta. In: Adam MP, Bick S, Mirzaa GM, Pagon RA, Wallace SE, Amemiya A, editors. GeneReviews((R)). Seattle (WA)1993.
3. Ventura L, Verdonk SJE, Zhytnik L, Ridwan-Pramana A, Gilijamse M, Schreuder WH, van Gelderen-Ziesemer KA, Schoenmaker T, Micha D, Eekhoff EMW. Dental Abnormalities in Osteogenesis Imperfecta: A Systematic Review. Calcif Tissue Int. 2024;115(5):461-79. Epub 20240918. doi: 10.1007/s00223-024-01293-2. PubMed PMID: 39294450; PMCID: PMC11531448.
4. Retrouvey JM, Taqi D, Tamimi F, Dagdeviren D, Glorieux FH, Lee B, Hazboun R, Krakow D, Sutton VR, Members of the BBDC. Oro-dental and cranio-facial characteristics of osteogenesis imperfecta type V. Eur J Med Genet. 2019;62(12):103606. Epub 20181226. doi: 10.1016/j.ejmg.2018.12.011. PubMed PMID: 30593885; PMCID: PMC6594916.
5. Andersson K, Dahllof G, Lindahl K, Kindmark A, Grigelioniene G, Astrom E, Malmgren B. Mutations in COL1A1 and COL1A2 and dental aberrations in children and adolescents with osteogenesis imperfecta - A retrospective cohort study. PLoS One. 2017;12(5):e0176466. Epub 20170512. doi: 10.1371/journal.pone.0176466. PubMed PMID: 28498836; PMCID: PMC5428910.
6. Kharazi. BWAMWKACBKAA. Anatomy, Head and Neck, Skull. (FL): SITI, editor: StatPearls Publishing; 2023.
7. SF. G. Developmental Biology. 6th edition. ed: Sunderland (MA): Sinauer Associates; 2000.
8. Yuan Y, Chai Y. Regulatory mechanisms of jaw bone and tooth development. Curr Top Dev Biol. 2019;133:91-118. Epub 20190211. doi: 10.1016/bs.ctdb.2018.12.013. PubMed PMID: 30902260; PMCID: PMC6986348.
9. Shen Z, Zhang R, Chen X, Yang G, Si Y, Yan T, Chen S, Cheng B, Wu X, Chen D, Zhang D, Xiao G, Zhu JK, Wang S. An atlas of early human mandibular endochondral and osteogenic paracrine signaling regions of Meckel's cartilage. Proc Natl Acad Sci U S A. 2025;122(12):e2420466122. Epub 20250317. doi: 10.1073/pnas.2420466122. PubMed PMID: 40096606; PMCID: PMC11962497.
10. Yao X, Carleton SM, Kettle AD, Melander J, Phillips CL, Wang Y. Gender-dependence of bone structure and properties in adult osteogenesis imperfecta murine model. Ann Biomed Eng. 2013;41(6):1139-49. Epub 20130328. doi: 10.1007/s10439-013-0793-7. PubMed PMID: 23536112; PMCID: PMC3703620.
11. Xiaohui T, Wang L, Yang X, Jiang H, Zhang N, Zhang H, Li D, Li X, Zhang Y, Wang S, Zhong C, Yu S, Ren M, Sun M, Li N, Chen T, Ma Y, Li F, Liu J, Yu Y, Yue H, Zhang Z, Zhang G. Sclerostin inhibition in rare bone diseases: Molecular understanding and therapeutic perspectives. J Orthop Translat. 2024;47:39-49. Epub 20240619. doi: 10.1016/j.jot.2024.05.004. PubMed PMID: 39007037; PMCID: PMC11245887.
12. Vanhoenacker FM, Balemans W, Tan GJ, Dikkers FG, De Schepper AM, Mathysen DG, Bernaerts A, Hul WV. Van Buchem disease: lifetime evolution of radioclinical features. Skeletal Radiol. 2003;32(12):708-18. Epub 20031001. doi: 10.1007/s00256-003-0675-4. PubMed PMID: 14520501.
13. Guo Y, Wu X, Jin Y, Gu Y, Lou Y, Miao P, Wang Y, Zhang B, Lin X, Zhang C, Feng J. Novel Loss of Function Variant in SOST From Chinese Family Results in Sclerosteosis 1. Mol Genet Genomic Med. 2025;13(7):e70109. doi: 10.1002/mgg3.70109. PubMed PMID: 40605263; PMCID: PMC12222177.

14. Appelman-Dijkstra NM, Avci TM, Schoeb M, Winter EM, van Lierop A, Papapoulos SE. Long-term clinical and bone mineral density changes of adult patients with sclerostin deficiency due to van Buchem disease: a follow-up study. JBMR Plus. 2025;9(4):ziae170. Epub 20250315. doi: 10.1093/jbmrpl/ziae170. PubMed PMID: 40092460; PMCID: PMC11910894.

15. Carpenter KA, Alkhatib DO, Dulion BA, Guirado E, Patel S, Chen Y, George A, Ross RD. Sclerostin antibody improves alveolar bone quality in the Hyp mouse model of X-linked hypophosphatemia (XLH). Int J Oral Sci. 2023;15(1):47. Epub 20231010. doi: 10.1038/s41368-023-00252-1. PubMed PMID: 37813865; PMCID: PMC10562382.

16. Scheiber AL, Barton DK, Khoury BM, Marini JC, Swiderski DL, Caird MS, Kozloff KM. Sclerostin Antibody-Induced Changes in Bone Mass Are Site Specific in Developing Crania. J Bone Miner Res. 2019;34(12):2301-10. Epub 20191107. doi: 10.1002/jbmr.3858. PubMed PMID: 31441963; PMCID: PMC7458133.

17. Sung HH, Kwon HH, Stephan C, Reynolds SM, Dai Z, Van der Kraan PM, Caird MS, Blaney Davidson EN, Kozloff KM. Sclerostin antibody enhances implant osseointegration in bone with Col1a1 mutation. Bone. 2024;186:117167. Epub 20240613. doi: 10.1016/j.bone.2024.117167. PubMed PMID: 38876270; PMCID: PMC11243590.

18. Cardinal M, Chretien A, Roels T, Lafont S, Ominsky MS, Devogelaer JP, Manicourt DH, Behets C. Gender-Related Impact of Sclerostin Antibody on Bone in the Osteogenesis Imperfecta Mouse. Front Genet. 2021;12:705505. Epub 20210810. doi: 10.3389/fgene.2021.705505. PubMed PMID: 34447412; PMCID: PMC8383339.

19. Haffner-Luntzer M, Fischer V, Ignatius A. Differences in Fracture Healing Between Female and Male C57BL/6J Mice. Front Physiol. 2021;12:712494. Epub 20210809. doi: 10.3389/fphys.2021.712494. PubMed PMID: 34434120; PMCID: PMC8381649.

20. Wang Y, Sakata T, Elalieh HZ, Munson SJ, Burghardt A, Majumdar S, Halloran BP, Bikle DD. Gender differences in the response of CD-1 mouse bone to parathyroid hormone: potential role of IGF-I. J Endocrinol. 2006;189(2):279-87. doi: 10.1677/joe.1.06351. PubMed PMID: 16648295; PMCID: PMC10745196.

21. Babey M, Wang Y, Kubota T, Fong C, Menendez A, ElAlieh HZ, Bikle DD. Gender-Specific Differences in the Skeletal Response to Continuous PTH in Mice Lacking the IGF1 Receptor in Mature Osteoblasts. J Bone Miner Res. 2015;30(6):1064-76. doi: 10.1002/jbmr.2433. PubMed PMID: 25502173; PMCID: PMC9045460.

22. Forlino A, Porter FD, Lee EJ, Westphal H, Marini JC. Use of the Cre/lox recombination system to develop a non-lethal knock-in murine model for osteogenesis imperfecta with an alpha1(I) G349C substitution. Variability in phenotype in BrtlIV mice. J Biol Chem. 1999;274(53):37923-31. doi: 10.1074/jbc.274.53.37923. PubMed PMID: 10608859.

23. Sinder BP, White LE, Salemi JD, Ominsky MS, Caird MS, Marini JC, Kozloff KM. Adult Brtl/+ mouse model of osteogenesis imperfecta demonstrates anabolic response to sclerostin antibody treatment with increased bone mass and strength. Osteoporos Int. 2014;25(8):2097-107. Epub 20140507. doi: 10.1007/s00198-014-2737-y. PubMed PMID: 24803333; PMCID: PMC4415164.

24. Vora SR, Camci ED, Cox TC. Postnatal Ontogeny of the Cranial Base and Craniofacial Skeleton in Male C57BL/6J Mice: A Reference Standard for Quantitative Analysis. Front Physiol. 2015;6:417. Epub 20160112. doi: 10.3389/fphys.2015.00417. PubMed PMID: 26793119; PMCID: PMC4709510.

25. Wei X, Thomas N, Hatch NE, Hu M, Liu F. Postnatal Craniofacial Skeletal Development of Female C57BL/6NCrl Mice. Front Physiol. 2017;8:697. Epub 2017/09/30. doi: 10.3389/fphys.2017.00697. PubMed PMID: 28959213; PMCID: PMC5603710.

26. Marulanda J, Ludwig K, Glorieux F, Lee B, Sutton VR, Members of the BBDC, Retrouvey JM, Rauch F. Craniofacial and dental phenotype of two girls with osteogenesis imperfecta due to mutations in CRTAP. Bone. 2022;164:116516. Epub 20220812. doi: 10.1016/j.bone.2022.116516. PubMed PMID: 35970273; PMCID: PMC10408670.

27. Prado HV, Teixeira SA, Rabello F, Vargas-Ferreira F, Borges-Oliveira AC, Abreu LG. Malocclusion in individuals with osteogenesis imperfecta: A systematic review and meta-analysis. Oral Dis. 2022;28(2):314-25. Epub 20201122. doi: 10.1111/odi.13715. PubMed PMID: 33222339.

28. Sinder BP, Eddy MM, Ominsky MS, Caird MS, Marini JC, Kozloff KM. Sclerostin antibody improves skeletal parameters in a Brtl/+ mouse model of osteogenesis imperfecta. J Bone Miner Res. 2013;28(1):73-80. Epub 2012/07/28. doi: 10.1002/jbmr.1717. PubMed PMID: 22836659; PMCID: PMC3524379.

29. Sinder BP, Salemi JD, Ominsky MS, Caird MS, Marini JC, Kozloff KM. Rapidly growing Brtl/+ mouse model of osteogenesis imperfecta improves bone mass and strength with sclerostin antibody treatment. Bone. 2015;71:115-23. Epub 20141023. doi: 10.1016/j.bone.2014.10.012. PubMed PMID: 25445450; PMCID: PMC4274252.

30. Chen S, Patel J, Katzmeyer T, Pei M. Sex-dependent variation in bone adaptation: from degeneration to regeneration. J Orthop Translat. 2025;52:325-43. Epub 20250505. doi: 10.1016/j.jot.2025.04.011. PubMed PMID: 40476066; PMCID: PMC12138372.

31. Modder UI, Hoey KA, Amin S, McCready LK, Achenbach SJ, Riggs BL, Melton LJ, 3rd, Khosla S. Relation of age, gender, and bone mass to circulating sclerostin levels in women and men. J Bone Miner Res. 2011;26(2):373-9. doi: 10.1002/jbmr.217. PubMed PMID: 20721932; PMCID: PMC3179347.

32. Delgado-Calle J, Sato AY, Bellido T. Role and mechanism of action of sclerostin in bone. Bone. 2017;96:29-37. Epub 20161012. doi: 10.1016/j.bone.2016.10.007. PubMed PMID: 27742498; PMCID: PMC5328835.

33. Shahid H, Morya VK, Noh KC. Sclerostin's role in bone-muscle crosstalk and osteoporosis pathogenesis. Osteoporos Sarcopenia. 2025;11(3):69-82. Epub 20250704. doi: 10.1016/j.afos.2025.06.004. PubMed PMID: 41127352; PMCID: PMC12537467.

34. Dreyer TJ, Keen JA, Wells LM, Roberts SJ. Novel insights on the effect of sclerostin on bone and other organs. J Endocrinol. 2023;257(2). Epub 20230403. doi: 10.1530/JOE-22-0209. PubMed PMID: 36802398.

35. Zhytnik L, Maasalu K, Reimann E, Martson A, Koks S. RNA sequencing analysis reveals increased expression of interferon signaling genes and dysregulation of bone metabolism affecting pathways in the whole blood of patients with osteogenesis imperfecta. BMC Med Genomics. 2020;13(1):177. Epub 20201123. doi: 10.1186/s12920-020-00825-7. PubMed PMID: 33228694; PMCID: PMC7684725.

36. Weyand CM, Goronzy JJ. The immunology of rheumatoid arthritis. Nat Immunol. 2021;22(1):10-8. Epub 20201130. doi: 10.1038/s41590-020-00816-x. PubMed PMID: 33257900; PMCID: PMC8557973.

37. Tilg H, Moschen AR, Kaser A, Pines A, Dotan I. Gut, inflammation and osteoporosis: basic and clinical concepts. Gut. 2008;57(5):684-94. doi: 10.1136/gut.2006.117382. PubMed PMID: 18408105.

38. Ono T, Nakashima T. Recent advances in osteoclast biology. Histochem Cell Biol. 2018;149(4):325-41. Epub 20180201. doi: 10.1007/s00418-018-1636-2. PubMed PMID: 29392395.

CHAPTER 6

Sclerostin antibody enhances implant osseointegration in bone with Col1a1 mutation

Hsiao H Sung [1,2,3], Hanna H Kwon [1], Chris Stephan [1], Skylar M Reynolds [1], Zongrui Dai [4], Peter M Van der Kraan [3], Michelle S Caird [1], Esmeralda N Blaney Davidson [3], Kenneth M Kozloff [1]

[1.] Orthopaedic Research Laboratories, Department of Orthopaedic Surgery, University of Michigan, Ann Arbor, MI, USA

[2.] Department of Oral and Maxillofacial Surgery, University of Michigan, Ann Arbor, MI, USA.

[3.] Experimental Rheumatology, Department of Rheumatology, Radboud Medical Centre, Nijmegen, the Netherlands.

[4.] Department of Biostatistics, University of Michigan, Ann Arbor, MI, USA.

Bone. 2024 Sep:186:117167. doi: 10.1016/j.bone.2024.117167. Epub 2024 Jun 13.

Abstract

We evaluated the potential of sclerostin antibody (SclAb) therapy to enhance osseointegration of dental and orthopaedic implants in a mouse model (Brtl/+) mimicking moderate to severe Osteogenesis Imperfecta (OI). To address the challenges in achieving stable implant integration in compromised bone conditions, our aim was to determine the effectiveness of sclerostin antibody (SclAb) at improving bone-to-implant contact and implant fixation strength. Utilizing a combination of micro-computed tomography, mechanical push-in testing, immunohistochemistry, and Western blot analysis, we observed that SclAb treatment significantly enhances bone volume fraction (BV/TV) and bone-implant contact (BIC) in Brtl/+ mice, suggesting a normalization of bone structure toward WT levels. Despite variations in implant survival rates between the maxilla and tibia, SclAb treatment consistently improved implant stability and resistance to mechanical forces, highlighting its potential to overcome the inherent challenges of OI in dental and orthopaedic implant integration. These results suggest that SclAb could be a valuable therapeutic approach for enhancing implant success in compromised bone conditions.

Keywords: Alveolar bone; Maxilla; Osteogenesis imperfecta; Sclerostin; Tibia.

Introduction

In contemporary healthcare, dental implants play a crucial role in restoring oral function and aesthetics for individuals suffering from tooth loss[1]. These implants are typically made from biocompatible materials such as titanium and require surgical placement into the bone. A key factor in their success is osseointegration, the process through which the implant integrates with the surrounding bone tissue[2]. Osseointegration is facilitated by the implant's stability and involves two stages: primary stability, which is mechanical and occurs immediately after placement, and secondary stability, a longer-term biological integration that ensures the implant's lasting stability[3, 4].

Excessively brittle and soft bone can compromise the primary and secondary stability of dental implants. Specifically, implants in the maxilla that lack primary stability often exhibit persistent fibrous encapsulation and mobility upon histological examination[5, 6]. Osteogenesis imperfecta (OI) results in impaired collagen synthesis due to mutations in collagen (COL1A1 and COL1A2) or collagen-associated genes, leading to reduced bone quality and quantity[7, 8]. Successfully achieving osseointegration in patients with OI is particularly challenging due to the complex nature of their bone condition. Although, some studies suggest a high success rate for dental implants in patients with OI, implying that implants could be a viable treatment [9, 10]. However, these findings are primarily based on a limited number of cases, predominantly involving mild forms of OI[9, 10]. The actual failure rates are not well documented, representing a significant gap in current research. These observations highlight the critical importance of achieving initial implant stability in OI to prevent long-term complications[11, 12].

Recent studies have highlighted the potential of Sclerostin antibody (SclAb) therapy in enhancing bone mineral density and improving the structural integrity of OI bones[13-17]. Sclerostin, a protein expressed by osteocytes that regulates bone metabolism, acts by inhibiting Wnt signaling, thus reducing bone formation [18, 19]. The inhibition of sclerostin by SclAb has been shown to improve bone quality and promote bone regeneration and osseointegration in preclinical studies involving both maxilla and long bones[20-25]. However, the efficacy of such treatments in OI models, which exhibit unique pathophysiological features affecting bone quality and biomechanics, remains unknown. Gaining insights from these preclinical studies could lead to a better understanding of this treatment and its potential applicability for OI patients.

Many SclAb-fixation studies in rat models are conducted in long bones and show increased osseointegration induced by SclAb[22, 23, 26, 27]. However, these findings are not directly extrapolatable to the clinical conditions of dental implant placement in humans, which typically occur in the jawbones (maxilla and mandible). The jawbones differ significantly in characteristics from long bones; for example, the maxilla presents a moist, microbially rich environment and is more challenging to access compared to the tibia. In contrast, the tibia, being easily accessible and shielded by muscle and skin, is a convenient model for studying implant osseointegration, yet it may not capture the full complexity of osseointegration in the jawbones[6, 28, 29].

Our study aims to analyze the effects of SclAb treatment on osseointegration around maxillary implants, using the Brtl/+ mouse model that closely resembles moderate to severe OI in humans[30]. We used the tibia as a reference to explore SclAb effects on osseointegration in long bones, commonly analyzed in fixation osseointegration studies. We propose that the structural and environmental uniqueness of the maxilla may respond differently to SclAb compared to tibia, potentially causing variations in implant osseointegration in an OI mouse model. This study allows us to examine the effects of SclAb on osseointegration in these bones, with the ultimate goal of improving oral rehabilitation for individuals affected by this condition.

Material and Methods

Animals

All protocols and procedures involving animals were approved by the University of Michigan's Committee on Use and Care of Animals (UM-IACUC PRO00011108, approved on 11/29/22). Wildtype (WT) and Brtl/+ mice with a mixed background of SV129/CD-1/C57BL/6S were derived from heterozygous Brtl/+ and WT parental strains. The Brtl/+ mouse is a heterozygous knock-in model for OI, featuring a Gly349Cys substitution in a COL1A1 allele, which has also been found in subjects affected by a moderately severe form of OI (type IV)[31]. A total of 48 female mice (3-month-old) underwent bilateral maxillary and tibial implant placement under inhaled isoflurane anesthesia. Buprenorphine was administered pre-operatively and again 12 hours later. Carprofen was administered immediately post-operatively and again 24 hours later, covering 48 hours post-surgery pain management. All surgical animals were housed in specific pathogen-free cages with standard 12-hour light/dark cycles and had access to a soft diet following surgery for up to 72 hours. Mice (n=48) were randomly assigned to SclAb (25mg/kg SclAb VI,

Amgen, Thousand Oaks, CA) or vehicle injection (PBS) subcutaneously starting on the day of the implant placement, two times per week for 5 weeks following our previously described protocol [15]. No antibiotics were administered to the animals after implantation surgery. These mice were euthanized at 5 weeks (35 days) post-implant placement by CO2 inhalation (Figure 1).

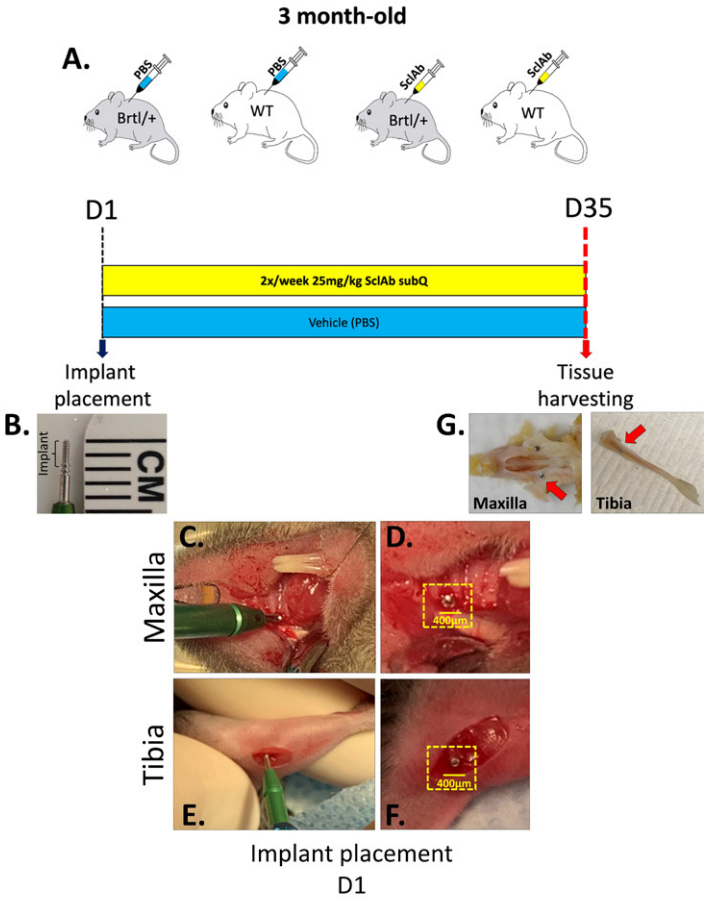

Figure 1. Experimental design. **A**. 3-month-old WT and Brtl/+ mice underwent bilateral maxillary and tibial implant with concomitant SclAb/PBS injections. **B**. 400µm diameter titanium implants. **C** and **D**. Maxillary implant placement and localization. **E** and **F**. Tibial implant placement and localization. **G**. Dissected specimens with the implants

Maxilla implant bed: Implants were placed transmucosally without incision or flap. An implant bed (0.4mm width x 1mm depth) was drilled with a bur at 650 rpm in the alveolar ridge between the upper central incisor and the first molar (Figure 1).

Tibia implant bed: 5 mm skin incisions were performed in the anteromedial of the proximal tibia without reflecting the periosteum. The implant bed (0.4mm width x 1mm depth) was drilled with a bur at 650 rpm in the union of the proximal metaphysis with the diaphysis. Incisions were re-approximated with a 6-0 nylon suture (Ethilon Monofilament 6-0, BV100-3, 5 in., Johnson & Johnson Medical, USA).

Implant selection: To simulate the clinical implant placement, we used 'Retopins' made with a titanium-6 aluminum-4 vanadium alloy (NTI Kahla GmbH, Thüringen, Germany). These screws, with a diameter of 0.4 mm are the smallest commercially available that fit the mouse maxilla, as demonstrated in previous studies using CD1 and C57Bl/6 mice[6, 32].

Implant placements: Each titanium implant, 1 mm in length, was screwed into the implant bed finger-tight using the integrated handle of the Retopins, which was then manually cut with a cutter after placement. Each mouse received bilateral maxillary and tibial implants (Figure 1).

The implant survival rate is determined by the number of implants that are successfully placed in the implant bed and remain stable for 35 days. Any implant that is lost during this period is classified as a failure.

Micro Computed Tomography (µCT)

Prior to scanning, maxilla (n=24) and tibia (n=24) samples (Table S1) were embedded in polymethyl methacrylate (PMMA). Samples were scanned at room temperature using an Xradia MicroXCT 520 (Zeiss, Jena, Germany) outfitted with a 0.4× objective lens. The X-ray source was configured to a voltage of 70 kV and a power of 10 W, with no X-ray prefilter utilized. Calibration phantoms were employed, and reference points for each sample were established using both air and implant standards. We developed a segmentation model using the deep learning tool in the Dragonfly 2022 software suite (Object Research Systems, Inc.; QC, Canada). This model was programmed to automatically segment bone, tooth, implant, and air within the sample. Subsequently, the model was employed to automate the segmentation process, enabling quantitative analysis of bone-implant contact and peri-implant bone volume fraction.

To confirm the systemic effect of SclAb treatment observed in our previous studies[13-15], we assessed the femoral trabecular and cortical phenotypes (without implants) of our samples. This evaluation served as an internal control to ascertain that the systemic action of SclAb is consistent with earlier findings, independent

of implant-related effects. We used high-resolution μCT (Bruker, Skyscan 1176, Kontich, Belgium), following methodologies previously described [30] to ensure that any changes observed in the surgical site could be attributed to the SclAb effect rather than being merely implant-induced secondary effects.

Push-in testing

For the mechanical testing of the implants, we used the push-in test because it is reported to be more sensitive than the pull-out test to changes in the mechanical properties at the bone-implant interfaces[33, 34]. We utilized an MTS 858 Mini-Bionix servo-hydraulic testing system (MTS Systems Corp., Eden Prairie, MN, USA) to administer a push-in force on the implants. We designed and fabricated a customized probe slightly smaller than the implant to facilitate proper testing of the osseointegration strength at the implant-bone interface. Prior to mechanical testing, each fresh specimen (n=24) (Table S1) was held and stabilized, but not infiltrated, in light-cured dental acrylic and maintained in a hydrated state using Phosphate-buffered Saline (PBS). Implants were subjected to a uniaxial compressive load until failure at a consistent displacement rate of 0.1 mm/s. During these tests, a 10-lb load cell (Sensotec, Columbus, OH, USA) continuously recorded the applied force, while an external linear variable differential transducer (LVDT; Lucas Schavitts, Hampton, VA, USA) monitored vertical displacements. Push-in load, defined as the force required to dislodge an implant from the murine maxillary or tibial bone, was precisely measured during these mechanical tests. We employed a customized LABVIEW program (NI, v21.0, Austin, Tx, USA) to perform comprehensive calculations of the mechanical properties under examination.

Immunohistochemistry (IHC) and Western blot.

Maxillae were harvested and fixed in 10% neutral buffered formalin. Samples (n=8) (Table S1) were decalcified in 20% EDTA for eight weeks and after complete demineralization, the implants were gently removed from the samples. Specimens were dehydrated through an ascending ethanol series prior to paraffin embedding. 5μm thick sagittal maxillary sections were cut and collected on Super Frost-plus slides for histology staining including Masson's trichrome. Sample slides were processed for immunohistochemistry (IHC). Before staining, slides were baked at 60 ºC for at least one hour, then deparaffinized with xylene and rehydrated through graded ethanol baths and MilliQ water. Antigen retrieval was performed in water bath at 65 ºC for 15 minutes using R-Universal epitope recovery buffer (EMS 62700-20, PA, USA). Sections were stained using mouse and rabbit specific HRP/DAB (ABC) detection IHC kit (ab64264, Abcam, Cambridge, UK) and processed according to the manufacturer's instructions. Slides were incubated with primary

antibody against Sost (ab63097, Abcam, Cambridge, UK) overnight at 4 ºC and used secondary anti-rabbit (HAF008, R&D systems, Minneapolis, MN, USA) for 1 hour at room temperature.

Harvested maxillae (n=24) (Table S1)were processed for western blot as previously described[30]. We used the same primary and secondary antibody for Sost as those used in the IHC) and the housekeeping was Gapdh (CS51724, Cell signaling technology, Boston, MA, USA).

Statistical analyses

Statistical comparisons among the genotype, control, and treated groups performed using ANOVA, with $p \leq 0.05$ considered significant. We checked the normality assumption using the Shapiro-Wilk test and tested the homoscedasticity assumption using Levene's Test for Homogeneity of Variance. Post hoc analysis was conducted with Welch's two-sample t-test to ensure robustness. Pairwise p-values were adjusted using the Benjamini-Hochberg (BH) procedure to avoid false positives. We performed linear regression to determine the effect of BIC and BV/TV on push-out force. Additionally, we used Fisher's exact test to assess the relationship between genotype and implant failure. Further analysis also included a comparison of Brtl/+ SclAb to the WT vehicle group, evaluating SclAb's ability to provide restorative anabolic gains as previously described[13-15].

Results

The bilateral implant model shows good postoperative recovery

To assess the healing and response of maxillary and tibial bone in the context of injury, we placed 400µm diameter implants in the maxilla and tibia of Brtl/+ and WT mice (Figure 1). Given the limited height of the maxillary alveolar ridge (400µm), all maxillary implants penetrated into the maxillary sinus, yet without any infections or need for antibiotics.

Implant survival rates are different in the maxilla compared with tibia

We assessed how these distinct anatomical locations, each with its unique characteristics, influence implant survival. The tibia, shielded by muscle, subcutaneous tissue, and skin, and in direct contact with bone marrow, contrasts with the maxillary environment, which is continuously exposed to moisture and the oral cavity's microbial load. Our findings reveal a significant disparity in immediate

post-op implant survival rates, with the tibia demonstrating a superior rate of 97% compared to 86% in the maxilla. Notably, in maxilla, failures were predominantly observed in Brtl/+ mice. The estimated odds ratio between genotype and maxilla implants is 0.13 (95%CI: 0.014, 0.68), indicating that there is significant association between the genotype and failed implants (p=0.006). In tibia, Brtl/+ presented higher failure, but there is no significant evidence to show that the genotype and tibial implants have strong association (p=0.35). The estimated odds ratio is 0.296 (95%CI:0.005,3.843). Table 1.

Table 1. Numbers of implants placed by genotypes.

Location	Genotype	Total implants By genotype Number (%)	Failed Implants Number (%)	Survived Implants	
				by genotype Number (%)	by bone location Number (%)
Maxilla	WT	50 (100%)	2 (4%)	48 (96%)	83 (86%)
	Brtl/+	46 (100%)	11 (24%)**	35 (76%)	
Tibia	WT	50 (100%)	1 (2%)	49 (98%)	92 (97%)
	Brtl/+	46 (100%)	3 (7%)	43 (93%)	

***p value ≤0.05*

SclAb increases peri-implant bone volume fraction (BV/TV) across bone types

To assess the peri-implant BV/TV, we delineated a ROI extending 250 micrometers (μm) radially around the implant surface. Our analysis highlighted notable differences in BV/TV between bone sites (maxilla vs tibia) and genotypes (WT vs Brtl/+). In Brtl/+ mice treated with Phosphate Buffered Saline (PBS-Brtl/+), the BV/TV was significantly lower in the maxilla (22.4% ± 10.6) compared to the tibia (41.8% ± 11.0). Similar patterns were observed in PBS-treated WT mice (PBS-WT), which exhibited higher BV/TV in the tibia (60.7% ± 6.5) compared to the maxilla (46.9% ± 8.4). When comparing PBS-Brtl/+ with PBS-WT, the BV/TV was significantly higher in PBS-WT for both the maxilla ($p<0.05$) and tibia ($p<0.05$). SclAb treatment markedly improved BV/TV in Brtl/+ mice, increasing to 38.3% ± 5.4 in the maxilla (a 71.3% increase) and 55.1% ± 6.4 in the tibia (a 31.9% increase), suggesting that SclAb treatment effectively mitigates the BV/TV insufficiency in Brtl/+ mice. In WT mice, SclAb administration increased BV/TV to 55.9% ± 3.3 in the maxilla, which is 19% higher than PBS-WT mice, but not statistically significant. In the tibia of SclAb-WT, BV/TV increased to 68.5% ± 7.8, representing a 12.9% increase compared to the PBS-WT though this increase was not statistically significant. Notably, the maxilla and tibia BV/TV in the SclAb-Brtl/+ mice were comparable to that of PBS-WT mice, highlighting the potential of SclAb treatment to normalize bone structure in Brtl/+ mice. (Figure 2).

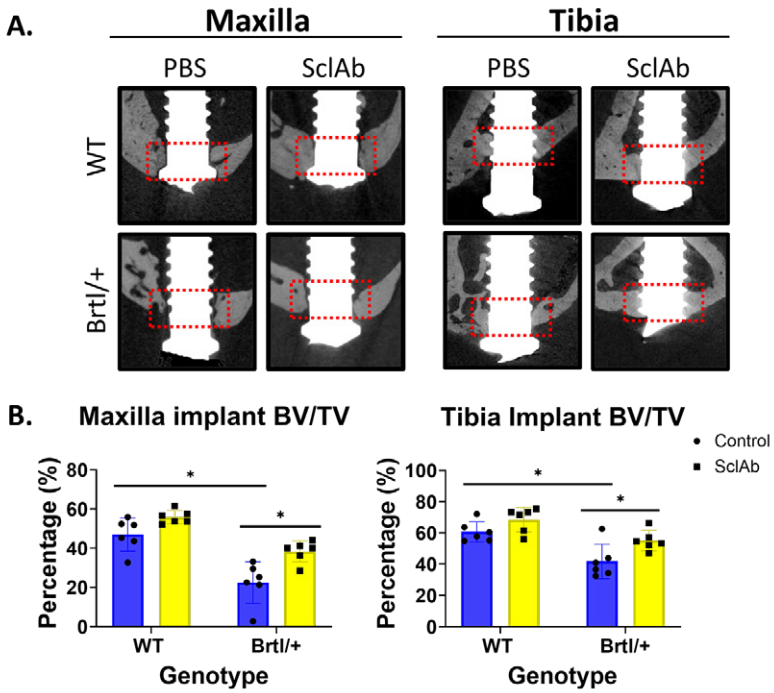

Figure 2. Bone volume fraction (BV/TV) of the peri-implant bone (within 250um of the implant). **A.** Figure shows the peri-implant bone in the PBS and SclAb treated groups in the maxilla and tibia of both genotypes. Red represents the region of interest (ROI). **B.** Graph represents the BV/TV of the red area in the maxilla and tibia. Asterisk represents $P<0.05$.

To confirm the effectiveness of SclAb in systemic gains, we analyzed the trabecular and cortical response in femur of our samples without implant placement. SclAb treatment significantly increased distal femoral trabecular BV/TV and mid-diaphyseal cortical thickness (Ct. Th.) in Brtl/+ mice (8.6% ± 2.8 and 0.21mm ± 0.01, respectively) compared to the PBS-Brtl/+ mice (5.1% ± 2.0 and 0.19mm ± 0.008, respectively). In wild-type mice, SclAb treatment also significantly improved trabecular BV/TV and Ct.Th (14.0% ± 3.7 and 0.23mm ± 0.01, respectively), demonstrating SclAb's positive impact systemically on bone structure and density (figure 3).

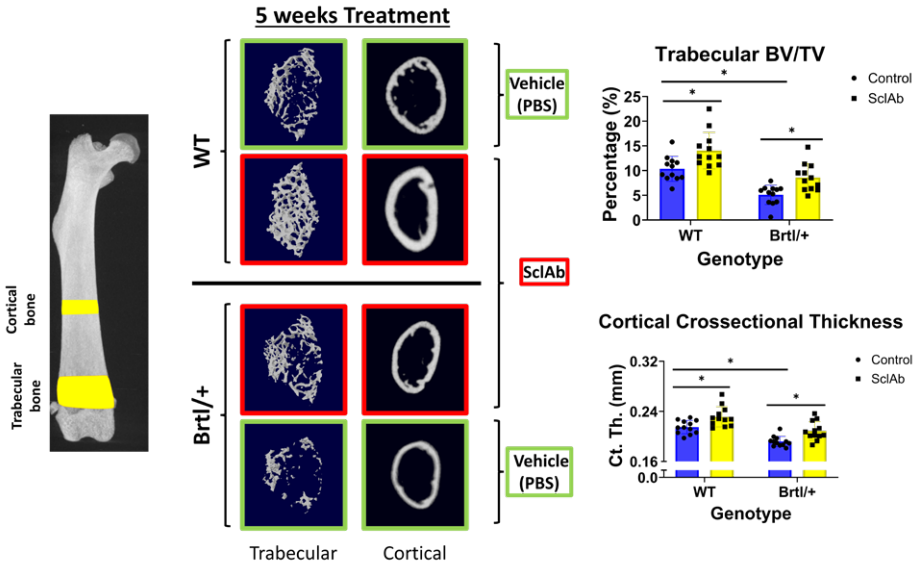

Figure 3. Micro computed tomography of the distal femur metaphysis. **A.** The cortical ROI defined as 15% of the total femur length situated equidistantly between the distal femur and the third trochanter, the trabecular ROI was defined as 10% of the total femur, located immediately proximal to the distal femoral end. Representative median BV/TV images reveal reduction in Brtl/+ bone mass and the anabolic effect of SclAb therapy. **B**. Graphs showing the increase in BV/TV and cortical thickness (ct.th) induced by SclAb for trabecular bone.

SclAb increases bone-implant contact (BIC) in WT and Brtl/+ mice

To assess osseointegration, we evaluated the bone-implant contact (BIC) in both the maxilla and tibia. In the maxilla, BIC for PBS-Brtl/+ mice were significantly lower at 3.4% ± 2.0 compared to PBS-WT mice, which had a BIC of 18.5% ± 1.3 ($p<0.05$), indicating that BIC in WT mice was 444% higher than in Brtl/+ mice. Following SclAb treatment, BIC in Brtl/+ mice increased to 15.9% ± 3.0, a significant enhancement of 373% ($p<0.05$), compared to PBS-Brtl/+. SclAb-WT mice exhibited a BIC of 25.3% ± 6.8, slightly, but not significantly, surpassing PBS-WT mice.

In the tibia, PBS-Brtl/+ mice demonstrated a BIC of 58.9% ± 2.9, substantially lower than PBS-WT mice, which had a BIC of 81.8% ± 5.1 ($p<0.05$). Similar to the maxillary findings, SclAb treatment in Brtl/+ mice improved tibial BIC to 77.1% ± 8.1 ($p<0.05$), corresponding to a 30.9% increase. The highest tibial BIC was observed in SclAb-WT mice, reaching 84.6% ± 5.3, marking a slight but non-significant improvement from PBS-WT mice (81.8% ± 5.1).

The BIC for both maxillary and tibial bone in SclAb-Brtl/+ mice reached the same levels as those observed in PBS-WT mice (Figure 4).

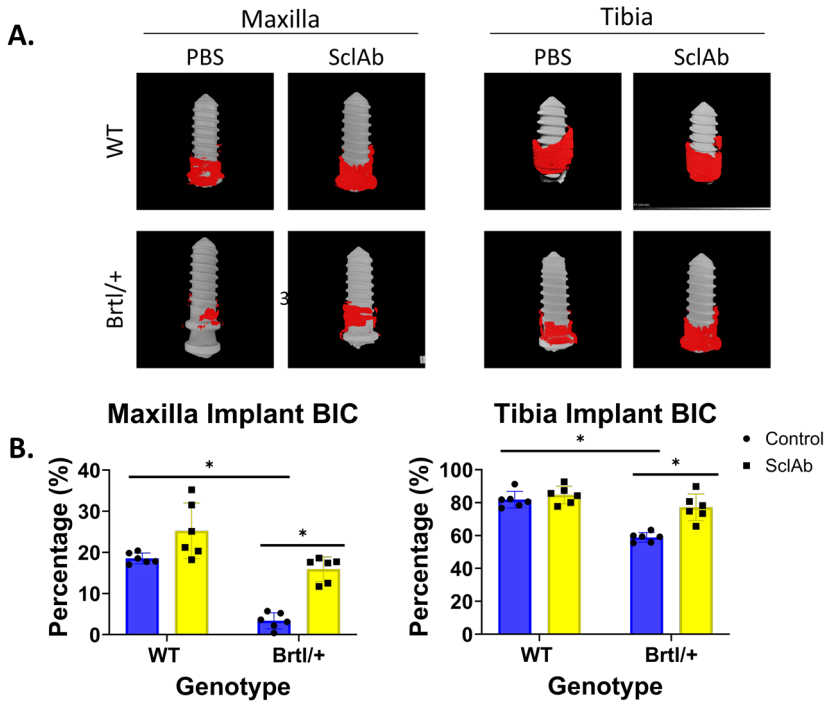

Figure 4. Bone-implant contact (BIC). **A**. Representative illustration of the BIC in the maxilla and tibia. **B**. Graph showing the percentage of bone -implant contact in the maxilla and tibia for both PBS and SclAb treated WT and Brtl/+ groups. Asterisk represents P<0.05.

SclAb increases the implant resistance to push-in forces in Brtl/+.

In our comparative study of mechanical resistance to push-in forces in implants, we noted distinct responses among our experimental groups. SclAb-Brtl/+ mice demonstrated a push-in force in the tibia that was nearly 150% higher (17.5N±7.5) compared to the PBS-Brtl/+ (7.1N±4.4, p<0.05). In the maxilla as well, these mice showed a 160% increased resistance (13.4N±3.2) versus the PBS-Brtl/+ (5.1N±3.4, p<0.05).

Both PBS-WT and SclAb-WT mice demonstrated high push-in resistance, with PBS-WT mice showing values of 14.7N±2.9 in the maxilla and 26.2N±6.1 in the tibia, and SclAb-WT mice showing a slight but non-significant increase in the resistance (17.1N±5.1 and 31.7N±3.4, respectively). The increase in push-in resistance induced by SclAb in WT mice did not reach statistical significance when compared with the PBS-WT, exhibiting only marginal improvements.

Further assessment revealed that the implant push-in resistance of the maxilla and tibia in SclAb-Brtl/+ mice was comparable to the PBS-WT, implying a restoration of mechanical properties toward normal WT levels. (Figure 5).

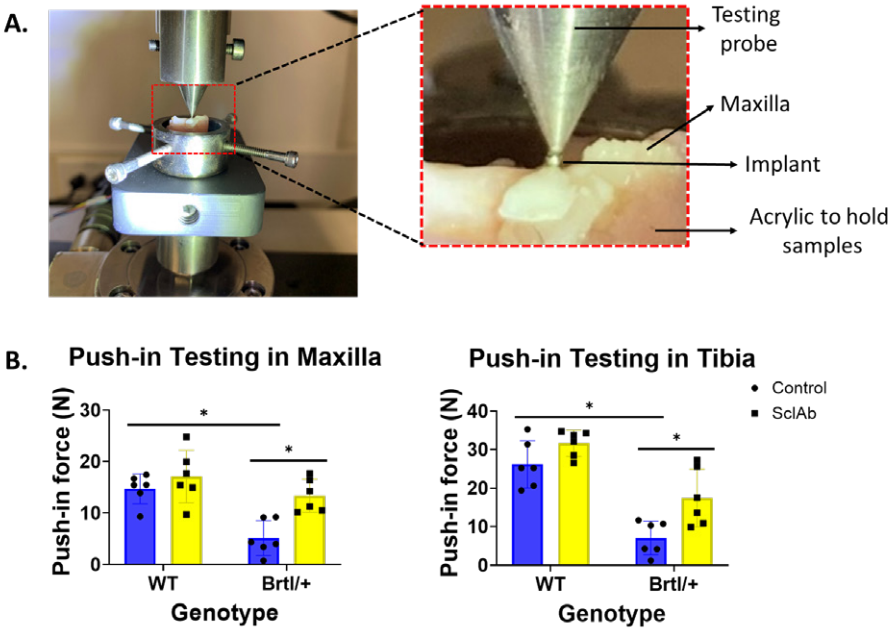

Figure 5. Push-in mechanical testing. **A**. Customized fixture aligned with the maxillary and tibial implants with the samples stabilized in light-cured acrylic to allow implant positioning directly beneath the probe. **B.** Graph showing maximum load measured in maxilla and tibia. Asterisk represents P<0.05.

BIC contributes significantly to the fixation push-in resistance.

We performed a regression analysis to determine if BIC or BV/TV influences the osseointegration resistance to push-in testing. For the maxilla, the BIC contributes more to the push-in resistance compared to BV/TV. The estimated BIC coefficient is 0.492 (95% CI: 0.214, 0.770, p<0.002), while the estimated BV/TV coefficient is 0.015 (95% CI: -0.156, 0.186, p<0.864). Also for the tibia, the BIC contributes more to the push-in resistance compared to BV/TV. The estimated BIC coefficient is 0.510 (95% CI: 0.115, 0.905, p<0.02), while the estimated BV/TV coefficient is 0.182 (95% CI: -0.181, 0.545, p<0.33).

SclAb induces compensatory production of sclerostin.

In a previous study examining the effects of SclAb treatment on alveolar bone regeneration in rats, an increase in sclerostin levels within the alveolar bone was observed [35]. Motivated by these findings, we aimed to determine if a similar

response occurred in our implant samples. Enhanced sclerostin immunostaining was observed in the osteocyte-containing lacunae and throughout the network of connecting canaliculi in the alveolar bone (Figure S1).

Quantification by Western blot, normalized against a housekeeping protein (GapdH), revealed that SclAb treatment significantly increased sclerostin levels in both Brtl/+ and WT samples compared to their respective controls. Specifically, the SclAb-WT group showed a relative sclerostin level increase to 1.72 times that of the control level ($p<0.05$), while the SclAb-Brtl/+ exhibited a relative increase to 1.82 times the control level ($p<0.05$).

Discussion

Successful osseointegration is critical to long-term health of patients receiving implants in compromised bone conditions, particularly in osteogenesis imperfecta, where impaired bone quality necessitates additional strategies for peri-implant osseointegration. Achieving optimal bone quantity and quality at the implant site is a crucial clinical goal before implant placement. However, understanding the effect of the sclerostin antibody during osseointegration is equally important. Our study investigated whether the sclerostin antibody can rescue osseointegration and implant stability to wild-type (WT) levels in osteogenesis imperfecta (OI) maxilla with poor bone quantity and quality. We found that systemic treatment with SclAb significantly improved implant fixation strength in Brtl/+ mice, as demonstrated by enhanced push-in test results and increased BIC after five weeks therapy. Notably, these improvements were significant in both the maxilla and tibia, indicating SclAb's effectiveness in enhancing osseointegration across different bone sites. In WT mice, however, the increase in BIC from SclAb treatment was modest, suggesting a potential saturation effect in unaffected bone. The increase in SclAb-induced osseointegration observed in this study not only aligns with previous research on osteoporotic rat models [21, 36] but also highlights SclAb's potential to improve both the quantity and quality of osseointegration in collagen-compromised bone. Thus, SclAb could enhance the stability and longevity of dental implants, particularly for OI clinical applications.

SclAb therapy effectively mitigated BV/TV deficits in the maxilla and tibia of Brtl/+ mice, demonstrating its efficacy in addressing bone structural alterations associated with OI. The increases in maxillary and tibial peri-implant BV/TV in Brtl/+ mice align with findings from studies on ovariectomized rats [22, 23], showcasing SclAb's broad

utility in enhancing bone quantity, even in the presence of genetically altered collagen and under injury stimuli like implant placement. Moreover, the SclAb-induced increase in BV/TV elevated the phenotypic characteristics of Brtl/+ mice to levels comparable to those in PBS-WT mice across bone types, underscoring SclAb's clinical relevance in restoring bone quantity under pathological conditions.

In WT mice, there is a response to SclAb in the tibia and maxilla, yet the effects are milder compared to the femoral BV/TV. This non-significant enhancement in peri-implant BV/TV for SclAb-WT mice is likely due to the restricted ROI analyzed (250 µm) and the nature of new bone, in comparison to the femoral BV/TV, which ROI represents 10% of the total femur. The enhancements in BV/TV observed in SclAb-Brtl/+ mice in both the maxilla and tibia are consistent with systemic gains in the femur (without implant placement). This supports the findings from our previous research on the SclAb-induced systemic bone gain [13-15]. Enhancements were noted across all examined bone sites, indicating SclAb's widespread efficacy. However, anatomical and structural differences likely affect the magnitude of SclAb's response, a factor that is also relevant to new bone formation induced by implants.

Our study highlighted the distinct processes of peri-implant osseointegration in the maxilla and tibia, corroborating previous research that demonstrated higher osseointegration in the tibia of healthy mouse models [6, 37]. Despite the collagen mutation in our Brtl/+ mice, we observed a pattern of osseointegration akin to that in healthy bone. The differences we observed can be attributed to the unique compositions and remodeling mechanisms of these bones. The maxilla, predominantly composed of trabecular bone, remodels through the periosteum, leading to less dense bone formation [37-39]. In contrast, the tibia, with its dense cortical structure, remodels via both the periosteum and bone marrow, facilitating stronger and more stable bone repair [6, 29]. This distinction is crucial for osseointegration, as the tibia's bone marrow and mechanical loading enhance osteoprogenitor cell availability and new bone formation [40]. Additionally, the differences in osseointegration between the tibia and maxilla could be influenced by the oral environment. The maxilla, exposed to a moist environment, faces additional challenges for implant integration, such as a higher risk of inflammation and infection [41, 42], compared to the tibia, which is protected by muscle and skin. All these factors may collectively contribute to the differences in osseointegration observed in these bones. In our Brtl/+ mice, SclAb treatment was more effective in enhancing osseointegration in the maxilla than in the tibia. This is likely due to the maxilla's lower baseline bone density, which provides greater potential for growth and improvement.

In this study, we observed an increased presence of sclerostin in the peri-implant alveolar bone of both WT and Brtl/+ mice following SclAb treatment. Western blot analysis confirmed a significant increase in sclerostin levels in both SclAb treated WT and Brtl/+ mice. This elevation was primarily localized within the osteocyte-containing lacunae and the extensive network of canaliculi in the alveolar bone. Previous research suggests that this increase of local sclerostin could be the accumulation of inactive, neutralized sclerostin protein trapped within the bone matrix [35]. Alternatively, the presence of sclerostin could counteract the enhanced bone formation induced by SclAb treatment, potentially through negative feedback regulation, where SclAb binding disrupts normal protein degradation or clearance, leading to sclerostin accumulation. Furthermore, SclAb treatment may alter cellular signaling, causing increased sclerostin synthesis via activated compensatory pathways. This explanation is supported by previous studies showing that SclAb treatment increases both gene expression and circulating levels of sclerostin [43], possibly due to the combined detection of unbound and antibody-bound sclerostin and the stabilization of the bound form by SclAb.

Our study encountered some limitations, with one notable challenge being the difficulty in standardizing the implant insertion process and achieving precise placement. This issue was exacerbated by the limited mouth opening and the fragility of the surgical site, particularly in Brtl/+ mice, where extreme care is necessary to prevent bone damage. Although the small diameter of the implant and its handle aids in insertion, sectioning of the implant handle after the positioning of the implant may disturb the bone at the implant bed, a concern that is especially relevant in the Brtl/+ mouse model as it could potentially compromise the implant's primary stability. We were not able to measure the implant insertion torque due to the small size of the implants, the restricted sites chosen for placement, and the design of the Retopin. As a result, we used finger-tight torque as an alternative measure. Previous study has shown that the finger-tight torque for female participants averaged 19 Ncm [44]. Additional studies support that lower insertion torques (< 20 Ncm) not only achieve comparable success rates for osseointegration with favorable gains in stability over the osseointegration phase but also reduce damage to the surrounding tissues [45, 46]. Based on these studies, the torque range achieved with finger-tight insertion is within the acceptable range for primary stability and osseointegration. All dental implants in our study were placed extending into the maxillary sinus due to the limited height of the alveolar bone. While this raises concerns about potential complications [47], clinical research supports the viability of such placements. Studies have shown that dental implants protruding into the maxillary sinus cavity by 4mm or less have a survival rate of

99.5%, suggesting that sinus penetration does not negatively impact implant success[48]. Our study corroborated these findings, with no instances of infection or the need for antibiotics observed.

In the general population, the dental implant survival rate is reported to be around 96% [49-53]. In contrast, for OI patients, this rate ranges between 80% to 94%, with those experiencing more severe OI exhibiting lower survival rates [9, 10]. Interestingly, in our study, the maxillary implant survival rates closely match these findings (WT:96%, Brtl/+: 76%). This similarity further supports our conclusions that the increase in osseointegration observed with the SclAb treatment in our model may have relevant implications for clinical application in OI patients.

Conclusion

Our research demonstrates that systemic administration of SclAb significantly enhances peri-implant osseointegration, highlighting its potential to improve implant success in conditions like OI, both anatomically and functionally. Dental implants in OI patients tend to have higher failure rates, particularly in severe forms of the disease. However, SclAb presents a promising solution for implant-supported dental rehabilitation, potentially reducing the risk of implant failure. This finding not only offers a new avenue of hope for OI patients but also suggests that targeted therapies can effectively address the challenges of dental implantation in the presence of compromised bone quality, thereby improving treatment outcomes and enhancing patients' quality of life.

References

1. Quadri MFA, Alamir AWH, John T, Nayeem M, Jessani A, Tadakamadla SK. Effect of prosthetic rehabilitation on oral health-related quality of life of patients with head and neck cancer: a systematic review. Transl Cancer Res. 2020;9(4):3107-18. Epub 2020/04/01. doi: 10.21037/tcr.2019.12.48. PubMed PMID: 35117674; PMCID: PMC8797697.
2. Walter N, Stich T, Docheva D, Alt V, Rupp M. Evolution of implants and advancements for osseointegration: A narrative review. Injury. 2022;53 Suppl 3:S69-S73. Epub 2022/08/11. doi: 10.1016/j.injury.2022.05.057. PubMed PMID: 35948509.
3. Javed F, Ahmed HB, Crespi R, Romanos GE. Role of primary stability for successful osseointegration of dental implants: Factors of influence and evaluation. Interv Med Appl Sci. 2013;5(4):162-7. Epub 2014/01/02. doi: 10.1556/IMAS.5.2013.4.3. PubMed PMID: 24381734; PMCID: PMC3873594.
4. Swami V, Vijayaraghavan V, Swami V. Current trends to measure implant stability. J Indian Prosthodont Soc. 2016;16(2):124-30. Epub 2016/05/04. doi: 10.4103/0972-4052.176539. PubMed PMID: 27141160; PMCID: PMC4837777.
5. Wazen RM, Currey JA, Guo H, Brunski JB, Helms JA, Nanci A. Micromotion-induced strain fields influence early stages of repair at bone-implant interfaces. Acta Biomater. 2013;9(5):6663-74. Epub 2013/01/23. doi: 10.1016/j.actbio.2013.01.014. PubMed PMID: 23337705; PMCID: PMC3622828.
6. Mouraret S, Hunter DJ, Bardet C, Brunski JB, Bouchard P, Helms JA. A pre-clinical murine model of oral implant osseointegration. Bone. 2014;58:177-84. Epub 2013/07/28. doi: 10.1016/j.bone.2013.07.021. PubMed PMID: 23886841; PMCID: PMC4962868.
7. Marini JC, Forlino A, Bachinger HP, Bishop NJ, Byers PH, Paepe A, Fassier F, Fratzl-Zelman N, Kozloff KM, Krakow D, Montpetit K, Semler O. Osteogenesis imperfecta. Nat Rev Dis Primers. 2017;3:17052. Epub 2017/08/19. doi: 10.1038/nrdp.2017.52. PubMed PMID: 28820180.
8. Marini JC, Forlino A, Cabral WA, Barnes AM, San Antonio JD, Milgrom S, Hyland JC, Korkko J, Prockop DJ, De Paepe A, Coucke P, Symoens S, Glorieux FH, Roughley PJ, Lund AM, Kuurila-Svahn K, Hartikka H, Cohn DH, Krakow D, Mottes M, Schwarze U, Chen D, Yang K, Kuslich C, Troendle J, Dalgleish R, Byers PH. Consortium for osteogenesis imperfecta mutations in the helical domain of type I collagen: regions rich in lethal mutations align with collagen binding sites for integrins and proteoglycans. Hum Mutat. 2007;28(3):209-21. Epub 2006/11/02. doi: 10.1002/humu.20429. PubMed PMID: 17078022; PMCID: PMC4144349.
9. Oelerich O, Kleinheinz J, Bohner L, Wiesmuller V, Hanisch M. Dental Implants in People with Osteogenesis Imperfecta: A Systematic Review. Int J Environ Res Public Health. 2022;19(3). Epub 2022/02/16. doi: 10.3390/ijerph19031563. PubMed PMID: 35162583; PMCID: PMC8835393.
10. Fogh FM, Jensen SS, Kofod T, Lauridsen E. Dental Implants in Patients with Osteogenesis Imperfecta - Clinical and Radiographic Outcome in Six Patients. Oral Health Prev Dent. 2023;21(1):33-40. Epub 2023/02/03. doi: 10.3290/j.ohpd.b3858615. PubMed PMID: 36727836.
11. Mouraret S, Hunter DJ, Bardet C, Popelut A, Brunski JB, Chaussain C, Bouchard P, Helms JA. Improving oral implant osseointegration in a murine model via Wnt signal amplification. J Clin Periodontol. 2014;41(2):172-80. Epub 2013/10/30. doi: 10.1111/jcpe.12187. PubMed PMID: 24164629; PMCID: PMC4993043.
12. Lioubavina-Hack N, Lang NP, Karring T. Significance of primary stability for osseointegration of dental implants. Clin Oral Implants Res. 2006;17(3):244-50. Epub 2006/05/05. doi: 10.1111/j.1600-0501.2005.01201.x. PubMed PMID: 16672018.
13. Sinder BP, Eddy MM, Ominsky MS, Caird MS, Marini JC, Kozloff KM. Sclerostin antibody improves skeletal parameters in a Brtl/+ mouse model of osteogenesis imperfecta. J Bone Miner Res. 2013;28(1):73-80. Epub 2012/07/28. doi: 10.1002/jbmr.1717. PubMed PMID: 22836659; PMCID: PMC3524379.

14. Sinder BP, Salemi JD, Ominsky MS, Caird MS, Marini JC, Kozloff KM. Rapidly growing Brtl/+ mouse model of osteogenesis imperfecta improves bone mass and strength with sclerostin antibody treatment. Bone. 2015;71:115-23. Epub 20141023. doi: 10.1016/j.bone.2014.10.012. PubMed PMID: 25445450; PMCID: PMC4274252.

15. Sinder BP, White LE, Salemi JD, Ominsky MS, Caird MS, Marini JC, Kozloff KM. Adult Brtl/+ mouse model of osteogenesis imperfecta demonstrates anabolic response to sclerostin antibody treatment with increased bone mass and strength. Osteoporos Int. 2014;25(8):2097-107. Epub 20140507. doi: 10.1007/s00198-014-2737-y. PubMed PMID: 24803333; PMCID: PMC4415164.

16. Glorieux FH, Devogelaer JP, Durigova M, Goemaere S, Hemsley S, Jakob F, Junker U, Ruckle J, Seefried L, Winkle PJ. BPS804 Anti-Sclerostin Antibody in Adults With Moderate Osteogenesis Imperfecta: Results of a Randomized Phase 2a Trial. J Bone Miner Res. 2017;32(7):1496-504. Epub 20170419. doi: 10.1002/jbmr.3143. PubMed PMID: 28370407.

17. Scheiber AL, Barton DK, Khoury BM, Marini JC, Swiderski DL, Caird MS, Kozloff KM. Sclerostin Antibody-Induced Changes in Bone Mass Are Site Specific in Developing Crania. J Bone Miner Res. 2019;34(12):2301-10. Epub 20191107. doi: 10.1002/jbmr.3858. PubMed PMID: 31441963; PMCID: PMC7458133.

18. Diegel CR, Kramer I, Moes C, Foxa GE, McDonald MJ, Madaj ZB, Guth S, Liu J, Harris JL, Kneissel M, Williams BO. Inhibiting WNT secretion reduces high bone mass caused by Sost loss-of-function or gain-of-function mutations in Lrp5. Bone Res. 2023;11(1):47. Epub 2023/08/24. doi: 10.1038/s41413-023-00278-5. PubMed PMID: 37612291; PMCID: PMC10447437 The Williams Laboratory has also received recent support from Janssen Pharmaceuticals for work unrelated to the studies reported here. C.M., J.L., I.K., M.K. and S.G. are employees and shareholders of Novartis.

19. Yavropoulou MP, Xygonakis C, Lolou M, Karadimou F, Yovos JG. The sclerostin story: from human genetics to the development of novel anabolic treatment for osteoporosis. Hormones (Athens). 2014;13(4):323-37. Epub 2015/01/03. doi: 10.14310/horm.2002.1552. PubMed PMID: 25555179.

20. Korn P, Kramer I, Schlottig F, Todtman N, Eckelt U, Burki A, Ferguson SJ, Kautz A, Schnabelrauch M, Range U, Kneissel M, Stadlinger B. Systemic sclerostin antibody treatment increases osseointegration and biomechanical competence of zoledronic-acid-coated dental implants in a rat osteoporosis model. Eur Cell Mater. 2019;37:333-46. Epub 2019/05/22. doi: 10.22203/eCM.v037a20. PubMed PMID: 31112281.

21. Liu S, Virdi AS, Sena K, Sumner DR. Sclerostin antibody prevents particle-induced implant loosening by stimulating bone formation and inhibiting bone resorption in a rat model. Arthritis Rheum. 2012;64(12):4012-20. Epub 2012/11/30. doi: 10.1002/art.37697. PubMed PMID: 23192793.

22. Virdi AS, Irish J, Sena K, Liu M, Ke HZ, McNulty MA, Sumner DR. Sclerostin antibody treatment improves implant fixation in a model of severe osteoporosis. J Bone Joint Surg Am. 2015;97(2):133-40. Epub 2015/01/23. doi: 10.2106/JBJS.N.00654. PubMed PMID: 25609440.

23. Virdi AS, Liu M, Sena K, Maletich J, McNulty M, Ke HZ, Sumner DR. Sclerostin antibody increases bone volume and enhances implant fixation in a rat model. J Bone Joint Surg Am. 2012;94(18):1670-80. Epub 2012/09/21. doi: 10.2106/JBJS.K.00344. PubMed PMID: 22992878; PMCID: PMC3444952.

24. Yu SH, Hao J, Fretwurst T, Liu M, Kostenuik P, Giannobile WV, Jin Q. Sclerostin-Neutralizing Antibody Enhances Bone Regeneration Around Oral Implants. Tissue Eng Part A. 2018;24(21-22):1672-9. Epub 2018/06/21. doi: 10.1089/ten.TEA.2018.0013. PubMed PMID: 29921173; PMCID: PMC6916116.

25. Yao Y, Kauffmann F, Maekawa S, Sarment LV, Sugai JV, Schmiedeler CA, Doherty EJ, Holdsworth G, Kostenuik PJ, Giannobile WV. Sclerostin antibody stimulates periodontal regeneration in large alveolar bone defects. Sci Rep. 2020;10(1):16217. Epub 20201001. doi: 10.1038/s41598-020-73026-y. PubMed PMID: 33004873; PMCID: PMC7530715.

26. Makhdom AM, Rauch F, Lauzier D, Hamdy RC. The effect of systemic administration of sclerostin antibody in a mouse model of distraction osteogenesis. J Musculoskelet Neuronal Interact. 2014;14(1):124-30. Epub 2014/03/04. PubMed PMID: 24583547.

27. Agholme F, Li X, Isaksson H, Ke HZ, Aspenberg P. Sclerostin antibody treatment enhances metaphyseal bone healing in rats. J Bone Miner Res. 2010;25(11):2412-8. Epub 2010/05/26. doi: 10.1002/jbmr.135. PubMed PMID: 20499342.

28. Son C, Choi MS, Park JC. Different Responsiveness of Alveolar Bone and Long Bone to Epithelial-Mesenchymal Interaction-Related Factor. JBMR Plus. 2020;4(8):e10382. Epub 2020/08/18. doi: 10.1002/jbm4.10382. PubMed PMID: 32803111; PMCID: PMC7422712.

29. Mavropoulos A, Rizzoli R, Ammann P. Different responsiveness of alveolar and tibial bone to bone loss stimuli. J Bone Miner Res. 2007;22(3):403-10. Epub 2006/12/22. doi: 10.1359/jbmr.061208. PubMed PMID: 17181394.

30. H.H. Sung H, W.J. Spresser, J.P. Hoffmann, Z. Dai, P.M. Van der Kraan, M.S. Caird, E. Blaney Davidson, K.M. Kozloff. Collagen mutation and age contribute to differential craniofacial phenotypes in mouse models of osteogenesis imperfecta. JBMR plus. 2024;8(1).

31. Forlino A, Porter FD, Lee EJ, Westphal H, Marini JC. Use of the Cre/lox recombination system to develop a non-lethal knock-in murine model for osteogenesis imperfecta with an alpha1(I) G349C substitution. Variability in phenotype in BrtlIV mice. J Biol Chem. 1999;274(53):37923-31. doi: 10.1074/jbc.274.53.37923. PubMed PMID: 10608859.

32. Biguetti CC, Cavalla F, Silveira EM, Fonseca AC, Vieira AE, Tabanez AP, Rodrigues DC, Trombone APF, Garlet GP. Oral implant osseointegration model in C57Bl/6 mice: microtomographic, histological, histomorphometric and molecular characterization. J Appl Oral Sci. 2018;26:e20170601. Epub 2018/06/14. doi: 10.1590/1678-7757-2017-0601. PubMed PMID: 29898187; PMCID: PMC5963915.

33. Seong WJ, Grami S, Jeong SC, Conrad HJ, Hodges JS. Comparison of push-in versus pull-out tests on bone-implant interfaces of rabbit tibia dental implant healing model. Clin Implant Dent Relat Res. 2013;15(3):460-9. Epub 20111215. doi: 10.1111/j.1708-8208.2011.00357.x. PubMed PMID: 22172015.

34. Chang PC, Seol YJ, Goldstein SA, Giannobile WV. Determination of the dynamics of healing at the tissue-implant interface by means of microcomputed tomography and functional apparent moduli. Int J Oral Maxillofac Implants. 2013;28(1):68-76. doi: 10.11607/jomi.2614. PubMed PMID: 23377049; PMCID: PMC4111564.

35. Taut AD, Jin Q, Chung JH, Galindo-Moreno P, Yi ES, Sugai JV, Ke HZ, Liu M, Giannobile WV. Sclerostin antibody stimulates bone regeneration after experimental periodontitis. J Bone Miner Res. 2013;28(11):2347-56. Epub 2013/05/29. doi: 10.1002/jbmr.1984. PubMed PMID: 23712325.

36. Liu M, Kurimoto P, Zhang J, Niu QT, Stolina M, Dechow PC, Feng JQ, Hesterman J, Silva MD, Ominsky MS, Richards WG, Ke H, Kostenuik PJ. Sclerostin and DKK1 Inhibition Preserves and Augments Alveolar Bone Volume and Architecture in Rats with Alveolar Bone Loss. J Dent Res. 2018;97(9):1031-8. Epub 2018/04/05. doi: 10.1177/0022034518766874. PubMed PMID: 29617179.

37. Covani U, Giammarinaro E, Panetta D, Salvadori PA, Cosola S, Marconcini S. Alveolar Bone Remodeling with or without Collagen Filling of the Extraction Socket: A High-Resolution X-ray Tomography Animal Study. J Clin Med. 2022;11(9). Epub 2022/05/15. doi: 10.3390/jcm11092493. PubMed PMID: 35566619; PMCID: PMC9100251.

38. Lin Z, Fateh A, Salem DM, Intini G. Periosteum: biology and applications in craniofacial bone regeneration. J Dent Res. 2014;93(2):109-16. Epub 2013/10/04. doi: 10.1177/0022034513506445. PubMed PMID: 24088412; PMCID: PMC3895334.

39. Jonasson G, Skoglund I, Rythen M. The rise and fall of the alveolar process: Dependency of teeth and metabolic aspects. Arch Oral Biol. 2018;96:195-200. Epub 2018/10/07. doi: 10.1016/j.archoralbio.2018.09.016. PubMed PMID: 30292055.

40. Ma Q, Miri Z, Haugen HJ, Moghanian A, Loca D. Significance of mechanical loading in bone fracture healing, bone regeneration, and vascularization. J Tissue Eng. 2023;14:20417314231172573. Epub 2023/05/30. doi: 10.1177/20417314231172573. PubMed PMID: 37251734; PMCID: PMC10214107.

41. Kunrath MF, Dahlin C. The Impact of Early Saliva Interaction on Dental Implants and Biomaterials for Oral Regeneration: An Overview. Int J Mol Sci. 2022;23(4). Epub 2022/02/27. doi: 10.3390/ijms23042024. PubMed PMID: 35216139; PMCID: PMC8875286.

42. Liao M, Shi Y, Chen E, Shou Y, Dai D, Xian W, Ren B, Xiao S, Cheng L. The Bio-Aging of Biofilms on Behalf of Various Oral Status on Different Titanium Implant Materials. Int J Mol Sci. 2022;24(1). Epub 2023/01/09. doi: 10.3390/ijms24010332. PubMed PMID: 36613775; PMCID: PMC9820730.

43. Carpenter KA, Davison R, Shakthivel S, Anderson KD, Ko FC, Ross RD. Sclerostin antibody improves phosphate metabolism hormones, bone formation rates, and bone mass in adult Hyp mice. Bone. 2022;154:116201. Epub 2021/09/20. doi: 10.1016/j.bone.2021.116201. PubMed PMID: 34537437; PMCID: PMC8671249.

44. Kanawati A, Richards MW, Becker JJ, Monaco NE. Measurement of clinicians' ability to hand torque dental implant components. J Oral Implantol. 2009;35(4):185-8. doi: 10.1563/1548-1336-35.4.185. PubMed PMID: 19813423.

45. Norton MR. The Influence of Low Insertion Torque on Primary Stability, Implant Survival, and Maintenance of Marginal Bone Levels: A Closed-Cohort Prospective Study. Int J Oral Maxillofac Implants. 2017;32(4):849-57. doi: 10.11607/jomi.5889. PubMed PMID: 28708918.

46. Rea M, Botticelli D, Ricci S, Soldini C, Gonzalez GG, Lang NP. Influence of immediate loading on healing of implants installed with different insertion torques--an experimental study in dogs. Clin Oral Implants Res. 2015;26(1):90-5. Epub 20131209. doi: 10.1111/clr.12305. PubMed PMID: 24313303.

47. Kim SW, Lee IH, Kim SW, Kim DH. Points to consider before the insertion of maxillary implants: the otolaryngologist's perspective. J Periodontal Implant Sci. 2019;49(6):346-54. Epub 2019/12/31. doi: 10.5051/jpis.2019.49.6.346. PubMed PMID: 31886027; PMCID: PMC6920034.

48. Ragucci GM, Elnayef B, Suarez-Lopez Del Amo F, Wang HL, Hernandez-Alfaro F, Gargallo-Albiol J. Influence of exposing dental implants into the sinus cavity on survival and complications rate: a systematic review. Int J Implant Dent. 2019;5(1):6. Epub 2019/02/06. doi: 10.1186/s40729-019-0157-7. PubMed PMID: 30719578; PMCID: PMC6362182.

49. Clark R, Burren CP, John R. Challenges of delivery of dental care and dental pathologies in children and young people with osteogenesis imperfecta. Eur Arch Paediatr Dent. 2019;20(5):473-80. Epub 2019/03/15. doi: 10.1007/s40368-019-00424-w. PubMed PMID: 30868445.

50. Howe MS, Keys W, Richards D. Long-term (10-year) dental implant survival: A systematic review and sensitivity meta-analysis. J Dent. 2019;84:9-21. Epub 2019/03/25. doi: 10.1016/j.jdent.2019.03.008. PubMed PMID: 30904559.

51. Ivanova V, Chenchev I, Zlatev S, Mijiritsky E. Correlation between Primary, Secondary Stability, Bone Density, Percentage of Vital Bone Formation and Implant Size. Int J Environ Res Public Health. 2021;18(13). Epub 2021/07/03. doi: 10.3390/ijerph18136994. PubMed PMID: 34208849; PMCID: PMC8297224.

52. Wang Y, Baumer D, Ozga AK, Korner G, Baumer A. Patient satisfaction and oral health-related quality of life 10 years after implant placement. BMC Oral Health. 2021;21(1):30. Epub 2021/01/16. doi: 10.1186/s12903-020-01381-3. PubMed PMID: 33446161; PMCID: PMC7807859.

53. Yang Y, Hu H, Zeng M, Chu H, Gan Z, Duan J, Rong M. The survival rates and risk factors of implants in the early stage: a retrospective study. BMC Oral Health. 2021;21(1):293. Epub 2021/06/11. doi: 10.1186/s12903-021-01651-8. PubMed PMID: 34107931; PMCID: PMC8188697.

Supplementals

Table S1. Summary of sample numbers per experiments

Experiments	Bone types	PBS		SclAb		Total
		WT	Brtl/+	WT	Brtl/+	
µCT	Maxilla	6	6	6	6	24
	Tibia	6	6	6	6	24
	Femur	12	12	12	12	48
Push-in testing	Maxilla	6	6	6	6	24
	Tibia	6	6	6	6	24
Western blot	Maxilla	6	6	6	6	24
Histology	Maxilla	2	2	2	2	8

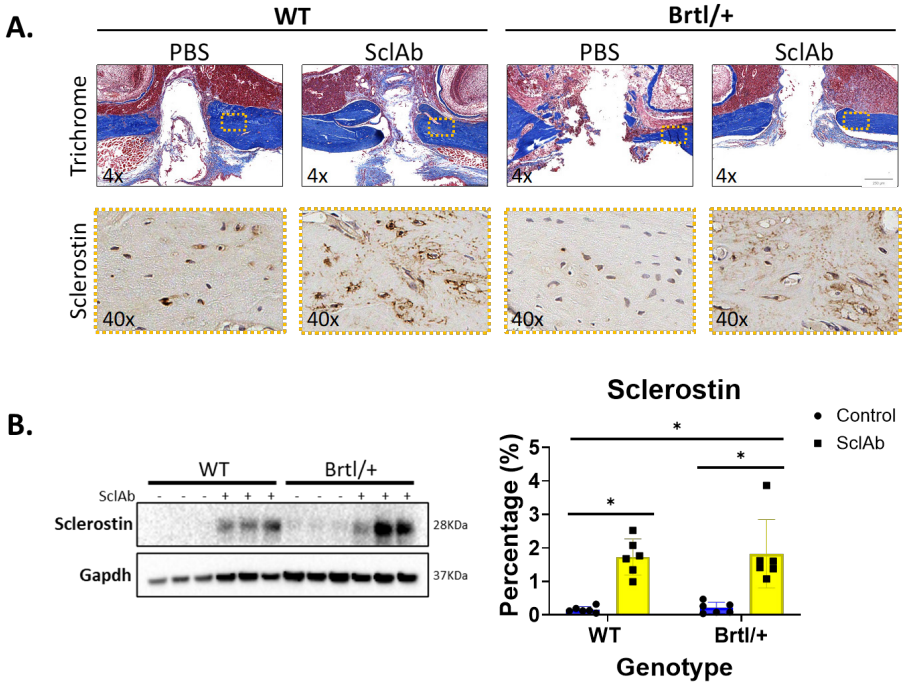

Figure S1. Sclerostin Level in the Maxilla. **A**. Histological slides showing Masson's trichrome staining and sclerostin immunostaining. Red arrows indicate the presence of sclerostin. **B**. Western blot and Graph depicting the relative sclerostin level in the peri-implant alveolar bone. An asterisk represents a statistically significant difference with $p<0.05$.

CHAPTER 7

General discussion and future directions

Aims

While OI has traditionally been defined by recurrent fractures in the long bones, clinical experience makes clear that the craniofacial consequences, for facial growth, dental development, and oral function are equally debilitating yet much less studied. The primary aim was to shift focus from limb fragility to the unique vulnerabilities of the craniofacial skeleton, and to provide a rigorous platform for innovation in therapeutic interventions.

Guided by four objectives, this work sought to illuminate the clinical burden and fracture patterns in the craniofacial skeleton using robust epidemiological data; unravel the molecular biology of bone fragility, with special emphasis on Wnt signaling as master regulators; validate preclinical OI models reflecting human craniofacial disease in order to study genotype, age, sex, and anatomical site; and rigorously test regenerative strategies, especially sclerostin inhibition, for their ability to restore bone mass, stability, and function, while identifying factors needed for individualized treatment response. Through multidisciplinary approaches spanning genetics, developmental biology, imaging, biomechanics, and molecular signaling, the thesis aimed to bridge fundamental discovery and practical solutions for patients and families living with OI.

This multidisciplinary approach, integrating genetics, developmental biology, advanced imaging, biomechanics, and molecular signaling, was designed not only to advance fundamental knowledge but to deliver actionable solutions for patient-centered care.

Major Findings and Their Scientific Context

The studies carried out in this thesis contribute significantly to the mechanistic understanding and clinical relevance of craniofacial bone fragility in OI, moving the field beyond its traditional focus on long bones. Beginning with an exploration of alveolar bone biology, Chapter 2 revealed how adaptation to mechanical forces and oral microbial exposure is tightly regulated by the Wnt/β-catenin pathway. While this chapter focused primarily on craniofacial bone remodeling during aging in the general context, the mechanisms identified, such as age-related suppression of Wnt signaling, have clear implications for oral bone loss and highlight the oral cavity as a uniquely vulnerable site. Though not centered on OI, these insights are directly relevant and extrapolatable to OI, providing a foundation for subsequent investigations into disease-specific fragility.

Building from this molecular framework, the epidemiological study in Chapter 3 provided the first nationwide, quantitative evidence for a disproportionately high

burden of craniofacial fractures in OI, mapped across jaw, skull, and facial bones. These fractures emerged with distinct demographic and disease-associated patterns, emphasizing that craniofacial sites, compared to previously studied skeletal regions, require targeted surveillance and intervention. This real-world population data not only confirmed the clinical significance of craniofacial bone involvement in OI but also highlighted gaps in existing management and prevention strategies.To prove the biological basis for these clinical observations, Chapter 4 employed genetically engineered mouse models to replicate patient-specific craniofacial defects. Detailed morphometric and bone turnover analyses demonstrated that both mutation type and aging significantly alter craniofacial bone structure, with different genotypes presenting unique developmental and remodeling deficits. By faithfully mirroring the variability seen in human OI, these models enabled rigorous preclinical evaluation of new therapies.

The translational significance of these models was realized in Chapter 5, where targeted molecular intervention using sclerostin antibody was shown to restore bone mass and architecture in Col1a1-mutated mice. Importantly, the findings revealed sex-dependent differences in therapeutic response, reflecting underlying hormonal regulation and underscoring the necessity for personalized approaches in craniofacial regeneration. These results moved beyond traditional concepts of bone turnover, demonstrating that successful intervention in OI must address site- and patient-specific biological complexity. From a clinical standpoint, these findings are especially notable: sclerostin antibody therapy demonstrated not only an anabolic effect, increasing bone quantity and improving bone architecture, but also a significant capacity to decrease established bone resorption and prevent further loss. This dual action brings new promises for the restoration of critical oral functions, such as eating, speaking, and social interaction, for patients with OI and other skeletal disorders who have previously had only limited rehabilitation options due to compromised bone integrity. Moreover, the potential application extends to periodontal disease, where balancing bone formation and resorption is a central therapeutic challenge. If future studies confirm these dual effects in human clinical settings, sclerostin antibody therapy could revolutionize treatment strategies for a wider population suffering from bone loss. However, it is essential to acknowledge that further research is required to fully validate these effects and establish safe, effective protocols for broader clinical use.

Chapter 6 translated molecular and regenerative advances into a practical clinical endpoint by investigating dental implant osseointegration. Mechanical and imaging analyses confirmed that sclerostin antibody not only improved bone quality but also enabled robust implant integration in OI mouse models, a

significant achievement given that implant placement is considered the gold standard for rehabilitation in modern dentistry. Despite this standard, patients with OI and others suffering from bone disease have historically faced persistent barriers to implant success owing to compromised bone quality and quantity. The results of this chapter highlight a promising pathway toward overcoming these limitations. While these findings do not immediately change clinical practice, they open the possibility for future translational research and clinical trials that could enable patients who were previously deemed unsuitable for implants, and others with low bone mass disorders, to benefit from the gold standard of dental restoration. This represents a meaningful step toward closing a gap in care that persists for some of the most challenging patient populations in skeletal and dental medicine.

Synthesizing all studies, these findings establish the oral and craniofacial skeleton as dynamic sites for both disease and therapeutic opportunity. Aging, mutation, and hormonal context all shape bone health in ways that are far more nuanced than previously recognized. The thesis validates sclerostin inhibition as a promising, individualized therapy for overcoming structural and functional deficits. From a scientific perspective, these results call for a reframing of OI pathobiology, and from a clinical viewpoint, they set new standards for interdisciplinary skeletal medicine and patient-focused treatment.

Future Directions: Scientific and Clinical Opportunities

The intricate nature of craniofacial bone fragility in OI demands a sophisticated approach rooted in precision medicine. Moving forward, the field is poised to benefit from several key developments. Foremost is the need for personalized regenerative strategies, where real-world patient registries and stratified clinical trials will be instrumental in tailoring therapies to the individual's genotype, sex, age, hormonal status, and specific anatomical site. This move toward customization will enable clinicians to optimize treatment efficacy and minimize adverse outcomes.

As molecular therapies evolve, the question of delivery becomes paramount. The potential of targeted local delivery, using biomaterial scaffolds or drug-eluting implants, promises to reduce systemic exposure and maximize bone regeneration precisely at sites of need. The engineering of such advanced delivery systems is set to become a cornerstone of safe and effective translation from bench to bedside.

Simultaneously, the future of bone regeneration is likely to rest on combination and adjunctive therapies. Synergistic approaches integrating Wnt pathway modulation with anabolic agents, anti-inflammatories, or stem cell technologies require active

exploration in both preclinical and clinical settings to determine the most effective context-specific treatments for OI and related conditions.

At the heart of these advances must be patient-centered outcomes. Incorporating standardized patient-reported outcome measures, functional performance evaluations, and aesthetic assessments into clinical trials will ensure that the scientific progress achieved actually translates into meaningful improvements in patients' daily lives, well-being, and satisfaction.

Moreover, the principles and therapeutic approaches validated in OI have implications far beyond this single disorder. There is considerable opportunity to systematically extend these findings to conditions such as periodontitis, traumatic injuries, cancer-related bone resections, and age-related bone degeneration, further broadening clinical impact.

Finally, deepening mechanistic understanding remains a top priority. The adoption of advanced molecular techniques, including single-cell sequencing, lineage tracing, and computational modeling, will refine our grasp of how regenerative therapies interact with diverse cellular microenvironments, immune responses, and complex signaling networks. By unraveling these intricacies, researchers will continue to sharpen interventions and uncover novel targets, ensuring sustained progress and innovation in craniofacial bone regeneration and repair.

Limitations and Challenges

No study is without limitations. The epidemiological analyses were constrained by the lack of direct clinical severity assessment and inability to study uninsured populations. Mouse models, while robust, cannot always recapitulate the variability of human disease. Long-term safety, optimal timing and dosing, and methods for localized drug delivery remain to be explored. The translation from animal studies to human OI for craniofacial treatment will require careful, staged clinical validation.

Clinical and Scientific Impact

This thesis advances a new paradigm for craniofacial medicine, not just in OI, but across skeletal disorders. By demonstrating that context-specific molecular targeting with sclerostin inhibition can fundamentally restore bone integrity and implant stability, even in severely compromised tissues, it shifts both scientific and clinical boundaries. The work argues for integrated multidisciplinary care, informed by genetics, molecular biology, engineering, and patient input, and prioritizes patient-centered outcome measures. The findings also suggest that the era of

"one-size-fits-all" skeletal therapy must be reassessed and ultimately replaced by precision, site-specific, and combinatorial approaches.

On a personal note, the resilience and optimism of patients and families living with OI shaped the values behind this work. It is my hope that these findings spark new collaborations, guide evidence-based practice, and ultimately restore function and dignity for those long underserved by conventional therapies. This is more than an academic exercise; it is a blueprint for future medicine.

Conclusion and Vision

In conclusion, this thesis elevates craniofacial fragility in osteogenesis imperfecta as both a clinical and scientific priority and lays important groundwork for future targeted regenerative interventions. While the findings here demonstrate that sclerostin inhibition and site-specific approaches may offer promising avenues to improve oral health, function, and quality of life, it is critical to recognize that current clinical trials for sclerostin inhibitors are focused mainly on long bones. Craniofacial applications, despite their potential, remain to be rigorously tested and validated in clinical settings. Thus, these strategies are not yet definitive solutions but rather represent foundational steps toward eventual clinical translation. Continued translational research and carefully designed, craniofacial-focused clinical trials will be essential before these approaches can be adopted in practice. The journey toward meaningful clinical impact is ongoing, and will require sustained innovation, collaborative effort, and patient-centered outcome evaluation. Even so, the principles and vision established here offer a clear direction for advancing the field and genuine hope for patients who have long been left behind by conventional therapies.

7

CHAPTER 8

Nederlandse samenvatting

Osteogenesis imperfecta (OI) is een erfelijke bindweefselaandoening die wordt gekenmerkt door broze botten, herhaalde fracturen en afwijkingen in collageen type I. Hoewel OI traditioneel vooral wordt benaderd vanuit de problematiek van de pijpbeenderen, blijkt uit de klinische praktijk dat de gevolgen voor het craniofaciale skelet minstens zo ingrijpend zijn. Afwijkingen in kaakbot, schedel en gebitselementen beïnvloeden functies als kauwen, spreken en esthetiek, en vormen daarmee een essentieel maar onderbelicht aspect van de ziektelast.

In dit proefschrift staat de vraag centraal hoe genetische defecten in collageen type I leiden tot craniofaciale botkwetsbaarheid, en in hoeverre gerichte modulatie van de Wnt-signaleringsroute (met name via remming van sclerostin met een antilichaam) mogelijkheden biedt voor regeneratie en functieherstel.

Hoofdstuk 2: Craniofaciale kwetsbaarheid en moleculaire regulatie

Craniofaciale botten verschillen duidelijk van pijbeenderen in embryonale oorsprong, vormingsmechanisme en mechanische belasting. Het alveolaire bot, dat voortdurend reageert op kauwkrachten en de orale microbiële omgeving, kent een hoge ombouwsnelheid en is sterk afhankelijk van een goed gereguleerde Wnt/β-catenine signaalroute. Verstoring van deze route kan leiden tot botverlies en afgenomen structurele integriteit: processen die in OI uitgesproken aanwezig zijn.

Hoofdstuk 3: Fracturen in de craniofaciale regio

Een landelijke (VS) epidemiologische analyse laat zien dat mensen met OI een duidelijk verhoogd risico hebben op fracturen van kaak, schedel en aangezichtsbeenderen. Deze fracturen volgen hun eigen patroon, afhankelijk van leeftijd, geslacht en ziekte-ernst. De resultaten tonen aan dat het craniofaciale skelet actief moet worden meegenomen in diagnostiek, monitoring en preventieve zorg.

Hoofdstuk 4: Muismodellen voor craniofaciale afwijkingen

Om de klinische observaties te vertalen naar het onderliggend biologisch mechanisme, zijn verschillende genetische muismodellen onderzocht. Deze modellen tonen aan dat zowel het type collageenmutatie als veroudering leiden tot specifieke afwijkingen in groei, vorm en remodellering van craniofaciale botten. De diermodellen blijken representatief voor menselijke fenotypes en vormen daarmee een robuust fundament voor preklinisch therapieonderzoek.

Hoofdstuk 5: Sclerostin remming als therapeutische benadering

Gerichte remming van sclerostin (SclAb) blijkt in staat om botvorming in OI-modellen te stimuleren en de botarchitectuur te verbeteren. De behandeling

laat bovendien duidelijke sekseverschillen zien, wat onderstreept dat regeneratieve strategieën baat hebben bij een gepersonaliseerde benadering. Deze bevindingen tonen aan dat modulatie van de Wnt-route een veelbelovend aanknopingspunt vormt voor versterking van craniofaciale botstructuren.

Hoofdstuk 6: Implantaatintegratie in compromitterend bot

Omdat succesvolle orale rehabilitatie vaak afhankelijk is van implantaat osseo-integratie, is onderzocht in hoeverre SclAb de bot-implantaat interactie versterkt. De resultaten laten zien dat de behandeling de stabiliteit en verankering van implantaten verhoogt, zelfs in bot dat door OI ernstig is verzwakt. Dit opent perspectieven voor patiëntengroepen die tot nu toe vaak als niet-geschikt werden beschouwd voor implantaatbehandeling.

Toekomstperspectief

De bevindingen uit dit proefschrift laten zien dat effectieve behandeling van craniofaciale afwijkingen bij OI vraagt om precisiegeneeskunde: afgestemd op genotype, leeftijd, sekse en anatomische locatie. Belangrijke toekomstige stappen zijn lokale toediening van regeneratieve middelen, combinatietherapieën met andere osteoanabole of immunomodulerende strategieën, en de ontwikkeling van patiëntgerichte uitkomstmaten die functie, esthetiek en kwaliteit van leven beter weerspiegelen.

Hoewel het remmen van sclerostin in het appendiculaire skelet klinisch wordt onderzocht, staan toepassingen in de craniofaciale regio nog aan het begin van translationele ontwikkeling. Dit proefschrift legt een fundament voor dergelijke studies en biedt handvatten voor verdere klinische validatie.

Conclusie

Dit proefschrift toont aan dat craniofaciale botkwetsbaarheid een wezenlijk en vaak onderschat onderdeel is van osteogenesis imperfecta. Door epidemiologische inzichten te combineren met moleculaire en preklinische studies etaleert dit werk dat het craniofaciale skelet niet alleen kwetsbaar is, maar ook goed kan reageren op gerichte, moleculair gestuurde regeneratie. Sclerostin remming vormt een veelbelovende therapeutische route, zowel voor structureel herstel als voor functionele revalidatie, waaronder implantaatintegratie. Samen schetsen deze bevindingen een toekomst waarin gepersonaliseerde en locatie-specifieke behandelingen bijdragen aan betere zorg en verbeterde levenskwaliteit voor mensen met OI.

APPENDIX

Research data management
Curriculum vitae
List of publications
Acknowledgments / dankwoord

Research data management

The data used for all chapters are not owned by Radboudumc. The data are archived by the University of Michigan. Questions about the data can be addressed to sunghsie@umich.edu

Medical and animal ethical approval

This thesis is based on two types of research. First, experiments involving mice were conducted in accordance with relevant national and international legislation, guidelines, codes of conduct, and University of Michigan policy. Animal care and use were reviewed and approved by the University of Michigan Institutional Animal Care and Use Committee (IACUC) under protocol number PRO00011108.

Second, secondary data analyses were conducted using fully de-identified data from human participants to ensure privacy and confidentiality. The University of Michigan Institutional Review Board determined that the use of these data was exempt from further review.

Privacy measures (i.e. pseudonymization / anonymization)

The privacy and confidentiality of human participants were protected by the use of fully de-identified and anonymous insurance claims data. No identifiable personal information was included in the analyses.

Informed consent

Not applicable. Only de-identified secondary data was used.

Data collection

Data for chapters 4, and 6 were obtained through laboratory experiments involving from experiments involving animals.

Data for Chapter 3 were obtained through fully de-identified secondary data, using patient-level insurance claims information from the IBM® Watson Health MarketScan® Research Databases. Access to these data was granted through a formal review and application process.

Data storage

Data from chapters 4, and 6 were analysed in The University of Michigan Orthopaedic Research Laboratory computers and server and stored in the Laboratory systems and University of Michigan Dropbox.

Data from chapter 3 were stored and analysed on the department server and are only accessible by the project member approved by the IBM® Watson Health MarketScan.

Describe which chapters have been published

Chapters 2, 3, 4, 6 are published with open access.

Chapters 5 are not published.

Describe which datasets are available for reuse and published in a data repository

The dataset from chapters 3, 4, 5, and 6 are accessible under request to the Senior investigator.

Describe which chapters were based on existing data

Chapter 2 is based on existing data which was obtained from published literature.

Chapter 3 is based on existing data, which was obtained from IBM® Watson Health MarketScan after the application process.

Describe which chapters are not available for reuse

The data used in the unpublished chapter 5 are archived at the department server. Upon publication of the chapter the data will be in open access.

Overview published and archived datasets

Chapter	DAC	RDC	DSC	NAME DATA REPOSITORY	License or Data Use Agreement (DUA)
2	Orthopaedic Research Laboratory U of M	Orthopaedic Research Laboratory U of M	DOI: 10.1111/jre.70085	Publication in Radboud repository Raw data in University of Michigan secure system	CC-BY-NC
3	Orthopaedic Department U of M	Orthopaedic Department U of M	https://doi.org/10.1016/j.bone.2025.117762	Publication in Radboud repository Raw data in University of Michigan secure system	CC-BY-NC
4	Orthopaedic Research Laboratory U of M	Orthopaedic Research Laboratory U of M	https://doi.org/10.1093/jbmrpl/ziad004	Publication in Radboud repository Raw data in University of Michigan secure system	CC-BY-NC
6	Orthopaedic Research Laboratory U of M	Orthopaedic Research Laboratory U of M	https://doi.org/10.1016/j.bone.2024.117167	Publication in Radboud repository Raw data in University of Michigan secure system	CC-BY-NC
5	Orthopaedic Research Laboratory U of M	Orthopaedic Research Laboratory U of M	-	Raw data in University of Michigan secure system	-

DAC = Data Acquisition Collection, RDC = Research Documentation Collection, DSC = Data sharing Collection

Curriculum Vitae

Hsiao Hsin Sung Hsieh was born on July 19, 1975, in Taiwan and grew up in Chile. She earned her DDS degree from the Universidad de Chile School of Dentistry in 2001. She then completed her residency training in Oral and Maxillofacial Surgery at the Universidad de Chile School of Dentistry in 2006. In 2008, she completed a fellowship in Implant Dentistry at Hospital San José, and in 2012 she earned a Master of Science degree from the Universidad de Chile School of Medicine. In 2023, she completed an additional fellowship in Implant Dentistry at the University of Nevada, Las Vegas School of Dental Medicine.

Following her training, Hsiao Hsin served as an Assistant Professor in the Department of Oral and Maxillofacial Surgery at the Universidad de Chile School of Dentistry. Since 2013, she has been a faculty member at the University of Michigan School of Dentistry, first as a Clinical Assistant Professor and currently as a Clinical Associate Professor in the Department of Oral and Maxillofacial Surgery.

Her clinical and academic work focuses on dentoalveolar surgery and bone regeneration, with a particular emphasis on the care of medically complex patients. Through her work, she integrates clinical practice, education, mentorship, and translational research to advance patient care and improve surgical outcomes.

In 2017, she began her doctoral research in the Orthopaedic Research Laboratory within the Department of Orthopaedic Surgery at the University of Michigan, in collaboration with the Department of Experimental Rheumatology at Radboudumc. Her work focuses on craniofacial bone biology and regeneration, with particular emphasis on the anabolic effects of sclerostin antibody therapy on craniofacial bone in mice with osteogenesis imperfecta. This research has been funded by the NIH/NIDCR K08 and the Osteo Science Foundation. Her doctoral work has been supervised by Prof. Dr. Peter van der Kraan, Prof. Dr. Kenneth Kozloff, and Dr. Esmeralda Blaney Davidson.

In 2025, she received the André Schroeder Preclinical Research Award from the International Team for Implantology (ITI) for her work entitled "Sclerostin Antibody Enhances Implant Osseointegration in Bone with Col1a1 Mutation." This recognition reflects her commitment to scientific discovery, clinical innovation, and the advancement of regenerative approaches in oral and maxillofacial surgery.

In addition to her clinical and scholarly work, Hsiao Hsin remains actively engaged in educating and mentoring undergraduate students, dental students, and residents.

List of Publications

Sung HH, Spresser WJ, Hoffmann JP, Dai Z, van der Kraan PM, Caird MS, Blaney Davidson EN, Kozloff KM
Collagen mutation and age contribute to differential craniofacial phenotypes in mouse models of osteogenesis imperfecta
Journal of Bone and Mineral Research Plus (2024)

Sung HH, Kwon HH, Stephan C, Reynolds SM, Dai Z, van der Kraan PM, Caird MS, Blaney Davidson EN, Kozloff KM
Sclerostin antibody enhances implant osseointegration in bone with Col1a1 mutation
Bone (2024)

Sung HH, Whitney DG, Caird MS, Kozloff KM
Craniofacial and whole-skeleton fracture patterns in osteogenesis imperfecta: Findings from a nationwide U.S. insurance claims database
Bone (2026)

Sung HH, Chalamalasetty N, Alzainal A, Liu H, Wang L, Colacrai-Arikita P, Wei ICX, Wang HL, van den Bosch MHJ, Caird MS, van der Kraan PM, Kozloff KM, Blaney Davidson EN
The Role of Wnt Signaling in Age-Related Alveolar Bone Loss and Regeneration
Journal of Periodontal Research (2026)

Acknowledgments / dankwoord

With the completion of this dissertation, a long, intense, educational, and deeply meaningful journey comes to an end. My path to this PhD has not been a traditional one. I began this journey as a clinician, carrying with me the questions, uncertainties, and hopes that arise when caring for patients. Those questions led me into the preclinical world, where I searched for answers that could one day return to the clinic and contribute to better patient care. Although the work in this dissertation was performed in mice, its motivation has always been deeply rooted in my clinical experience. The patients I have cared for, with their resilience and trust, reminded me again and again why this work mattered.

Starting a PhD at a later stage in my career, while continuing to grow clinically and professionally, was not always easy. At times, it felt like this journey was taking forever; yet my clinical work continually gave meaning to the research and gave me the motivation to keep going.

Fortunately, I did not walk this path alone. This dissertation reflects not only years of scientific work, but also the mentorship, patience, friendship, generosity, and unwavering support of many people. I would like to take this moment to thank everyone who, in one way or another, helped make this work possible.

Beste **Peter**, Dank je wel dat je mij in 2017 als promovendus hebt aangenomen en mij de kans hebt gegeven om dit traject met jou te beginnen. Ik ben je ontzettend dankbaar dat je mij de ruimte hebt gegeven om tegelijkertijd te werken en te studeren, en voor je geduld en begrip voor mijn bijzondere situatie. Ondanks de afstand en de soms complexe weg die ik heb afgelegd, bleef je mij gedurende dit hele proces ondersteunen en begeleiden. Dank je wel voor je vertrouwen in mij en in dit project, voor je voortdurende steun, en voor de begeleiding die je mij onderweg hebt gegeven. Ik ben oprecht dankbaar voor de kans die je mij hebt geboden en voor jouw rol in deze reis.

Dear **Ken**, I am especially thankful to you for welcoming me into your lab and for your outstanding mentorship, friendship, and unwavering support. From the very beginning, you created an environment where I felt trusted, encouraged, and valued. Your support has helped me grow not only as a scientist, but also as a mentor, a teammate, and a person. I have learned so much from your example, not only in how to ask meaningful scientific questions and pursue rigorous research, but also in how to lead with kindness, patience, respect, and integrity. You were always fully

supportive, patient, and understanding. You never pushed me in a way that made me feel pressured, but instead guided me with compassion, confidence, and steady encouragement. Your mentorship gave me the space to grow, make mistakes, learn, and become more independent. I am deeply grateful for your belief in me, for your friendship, and for the many ways you have supported me throughout this journey.

Beste **Esmeralda**, Wat ben ik ontzettend dankbaar dat jij mijn copromotor, mentor en vriendin bent geweest tijdens dit traject. Je steun, begeleiding en aanmoediging hebben ontzettend veel voor mij betekend. Jouw intelligentie, toewijding en warmte zijn werkelijk inspirerend. Je stond altijd klaar om mee te denken, te helpen en mij te begeleiden, zowel op wetenschappelijk als persoonlijk vlak. Ik zal onze vroege Zoom-overleggen hier in Ann Arbor nooit vergeten, en ook niet het geduld en de energie die je me gaf, ondanks de afstand. Ik bewonder hoe je je altijd met zoveel diepgang in een onderwerp kunt verdiepen en scherpe, waardevolle feedback geeft die het werk telkens verbetert. Bovenal ben je voor mij een mentor in het leven en een echte inspiratiebron geworden. Dank je wel voor je vriendschap, je vertrouwen en het voorbeeld dat je bent.

I am deeply grateful to the members of my Manuscript Committee, Dr. **van den Beucken**, Prof. Dr. **Bakker**, and Prof. Dr. **Forlino**, for your time, thoughtful reading, careful assessment, and valuable feedback on this dissertation.

I would also like to thank the members of my defense committee for your time, support, and willingness to participate in my defense. I am grateful for your careful consideration of my work and for the valuable perspectives and expertise you bring to this important milestone in my PhD journey.

I gratefully acknowledge the financial support that made this work possible, including funding from the **National Institutes of Health/National Institute of Dental and Craniofacial Research (NIH/NIDCR)** and the **Osteo Science Foundation**. This support was essential for the completion of the studies presented in this dissertation.

This journey would not have been possible without the support of the department chairs who led the Department of Oral and Maxillofacial Surgery at the University of Michigan during the years of my PhD. I would like to sincerely thank Dr. **Joseph Helman**, Dr. **Brent Ward**, and Dr. **Sean Edwards** for your understanding, support, and encouragement throughout the many years it took me to complete this work. Your patience, flexibility, and trust allowed me to balance my clinical

responsibilities, research, and professional growth, and I am deeply grateful for the space and support you gave me along the way.

Dear **Michelle**, I am grateful that you introduced me to Ken and to the lab, and for your continued support throughout this process. Your help was essential in connecting me with the people and environment where this work could grow. Dear **Deb**, thank you for your friendship and for introducing me to Michelle, a connection that truly changed the course of this journey. Without both of you, your support, and the doors you helped open, I may not have been able to complete this work. I am deeply grateful.

Dear **Laurie**, I am deeply grateful for your support with my K08 grant and for your strong commitment to promoting women in research. As an exceptional researcher and leader at the University of Michigan, including in your roles as Dean and Provost, you have been a true source of inspiration. Despite your very busy schedule, you always made time for me and were willing to offer guidance, encouragement, and support whenever I needed it. Your advocacy, generosity, and belief in me meant a great deal, and I am sincerely thankful for the important role you played in this journey.

Dear **Kurt**, I am deeply grateful for your support of my research career. Your guidance and help have been crucial throughout this process. Your encouragement and commitment to supporting my development as a researcher have meant a great deal to me, and I sincerely appreciate everything you and your team have done to help me move forward.

I would also like to thank **Andrea, Tristan, Megan, Adam, Karl**, and Dr. **Mishina** for your generous support throughout this journey. Thank you for sharing your lab resources, offering guidance, and always being willing to help when needed. Your support, expertise, and openness made an important difference in the completion of this work.

Dear **Rob**, I am especially grateful for your constant support, friendship, and collaboration. Your help with imaging, computing, and problem-solving were absolutely essential; without your expertise, patience, and willingness to help, I truly do not know how I would have completed this work. I am deeply grateful for the important role you played in this dissertation.

Dear **Karen**, I want to give you a very special thank you for all your help throughout this journey. You were absolutely essential, from animal training and handling to

answering all my questions and taking care of the orders. Without you, we could never have performed the surgeries. More than that, I truly value you as a friend. The wonderful talks and all the laughs we shared made the work not only easier, but so much more enjoyable.

Dear **Chris, Rachel, Alex, Christina, Diana, Lindsey, Danny,** and **Buchan**, thank you for your friendship, support, and companionship throughout this journey. Thank you for the conversations, laughter, shared frustrations, encouragement, and all the small moments that made the long days in the lab more enjoyable. Having people to chat with, laugh with, and navigate the ups and downs of research alongside made this experience much lighter, more meaningful, and much more enjoyable.

I would like to sincerely thank my students and research assistants, **Wyatt, Joe**, **Skylar, Jiayu, Ali, Pietra, Lexuang, Hane, Asal,** and **Paige**, for your hard work, dedication, and enthusiasm throughout this project. Your help with surgeries, animal care, tissue harvesting, wet lab experiments, imaging, and countless other tasks was essential to this work. I am deeply grateful for your reliability, curiosity, patience, and willingness to learn, even during the long and demanding days in the lab. Working with you and mentoring you has been one of the most rewarding parts of this journey.

Dear **Conor, Melissa, Andrea,** and **Bonnie** for your support, expertise, and constant willingness to help. Each of you, in your own area, made this journey easier and helped things move forward. I am grateful not only for your knowledge and assistance, but also for the kindness, patience, and smiles you brought along the way. Thank you for always being open to help whenever I needed it.

I would also like to thank my collaborators, **Dan** and **Zongrui**, for sharing your expertise, time, and thoughtful insights throughout this project. Your contributions were invaluable, and your willingness to collaborate and help whenever needed made a meaningful difference in this work. I am truly grateful for your support and collaboration.

I would also like to thank the animal care and vivarium staff for their support, dedication, and care throughout this project. I am especially grateful to **Chris** for his invaluable help with breeding and maintaining the mouse colonies. Your careful work, organization, and support behind the scenes were essential to the success of this dissertation.

Dear **Genny**, thank you for being such an exceptional friend and such a wonderful person. I honestly do not know how you manage everything — your children, family, dental school, PhD, and so much more — and still make it look effortless. Your strength, organization, generosity, and dedication inspire me constantly. Thank you for your constant support, for sharing your knowledge, for encouraging me, and for always being willing to listen and help. I am especially grateful for your support with grant applications and for the time, advice, and thoughtful feedback you gave me throughout that process. Your friendship, wisdom, and encouragement have meant so much to me during this journey, and I am truly grateful to have you in my life.

Querida profe **Julieta, Isa, Kote** y **Vero**, gracias por acompañarme en mis primeros pasos en la ciencia. Gracias por abrirme puertas, por inspirarme, por enseñarme a hacer preguntas, y por sembrar en mí la curiosidad que finalmente me trajo hasta aquí. Sus enseñanzas y apoyo han sido parte fundamental de este camino.

To my friends **Amy** and **Ivy**, thank you for always being there and for helping with whatever was needed so that I could focus on my research. Your support, kindness, and willingness to step in made an enormous difference during this journey. I am so grateful for your friendship and for the many ways you helped me keep going.

A mis queridos amigos **Carito, Moncha, Isa, Lore, Sandra, Caro, Yeli, Eli, Angélica,** y **Lucho**, gracias por acompañarme siempre, incluso desde la distancia. Gracias por sus palabras de aliento, por sus mensajes llenos de cariño, por celebrar mis logros y por sostenerme en los momentos difíciles. Aunque la vida nos haya puesto en lugares distintos, siempre he sentido su cercanía y he sabido que puedo contar con ustedes. Su amistad incondicional ha sido un regalo inmenso y una fuente constante de fuerza, alegría y esperanza durante este camino.

我要把最深的感谢献给我的家人。谢谢你们始终无条件地支持我、相信我、爱我。你们从来没有给我压力，也从来没有要求我必须成为某一种样子；无论我追求什么梦想、走向哪里，你们都只是希望我过得好，希望我快乐、健康、平安。你们一直是我最坚强的后盾，也是我最温暖的港湾。能够拥有你们的爱与支持，是我人生中最大的幸运。谢谢你们一直在那里，陪我走过这一切。

To everyone who supported me, encouraged me, taught me, challenged me, and believed in me throughout this journey: thank you, gracias, 谢谢. This dissertation represents far more than the completion of a scientific project. It represents years of persistence, growth, uncertainty, learning, friendship, and hope. I am deeply grateful to have been surrounded by people who helped me continue, even when

the road was long. To those whose names may not appear here, please know that your support, kindness, and encouragement have mattered deeply and remain in my heart. Thank you for walking this path with me.

Fine, al tiuj, kiuj ne plu estas korpe ĉe mi en ĉi tiu vivo, sed kiuj ĉiam vivas en mia koro: dankon pro via spirita akompano. En ĉiuj altaj kaj malaltaj momentoj de ĉi tiu vojaĝo, mi sentis vian kuraĝigan spiron gvidi min la tutan vojon.

We kunnen niet voorkomen dat de boom ouder wordt, maar we kunnen zijn wortels versterken tegen de storm.
Oud worden is geen kwetsbaarheid, geen mislukking, geen strijd en geen probleem dat moet worden teruggedraaid, het is een levensfase. De vraag is niet of botten met de tijd veranderen, maar of we kunnen leren om ze betere redenen te geven om stand te houden.
Sommige reizen duren langer. Dat is geen tekortkoming.
Het is simpelweg een andere manier van aankomen.

9 789465 153018 >

Radboudumc university medical center
IN DEI NOMINE FELICITER
Radboud University